Dissertation
submitted to the
Combined Faculties for the Natural Sciences and for Mathematics
of the Ruperto-Carola University of Heidelberg, Germany
for the degree of
Doctor of Natural Sciences

presented by
Diplom-Biologe Andre Engling
born in Marl

Mutational Analysis of the Export Targeting Motif of Fibroblast Growth Factor 2, a Mediator of Tumor-Induced Angiogenesis

Referees:

Prof. Dr. Walter Nickel

Prof. Dr. Michael Brunner

Summary

The majority of secretory proteins is exported from mammalian cells by the classical secretory pathway involving subcellular compartments such as the endoplasmic reticulum (ER) and the Golgi apparatus. However, basic fibroblast growth factor (FGF2), a potent mediator of tumor-induced angiogenesis, has been shown to be secreted by a non-classical pathway that does not depend on the functions of the ER and the Golgi apparatus. The molecular characterization of the FGF2 export mechanism is not only a fundamental problem in cell biology but also of great interest for biomedical research since it may pave the way for the development of a novel class of anti-angiogenic drugs.

In this thesis, a robust model system designed to quantitatively assess FGF2 secretion under various experimental conditions was developed. A retroviral expression system was established in CHO cells that allows for a stable integration of reporter constructs whose expression can be induced by doxicycline. In order to monitor expression of FGF2 reporter molecules they were constructed as GFP fusion proteins. Based on this experimental system, secretion of FGF2-GFP can be quantified by flow cytometry, confocal microscopy and biochemical methods since exported FGF2-GFP binds to cell surface heparan sulfate proteoglycans and, therefore, is accessible by membrane-impermeable tools such as antibodies and biotinylation reagents.

In the second part of this thesis, a systematic mutational analysis of the FGF2 open reading frame was conducted in order to identify *cis* elements that direct FGF2 to its export machinery. Initial experiments revealed the identification of FGF2 mutants that are defective in binding to heparan sulfate proteoglycans. Such mutants were neither detectable on the cell surface nor in the medium of cells suggesting that the interaction of FGF2 with heparan sulfate proteoglycans does not only play a role in FGF2 signaling but also in the overall process of FGF2 externalization from mammalian cells. A collection of more than a hundred FGF2 mutants and corresponding stable cell lines described in this thesis now provide a basis for future studies in order to conduct a detailed analysis of determinants required for FGF2 secretion.

1 Introduction

Eukaryotic cells possess an elaborate endomembrane system, compartmenting the cell into different organelles. Each compartment provides a specialized environment for certain biological processes. The transport of proteins into the lumen of these organelles involves polypeptide translocation across membranes. Well characterized translocation processes are transport in and out of the nucleus (Gorlich and Kutay, 1999; Weis, 2003), import into mitochondria (Gordon et al., 2000; Endo et al., 2003) and peroxisomes (McNew and Goodman, 1994; Walton et al., 1995; Holroyd and Erdmann, 2001). Secretory proteins pass the membrane of the endoplasmatic reticulum, are modified in different organelles and finally reach the extracellular space by fusion of secretory vesicles with the plasma membrane.

1.1 Classical Protein Secretion

The transport of soluble secretory proteins to the extracellular space is understood in great detail. The first step of this process called classical protein secretion is the cotranslational transport of the nascent polypeptide chain into the endoplasmatic reticulum (ER). Soluble secretory proteins contain N-terminal signal peptides directing them to the transport machinery of the ER (Walter et al., 1984). Interaction of this signal peptide with its receptor, the signal recognition particle (SRP) leads to an arrest in translation elongation (Sakaguchi et al., 1987; Wessels and Spiess, 1988; Kuroiwa et al., 1996). The complex of SRP, nascent polypeptide chain and ribosome diffuses to the ER membrane where SRP binds to the SRP receptor (Rapoport et al., 1992). The arrest in protein elongation is released (Gilmore et al., 1982a) and the nascent polypeptide is synthesized into the lumen of the ER (Gilmore et al., 1982b; Walter et al., 1984; Brodsky, 1998). Subsequently, the signal peptide is cleaved off by specific peptidases and luminal chaperones ensure correct folding of the polypeptide chain (Hebert et al., 1995). Once present in the lumen of the ER, disulfide bonds are formed and the protein gets N-glycosylated by oligosaccharyl transferase, transferring N-linked oligosaccharide precursor chains to asparagine

residues of the protein (Sharma et al., 1981). Subsequently, glucose and mannose moieties are trimmed from these precursor chains by glucosidases or mannosidases (Lucocq et al., 1986; Roth et al., 1990; Roth et al., 2003). The modified and correctly folded protein leaves the ER via small vesicles and enters the Golgi apparatus, which is composed of different cisternae, mediating typical modifications, like sulfatation (Hille et al., 1984; Baeuerle and Huttner, 1987), O-glycosylation (Sadeghi and Birnbaumer, 1999; Ernst and Prill, 2001; Hanisch, 2001) and further trimming of sugar moieties from N-glycans (Zuber et al., 2000). Secretory proteins are transported through the distinct cisternae, are specifically modified there, and finally packaged into secretory vesicles (Pearse, 1976; Tooze and Tooze, 1986; Seeger and Payne, 1992), leaving the donor membrane (trans-Golgi cisternae) and targeted to the acceptor membrane (plasma membrane). The vesicles travel along the microtubule network (Wacker et al., 1997; Pruyne et al., 1998; Vega and Hsu, 2001; Martin-Verdeaux et al., 2003) and finally fuse with the plasma membrane thereby releasing the protein into the extracellular space (Guo et al., 1999; Sivaram et al., 2005; Tsuboi et al., 2005).

Two non-clathrin coats, COPI and COPII, drive the formation of vesicles that mediate transport between the ER and the Golgi and between the compartments of the Golgi (Salama and Schekman, 1995). COPII vesicles mediate anterograde transport from the ER to the Golgi (Barlowe et al., 1994; Schekman and Orci, 1996). The general consensus for COPI vesicles is that they are involved in the retrograde transport (Lippincott-Schwartz et al., 1998) of cargo proteins. Additionally evidence is accumulating that COPI vesicles also transport cargo proteins in an anterograde manner (Rothman and Wieland, 1996; Nickel et al., 1998). The formation of a vesicle is mediated by coat components, which are recruited to the appropriate sites, interact with cargo proteins and drive vesicle budding. GTP-binding proteins drive the initial recruitment of the coat and act as molecular switches to facilitate coat assembly (Lee et al., 2004).

Once budded off the donor membrane, the vesicle is targeted specifically to an acceptor membrane involving a complex molecular machinery that mediates specificity and vesicle fusion with the acceptor membrane. Small receptor molecules, the SNARES (soluble NSF attachment protein receptors), located in the membrane

of the vesicle (v-SNARE) and in the target membrane (t-SNARE; (Sollner et al., 1993)) are involved in membrane fusion (Rothman, 1996; Weber et al., 1998; Nickel et al., 1999). Leading a vesicle to its correct acceptor membrane is likely mediated by rab proteins and other tethering factors. Once the vesicle is localized at the correct target membrane, the fusion process is facilitated by the assembly of v- and t-SNAREs, interacting in specific combinations. The assembly converts trans-SNARE complexes from an instable high-energetic state into a stable low-energetic cis-SNARE conformation. The energy provided is used to overcome the natural energy barrier of two negatively charged and hydrated surfaces allowing fusion of opposing membranes. Following fusion, N-ethylmaleimide-sensitive factor (NSF) provides energy by ATP hydrolysis, which is required for the disassembly of the cis-SNARE complex. The t-SNAREs remain in the acceptor membrane and are available again for further rounds of fusion processes (Hanson et al., 1997), whereas the v-SNAREs are recycled back to their donor membrane by retrograde transport (Ballensiefen et al., 1998), although recent studies on yeast vacuoles suggest that recycling of v-SNAREs might also be mediated by a mechanism independent of retrograde transport (Dietrich et al., 2005).

The ER/Golgi dependent secretory pathway can be selectively blocked by inhibitors like monensin, which irreversibly inhibit trans-Golgi transport (Maxfield et al., 1979; Tartakoff, 1983) and brefeldin A, which induces the redistribution of Golgi components into the ER, thereby reversibly destructing the Golgi apparatus (Misumi et al., 1986; Lippincott-Schwartz et al., 1990; Ivessa et al., 1995).

1.2 Unconventional Protein Secretion

In contrast to the well characterized conventional protein secretion, unconventional protein secretion (also known as “nonclassical protein export”) was discovered about 15 years ago, but the molecular mechanisms and the identity of machinery components remain elusive (Rubartelli et al., 1992; Florkiewicz et al., 1995; Cleves et al., 1996; Nickel, 2003). However, unconventionally secreted proteins share the following common features:

- they can not be detected in the lumen of ER or the Golgi apparatus
- they lack a conventional signal peptide.
- they do not contain ER/Golgi dependent post-translational modifications.
- their secretion is not blocked by brefeldin A, a typical inhibitor of the classical secretory pathway.

Although unconventionally secreted proteins demonstrate the same characteristics, it has been shown that they do not take the same export route, but use different secretion pathways (Hughes, 1999; Nickel, 2003; Nickel, 2005). The potential mechanisms for unconventional secretory processes are summarized in the following figure 1.1:

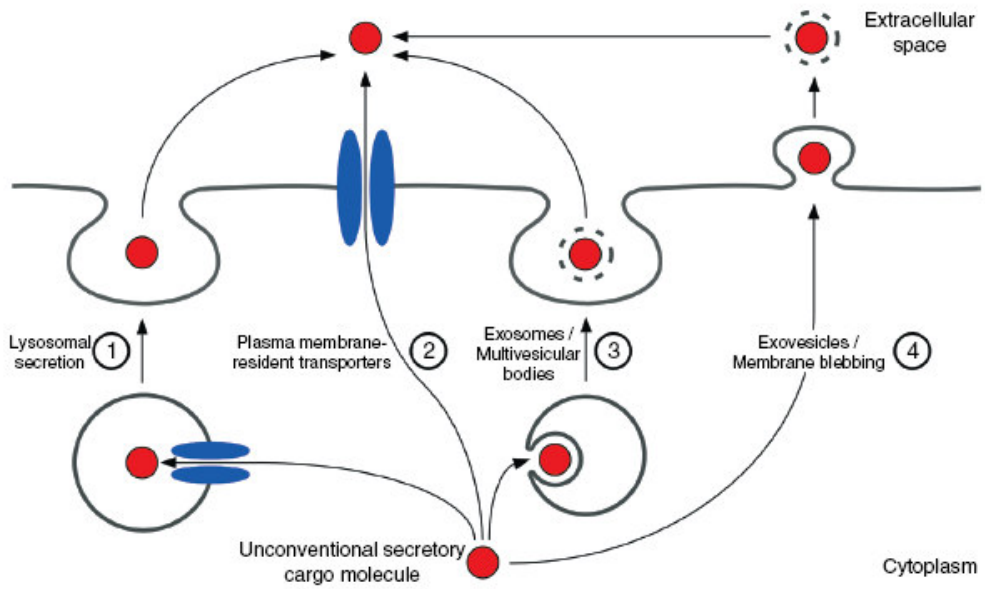

Figure 1.1: Current models of pathways potentially involved in unconventional secretory processes (Nickel, 2005)

1) Export by secretory lysosomes.

   Lysosomal contents gain access to the exterior of cells when specialized endocytic structures such as secretory lysosomes of cytotoxic T lymphocytes or melanosomes of melanocytes fuse with the plasma membrane (Stinchcombe et al., 2004). A classical example of an unconventional secretory protein whose export mechanism involves endo-lysosomal vesicles is IL-1β (Rubartelli et al., 1990).

2) Export mediated by plasma membrane-resident transporters.
   Direct translocation of cytosolic factors across the plasma membrane using protein conducting channels such as adenosine triphosphate-binding cassette (ABC) transporters (Cleves and Kelly, 1996). Examples are the *leishmania* protein HASPB which translocation is likely to be mediated by a plasma membrane-resident transporter (Stegmayer et al., 2005) and FGF1 that is also suggested to rely on a direct transport mechanism at the level of the plasma membrane (Prudovsky et al., 2002).

3) Export through the release of exosomes derived from multivesicular bodies.
   Luminal contents of endocytic structures can be released into the extracellular space when multivesicular bodies fuse with the plasma membrane, a process that results in the release of exosomal vesicles along with their cargo molecules (Stoorvogel et al., 2002).

4) Export mediated by plasma membrane shedding of microvesicles.
   Direct translocation of cytosolic factors across the plasma membrane using a process called membrane blebbing being characterized by shedding of plasma membrane-derived microvesicles that are released into the extracellular space (Hugel et al., 2005; Martinez et al., 2005). Evidence existing in a number of studies indicates that the secretory process for members of the galectin family involves the formation of exovesicles generated by membrane blebbing (Hughes, 1999).

1.3 Unconventionally secreted proteins

Nowadays it is not known how many proteins are secreted using mechanisms distinct from the classical secretory pathway. Since the discovery of the existence of non-classical secretion (Cooper and Barondes, 1990; Muesch et al., 1990; Florkiewicz et al., 1995), the list of proteins demonstrated to be externalized by unconventional means is steadily growing. The following proteins are known to be secreted in an ER/Golgi-independent manner and are introduced in the following sections.

- Cytokines: Thioredoxin, interleukin-1 and migration inhibitory factor (MIF)
- Leishmania HASPB
- Viral proteins: HIV-Tat, FV Bet and HSV VP22
- Homeodomain-containing transcription factors and HMG chromatin-binding proteins
- Lectins of the extracellular matrix: Galectin-1 and -3
- Pro-angiogenic growth factors: Fibroblast growth factor 1 and 2

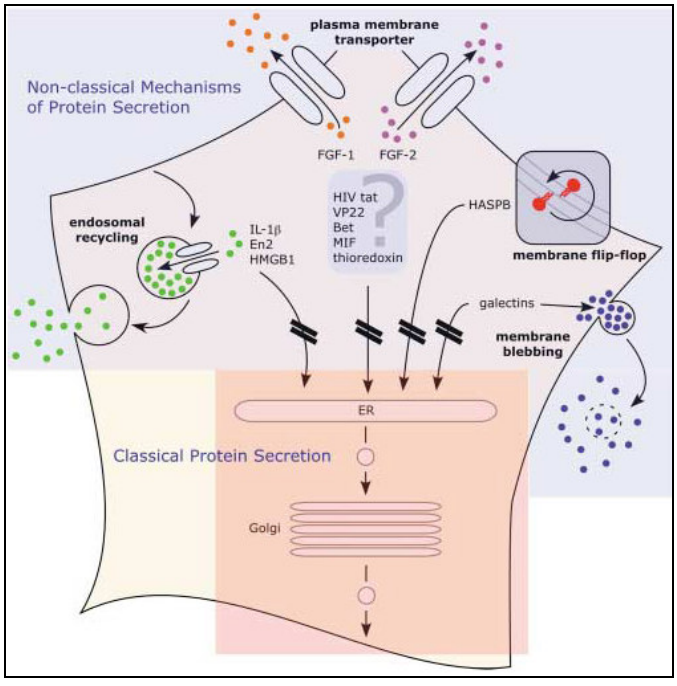

Figure 1.2: Proteins exported by unconventional means and their potential export routes (Nickel 2003).

The various proteins secreted in an unconventional manner and their proposed export routes are summarized in figure 1.2.

1.3.1 Interleukin-1

Interleukin-1 (IL-1) is the prototypic pro-inflammatory cytokine. Two forms of IL-1, IL-1α and IL-1β have been identified, mediating a wide range of indistinguishable biological activities. IL-1 affects nearly every cell type, is a highly inflammatory cytokine and plays an important role in immune response and host defences (Dinarello, 1985). Regulation of IL-1 activity is mediated by low numbers of surface receptors, circulating soluble receptors and a cell surface "decoy" receptor, which down-regulates responses to IL-1β (Dinarello, 1997).
Both forms of Interleukin-1 lack a classical secretion signal and are exported from activated monocytes (Auron et al., 1987).

1.3.1.1 Interleukin-1α

IL-1α is synthesized as an 31 kDa precursor form (pro IL-1α) from cytoskeleton-associated polyribosomes (Stevenson et al., 1992). Intracellular IL-1α is distributed asymmetrically between cytosol, microtubules and nuclear compartments and is modified by myristoylation (Stevenson et al., 1993), therefore inserted into the plasma membrane and finally a target for specific cysteine proteases, the calpains (Kobayashi et al., 1990; Miller et al., 1994). However, IL-1α is also found on the surface of monocytes and lymphocytes (Kurt-Jones et al., 1985). The molecular mechanism of IL-1α secretion has not been classified at a molecular level, but it has been shown that shear stress increases the release of interleukin 1α (Sterpetti et al., 1993) and that IL1-α is secreted upon heat shock treatment (Tarantini et al., 2001).

1.3.1.2 Interleukin-1β

Interleukin-1β is also synthesized as a 31 kDa proIL-1β form that is mainly distributed in the cytosol. The precursor form is processed by the IL-1β converting enzyme (ICE) to the mature form of 17 kDa size. The protein is not glycosylated despite bearing multiple consensus sites for N-glycosylation.

It was shown that only the processed form is secreted from IL-1β expressing cells, whereas the precursor remains in the cell. IL-1β was found to be partially present within intracellular vesicles only in cells also secreting IL-1β, indicating that packaging of IL-1β into these vesicles may be a part of the secretion pathway. Recently it was shown that these intracellular vesicles fuse with the plasma membrane, releasing their content to the extracellular space (Andrei et al., 1999). The secretion of IL-1β is blocked by methylamine, low temperature or serum free medium. In contrast, the secretion is increased by heat shock treatment or by the presence of calcium ionophores, brefeldin A, monensin, dinitrophenol or carbonyl cyanide chlorophenylhydrazone (Rubartelli et al., 1990). Moreover, the ABC transporter ABCA1 has been implicated to be involved in the overall process of IL-1β secretion since secretion of IL-1β is sensitive to glyburide, a drug targeted to the ABC1 family of membrane transporters (Hamon et al., 1997). However ABCA1 has been implicated in the membrane translocation of cholesterol (Raggers et al., 2000) and therefore, it seems unlikely that a defined type of ABC transporter is capable of translocating two classes of molecules structurally as different as a small protein and a membrane lipid. It was shown that IL-1β secretion is dependent on this ABC transporter in macrophages, but not in monocytes (Zhou et al., 2002). However, for this cell type it was proposed that microvesicle shedding plays a central role in the mechanism of IL-1β secretion (MacKenzie et al., 2001).

1.3.2 Thioredoxin

Thioredoxin (TRX) is an ubiquitous intracellular protein (12 kDa) that contains an active site with a redox-active disulfide, which is involved in the redox-system of mammals (Holmgren, 1989) and plants (Balmer et al., 2004). Besides intracellular thioredoxin, two isoforms (10 and 12 kDa) have been detected extracellularly, although they do not contain a signal peptide. The secretory pathway postulated for thioredoxin occurs independently of its redox state (Tanudji et al., 2003) by an unknown mechanism. However, secretion of TRX shows several features which are also described for the unconventional secretion pathway of interleukin-1β (IL-1β). Both pathways are shown to be sensitive to methylamine and are stimulated by brefeldin A (Rubartelli et al., 1992). In contrast to IL-1β, TRX is not inhibited by

reagents that interfere with ABC transporters and is not found to be incorporated into intracellular vesicles (Rubartelli et al., 1995).

1.3.3 Macrophage migration inhibitory factor (MIF)

Macrophage inhibitory factor (MIF) is a pleiotropic cytokine mediating a number of immune and inflammatory conditions. Monocytes, macrophages and lymphocytes constitutively express MIF, which is rapidly released after stimulation with bacterial endotoxins, exotoxins, and cytokines (Calandra, 2003). Its immunological functions include the modulation of host macrophage T and B cell response (Bernhagen et al., 1998).

MIF lacks a classical signal sequence for the translocation into the ER and is found to be mainly localized to the cytosol. Additionally, MIF is not glycosylated and secretion from monocytes is not blocked by inhibitors of the classical pathway, such as BFA or monensin but is stimulated by heat and redox stress (Flieger et al., 2003). The secretion mechanism of MIF remains elusive, however in 2001 it was suggested that MIF is exported by membrane blebbing as it was observed that MIF containing vesicles pinch off the plasma membrane (Eickhoff et al., 2001). In addition, it was reported that MIF export is fully blocked by the ABC transporter inhibitors glyburide and probenecide (Flieger et al., 2003), suggesting a pathway depending on the function of ABC transporters. It has been proposed that the export pathway taken by MIF could be similar to the secretion mechanism that has been suggested for IL-1β, since both cytokines share similar pro-inflammatory activities and involve ABC transporters during their secretion.

1.3.4 *Leishmania* hydrophilic acylated surface protein B (HASPB)

HASPB is a lipoprotein synthesized on free ribosomes in the cytoplasm of *Leishmania* parasites. It gets modified with both myristoyl and palmitoyl residues covalently attached to an SH4 domain present at the N-terminus by which it is anchored within membranes. The palmitoylation occurs at the Golgi membrane, where the palmitoylacyltransferase is localized which is required for the thioester-based acylation of a distinct cysteine residue present in the SH4 domain (Denny et al., 2000).

Only the infectious forms of *Leishmania* parasites express HASPB which is then found to be associated with the outer leaflet of the plasma membrane (Flinn et al., 1994). It is currently unclear how this transport step is mediated; however, there are in principle three options: (1) HASPB might be transported to the plasma membrane associated with the cytoplasmic leaflet of secretory vesicles, (2) HASPB might be targeted first to endosomal structures followed by translocation to the plasma membrane or (3) HASPB transport from the Golgi to the plasma membrane might not rely on transport vesicles (Nickel, 2005). The translocation mechanism of HASPB to the outer leaflet remains elusive, however it was demonstrated that the plasma membrane is the subcellular site of membrane translocation of HASPB (Stegmayer et al., 2005). It also has been reported that HASPB when expressed in mammalian cells can be detected on the cell surface of CHO cells, suggesting a conserved machinery among eukaryotes (Denny et al., 2000).

1.3.5 Viral proteins: HIV Tat, FV Bet and HSV VP22

Viral proteins have been reported to be secreted by nonclassical means. Among them are many factors whose localization-dependent functions are of high biomedical relevance. Such proteins include virus-encoded factors that are critical for the viral replication cycle.

1.3.5.1 HIV Tat

The Human immunodeficiency virus type 1 (HIV-1) encodes an early trans-activator protein (HIV Tat), which is necessary for the replication of the viral genome (Wong-Staal and Haseltine, 1992; Goldstein, 1996). HIV-infected T cells, as well as HIV-transfected cultured cells release Tat into the extracellular space in the absence of cell death, followed by its binding to heparan sulfate proteoglycans (Chang et al., 1997) mediated by a basic region present at position 49-57 of its amino acid structure. This region, also called basic transduction domain, is also thought to mediate the transport over the plasma membrane (Becker-Hapak et al., 2001). The translocation across the plasma membrane is most probably mediated by a non-proteinaceous machinery, because it has been shown for basic transduction domains containing proteins that they are able to cross the lipid bilayer in protein free membranes

(Derossi et al., 1998). Furthermore it has been shown that translocation of these proteins across membranes occurs at 4°C (Thoren et al., 2000). However, the translocation properties of the basic transduction domain have been discussed in a controversial way recently. It was suggested that basic transduction domains do not act to enhance translocation, but instead merely to increase binding to the cell surface, because it was demonstrated that the most dramatic demonstrations of basic transduction domain efficiency have been obtained using fixed cells and/or denatured proteins (Leifert et al., 2002).

1.3.5.2 HSV VP22

Herpes simplex virus type 1 (HSV-1) protein VP22 is a structural protein of 38 kDa size present in the viral tegument. Upon expression in the cytosol it travels along an unknown pathway to the cell periphery (Elliott and O'Hare, 1999). Features of VP22 include intercellular transport, binding to and bundling of microfilaments, thereby inducing cytoskeleton collapse, nuclear translocation during mitosis, and binding to chromatin and the nuclear membrane (Aints et al., 2001).
The secretion of VP22 is an ER/Golgi independent process shown by its insensitivity to brefeldin A. A classical signal sequence was not identified, but mutations in the C-terminal half of the protein prevent its secretion (Elliott and O'Hare, 1997). Interestingly, cytochalasin D, which inhibits actin polymerization, blocks export of VP22 suggesting an unconventional export route depending on the cytoskeleton.
VP22 re-enters surrounding cells upon release from expressing cells (Wybranietz et al., 1999). Once imported into target cells, VP22 is transported into the nucleus during mitosis, binds to the condensing cellular chromatin and remains bound through all stages of mitosis and chromatin decondensation until the G(1) stage of the next cycle (Elliott and O'Hare, 2000). This effect mediated by imported VP22 is discussed in a controversary way, because recently experimental evidence was reported demonstrating nuclear targeting after import to be an artefact (Lundberg and Johansson, 2001).

1.3.5.3 FV Bet

Foamy viruses (FV) are retroviruses inducing persistent infections in their host without causing any apparent disease. Foamy viruses infect most cell lines in culture, but circulating lymphocytes seem to be their major reservoir *in vivo* (Tobaly-Tapiero et al., 2005). The major host of FV are non-human primates, but it has been reported that the virus is transmitted to humans, although with low transmission rate and resulting in non-pathogenic diseases (Heneine et al., 2003).

Foamy viruses express a cytosolic protein of 160 kDa size, termed Bet (Giron et al., 1998), which is capable to spread between cultured cells (Lecellier et al., 2002). The function of foamy FV Bet during the viral replication cycle has yet to be reported, but it seems to play a key role in the establishment and persistence of viral infection.

Since Bet is found outside of expressing cells and a classical secretory signal was not identified, it has been proposed that FV Bet makes use of an ER/Golgi independent export route. This hypothesis is affirmed by the observation that Bet export is insensitive to brefeldin A (Lecellier et al., 2002). However, the mechanism of FV Bet secretion has not yet been elucidated.

1.3.6 Homeodomain-containing transcription factors and HMG chromatin-binding proteins

The transcription factor Engrailed homeoprotein isoform 2 (En2) is mainly localized to the nucleus of neurons. The protein induces the transcription of genes with a homeodomain motif thus playing a decisive role in the establishment of cerebral structures and cell differentiation (Retaux et al., 1999).

However, significant amounts of the protein are also found in the cytoplasm or associated with membrane microdomains enriched in cholesterol and glycosphingoglycolipids. In addition, En2 is associated with caveolae-like vesicles that localize to the cell surface (Joliot et al., 1997). It has access to these vesicles targeted to the cell surface but lacks a signal sequence for secretion (Maizel et al., 2002). It has been suggested, that a short sequence, overlapping with the nuclear import signal of Engrailed 2 is responsible for its non-classical secretion. These results have been taken to mean that retrotranslocation of En2 from the nucleus to the cytoplasm is a prerequisite for nonclassical export of En2 (Maizel et al., 1999).

However, recently it was shown that phosphorylation of a serine-rich domain within Engrailed 2 is required for its unconventional export (Maizel et al., 2002) .

The high mobility group protein B 1 (HMGB1), also localized to the nucleus, does not contain a signal peptide, but nevertheless it has been reported to be secreted from monocytes after stimulation with bacterial lipopolysaccharides (Gardella et al., 2002). Its unconventional secretion is enhanced by raising the intracellular Ca^{2+}-level (Passalacqua et al., 1997).
After stimulation of monocytes, HMBG1 is redistributed from the nucleus to the cytoplasm. Following relocalization, HMBG1 is targeted by an unknown mechanism to an endo-lysosomal compartment, from which it is secreted (Gardella et al., 2002). Since the secretion pathway shows similarities to the mechanism of IL-1β secretion, it is possible that, although the physiological triggers of secretion are different, both proteins are externalized in a similar way.

1.3.7 Galectins

The members of the galectin family are β-galactoside-binding lectins of the extracellular matrix. A common feature of all galectins is the highly conserved carbohydrate recognition domain (CRD (Leffler, 2001). Most galectins possess two CRDs, enabling multivalent binding properties.
Galectins act intra- and extracellularly (Harrison, 1991; Liu et al., 2002) mediating many biological activities, such as cell proliferation, apoptosis, inflammation and cell differentiation (Perillo et al., 1995; Perillo et al., 1998; Pace et al., 1999; Liu, 2000). Inside the cell, galectins are mainly found in the cytoplasm, but were also shown to be localized inside the nucleus (Wang et al., 1991). Upon secretion, galectins are found to be present as components of the extracellular matrix (Cooper and Barondes, 1990), or they interact with the cell surface by β-galactose-terminated oligosaccharide side chains of glycoproteins and galactose-containing glycolipids, such as the ganglioside GM_1 (Mehul et al., 1995; Kopitz et al., 1998).

1.3.7.1 Galectin-1

Galectin-1 (Gal-1) is a homodimeric low molecular weight protein of 14 kDa size. It is synthesized on free ribosomes (Wilson et al., 1989) and mainly found in the cytoplasm of most galectin-expressing cells (Briles et al., 1979). It lacks intramolecular disulfide bonds but contains free sulfhydryls and is unstable and inactive in the absence of reducing agents (Hirabayashi and Kasai, 1991; Tracey et al., 1992).

Additionally, galectin-1 lacks a signal peptide, which would target the protein to the classical secretory pathway (Couraud et al., 1989). Nevertheless it is found to be secreted from mammalian cells in a brefeldin A-resistant manner (Sato et al., 1993). Galectin-1 binds to counter receptors, such as laminin (Zhou and Cummings, 1990), fibronectin (Ozeki et al., 1995) and cell type specific receptors as T cell CD43 and CD45 (Pace et al., 1999) as well as to the tumour specific cell surface antigen CA125 (Seelenmeyer et al., 2003). Unlike interleukin 1β, galectin-1 is not packaged into intracellular vesicles prior to export. In contrast, galectin-1 was shown to accumulate directly below the plasma membrane, followed by an export mechanism that involves the formation of membrane-bound vesicles that pinch off the plasma membrane in order to be released into the extracellular space. This process has been termed “membrane blebbing” (Hughes, 1999). However, based on various experimental systems, evidence is accumulating that galectin-1 export is mediated by direct translocation from the cytoplasm across the plasma membrane into the extracellular space (Schäfer et al., 2004). So far, it has been assumed that galectins do not interact with their counter receptors until they have been released into the extracellular space. However, it has been shown that these interactions are an integral part of the export mechanism itself, because galectin counter receptors (i.e. β-galactoside-containing cell surface glycolipids and/or glycoproteins) were identified to be essential components of the overall process of gal-1 secretion. It was shown that both Gal-1 mutants, deficient in β-galactoside binding and mutant cell lines deficient in the biogenesis of galectin counter receptors, are defective with regard to gal-1 secretion (Seelenmeyer et al., 2005).

1.3.7.2 Galectin-3

Galectin-3 is a high molecular weight β-galactoside-binding protein (30 kDa) and is synthesized on free ribosomes. The protein contains a large flexible N-terminal domain that appears to be involved in oligomerization.
As an unconventionally secreted protein, galectin-3 does not contain a signal sequence and its secretion is not blocked by brefeldin A. Fetuin, a serum protein, which is abundant in fetal serum is able to induce the rapid release of galectin-3 from breast carcinoma cells (Zhu and Ochieng, 2001). Galectin-3 was also found to be secreted in vesicles, which pinch off the plasma membrane. This process of "membrane blebbing" was also observed for the secretion of galectin-1.
Once secreted, galectin-3 is found bound to receptors present on the cell surface, such as laminin (Hughes, 1997), AGE (advanced end product) receptors that mediate multiple biological activities (Thornalley, 1998) and various cell surface glycoproteins.

1.3.8 Fibroblast growth factors

The fibroblast growth factors (FGFs) belong to a family of proteins currently thought to consist of at least 23 different members. In vertebrates, the members of the mammalian FGF family range in molecular mass from 17 to 34 kDa (*Drosophila* FGF is 84 kDa) and share 13-71% amino acid identity (Ornitz and Itoh, 2001). Most of the FGF family members contain 6 identical and 28 highly conserved amino acids from which ten are thought to mediate the interaction with FGF receptors (Plotnikov et al., 2000). The FGFR tyrosine kinase receptors contain two or three immunoglobulin-like domains and one heparin-binding domain (McKeehan et al., 1998). Alternative mRNA splicing, regulated in a tissue-specific manner, of the FGFR gene specifies the sequence of the carboxy terminal half of immunoglobulin-domain II, resulting in two different isoforms (Miki et al., 1992) and affecting ligand-receptor specificity (Ortega et al., 1998).

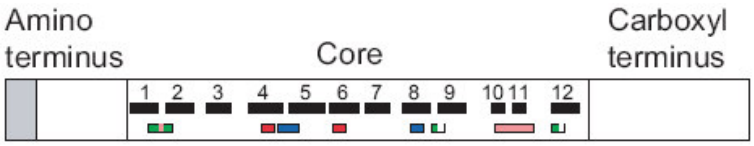

Figure 1.3: Structural features of the FGF polypeptide. The amino terminus of some FGFs contains a signal sequence (shaded). All FGFs have a core region that contains conserved amino-acid residues and conserved structural motifs. The location of β-strands within the core region are numbered and shown as black boxes. The heparin-binding region (pink) includes residues in the loop between β-strands 1 and 2 and the β-strands 10 and 11. Residues that contact the FGFR are shown in green, blue and red. Picture taken from (Ornitz and Itoh, 2001).

As depicted in figure 1.3, structural studies on FGF1 and FGF2 identified 12 antiparallel β-strands in the conserved core region of these proteins (Eriksson et al., 1991). They have a β–trefoil structure that contains four-stranded β sheets arranged in a triangular array (Faham et al., 1996). Two β-strands (strands 10 and 11) contain several basic amino acid residues that form the primary heparin-binding site of FGF2. Regions thought to be involved in receptor binding are distinct from those regions that bind to heparin.

Most FGFs (FGFs 3-8, 10, 15, 17-19 and 21-23) have amino-terminal signal peptides and are secreted from cells via the ER/Golgi-dependent route. FGFs 9, 16 and 20 lack an obvious amino-terminal signal peptide but are also nevertheless secreted via the classical secretory pathway (Miyake et al., 1998; Miyakawa et al., 1999). Therefore, it can be concluded that the lack of a signal peptide does not conclusively lead to a secretion in an unconventional manner. A subset of FGFs (FGF 11-14) lack signal sequences and are thought to remain intracellular. It is not known whether these FGFs interact with known FGF receptors or function in a receptor-independent manner within the cell (Ornitz and Itoh, 2001).

An important characteristic of FGFs is their interaction with heparin, heparin sulfate (HS) or heparan sulfate proteoglycans (HSPG) (Gleizes et al., 1995). These interactions stabilize FGFs with regard to thermal denaturation and proteolysis and may limit their diffusion and release into the interstitial space (Moscatelli, 1987; Flaumenhaft et al., 1990). It was suggested that FGFs must saturate nearby HS-binding sites before exerting an effect on other tissues or must be mobilized by heparin/HS-degrading enzymes. The interaction between FGFs and HS results in the formation of dimers and higher ordered oligomers (Mach et al., 1993; Herr et al., 1997). It has been shown that a ternary complex of HSPG, FGF and FGFR is required for the biological activity of FGF2 (Pellegrini et al., 2000).

FGF1 and FGF2 are exported in an unconventional manner independently from the ER-Golgi pathway (Mignatti et al., 1992; Engling et al., 2002; Prudovsky et al., 2003).

1.3.8.1 Fibroblast growth factor 1

The primary structure of FGF1, also known as acidic FGF, contains a nuclear localization signal (NLS) which plays an important role for its mitogenic activity (Imamura et al., 1990; Imamura et al., 1992). When extracellular FGF1 binds to cell-surface receptors (FGFR 1-4) or to heparan sulfates, it is internalized in association with its receptor via an uncharacterized pathway. It has been reported that externally added FGF1 was localized to sorting/early endosomes after 15 min at 37°C (Haugsten et al., 2005). The endosomal compartment acts as a sorting station for FGF1 bound to its receptor. Depending on the association with its different receptors, FGF1 is sorted to the recycling compartment (FGFR 4) or sorted for degradation into lysosomes (FGFR 1-3) (Haugsten et al., 2005). Internalized FGF1 which is not destined for degradation is able to cross cellular membranes (Wiedlocha and Sorensen, 2004), is found in the cytosol and is then shown to translocate to the nucleus in a cell-cycle dependent manner (Zhan et al., 1992). Both the activation of FGF receptors and the internalization of FGF1 are necessary to induce proliferation (Wiedlocha et al., 1994). In addition to internalized FGF1, endogenously expressed FGF1 is also found predominantly in the cytosol, which is consistent with the absence of a signal sequence in its primary structure (Shi et al., 1997). However, export of intracellular FGF1 is induced upon heat shock (Jackson et al., 1992; Tarantini et al., 1998) or serum starvation (Shin et al., 1996) and occurs in presence of brefeldin A (Jackson et al., 1992).

The formation of a Cys 30-mediated FGF1 homodimer is a prerequisite for its secretion (Jackson et al., 1995; Tarantini et al., 1995). Dimerized FGF1 is associated with the extravesicular p40 fragment of p65 Syt1 - an integral transmembrane protein participating in secretory vesicle docking (LaVallee et al., 1998) - and S100A13, a member of the family of intracellular calcium-binding S100 proteins (Mouta Carreira et al., 1998; Landriscina et al., 2001b). The formation of this multiprotein release complex (FGF1, S100A13, and p40) requires the oxidative function of copper (Landriscina et al., 2001a). It was suggested that FGF1 is transported to the inner surface of the plasma membrane where the multiprotein complex is assembled and

exported (Prudovsky et al., 2002). FGF1 redistribution is inhibited by amlexanox, which specifically binds to S100A13 (Shishibori et al., 1999) and attenuates actin assembly (Landriscina et al., 2000), suggesting that actin stress fibers may be used to transport FGF1 to the inner leaflet of the plasma membrane.

1.3.8.2 Fibroblast growth factor 2

Five isoforms of FGF2, with molecular weights of 18, 22, 22.5, 24 and 34 kDa, have been identified, all derived from a single messenger RNA. The translation of the 18 kDa form is initiated from an AUG codon, whereas the high molecular weight isoforms are translated using alternative upstream CUG start codons (Florkiewicz and Sommer, 1989; Prats et al., 1989). The 18 kDa FGF2 is primarily a cytosolic protein and lacks a classical hydrophobic signal sequence. It is exported out of the cells in an unconventional manner and stored within the extracellular matrix, whereas the high molecular weight isoforms are predominantly localized to the nucleus (Renko et al., 1990).

Structural characteristics

FGF2 is very well conserved during evolution. For bovine and human FGF2, only two amino acids are different, resulting in an overall amino acid homology of 98.7% (Abraham et al., 1986). Comparison of the primary structure of FGF2 and FGF1 has shown that 55% of their amino acids are identical. A weak homology of 25% exists in the primary structure between FGF2 and Interleukin-1β (Gimenez-Gallego et al., 1985). However, their 3-dimensional structures share significant similarities (Ago et al., 1991; Eriksson et al., 1991).

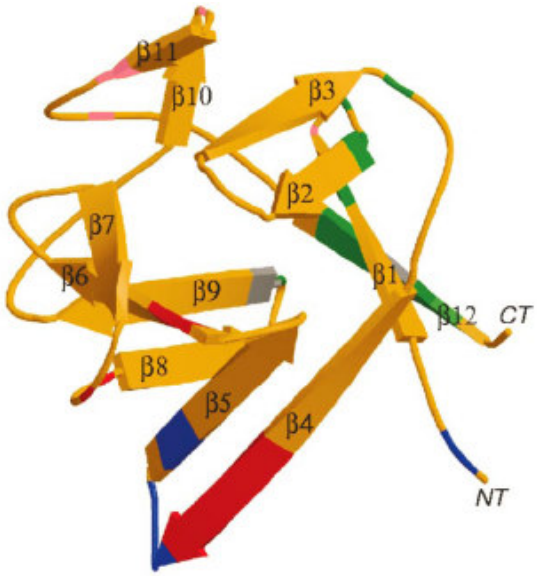

Figure 1.4: Three-dimensional structure of FGF2. A ribbon diagram shows β-strands (labelled from 1 to 12) and regions in contact with FGFR and heparin are labelled as in figure 1.3. Picture taken from Ornitz and Itoh, 2001.

As depicted in figure 1.4, the 12 β-sheets have a β–trefoil structure that contains four-stranded β-sheets arranged in a triangular array (Faham et al., 1996). 10 out of the 12 β-sheets meet the criteria of Kabsch and Sander for β-sheet strands (Kabsch and Sander, 1983). Additionaly, two segments exist, comprising residues 117-119 and 124-129 that do not meet these criteria for β-sheet strands, but, nevertheless, form the 10th and 11th of the 12 β-strands that comprise the overall framework of the FGF2 structure (Eriksson et al., 1991). Three motifs are present in the structure of FGF2 mediating high-affinity binding to immunoglobuline-like domains (Ig-domain) of the receptor (Lee et al., 1989). The motifs are present in different β-sheets, and are widely spread over the protein. Residues contacting Ig-domain 2 of the receptor (figure 1.4, green) are present in β11 and 12, close to the C-terminus, those contacting Ig-domain 3 (blue) link β4 and 5 and are also part of β5. Additionally amino acids present in β4 and 6 contact the alternatively spliced region of the receptors Ig-domain (red). Importantly, two β-strands (strands 10 and 11) contain several basic amino-acid residues that form the primary heparin-binding site in FGF2 (pink). A second heparin binding site is located in the linking region between sheets β1 and β2 (Faham et al., 1996; Plotnikov et al., 2000).

Binding to heparin and heparan sulfate proteoglycans

An intact three-dimensional structure is required for binding of FGF2 to heparin (Seddon et al., 1991). From the crystal structure of FGF2, two pairs of basic residues, K128 and K138, and R129 and K134, respectively, were found to form binding sites for two sulfate molecules (Li et al., 1994). It was shown that heparin binding is also mediated by N-terminal amino acids located at position 20-30 (Baird et al., 1988), suggesting that binding of heparin to the growth factor is not mediated by a single heparin binding site, but rather by cumulative effects of heparin binding sequences.
Binding of FGF2 *in vivo* is mediated by high affinity receptors and heparan sulfate proteoglycans present on the cell surface of mammalian cells. The latter consist of proteoglycan core protein (e.g. perlecan, syndecan) and heparan sulfates (HS). Heparan sulfates exist in a broad structural variety, up to date 23 different disaccharides have been identified to be present in heparin (Esko and Selleck, 2002). To mediate biological activity, a ternary complex composed of FGF2, heparin and FGF receptor must be assembled to activate signalling by the tyrosine kinase of FGFR (depicted in figure 1.5).

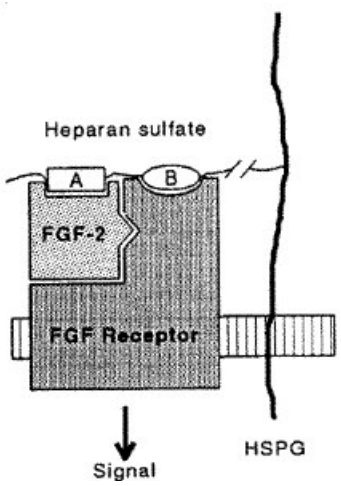

Figure 1.5: Receptor signalling requires the formation of a trimeric complex as indicated, where the polysaccharide binds both to the growth factor, through Site A, and to the receptor, through Site B. Picture taken from (Guimond et al., 1993).

The addition of heparin, which is too short to span both binding regions, may block the activity induced by full-size heparin (or heparan sulfate) due to competitive binding to the growth factor (Ishihara et al., 1993).

Biological functions of FGF2

FGF2 is a pleiotropic growth factor mediating many different biological activities. Binding of FGF2 to HSPGs and its receptor present on the plasma membrane activates signalling cascades inside the target cells.

FGF2 induces cell proliferation or differentiation in a variety of cell types of mesodermal and neuroectodermal origin (Gospodarowicz, 1991). It was also shown to induce chemotaxis and protease production in cultured endothelial cells (Presta et al., 1986).

The most important biological activity of FGF2 is its role as a mediator of angiogenesis by the stimulation of VEGF (vascular endothelian growth factor) receptors and direct stimulation of endothelial cells. FGF2 was one of the first identified angiogenic growth factors (Moscatelli et al., 1986; Shin et al., 1996).

In vivo, FGF2 is thought to play a role in the growth and neovascularization of solid tumours. Various tumour cell lines express FGF2 *in vitro* (Moscatelli et al., 1986; Okumura et al., 1989; Nakamoto et al., 1992), as shown by *in situ* hybridization and immunolocalization experiments, in which FGF2 mRNA and protein was found to be present in neoplastic cells, endothelial cells, and infiltrating cells within human tumours of different origin (Schulze-Osthoff et al., 1990; Zanetta, 1998; Tanudji et al., 2002). Additionally, neovascularization and growth of human melanomas were inhibited by expression of antisense cDNAs for FGF2 and FGFR-1 (Wang and Becker, 1997).

FGF2 is released from producing cells in an unconventional manner (Mignatti et al., 1992; Florkiewicz et al., 1995) and accumulates in the ECM, where it is mobilized by ECM-degrading enzymes (Ribatti et al., 1999).

Unconventional secretion of FGF2

About 15 years ago, it was believed that FGF2 is primarily released from injured or dead cells thereby mediating its biological activities. In 1990 it was reported that the structurally related cytokine Interleukin-1β is secreted, although lacking a signal peptide, by a pathway independent from the classical, Golgi-dependent secretion (Rubartelli et al., 1990). In 1991, Mignatti and Rifkin were the first to report that FGF2,

despite lacking a signal sequence, might be exported by a controlled mechanism, because FGF2 was shown to be released from a single, uninjured cell, mediating its biological functions in an autocrine manner (Mignatti and Rifkin, 1991). In 1995, Florkiewicz et al. demonstrated that FGF2 is selectively and quantitatively exported from transiently transfected Cos-1 cells. FGF2 export was found not to be blocked by brefeldin A, a known inhibitor of the classical secretory pathway. Additionally, export of FGF2 was shown to be ATP-dependent since depletion of ATP blocked the release of the growth factor. As shown by pulse label experiments, FGF2 required two hours to appear in the extracellular space (Florkiewicz et al., 1995). Three years later, Florkiewicz et al. could show that export of FGF2 is specifically blocked by cardenolides such as ouabain, a known inhibitor of the Na^+/K^+ ATPase. FGF2 was copurified with the α-subunit of the plasma membrane resident Na^+/K^+ ATPase, suggesting a direct interaction of the growth factor with the transmembrane protein (Florkiewicz et al., 1998). This observation was underlined by the finding that an ouabain resistant mutant of the rodent α-1 subunit of the Na^+/K^+ ATPase was capable of rescuing ouabain-inhibitable FGF2 export (Dahl et al., 2000). In 2000, the existence of an unconventional pathway for the secretion of FGF2 was further substantiated. By performing biochemical studies like biotinylation of cell surface proteins and purification of those using streptavidin beads, it was demonstrated that FGF2 is translocated to the outer surface of the plasma membrane and is retained there by binding to HSPGs. It was also suggested that release of FGF2 into the medium of expressing cells is uncoupled from the transport process itself. To be able to perform biological activities as a growth factor, cell surface FGF2 must then be released from sequestration on the cell surface into the extracellular matrix or biological fluids (Trudel et al., 2000). In 2002, another model for the secretion of FGF2 was proposed, as it was shown that FGF2 is released from endothelial cells after stimulation by shear stress and under the tight control of a specific integrin (Gloe et al., 2002). The observation that shear stress has been found to promote microvesicle shedding (Martinez et al., 2005) is consitent to yet another model for FGF2 secretion which was proposed one year later. In 2003, Taverna et al. showed, that three isoforms of FGF2 (18, 22 and 24 kDa) were present in vesicles which were shed from the plasma membrane after stimulation by serum addition to serum-starved cells (Taverna et al., 2003). However, this model is discussed in a controversial way, since FGF2-containing vesicles found in cell culture supernatants

could be affinity-purified using immobilized annexin V, a well known binding protein of phosphatidylserine. Thus, annexin V affinity-purified vesicles are likely to be derived from apoptotic cells as translocation of phosphatidylserine to the outer leaflet of the plasma membrane is a hallmark of programmed cell death. Moreover, readdition of medium to cells serum-starved for longer periods of time is a procedure which is commonly used to artificially induce apoptosis. Although it appears to be unlikely that FGF2 secretion involves shedding of plasma membrane vesicles, it can not be excluded (Nickel, 2005).

In 2004, the translocation process of FGF2 at the plasma membrane was characterized by reconstitution of the translocation of FGF2 using inside-out vesicles obtained from the plasma membrane. The translocation was observed to be temperature- and incubation time-dependent. In contrast, right side-out vesicles were not shown to translocate FGF2-GFP into the lumen of the vesicle. Moreover, galectin-1 was found to traverse the membrane of inside-out vesicles, whereas the unconventional secretory protein MIF and the classical secretory protein FGF4 were not found to be translocated. Additionally, removal of vesicle-associated proteins by high salt conditions or protease treatment resulted in a loss of FGF2 translocation across the membrane, indicating that proteins present on the extracellular site of the plasma membrane (e.g. heparan sulfate proteoglycans) are involved in the translocation process. These data, obtained by Tobias Schäfer from our working group suggest that FGF2 translocation is mediated by a plasma membrane resident protein transporter (Schäfer et al., 2004).

1.4 Aim of the present thesis

The molecular machinery involved in unconventional secretion of fibroblast growth factor 2 is poorly understood. Therefore, in the first part of this thesis, a novel experimental system was implemented that will greatly facilitate studies on the molecular machinery of FGF2 secretion. A key aspect was to reconstitute FGF2 secretion in living cells based on a read-out method that provides a precise and quantitative analysis of this process. A considerable advantage of the FGF2-GFP-based system is that total protein expression (GFP-derived fluorescence) and secreted FGF2-GFP (APC-derived cell surface staining) can be measured simultaneously. Therefore, a phenotype determined by cell surface staining can be

corrected by normalization based on the degree of total FGF2-GFP expression. Moreover, by using FGF receptor-deficient CHO cells, secondary effects based on FGF2 induced signal transduction can be avoided. This robust and efficient FACS-based assay was then used in our group to elucidate unconventional secretion of FGF2, HASPB and galectin-1. Another obvious application is a systematic high throughput screening for inhibitors of FGF2 secretion and the subsequent functional identification of their cellular targets. Given the biological function of FGF2 as a direct stimulator of tumour angiogenesis, inhibitors of FGF2 secretion might have strong biomedical implications as potential lead compounds for the development of anti-angiogenic drugs.

The second part of this thesis deals with the question of how FGF2 is recognized by its transport machinery. A targeting motif, directing the protein to its interaction partners of the membrane translocation apparatus has so far not been reported. Therefore, a mutational analysis was conducted in order to screen for amino acids which might play a major role in the overall transport process. The FACS-based assay, established in the first part of this thesis, and other assays were used as a read-out systems to elucidate amino acids mediating heparin binding and influence export of FGF2. By performing the mutational analysis, it was not possible to find distinct amino acids serving as a targeting motif for the secretion of FGF2. Additionally, single amino acid exchanges and truncations of the N-terminus did not result in a knock-out of heparin-binding capabilities of FGF2. However, C-terminal truncations of FGF2 demonstrated a loss of binding ability to heparan sulfate proteoglycans and heparin, resulting in FGF2-GFP secretion deficiency. Therefore, it can be suggested that binding of FGF2 to its low affinity receptors present on the extracellular site of the plasma membrane is a prerequisite for the translocation of FGF2 across the lipid bilayer, thereby providing a mechanism for quality control, since only correctly folded and biological active forms of the growth factor are secreted from mammalian cells.

2 Material and Methods

2.1 Material

2.1.1 Chemicals

Chemicals	Manufacturers
Agar	Beckton Dickinson, Le Pont de Claix, France
Agarose electrophoresis grade	Invitrogen Ltd., Paisley, UK
αMEM	Biochrom KG, Berlin
Ampicillin sodium salt	Gerbu Biotechnik GmbH, Gaiberg
APS (Ammonium peroxo disulfate)	Carl Roth GmbH, Karlsruhe
β-Mercaptoethanol	Merck , Darmstadt
Bromphenol Blue Na-salt	Serva Electrophoresis GmbH, Heidelberg
BSA (Bovine serum albumine, Albumin fraction V)	Carl Roth GmbH, Karlsruhe
Calcium chloride dihydrate	Applichem, Darmstadt
Cell dissociation buffer (CDB)	Invitrogen, Paisley, UK
Chloroquine	Sigma-Aldrich Chemie GmbH, Steinheim
CL-4B Sepharose (Beads)	Amersham Biosciences Pharmacia, , Sweden
Clear Nail Protector	Wet'n Wild USA, North Arlington, USA
Complete Mini (Protease Inhibitor Cocktail Tablets)	Roche Diagnostics, Mannheim
Deoxycholic acid sodium salt	Sigma-Aldrich Chemie GmbH, Steinheim
DMEM	Biochrom KG, Berlin
DMSO (Dimethyl sulfoxide)	J.T. Baker, Deventer, USA
dNTP-Mix	Peqlab, Erlangen
Doxicycline	Clontech, Palo Alto, USA
ECL Western Blotting Detection Reagent	Amersham Biosciences Pharmacia, Sweden
EDTA (Ethylene diamine tetraacetic acid)	Merck, Darmstadt
Ethanol pro analysis	Riedel-de Haën, Seelze
FCS (Fetal Calf Serum)	PAA Laboratories GmbH, Linz, Austria
Fluoromount G	Southern Biotechnologies Inc USA
Glacial acidic acid	Carl Roth GmbH, Karlsruhe
Glycerine	Carl Roth GmbH, Karlsruhe
Glycine	Applichem, Darmstadt
Isopropanol	Merck , Darmstadt
L-Glutamine	Biochrom AG, Berlin

Magnesium chloride hexahydrate	Applichem, Darmstadt
Mangan chloride	Merck, Darmstadt
Methanol pro analysis	Merck , Darmstadt
Milk Powder	Carl Roth GmbH, Karlsruhe
Nonidet P40 (NP-40)	Roche, Mannheim
Paraformaldehyde	Electron Microscope Sciences, Hatfield, UK
Penicillin/Streptomycin for cell culture	Biochrom AG, Berlin
Ponceau S	Serva Electrophoresis GmbH, Heidelberg
Potassium dihydrogen carbonate	Carl Roth GmbH, Karlsruhe
Potassium hydroxide	J.T.Baker, Deventer, USA
Protein A CL-4B-Sepharose(Beads)	Amersham Biosciences Pharmacia, Sweden
PVDF Membrane Immobilon P Blotting	Millipore Corporation, Bedford
PVDF Membrane Immobilon XL	Millipore Corporation, Bedford
Rotiphorese Gel 30 (37.5:1)	Carl Roth GmbH, Karlsruhe
Sodium chloride	J.T. Baker, Deventer, USA
Sodium dodecyl sulfate	Serva Electrophoreis GmbH, Heidelberg
Sodium hydrogen carbonate	J.T. Baker, Deventer, USA
Sodium hydroxide	J.T. Baker, Deventer, USA
Temed (*N*,*N*,*N*',*N*'-tetramethylethylenediamine)	Bio-Rad Laboratories GmbH, München
Tris	Carl Roth GmbH, Karlsruhe
Trition X-100	Roche, Mannheim
Trypsin / EDTA for cell culture	Biochrom KG, Berlin
Trypsine (Protease Protection)	Sigma-Aldrich Chemie GmbH, Steinheim
Tryptone	Beckton Dickinson, Le Pont de Claix
Tween 20 (Polyoxyethylenesorbitan monolaurate)	Carl Roth GmbH, Karlsruhe
UltraLink immobilized streptavidin (Beads)	Pierce, Perbio Sciences, Bonn
Whatman MM	Whatman AG, Würzburg
Xylencyanol FF	Serva Electrophoresis GmbH, Heidelberg
Yeast Extract	Beckton Dickinson, Le Pont de Claix

2.1.2 Enzymes

Restriction enzymes were purchased from New Englang Biolabs. The restriction enzymes listed below were used for cloning of the different cDNA constructs.

Age I
Sph I
BamH I
Not I
Apa I

2.1.3 Antibodies

For flow cytometry analysis, immunoprecipitation experiments and Western blot detection of FGF2-GFP fusion proteins, affinity-purified polyclonal rabbit anti-GFP antibodies were used (Engling et al., 2002). Secondary antibodies used for flow cytometry (Allophycocyanin (APC)-conjugated or Phycoerythrin (PE)-conjugated goat anti-rabbit antibodies) were purchase from Molecular Probes, HRP-coupled mouse anti-rabbit secondary antibodies used for Western blot detection of immunoprecipitates using ECL were from Sigma (clone RG-16). Alexa 680-coupled goat anti-rabbit antibodies used for quantitative analysis of antigens processed by Western blotting employing the LI-COR Odyssey system were purchased from Molecular Probes.

2.1.4 Equipment

Technical devices	manufacturers
Bacterial Incubator Infors HT ITE	Infors AG, Einsbach
Bacterial Shaker Centromat R	Braun, Melsungen
FACSAria	Becton Dickinson, Heidelberg
FACSVantage	Becton Dickinson, Heidelberg
FASCCalibur	Becton Dickinson, Heidelberg
Gel Doc 2000	Bio-Rad, München

Microscope Axiovert 40 C	Zeiss, Göttingen
Microscope LSM 510 Meta Confocal	Zeiss, Göttingen
Mini-PROTEAN 3 Electrophoresis System	Bio-Rad, München
Nanodrop ND-1000 Spectrophotometer	Peqlab, Erlangen
Odyssey Infrared Imaging System	LI-COR Biosciences, Bad Homburg
PCR Primus Advanced 25 and 96	Peqlab, Erlangen
Sonifier Cell Disruptor B 30	Heinemann, Schwäbisch Gmünd
Sonorex Super RK 103 h	Bandelin, Berlin

2.1.5 Plasmids and Primers

pVPack Eco	BD Bioscience, Clontech
pVPack GP	BD Bioscience, Clontech
pRevTRE2	BD Bioscience, Clontech, Mountain View
pBI-rtTA2M2/CD2	kindly provided by Dr. Blanche Schwappach
pGEM-T	Promega

Primers for Random Mutagenesis

In the following table, the primer specific sequence and its melting temperature are listed in column “Sequence” and “Tm”, respectively.

Primer	Sequence	T_m (°C)
FGF2-MUT-FOR	CGGGATCCCGCATCGATCGCCACCATGG	78,4°
FGF2-MUT-REV	CCTAGGTTTTGTCCTGGACCG	55,0°

Primers for Point Mutations

In the following table, primer specific sequences are listed. The triplet encoding the original amino acid is listed in column “Codon” whereas the triplet encoding the amino acid for mutation is marked with bold letters in column “Sequence”.

Additionally, the melting temperature of the specific primer is indicated in column "T_m" as well as the length of the primer in nucleotides in column "N".

Primer	Sequence	T_m (°C)	N	Codon
A-3-V-For	ATCGCCACCATG**GTA**GCCGGGAGCATC	80,1	27	GCC
A-3-V-Rev	GATGCTCCCGGC**TAC**CATGGTGGCGAT	80,1	27	
G-4-A-For	GCCACCATGGCA**GTC**GGGAGCATCACC	78,4	25	GGG
G-4-A-Rev	GGTGATGCTCCC**GAC**TGCCATGGTGGC	78,4	25	
S-5-A-For	CATGGCAGCC**GCG**AGCATCACCACG	79,5	27	AGC
S-5-A-Rev	CGTGGTGATGCT**CGC**GGCTGCCATG	79,5	27	
I-6-A-For	TGGCAGCCGGG**GCC**ATCACCACGCTGC	79,3	25	ATC
I-6-A-For	GCAGCGTGGTGAT**GGC**CCCGGCTGCCA	79,3	25	
T-7-A-For	CAGCCGGGAGC**GCC**ACCACGCTGCC	79,9	23	ACC
T-7-A-Rev	GGCAGCGTGGT**GGC**GCTCCCGGCTG	79,9	23	
T-7-E-For	CGGGAGCATC**GCC**ACGCTGCCCG	79,1	31	ACC
T-7-E-Rev	CGGGCAGCGT**GGC**GATGCTCCCG	79,1	31	
T-7-D-For	CAGCCGGGAGCATC**GAG**ACGCTGCCCGCCTT	80,5	33	ACC
T-7-D-Rev	AAGGCGGGCAGCGT**CTC**GATGCTCCCGGCTG	80,5	33	
T-8-M-For	GGGAGCATCACC**ATG**CTGCCCGCCT	78,4	25	ACG
T-8-M-Rev	AGGCGGGCAG**CAT**GGTGATGCTCCC	78,4	25	
P-13-H-For	GCCCGCCTTG**CAC**GAGGATGGCG	78,1	23	CCC
P-13-H-Rev	CGCCATCCTC**GTG**CAAGGCGGGC	78,1	23	
E-14-D-For	CGCCTTGCCC**GAC**GATGGCGGCA	78,1	23	GAG
E-14-D-Rev	TGCCGCCATC**GTC**GGGCAAGGCG	78,1	23	
F-21-I-For	CAGCGGCGCC**ATC**CCGCCCGGCC	83,5	23	TTC
F-21-I-Rev	GGCCGGGCGG**GAT**GGCGCCGCTG	83,5	23	
P-23-S-For	CGCCTTCCCG**TCC**GGCCACTTCAAG	78,4	25	CCC
P-23-S-Rev	CTTGAAGTGGCC**GGA**CGGGAAGGCG	78,4	25	
F-26-A-For	CGCCCGGCCAC**GCC**AAGGACCCCAAGC	81,0	27	TTC
F-26-A-Rev	GCTTGGGGTCCTT**GGC**GTGGCCGGGCG	81,0	27	
K-30-E-For	TTCAAGGACCCC**GAG**CGGCTGTACTGC	78,6	27	AAG
K-30-E-Rev	GCAGTACAGCCG**CTC**GGGGTCCTTGAA	78,6	27	
Y-33-A-For	CCCAAGCGGCTG**GCC**TGCAAAAACGGGGG	79,6	29	TAC
Y-33-A-Rev	CCCCCGTTTTTGCA**GGC**CAGCCGCTTGGG	79,6	29	
F-39-L-For	CAAAAACGGGGGC**CTC**TTCCTGCGCATCC	80,2	29	TTC
F-39-L-Rev	GGATGCGCAGGAA**GAG**GCCCCCGTTTTTG	80,2	29	
F-39-A-For	CAAAAACGGGGGC**GCC**TTCCTGCGCATCC	78,2	29	TTC
F-39-A-Rev	GGATGCGCAGGAA**GGC**GCCCCCGTTTTTG	78,2	29	

Primer	Sequence	T_m (°C)	N	Codon
F-40-L-For	CGGGGGCTTC**CTC**CTGCGCATCC	78,1	23	TTC
F-40-L-Rev	GGATGCGCAG**GAG**GAAGCCCCCG	78,1	23	
R-42-H-For	GGCTTCTTCCTG**CAC**ATCCACCCCGAC	78,6	27	CGC
R-42-H-Rev	GTCGGGGTGGAT**GTG**CAGGAAGAAGCC	78,6	27	
V-52-A-For	GAGTTGACGGG**GCC**CGGGAGAAGAG	78,4	25	GTC
V-52-A-Rev	CTCTTCTCCCG**GGC**CCCGTCAACTC	78,4	25	
R-53-A-For	AGTTGACGGGGTC**GCG**GAGAAGAGCGACC	78,2	29	CGG
R-53-A-Rev	GGTCGCTCTTCTC**CGC**GACCCCGTCAACT	78,2	29	
K-55-T-For	GGTCCGGGAG**ACG**AGCGACCCTC	78,1	23	AAG
K-55-T-Rev	GAGGGTCGCT**CGT**CTCCCGGACC	78,1	23	
K-55-R-For	GGTCCGGGAG**AGG**AGCGACCCTC	78,1	23	AAG
K-55-R-Rev	GAGGGTCGCT**CCT**CTCCCGGACC	78,1	23	
H-59-P-For	AGAAGAGCGACCCT**CCC**ATCAAGCTACAACTTC	79,1	33	CAC
H-59-P-Rev	GAAGTTGTAGCTTGAT**GGG**AGGGTCGCTCTTCT	79,1	33	
K-61-E-For	GCGACCCTCACATC**GAG**CTACAACTTCAAGCAG	80,4	33	AAG
K-61-E-Rev	CTGCTTGAAGTTGTAG**CTC**GATGTGAGGGTCGC	80,4	33	
L-64-P-For	TCACATCAAGCTACAA**CCT**CAAGCAGAAGAGAGAG	78,1	35	CTT
L-64-P-Rev	CTCTCTCTTCTGCTTG**AGG**TTGTAGCTTGATGTGA	78,1	35	
Q-65-A-For	CTCACATCAAGCTACAACTT**GCA**GCAGAAGAGAGAGGAGTT	79,2	41	CAA
Q-65-A-Rev	AACTCCTCTCTCTTCTGC**TGC**AAGTTGTAGCTTGATGTGAG	79,2	41	
E-67-V-For	GCTACAACTTCAAGCA**GTA**GAGAGAGGAGTTGTGT	78,1	35	GAG
E-67-V-Rev	ACACAACTCCTCTCTC**TAC**TGCTTGAAGTTGTAGC	78,1	35	
E-68-A-For	TACAACTTCAAGCAGAA**GCG**AGAGGAGTTGTGTCT	78,1	35	GAG
E-68-A-Rev	AGACACAACTCCTCT**CGC**TTCTGCTTGAAGTTGTA	78,1	35	
E-68-G-For	TACAACTTCAAGCAGAA**GGG**AGAGGAGTTGTGTCT	78,1	35	GAG
E-68-G-Rev	AGACACAACTCCTCT**CCC**TTCTGCTTGAAGTTGTA	78,1	35	
R-69-A-For	ACAACTTCAAGCAGAAGAG**GCA**GGAGTTGTGTCTATCAAAG	78,2	41	AGA
R-69-A-Rev	CTTTGATAGACACAACTCC**TGC**CTCTTCTGCTTGAAGTTGT	78,2	41	
V-72-A-For	AGAAGAGAGAGGAGTT**GCG**TCTATCAAAGGAGTGT	78,1	35	GTG
V-72-A-Rev	ACACTCCTTTGATAGA**CGC**AACTCCTCTCTCTTCT	78,1	35	
I-74-T-For	GAGAGGAGTTGTGTCT**ACC**AAAGGAGTGTGTGCTA	79,3	37	ATC
I-74-T-Rev	TAGCACACACTCCTTT**GGT**AGACACAACTCCTCTC	79,3	37	
K-75-I-For	AGGAGTTGTGTCTATC**ATA**GGAGTGTGTGCTAACC	78,1	35	AAA
K-75-I-Rev	GGTTAGCACACACTCC**TAT**GATAGACACAACTCCT	78,1	35	
V-77-A-For	TGTGTCTATCAAAGGA**GCG**TGTGCTAACCGTTACC	79,3	35	GTG
V-77-A-Rev	GGTAACGGTTAGCACA**CGC**TCCTTTGATAGACACA	79,3	35	
C-78-A-For	GTGTCTATCAAAGGAGTG**GCT**GCTAACCGTTACCTGG	78,9	37	TGT

Primer	Sequence	T_m (°C)	N	Codon
C-78-A-Rev	CCAGGTAACGGTTAGC**AGC**CACTCCTTTGATAGACAC	78,9	37	
N-80-A-For	CAAAGGAGTGTGTGCT**GCC**CGTTACCTGGCTATGA	78,8	35	AAC
N-80-A-Rev	TCATAGCCAGGTAACG**GGC**AGCACACACTCCTTTG	78,8	35	
Y-82-A-For	AGTGTGTGCTAACCGT**GCC**CTGGCTATGAAGGAAG	78,8	35	TAC
Y-82-A-Rev	CTTCCTTCATAGCCAG**GGC**ACGGTTAGCACACACT	78,8	35	
E-87-K-For	GTTACCTGGCTATGAAG**AAA**GATGGAAGATTACTGGC	78,3	37	GAA
E-87-K-Rev	GCCAGTAATCTTCCATC**TTT**CTTCATAGCCAGGTAAC	78,3	37	
D-88-A-For	CCTGGCTATGAAGGAA**GCT**GGAAGATTACTGGCTT	79,3	35	GAT
D-88-A-Rev	AAGCCAGTAATCTTCC**AGC**TTCCTTCATAGCCAGG	79,3	35	
L-92-A-For	GAAGGAAGATGGAAGATTA**GCG**GCTTCTAAATGTGTTACGG	78,2	41	CTG
L-92-A-Rev	CCGTAACACATTTAGAAGC**CGC**TAATCTTCCATCTTCCTTC	78,2	41	
C-96-A-For	GGAAGATTACTGGCTTCTAAA**GCT**GTTACGGATGAGTGTTTCT	78,3	43	TGT
C-96-A-Rev	AGAAACACTCATCCGTAAC**AGC**TTTAGAAGCCAGTAATCTTCC	78.3	43	
F-102-A-For	CTAAATGTGTTACGGATGAGTGT**GCC**TTTTTTGAACGATTGGAATCTAATA	78,8	49	TTC
F-102-A-Rev	TATTAGATTCCAATCGTTCAAAAAA**GGC**ACACTCATCCGTAACACATTTAG	78,8	49	
F-104-A-For	GTGTTACGGATGAGTGTTTCTTT**GCT**GAACGATTGGAATCTAATAACTA	78,7	47	TTT
F-104-A-Rev	TAGTTATTAGATTCCAATCGTTC**AGC**AAAGAAACACTCATCCGTAACAC	78,7	47	
Y-112-A-For	GAACGATTGGAATCTAATAAC**GCC**AATACTTACCGGTCAAGGA	78,3	41	TAC
Y-112-A-Rev	TCCTTGACCGGTAAGTATT**GGC**GTTATTAGATTCCAATCGTTC	78,3	41	
S-122-A-For	CGGTCAAGGAAATACACC**GCT**TGGTATGTGGCACTGAAA	79,0	39	AGT
S-122-A-Rev	TTTCAGTGCCACATACCA**AGC**GGTGTATTTCCTTGACCG	79,0	39	
K-128-E-For	GGTATGTGGCACTG**GAA**CGAACTGGGCAG	78,8	29	AAA
K-128-E-Rev	CTGCCCAGTTCG**TTC**CAGTGCCACATACC	78,8	29	
R-129-Q-For	GGTATGTGGCACTGAAA**CAA**ACTGGGCAGTATAAACT	78,3	37	CGA
R-129-Q-Rev	AGTTTATACTGCCCAGT**TTG**TTTCAGTGCCACATACC	78,3	37	
Q-132-R-For	CTGAAACGAACTGGG**CGG**TATAAACTTGGATCCAA	78,1	35	CAG
Q-132-R-Rev	TTGGATCCAAGTTTATA**CCG**CCCAGTTCGTTTCAG	78,1	35	
Y-133-H-For	GAAACGAACTGGGCAG**CAT**AAACTTGGATCCAAAACA	78,3	37	TAT
Y-133-H-Rev	TGTTTTGGATCCAAGTTT**ATG**CTGCCCAGTTCGTTTC	78,3	37	
Y-133-A-For	CTGAAACGAACTGGGCAG**GCT**AAACTTGGATCCAAAACAGG	80,2	41	TAT
Y-133-A-Rev	CCTGTTTTGGATCCAAGTTT**AGC**CTGCCCAGTTCGTTTCAG	80,2	41	
K-138-A-For	GCAGTATAAACTTGGATCC**GCG**ACAGGACCTGGGCAGAA	78,6	39	AAA
K-138-A-Rev	TTCTGCCCAGGTCCTGT**CGC**GGATCCAAGTTTATACTGC	78,6	39	
S-152-A-For	TATACTTTTTCTTCCAATG**GCT**GCTAAGAGCATGGTGAG	78,4	39	TCT
S-152-A-Rev	CTCACCATGCTCTTAGC**AGC**CATTGGAAGAAAAAGTATA	78,4	39	
C-96-A-For	GGAAGATTACTGGCTTCTAAA**GCT**GTTACGGATGAGTGTTTCT	78,3	43	TGT
C-96-A-Rev	AGAAACACTCATCCGTAAC**AGC**TTTAGAAGCCAGTAATCTTCC	78.3	43	

Primers for FGF2 truncations

The primers used for the generation are listed in the following tables.

N-terminal Truncations

Primer	Sequence
N-10	CGGGATCCCGCCACCATGGGCCCCGAGGATGGCGGCAGCG
N-20	CGGGATCCCGCCACCATGGGCCCCGGCCACTTCAAGGACCCC
N-30	CGGGATCCCGCCACCATGGGCTACTGCAAAAACGGGGGCTTCTTCC
N-40	CGGGATCCCGCCACCATGGGCATCCACCCCGACGGCCG
N-50	CGGGATCCCGCCACCATGGGCCGGGAGAAGAGCGACCCTCAC
REV	CGGGATCCGTAAGTATTGTAGTTATTAGATTCCAATCG

C-terminal Truncations

Primer	Sequence
FOR	CCAAGCTTGCGGCCGCACCG
C_{1-146}	GACGGGGCCCTATAGCTTTCTGCCCAGGTCCTGTTTTGG
C_{1-136}	GACGGGGCCCTCCAAGTTTATACTGCCCAGTTCG
C_{1-126}	GACGGGGCCCTGCCACATACCAACTGGTGTATTTCC
C_{1-116}	GACGGGGCCCCCGGTAAGTATTGTAGTTATTAGATTCC
C_{1-106}	GACGGGGCCCTCGTTCAAAAAGAAACACTCATCCGTAAC
C_{1-96}	GACGGGGCCCACATTTAGAAGCCAGTAATCTTCCATCTTC
C_{1-86}	GACGGGGCCCCTTCATAGCCAGGTAACGGTTAGCAC
C_{1-66}	GACGGGGCCCTGCTTGAAGTTGTAGCTTGATGTGAGGG
C_{1-56}	GACGGGGCCCGCTCTTCTCCCGGACCCCG
C_{1-46}	GACGGGGCCCGTCGGGGTGGATGCGCAGG
C_{1-36}	GACGGGGCCCGTTTTTGCAGTACAGCCGCTTGGGG
C_{wt}	GACGGGGCCCGCTCTTAGCAGACATTGGAAGAAAAAG
$GFP_{forapaI}$	GACGGGGCCCATGGTGAGCAAGGGCGAGG
$GFP_{revsphI}$	ATCGATGCATGCTTAGTGATGGTGATGG

2.1.6 Bacteria and Media

The following *E.coli* strains were used for cloning and amplification. They were grown in LB (Luria Bertani) medium or on LB agar plates supplied with ampicillin in a final concentration of 100 µg/ml to select for successfully transformed cells carrying plasmids containing the appropriate resistance gene.

DH5α	Invitrogen, Karlsruhe
XL1-Blue supercompetent cells	Stratagene, La Jolla

LB medium	
5 -10g	NaCl
10g	Tryptone
5g	Yeast extract
ad 1 l	H_2O_{milliQ}

LB_{Amp} plates	
5 -10g	NaCl
10g	Tryptone
5g	Yeast extract
15g	Agar
ad 1 l	H_2O_{milliQ}

2.1.7 Eukaryotic Cells and Media

Chinese Hamster Ovary (CHO) cell lines

Several CHO model cell lines expressing different mutated versions of FGF2-GFP in a doxicycline dependent manner were generated during this thesis. They were stably transduced with the corresponding reporter constructs and were used to function as a eukaryotic system to investigate FGF2 in a living cell. For the procedure of retroviral transduction see section 2.5.2.

Human Embryonic Kidney (HEK) cells

The cell line HEK 293T was used for the production of retroviral particles carrying different reporter constructs.

α-Modification of the Minimal Essential Medium (α-MEM)

The α-Modification of the Minimal Essential Medium was used for cultivation of CHO cells. The appropriate amount of α-MEM powder (Biochrom KG, Berlin) was dissolved in 5 l of ultrapure water and 10 g of sodium hydrogen carbonate was added to adjust the pH to 7.4. The prepared medium was filter sterilized into autoclaved bottles and stored at 4°C. If the medium was stored for more than six weeks, 2 mM L-glutamine were added before use. The medium was supplemented with 10% (v/v) fetal calf serum (FCS) and 500 U Penicillin/Streptomycin before it was added to cultured cells.

Dulbecco´s Modified Eagle Medium (DMEM)

The Dulbecco´s Modified Eagle Medium was used for the cultivation of HEK cells. Dry medium (Biochrom KG) was dissolved in 5 l of ultrapure water, and 10g of sodium hydrogen carbonate was added to adjust the pH to 7.4. The prepared medium is sterile filtered into autoclaved bottles and stored at 4°C. If the medium was stored for more than 6 weeks, 2 mM L-glutamine were added before use. Before addition to cultured cells, the medium was supplemented with 10% (v/v) fetal calf serum (FCS) and 500 U Penicillin/Streptomycin.

Maintaining CHO cells

CHO cells were maintained at 37°C in 5% CO_2 (Heraeus incubator), in Minimal Essential Medium (α-MEM) supplemented with 10% (v/v) fetal calf serum (FCS) and 500 U Penicillin/Streptomycin. Cells were passaged when confluent by removing the old medium and washing the cells with PBS. After trypsinization of the cell monolayer with 1 ml trypsin (0.125% trypsin in PBS, 0.5 mM EDTA), the cells were resuspended in 10 ml of fresh culture medium and finally seeded into cell culture dishes at desired densities, depending on the experiment requirements.

Freezing of eukaryotic cells

Frozen stocks for long time use were prepared from cells grown to 100% confluency on a 10 cm culture plate. The cells were washed once with PBS and detached using 1 ml trypsin/EDTA. Subsequently, the cells were resuspended in growth medium, transferred to a 10 ml tube and pelleted by low speed centrifugation at 200 g for 5 min at 4°C. The pellet was carefully resuspended in 2 ml freeze medium and transferred to 2 ml cryo tubes which were frozen at -80°C. For long term storage the frozen cryo tubes were transferred to liquid nitrogen cell storage tanks.

Freeze medium	
20%	FCS (v/v)
10%	DMSO (v/v)
1 mg/ml	Streptomycin/Penicillin
70%	αMem or DMEM

Thawing of eukaryotic cells

To defreeze cells the cryo tube was removed from liquid nitrogen and immediately thawn in a water bath at 37°C. The cells were transferred to 20 ml of prewarmed culture medium in a 50 ml tube and sedimented by low speed centrifugation (200 g, 5 min, 4°C). DMSO was removed by discarding the medium followed by resuspension of cells using fresh growth medium. The cells were then seeded on culture plates (Ø 10 cm) and incubated at 37°C supplemented with 5% CO_2.

2.2 Molecular biological methods

2.2.1 Polymerase Chain Reaction (PCR)

2.2.1.1 Random Mutagenesis

A low fidelity PCR based on the addition of $MnCl_2$ was performed to introduce randomly distributed base pair alterations into the open reading frame of FGF2. (Shafikhani et al., 1997).

The used primers were FGF2-MUT-FOR and FGF2-MUT-REV respectively and are listed in section 2.1.6.
PCR reaction mix:

PCR for random Mutagenesis	
30 ng	template DNA (PRevTRE2 FGF2-GFP)
25 pmol	FGF2-MUT-FOR
25 pmol	FGF2-MUT-REV
10 µl	2.5 mM dNTP-Mix
12 µl	25 mM $MgCl_2$
10 µl	5 mM $MnCl_2$
10 µl	10x PCR buffer
0.5 µl	5 U Ampli-Taq Polymerase
Ad 100 µl	H_2O_{MilliQ}

PCR program:

Start: 2 min at 95°C

Amplification:	1 min at 94°C	Denaturation
20 cycles	1 min at 50°C	Hybridization
	1 min at 72°C	Elongation
End:	10 min at 72°C	

The PCR product was then subjected to an agarose gel electrophoresis, proving correct size of the amplified DNA, followed by purification of the PCR product using the QIAquick PCR Purification Kit (Qiagen).

2.2.1.2 Point mutations

Point mutations were introduced into FGF2 using the QuickChange Site-Directed Mutagenesis kit. PCR reactions were performed using PfuTurbo Polymerase, a dsDNA vector with the insert of interest (pGEM-T-FGF2-GFP) and two synthetic complementary primers containing the desired mutation (see chapter 2.1.6).

Incorporation of the oligonucleotide primers generated a mutated plasmid containing staggered nicks.

PCR reaction mix:

PCR for point mutations	
50 ng	template DNA (PGemT-FGF2-GFP)
125 pmol	Forward primer
125 pmol	Reverse primer
10 µl	2.5 mM dNTP-Mix
5 µl	10x PCR buffer
0.5 µl	5 U PfuTurbo Polymerase
Ad 50 µl	H_2O_{MilliQ}

PCR program:

Start:	1 min at 30°C	
Amplification:	30 s at 95°C	Denaturation
16 Cycles	1 min at 55°C	Hybridization
	4 min at 68°C	Elongation
End:	store at 4°C	

The PCR products were treated with 10U of the endonuclease *Dpn I* for 1h at 37°C, which specifically cuts methylated DNA. *Dpn I* was used to digest the parental DNA template derived from a dam methylase containing E.coli strain, therefore selecting for mutated newly synthesized DNA. The nicked vectors containing the desired mutations were subsequently introduced into DH5α- or XL1-Blue supercompetent cells.

2.2.1.3 Truncations

Specific primers were used for the generation of N- and C-terminal truncations which are listed in section 2.1.6.

PCR reaction mix:

PCR for N- and C-terminal Truncation	
30 ng	template DNA (PGemT-FGF2-GFP)
25 pmol	Forward primer
25 pmol	Reverse primer
10 µl	2.5 mM dNTP-Mix
10 µl	10x PCR buffer
0.5 µl	5 U Ampli-Taq Polymerase
Ad 100 µl	H_2O_{MilliQ}

For primers used see chapter 2.1.7

PCR program:

Start:	2 min at 95°C	
Amplification:	1 min at 94°C	Denaturation
35 cycles	1 min at 47°C	Hybridization
	1 min at 72°C	Elongation
End:	10 min at 72°C	

The PCR product was then subjected to an agarose gel electrophoresis, proving correct size of the amplified DNA, followed by purification of the PCR product using the QIAquick PCR Purification Kit (Qiagen).

2.2.2 PCR Purification

PCR products were purified using the QIAquick PCR Purification (Qiagen) according to the manufacturers instructions. The DNA was eluted with 30 µl H_20_{MilliQ}.

2.2.3 Restriction digestion and Dephosphorylation

Restriction digestions of DNA with endonucleases were performed after a procedure described by (Maniatis et al., 1989). Reactions were carried out as recommended by New England BioLabs. According to used enzymes, the appropriate buffer and supplements were used. About 2-4 U of the corresponding enzyme was used to digest 1 µg DNA. The reaction mix was incubated up to 4 h at 37°C.
To remove 5´-phosphates at the ends of linearised vectors (to prevent self-ligation of vector) the restriction product was treated with 1 U calf intestinal alkaline phosphatase (CIP, New England Biolabs) per 1 µg DNA for 30 min at 37°C.

2.2.4 Ligation of DNA fragments

Ligations of linearised vectors and inserts digested with the same restriction enzymes were conducted using the TAKARA ligation kit. 50 ng of vector were used in the reaction, the amount of insert was calculated using the following equation:

$$\frac{\text{amount (ng) vector x size (bp) insert}}{\text{size (bp) vector}} = \text{amount (ng) insert}$$

5 µl Solution 1, containing the ligase, was added to the DNA and the reaction mix was filled up with H_2O to a final volume of 10 µl. The ligation was performed for 3 h at 37°C or over night at 16°C followed by heat inactivation of the ligase at 60°C for 10 min.

2.2.5 Transformation of *E.coli* with plasmid DNA

1-10 ng DNA or 5µl from a ligation reaction were incubated with 30 µl of competent E.coli DH5α cells for 30 min on ice, followed by heat shock at 37°C for 20 s and incubation on ice for additional 2 min. 1 ml of LB medium was added followed by incubation for 1h at 37°C under constant shaking (300 /min). The cells were then spread on LB plates containing 100 µg/ml ampicillin and cultivated at 37°C over night.

2.2.6 Selection of clones

After incubating LB_{Amp} plates over night, bacteria resistant to ampicillin form colonies on the plates. For amplification of single colonies, they were transferred with a pipette tip to 5 ml LB medium containing ampicillin (100 µg/ml) and incubated for 12-16 h at 37°C under constant shaking (200 U/min).

2.2.7 Isolation of plasmid DNA from bacteria

Plasmid DNA from over night cultures incubated with individual colonies from LB_{Amp} plates was prepared using kits supplied by Macherey & Nagel or Qiagen according to the manufacturers manual. Following alkaline lysis of bacterial cells the DNA was bound to a silica-membrane in presence of high salt concentrations. After washing the membrane, the purified DNA was eluted using H_2O_{MilliQ}. Depending on the volume of the over night cultures, the following kits were used:

Volume of bacterial cells	Qiagen Kit	Machery & Nagel Kit
5 – 10 ml	QIAprep Spin Miniprep Kit	Nucleospin Plasmid
20 – 150 ml	QIAprep Plasmid Midi Kit	Nucleobond-PC 100
More than 150 ml	QIAgen Plasmid Maxi Kit	Nucleobond-PC 500

2.2.8 Agarose gel electrophoresis

Size and purity of DNA fragments were analyzed by agarose gel electrophoresis. For the preparation of agarose gels, 1% (w/v) agarose was dissolved in 1x TAE using a microwave and poured in a casting device after addition of ethidiumbromide to a final concentration of 0.5 µg/ml.

50x TAE buffer	
242 g	Tris
57.1 ml	Glacial acidic acid
100 ml	EDTA, 0.5 M, pH 8
ad 1 l	H_2O_{milliQ}

After addition of the appropriate amount of sample buffer containing glycerol (30% w/v), the samples were loaded on the gel.

5x sample buffer	
0.25% (w/v)	Bromphenol blue
0.25% (w/v)	Xylencyanol FF
30% (w/v)	Glycerol

Electrophoresis was conducted in 1x TAE buffer at 100 V for approximately 20 min. For visualization BioRad Gel Doc System was used.

2.2.9 DNA extraction from agarose gels

Bands were visualized with UV light (366 nm) and cut out of the agarose gel. The extraction of DNA was carried out following the manual from the DNeasy gel extraction kit. The DNA was eluted with 30 µl elution buffer or H_20_{MilliQ}.

2.2.10 DNA Sequencing

All obtained constructs were verified by DNA-Sequencing. Therefore the demanded amount of DNA was sent to specialized companies (Seqlab, Göttingen or GATC, Konstanz). Editing, assembly and analysis of DNA sequences was performed using LaserGene Software.

2.3 Biochemical Methods

2.3.1 SDS-Polyacrylamid-gel electrophoresis

SDS polyacrylamide gel electrophoresis was performed as described by (Laemmli, 1970). The Mini-PROTEAN III-Gel system (Bio-Rad) was used. The gels used had a size of 80 x 73 mm and a thickness of 0.75 mm, consisting of a separating and a stacking gel.

For preparation of the separating gel the following solutions were mixed and poured between two glass plates fixed in the casting device:

Separation gel	10 %	13 %
H_2O_{MilliQ}	2 ml	1.68 ml
1.5 M Tris-HCl pH 8.8	1.25 ml	1.25 ml
10% (w/v) SDS	50 µl	50 µl
Acrylamide/Bis 30% (w/v)	1.66 ml	2 ml
10 % (w/v) Ammonium persulphate (APS)	25 µl	25 µl
N,N,N',N'-Tetramethylendiamin (TEMED)	2.5 µl	2.5 µl

To achieve an even surface, isopropanol was carefully poured over the not yet polymerized gel surface. After polymerization was completed, isopropanol was removed with Whatman paper.

For the 4.8 % stacking gel the following solutions were mixed and poured on the separation gel:

Stacking Gel	
1.53 ml	H_2O_{MilliQ}
0.625 ml	0.5 M Tris-HCl pH 6.8
25 µl	10% (w/v) SDS
335 µl	Acrylamide/Bis 30% (w/v)
12.5 µl	25 % (w/v) Ammonium persulphate (APS)
2.5 µl	N,N,N',N'-Tetramethylendiamin (TEMED)

The samples were mixed in a ratio of 3:1 with sample buffer and heated for 10 min at 95°C before loading onto the gel.

4x Sample Buffer	
200 mM	Tris-HCl, pH 6.8
25% (w/v)	Glycerol
2% (w/v)	SDS
0.2% (w/v)	Bromphenol blue
0.7 M	β-Mercaptoethanol

Running Buffer	
25 mM	Tris pH 8.3
192 mM	Glycine
0.1% (w/v)	SDS

Electrophoresis was performed in running buffer at 200 V until the bromphenol blue marker front reached the end of the gel.

2.3.2 Western Blot Analysis

Western blotting was performed as described by (Towbin et al., 1979). Proteins separated by SDS-PAGE were blotted on a polyvinylidene fluoride (PVDF) membrane (Immobilon™-P/FL, Millipore) using a wet blotting apparatus (MiniProtean Trans Blot®, Bio-Rad).

Solutions:

Blotting / transfer buffer	
192 mM	Glycine
25 mM	Tris-Base
20% (v/v)	Methanol

Ponceau S	
0.25% (w/v)	Ponceau S
3% (v/v)	TCA

1x PBS	
140 mM	Sodium chloride (NaCl)
2.7 mM	Potassium chloride (KCl)
10 mM	Sodium hydrogen phosphate (Na_2HPO_4)
1.8 mM	Potassium dihydrogen phosphate (KH_2PO_4)

PBS-Tween	
0.05% (w/v)	Tween 20
	PBS

Blocking buffer	
5% (w/v)	Milk powder
	PBS-Tween

Primary antibody buffer	
3% (w/v)	Bovine serum albumin (BSA)
0.02 % (w/v)	Sodium azid (NaN_3)
	PBS-Tween

Secondary antibody buffer (HRP system)	
3% (w/v)	Milk powder
	PBS-Tween

Secondary antibody buffer (Licor system)	
3% (w/v)	Milk powder
0.01%	SDS
	PBS-Tween

2.3.2.1 Transfer of proteins to polyvinylidene fluoride (PVDF) membrane

A PVDF membrane sheet of the same dimensions as the gel was prepared, soaked in methanol and equilibrated in blotting buffer. Two pieces of filter paper (Whatman 3MM) of the same size as the gel were soaked in blotting buffer, as well as two sponges. The blotting apparatus was assembled, taking care to remove air bubbles, and placed in the transfer tank with the PVDF membrane towards the anode. An ice block was placed in the tank, which was then filled up with blotting buffer. Protein transfer to the PVDF membrane was performed at constant voltage (100 V) for 1h.

Anode (+)

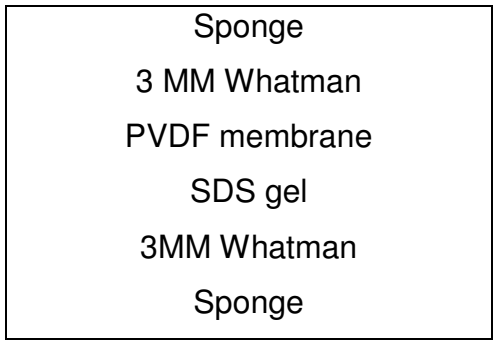

Kathode (-)

Figure 2.1: Assembly of the Western Blot apparatus

2.3.2.2 Ponceau S staining

Following transfer to the membrane, proteins were visualized by staining with Ponceau S for one minute while shaking. Background staining was removed with H_2O_{MilliQ} until the bands were clearly observed and the position of the molecular weight marker proteins was labeled on the membrane. Complete destaining was reached by washing the membrane in PBS-Tween. When using the Licor System, Ponceau S staining was not performed, since this resulted in an enhanced background.

2.3.2.3 Immunochemical detection of proteins (HRP system)

The membrane was treated with blocking buffer for one hour at room temperature or overnight at 4°C, and subsequently incubated for 1h with affinity-purified polyclonal antibodies directed against the protein of interest. The membrane was washed three times with PBS-Tween followed by treatment with the appropriate horseradish peroxidase (HRP)-conjugated secondary antibodies for 1h. After three washing steps, remaining secondary antibody was removed with PBS-Tween. Visualization was performed using the enhanced chemi-luminescence mixture (ECL; Amersham): The membrane was incubated for 60 s in the reagent, patted dry, covered in Saran wrap and exposed to Super RX Medical X ray film (Fuji) for up to thirty minutes.

2.3.2.4 Immunochemical detection of proteins (Licor System)

The membrane was treated with blocking buffer without Tween-20 for one hour at room temperature, and subsequently incubated for one hour with affinity-purified polyclonal antibodies directed against the protein of interest. The membrane was washed four times with PBS-Tween followed by treatment with the appropriate Alexa 680-conjugated secondary antibodies for 30 min. After four times of washing, remaining secondary antibodies were removed using PBS-Tween, followed by one washing step using PBS without Tween-20. Visualization was performed by the Odyssey System (Licor).

2.3.3 Biochemical assay to estimate the amount of secreted FGF2-GFP

CHO cells were grown on 6-well plates for 48 h at 37°C in the presence of 1 µg/ml doxicycline and 125 µg/ml heparin. The medium was removed followed by the dissociation of the cells from the culture plates using a protease-free buffer (Cell dissociation buffer) supplemented with 125 µg/ml heparin. Following sedimentation of cells, the supernatant was combined with the original medium, diluted 1:10 in a Tris buffer (10 mM, pH 7.4) containing 1 mM EDTA and 1% (w/v) Triton X-100. The cells were lysed in the same buffer. Both the cellular extracts and the corresponding supernatants were then subjected to affinity purification using heparin sepharose (Amersham Pharmacia). Bound material was eluted with SDS sample buffer followed by SDS-PAGE and western blot analysis using affinity-purified anti-GFP antibodies and ECL detection.

2.3.4 Isolation of detergent-insoluble microdomains

$CHO_{FGF2\text{-}GFP}$ cells were grown on large culture plates (ø 15 cm) for 36 h in the presence of doxicycline (1 µg/ml). The cells were washed twice with PBS followed by the addition of PBS supplemented with 10% (w/v) sucrose. After dissociation from the culture plates using a rubber policeman, cell disruption was achieved using a Balch homogenizer (Balch and Rothman, 1985). The resulting suspension was subjected to differential centrifugation at 1000 g and 5000 g, respectively. The 5000 g supernatant was loaded onto a 20% sucrose cushion followed by ultracentrifugation

at 100,000 g for 60 min at 4°C. The resulting membrane sediment represents a microsomal membrane fraction containing intracellular as well as plasma membranes. The preparation of detergent-soluble and –insoluble fractions as well as a flotation analysis employing sucrose gradients were performed as described by (Gkantiragas et al., 2001).

2.3.5 Biotinylation of proteins associated with the cell surface

Biotinylation was performed as described by Seelenmeyer et al, 2005. Extracellular proteins were labeled with a membrane impermeable biotin reagent and in this way discriminated from the intracellular fraction.

Solutions:

PBS Ca^{2+}/Mg^{2+}	
1x	PBS
1 mM	$MgCl_2$
0.1 mM	$CaCl_2$

Incubation buffer	
150 mM	$MgCl_2$
10 mM	Triethanolamine pH 9
2 mM	$CaCl_2$

Quenching buffer	
	PBS Ca^{2+}/Mg^{2+}
100 mM	Glycine

Lysis buffer	
62.5 mM	EDTA
50 mM	Tris-HCl pH 7.5
0.4%	Deoxycholate
1%	NP-40
	Protease inhibitor tab (1 in 10 ml)

Washing buffer 1	
62.5 mM	EDTA
50 mM	Tris-HCl pH 7.5
0.4%	Deoxycholate
1%	NP-40
0.5 M	NaCl

Washing buffer 2	
62.5 mM	EDTA
50 mM	Tris-HCl pH 7.5
0.4%	Deoxycholate
0.1%	NP-40
0.5 M	NaCl

The CHO model cell lines were grown on 12-well plates in presence of 1µg/ml doxicycline to a confluency of 70%. Cells were washed twice with cold PBS Ca^{2+}/Mg^{2+} and subsequently incubated for 30 min at 4°C with 350 µl of incubation buffer containing 0.5mg/ml membrane-impermeable biotin (EZ-link Sulfo-NHS-SS-biotin, Pierce). To quench remaining biotin reagent, cells were washed with Quenching buffer, followed by incubation at 4°C for 20 min with 350 µl Quenching buffer. A washing step with PBS was introduced to remove residual Quenching buffer, followed by incubation for 10 min at 37°C with 110 µl Lysis buffer. Cells were scraped off using a rubber policeman, resuspended and transferred to an Eppendorf tube. Cell lysates were produced by sonication in a sonication bath for 3 min, followed by incubation for 15 min at RT, pipetting the sample up and down several times. To remove insoluble material, a centrifugation at 16,000 g was performed. An aliquot of 10% was stored as the input material. The remaining lysate was subjected to a streptavidin affinity chromatography, using 20 µl packed beads, equilibrated with lysis buffer. After incubation of lysates with the beads for 1 h at room temperature under constant head-over-head rolling, a centrifugation at 3000 g was performed to pellet the beads. The supernatant was discarded. To remove non-specific bound material, the pellet was washed three times with Washing Buffer 1, followed by two washing steps with Washing Buffer 2. The residual Washing Buffer 2 was carefully removed and the biotinylated protein, bound to streptavidin beads was eluted with 20 µl of

Sample Buffer. Input and eluate were subsequently analyzed by SDS-PAGE and Western blotting using anti-GFP antibodies.

2.3.6 Preparation of cell free supernatant

FGF2-GFP fusion proteins were expressed in CHO cells by incubating the cells in the presence of doxicycline (1 µg/ml) for 48 h at 37°C. After removing growth medium and washing cells with PBS, they were detached from the culture plate using Cell Dissociation Buffer. Cells in solution were transferred to an Eppendorf tube und submitted to a low speed centrifugation step for 3 min at 200 g to pellet cells. Resuspension was carried out by adding 500 µl of PBS. Cell-free supernatants were then prepared by homogenization combining freeze-thaw cycles with sonication. Membranes were removed in two steps by centrifugation at 14000 g (10 min at 4°C) and 100000 g (1h at 4°C) The resulting supernatants were analyzed for the amounts of fusion protein based on GFP fluorescence as measured with a fluorescence plate reader (Molecular Devices Spectra Max Gemini XS).

2.3.7 Binding of FGF2 to heparin beads

Cell free supernatant was produced as described in 2.3.4. Normalized amounts of the supernatant (50 GFP units corresponding to about 0.5 µg GFP) were then incubated with heparin beads (Sigma), equilibrated with PBS, for 1h at 4°C. An input fraction, corresponding to 10% of the total protein was removed prior to binding and stored at 4°C. Beads were centrifuged at 800 g and the supernatant (non-bound material) was stored at 4°C. Following extensive washing with PBS, bound material was eluted using SDS sample buffer. Input, flow-through fraction and SDS eluates were analyzed by SDS PAGE and Western blotting using anti-GFP antibodies.

2.3.8 Precipitation of FGF2-GFP from culture media using heparin beads

Medium was removed from the cells which were additionally washed with PBS. Heparin beads were equilibrated using PBS. Both, medium and PBS were subjected to heparin beads for 1h at 4°C to allow binding of FGF2-GFP, present as a soluble protein in the medium, to heparin beads. After centrifugation at 3000 g to pellet

beads, the supernatant (non-bound material) was removed. The pellet was extensively washed using PBS, followed by eluating bound material from heparin beads using SDS-sample buffer. The SDS eluate was then subjected to SDS-PAGE and Western blotting using anti-GFP antibodies.

2.3.9 Binding of FGF2-GFP to $CHO_{MCAT/TAM2}$ Cells

Cell free supernatant was produced as described in 2.3.4. Normalized amounts of the supernatant (50 GFP units corresponding to about 0.5 µg GFP) were then incubated with $CHO_{MCAT/TAM2}$ cells for 1h at 4°C to allow binding of FGF2-GFP to receptors present on the cell surface of the cells. Cells were subsequently washed using PBS and prepared for FACS analysis (see 2.4.2).

2.3.10 Immunoprecipitation of FGF2-GFP from growth medium

20 µl of a 1:1 Protein A and CL-4B-sepharose mix were transferred to an Eppendorf tube, followed by extensive washing with IP-buffer 1.

IP-buffer 1	
25 mM	Tris-HCl 7.4
150 mM	NaCl
1 mM	EDTA
0.5%	NP-40

To bind antibodies to sepharose, affinity-purified anti-GFP antibodies in IP-buffer 1 was added to the beads and incubated over night at 4°C under constant shaking. Sepharose was then extensively washed using IP buffer 2.

IP-buffer 2	
25 mM	Tris-HCl 7.4
150 mM	NaCl
1 mM	EDTA
0.5%	NP-40
1%	BSA

Subsequently, the sepharose was pelleted and the supernatant was carefully

removed. Growth medium and PBS-wash solution obtained from the corresponding CHO model cell lines were added to the sepharose and incubated for 2 h at 4°C. After three of washing steps with IP-buffer 0, the protein was eluted using SDS-containing sample buffer.

IP-buffer 0	
25 mM	Tris-HCl 7.4
150 mM	NaCl
1 mM	EDTA

The eluate was then applied to SDS-PAGE and Western blotting using affinity-purified anti-GFP antibodies.

2.4 FACS Analysis

2.4.1 Antibody labelling of cells in suspension

The following solutions were used during the antibody labelling procedure:

PBS EDTA	
1x	PBS
0.5 mM	EDTA

Primary antibody	
	α-MEM (growth medium)
1:200	Affinity-purified anti-GFP antibodies

Secondary antibody	
	α-MEM (growth medium)
1:750	Goat anti rabbit IgG coupled to allophycocyanin (APC)

Sorting medium	
	α-MEM without FCS
0.2%	FCS
5%	CDB

Cells were washed with PBS and detached from the culture plate using Cell Dissociation Buffer (Invitrogen) or PBS/EDTA and sedimented by low speed centrifugation at 200 g for 3 min. The supernatant was removed and the pellet was washed once with PBS. Cells were then incubated with 500 µl of primary antibodies for 1h at 4°C. Antibody solution was removed by washing cells two times with PBS. 500 µl of secondary antibodies was applied to the cells for 30 min at 4°C, followed by two washing steps using PBS. Cells were resuspended in 500 µl sorting medium subsequently analyzed via flow cytometry (FACS Calibur, Becton Dickinson).

2.4.2 Antibody labelling of Cells Attached to the culture plate

PBS/EDTA	
1x	PBS
0.5 mM	EDTA

Primary antibody	
	Alpha-MEM (growth medium)
1:200	Affinity-purified anti-GFP antibody

Secondary antibody	
	Alpha-MEM (growth medium)
1:750	Goat anti rabbit IgG coupled to allophycocyanin (APC)

Sorting medium	
	Alpha-MEM without FCS
0.2%	FCS
5%	CDB

Cells were washed with PBS followed by incubation with 350µl primary antibodies for 1h at 4°C. Following one washing step with PBS, secondary antibodies were added to attached cells for 30 min at 4°C. To remove free antibodies, cells were extensively washed with PBS prior to their detachment of cells using 200 µl cell dissociation buffer or PBS/EDTA. Cells were transferred in Eppendorf tubes containing 300 µl sorting medium and subsequently analyzed via flow cytometry (FACS Calibur, Becton Dickinson).

2.5 Production of stable Cell Lines

2.5.1 Retroviral Transduction

CHO cell lines were generated by retroviral transduction of $CHO_{MCATTAM}$ cells with the corresponding reporter constructs. All plasmids used are listed in chapter 2.1.6.

Principle of this method:
HEK 293T cells were cotransfected with the plasmid pVPack Eco encoding a retroviral *envelope*-protein and the reporter construct cloned into pRevTRE2 or pFB-GFP as a control. The transfected cells produce retroviral particles containing the RNA of interest which accumulate in the cell culture medium. The medium is then transferred to the $CHO_{MCATTAM}$ target cells that are infected by the retrovirus followed by reverse transcription and the integration of the reporter DNA into the host cell genome.

Experimental procedure:
The retroviral transduction was conducted using the MBS Mammalian Transfection Kit, (Stratagene) according to the protocol supplied by the manufacturer. In the following the procedure is described briefly: On the first day, the required plasmids were precipitated and HEK 293T cells were splitted. On the second day, HEK 293T cells were transfected with the prepared DNA and production of retroviral particles starts. On the next day, $CHO_{MCAT/TAM2}$ target cells were splitted 1:20. On the fourth day, the medium from virus producing HEK 293T cells was sterile filtered and transferred to the target $CHO_{MCAT/TAM2}$ cells. After adding growth medium to medium containing virus particles, cells were incubated for another two days prior to FACS analysis to prove the expression of the integrated reporter molecules.

2.5.2 FACS Sort

Sorting of cells expressing the desired GFP fusion protein was conducted in collaboration with Dr. Blanche Schwappach from the Center of Molecular Biology Heidelberg (ZMBH). Transduced cells were induced to synthesize the desired protein by adding doxicycline (1µg/ml) for 16 h to the growth medium of transduced cells.

Detachment of cells occurred with sterile cell dissociation buffer (Invitrogen), followed by addition of 500 µl of sorting medium.

Sorting medium	
	α-MEM without FCS
0.2%	FCS
5%	CDB

Cells were subsequently passed through a cell strainer cap into a sterile round bottom FACS tube (Becton Dickinson) and analyzed via flow cytometry (FACS Vintage or FACSAria, Becton Dickinson). GFP positive cells were collected in 6-well plates and propagated for a week. A second sorting step was conducted without prior induction of protein synthesis and cells were collected for negative GFP fluorescence on 6-well plates. After propagation of these cells for a week and incubation with 1 µg/ml doxicycline for 16 h a final sorting step was conducted, sorting cells for enhanced GFP-fluorescence. The cells were either sorted as single cell events in a 96-well plate to generate clonal cell lines or as cell populations in 6-well plates.

2.6 Confocal Microscopy

Cells were grown on cover slips placed in 12 well plates. After washing with PBS, cells were fixed without permeabilization for 20 min on ice using 3% paraformaldehyde. Remaining PFA was washed away using PBS and cells were quenched for 10 min with 50 mM NH_4Cl. Unspecific antibody binding was avoided by incubating cells with 1% BSA in PBS for 10 min. Subsequently, cells were processed with primary antibodies (1:50 affinity-purified anti-GFP antibody, 1h, RT) and secondary antibodies (1:250 goat anti-rabbit Alexa 546, 1h, RT). After removing antibody solution by multiple washing steps, specimens were mounted in Fluoromount G (Southern Biotechnology Associates), sealed and viewed with a Zeiss LSM 510 confocal microscope.

3 Results

Most of the examples of protein translocation across a membrane (such as the import of classical secretory proteins into the endoplasmic reticulum (ER), import of proteins into mitochondria and peroxisomes, as well as protein import into and export from the nucleus), are understood in great detail. Generally, proteins are targeted to the corresponding translocation apparatus by “transport” signals which are specific for protein import into distinct organelles. Proteins imported into the ER contain N-terminal signal peptides directing the protein to the translocation apparatus (Walter et al., 1984). Proteins that are translocated over mitochondrial membranes contain either N-terminal cleavable signal sequences or internal targeting sequences (Schatz, 1996; Neupert, 1997; Gordon et al., 2000). Peroxisomal proteins contain peroxisomal targeting sequences (PTS) which direct the protein to the peroxisomal transport machinery. (Johnson and Olsen, 2001). The nuclear import of proteins into the cell nucleus involves the recognition of a nuclear localization signal sequence which is recognized by the translocation apparatus of the nuclear transport machinery (Christophe et al., 2000).

In contrast, unconventional protein secretion from eukaryotic cells was discovered about 15 years ago, but the transport mechanism is still poorly understood. In 1991, Interleukin-1β has been suggested to be exported in an unconventional manner (Rubartelli and Sitia, 1991) and only two years later FGF2 has been proposed to be exported independently from the classical secretion pathway (Mignatti and Rifkin, 1991). However, the molecular mechanism and the molecular identity of machinery components that mediate this process remain elusive. An export targeting motif that directs unconventional secretory proteins to their translocation machinery has not yet been identified.

This thesis was aimed on identifying such a motif which targets FGF2 to its putative transport machinery. Therefore, the open reading frame (ORF) of FGF2 was screened for amino acids potentially forming a motif which might interact with the machinery of the unconventional secretion pathway. The nature of this motif remains elusive and it has to be identified if it is composed of consecutive amino acids, thereby building a linear motif, or of amino acids distributed over the open reading frame of FGF2, building a three dimensional motif.

In order to be able to screen for amino acids potentially forming an export targeting

motif, a suitable tool for the quantitative analysis of FGF2 secretion had to be developed first. Therefore, a model CHO cell line was generated, expressing a FGF2-GFP fusion protein in a doxicycline dependent manner. The first part of this thesis describes the establishment of an *in vivo* assay, which allows direct quantification of secreted FGF2-GFP based on flow cytometry. Furthermore, additional assays were developed allowing the characterization of FGF2 secretion. These assays were used in the second part of this thesis to perform a mutational analysis of FGF2, in order to elucidate an export targeting motif. Therefore more than 100 different FGF2 mutants were generated and analyzed with regard to export efficiency. The individual mutants were selected by random mutagenesis employing low-fidelity PCR, in order to hit a broad range of multiple amino acids, by point mutations to hit specific single amino acids and to complete the mutational analysis of FGF2, and finally by systematic truncations of the C- and N-terminus of FGF2.

3.1 Generation of model cell lines expressing FGF2-GFP in a doxicycline-dependent manner

In order to establish a FGF2 export model system, CHO cells were genetically modified to express a GFP-tagged version of FGF2 (FGF2-GFP) and GFP, respectively, in a doxicycline-dependent manner.

The generation procedure of the model cell lines is depicted in figure 3.1:

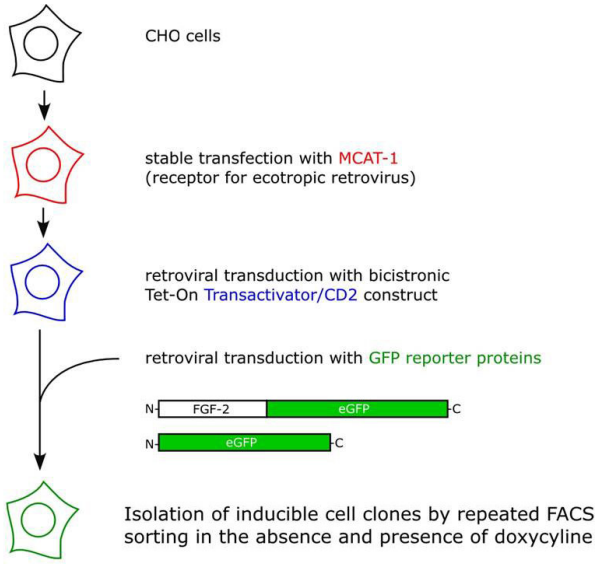

Figure 3.1: schematic overview of the generation of model cell lines expressing FGF2-GFP in a doxicycline dependent manner. CHO cells were first stably transfected with the receptor for an ecotropic virus (MCAT), followed by retroviral transduction with a bicistronic Tet-On Transactivator/CD2 construct to facilitate the doxicycline dependent expression. A second retroviral transduction with FGF2-GFP inserted the reporter protein into the genomic DNA. Single cell clones were isolated employing repeated FACS sortings in the presence and absence of doxicycline. For more detail see Material and Methods, chapter 2.5

CHO cells were stably transfected with the mouse cationic amino acid transporter-1 (MCAT-1; (Albritton et al., 1989; Davey et al., 1997), which serves as a receptor for an ecotropic envelope protein of a murine virus carrying appropriate constructs. In a second step, cells where transduced with an ecotropic retrovirus carrying a bicistronic construct consisting of the doxicycline-sensitive transactivator (rtTA2-M2) (Urlinger et al., 2000) and a truncated version of CD2 (Liu et al., 2000) that serves as a cell surface marker. A pool of CD2 positive cells was isolated by fluorescence activated cell sorting (FACS) sorting and subjected to another round of retroviral transduction using a vector carrying a doxicycline/transactivator-dependent promotor to generate a cell line expressing FGF2-GFP or GFP, respectively.

To demonstrate the generation of cell lines the results of the sorting procedure displayed for the cell line $CHO_{FGF2\text{-}GFP\text{-}His6}$ was used as an example in figure 3.2.

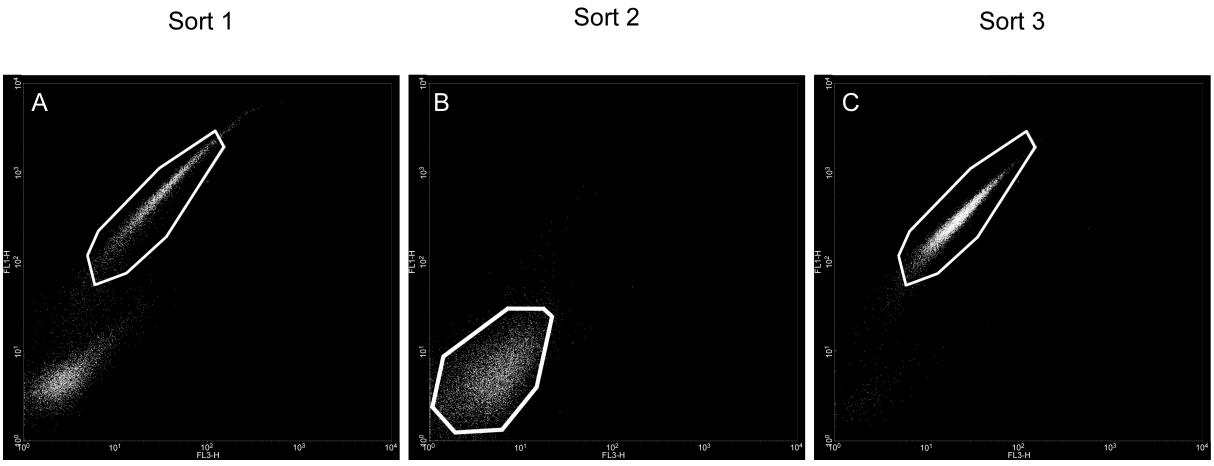

Figure 3.2: FACS sorting based on GFP fluorescence to generate the reporter cell line FGF2-GFP.
Cells were detached from culture dishes using cell dissociation buffer and processed for FACS analysis to measure GFP fluorescence. Sort 1 displays cells 3 days after viral transduction incubated in the presence of 1 µg/ml doxicycline for 12 h (panel A). FL1-H represents the green channel measuring GFP fluorescence, FL3-H shows the red channel displaying propidium iodide staining (dead cells). 50000 cells were sorted within the sorting gate (marked area). Sort 2 shows cells grown for 7 days in the absence of doxicycline after sort 1 (panel B). Again 50000 cells were sorted within the sorting gate. Sort 3 shows cells 7 days after sort 2 incubated in the presence of 1 µg/ml doxicycline for 12 h. Single clones were sorted within the sorting gate and propagated to generate clonal cell lines or 50000 cells were sorted to generate cell pools expressing the reporter constructs in a doxycycline-dependent manner.

Three days after retroviral transduction, 1 µg/ml doxicycline was added to the culture medium for 12 h. Following this incubation period, cells were detached from culture plates using cell dissociation buffer and processed for flow cytomery. Dead cells were excluded by staining with propidium iodide which intercalates into the DNA after membrane damage (Crissman et al., 1976).
Based on GFP fluorescence using a FACSVantage sorting device, 50000 cells from

each cell line were isolated (figure 3.2, panel A). The obtained pools of cells were incubated for 7 days in the absence of doxicycline followed by the isolation of 50,000 cells from each population that did not display any GFP fluorescence at this point (figure 3.2, panel B). Each population was now cultured for another 7 days including 12 h in the presence of 1 µg/ml doxicycline at the end of this period (figure 3.2, panel C) and single cells were isolated by FACS-sorting based on GFP fluorescence.

3.1.1 Verification of the stable integration of FGF2-GFP into the genome of CHO cells

After retroviral transduction, the integration of the FGF2-GFP construct into the CHO genome was verified.

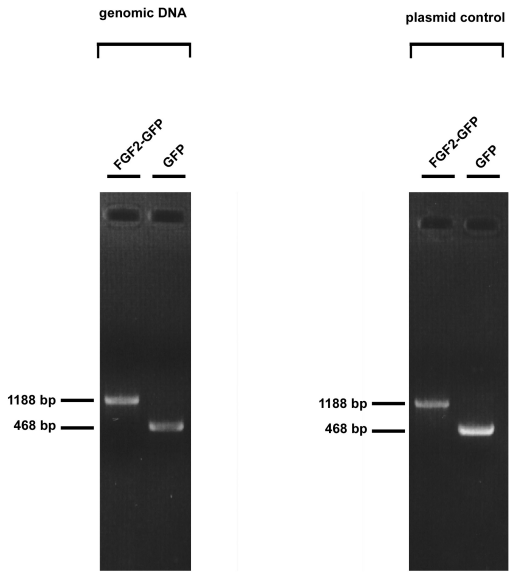

Figure 3.3: PCR analysis to verify integration of FGF2-GFP into the genome of CHO cells.
Genomic DNA was extracted from CHO cells grown on a culture plate (Ø 10 cm) to 100% confluency. After cell lysis a PCR with primers complementary to the flanking LTR of the retroviral system was performed. PCR from genomic DNA (10% of total), as well as from original plasmid (10% of total, positive control) were subjected to electrophoresis on a 1% agarose gel and visualized using the Biorad Geldoc System.

Therefore, the corresponding cells from a 100% confluent culture plate (∅ 10 cm) were lysed, the genomic DNA was extracted and a PCR using genomic DNA as a template was performed, using specific primers complementary to the long terminal repeats (LTR) at the 5´and 3´ends of the retroviral genome.

As depicted in figure 3.3, the PCR analysis of genomic DNA revealed the presence of DNA fragments of the expected size of 1188 bp for FGF2-GFP and 468 bp for

GFP, respectively. The same size of PCR products was observed for the control reaction using the original vector for retroviral transduction. This experiment confirmed the stable integration of FGF2-GFP into the genome of CHO host cells.

3.1.2 Characterization of $CHO_{FGF2\text{-}GFP}$ and CHO_{GFP} cells employing fluorescence microscopy, Western blotting and FACS analysis

The doxicycline dependent expression of FGF2-GFP was characterized employing Fluorescence Microscopy, Western blot and FACS analysis. For all experiments, cells were incubated in the presence of doxycyline (1 µg/ml) for 16 h to induce the expression of the reporter protein. As a control, cells were grown in the absence of doxycyline.

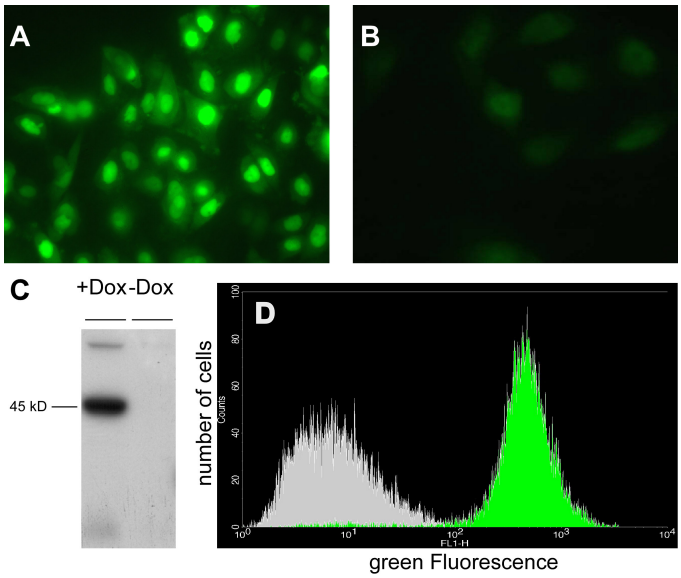

Figure 3.4: Characterization of $CHO_{FGF2\text{-}GFP}$ cells.
The model cell line generated was characterized with regard to doxicycline dependent protein expression based on fluorescence microscopy (**A**, +dox; panel B, -dox), Western blot analysis of doxycyline dependent protein expression (**C**) and analysis of doxicycline dependent protein expression based on FACS (**D**). Fluorescence microscopy. Cells were grown on cover slips to 50% confluency and incubated for 16 h in presence (**A**, 1 µg/ml) and absence (**B**) of doxycyline and analyzed employing fluorescence microscopy (oil immersion objective, 63x, identical exposure time). Western blot analysis (**C**). Total cell lysates from a confluent 6-well plate were subjected to SDS-PAGE (20 µg/lane) followed by Western blot analysis employing affinity-purified anti-GFP antibodies. FACS analysis (**D**). Cells were grown on 10 cm plates to 90% confluency and incubated in absence (grey histogram), and in presence of doxicycline (dark grey histogram), detached by cell dissociation buffer (CDB) and analyzed by flow cytometry using affinity-purified anti-GFP antibodies and PE-conjugated mouse anti-rabbit antibodies.

Fluorescence microscopy was performed after fixation of cells grown on cover slips to a confluency of about 50%. GFP-derived fluorescence was detectable in the presence of doxicycline (A), indicating the expression of the FGF2-GFP fusion protein. GFP-derived fluorescence was not detectable in cells not induced with doxicycline (B).

A western blot analysis was performed after lysis of cells with SDS-containing buffer, followed by separation of total cell lysates (20 µg/lane) on an SDS-gel, transfer to a PVDF membrane and immunodetection using affinity-purified anti-GFP antibodies. After inducing the cells with doxicycline an immunoreactive band with an apparent molecular weight of 45 kDa corresponding to the expected size of FGF2-GFP was observed (C, +dox). Without induction, FGF2-GFP expression could not be observed (C, -dox).

For FACS experiments, cells were grown on culture plates (∅ 10 cm) to about 90% confluency. The cells were detached using cell dissociation buffer (CDB). The expression level was detected by exciting GFP with a blue laser at 488 nm. $CHO_{FGF2\text{-}GFP}$ cells not induced to express the fusion protein were used to calibrate the flow cytometer. The cells intrinsic fluorescence (autofluorescence) was thereby manually set to 10 arbitrary units. Inducing the expression of FGF2-GFP with doxicycline led to an approximately 50-100 fold increase of GFP-derived fluorescence as compared to autofluorescence (D).

As demonstrated by all three independent methods, FGF2-GFP expression was strictly regulated by the doxicycline-dependent transactivator system, as FGF2-GFP was exclusively expressed in the presence of doxicycline.

3.2 Establishing an in vivo system to quantitatively asses FGF2-GFP secretion

FGF2 binds to low and high affinity receptors present on the cell surface which mediate its role as a growth factor. These molecules are on the one hand high-affinity FGF-receptors (FGFR1-4) and on the other hand receptors like heparan sulfate proteoglycans (HSPG) and the glycolipid GM_1. Since CHO cells lack high affinity FGF-receptors (Rusnati et al., 2002), binding of FGF2 to the cell surface is only mediated by heparan sulfate proteoglycans and the glycolipid GM1. Following its secretion, FGF2 binds to these low affinity receptors and therefore, is detectable with specific antibodies on the cell surface of non-permeabilized cells.

3.2.1 Secreted FGF2-GFP is detected on the cell surface of CHO cells

Since an intact plasma membrane is impermeable for antibodies, only secreted FGF2-GFP, bound to the cell surface is detectable with FGF2- or GFP-antibodies and can be quantified using flow cytometry. To verify this detection method, the following experiments were performed:

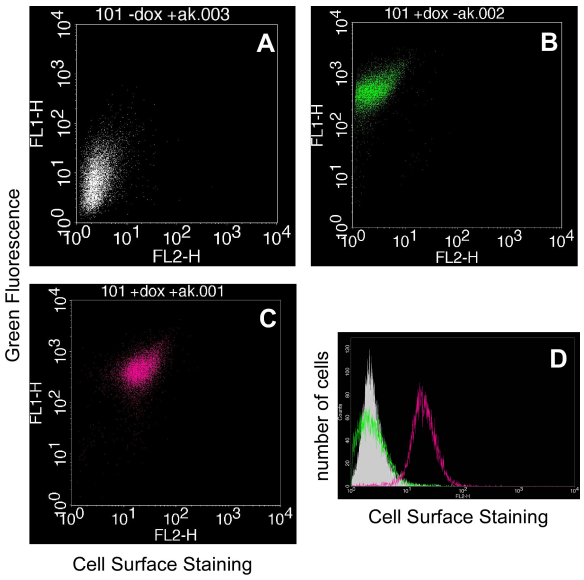

Figure 3.5: FGF2-GFP is detected on the cell surface of CHO cells.
Cells were grown for 18 hours at 37° C under the conditions indicated followed by dissociation from the culture plates employing a protease free protocol. The cell suspension was then processed for FACS analysis as indicated. Panel A to C represent dot blots, blotting total GFP-derived fluorescence against cell surface derived PE fluorescence. Panel A, cells grown in absence of doxicycline. Cells grown in presence of doxicycline and processed without (panel B) and with antibodies (panel C, 1:30 anti-GFP; 1:300 goat-anti-rabbit PE-conjugated). Panel D represents the corresponding histograms of the cell surface staining. The colours correspond to the conditions shown in panel A to C.

$CHO_{FGF2\text{-}GFP}$ cells grown on culture plates (∅ 10 cm) to a confluency of about 90% in presence or absence of doxicycline (1 µg/ml) were detached using a protease free reagent (cell dissociation buffer, CDB) and processed with primary antibodies (affinity-purified anti-GFP antibodies, 1:30, 1h), followed by secondary antibody treatment (Phycoerythrin (PE)-coupled, 1:300, 30 min) and FACS analysis. Non-induced cells do not express the fusion protein and did not show any signal in GFP-derived fluorescence as well as in cell surface staining (A, white dot plot).

Cells cultivated with doxicycline (1 µg/ml) were characterized by an increased GFP-derived fluorescence (50-100 fold) and Phycoerythrin (PE)-derived cell surface staining (10-20 fold) as compared to non-induced cells (C, pink dot plot). Without antibody processing, GFP-derived fluorescence, but no cell surface staining could be detected (B, green dot plot). The data described above are also shown as an overlay

of histograms (D).

This experiment confirmed that FGF2-GFP is translocated to the cell surface and can be detected by specific antibodies. Accordingly, PE-derived fluorescence corresponding to cell surface localized FGF2-GFP could only be observed when FGF2-GFP expression was induced by doxicycline, demonstrating the monospecificity of the affinity-purified anti-GFP antibodies used.

3.2.1.1 Cell surface staining is removable by trypsin and heparin treatment

To ensure that PE-derived fluorescence exclusively represents FGF2-GFP bound to the cell surface, a control experiment was conducted. In this experiment, the proteolytic activity of trypsin was used to degrade cell surface proteins as for example heparan sulfate proteoglycans.

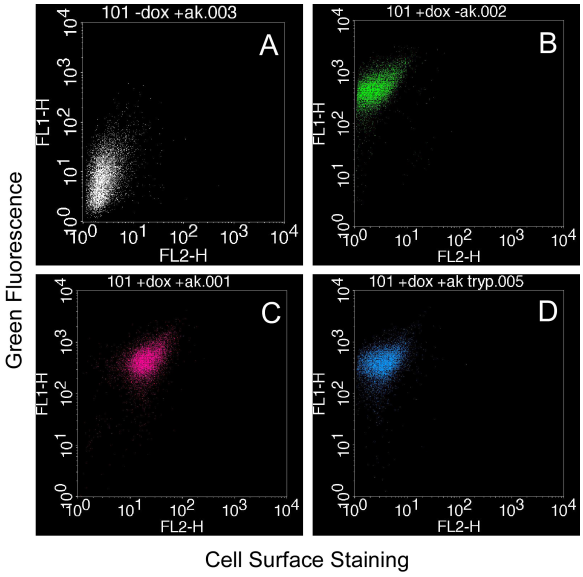

Figure 3.6: Trypsin treatment of cells expressing FGF2-GFP reduces the signal for fusion protein bound to the cell surface.
Cells were grown on culture plates (Ø 10 cm) to a confluency of 90%, incubated in absence (panel A) and presence of doxicycline (1µg/ml, 18h, panel B-D), followed by detachment of cells using cell dissociation buffer (A-C) or trypsin/EDTA (0.125% (v/v), 10 min). Cells were processed without (panel B) and with anti GFP primary antibodies and PE coupled secondary antibodies and analyzed by FACS analysis (panel A, C, D).

Cells were cultivated on culture plates (∅ 10 cm) to a confluency of about 90% in absence and presence of doxycyline (1 µg/ml, 18h), detached from the culture plate using either cell dissociation buffer (Invitrogen) or 0.125% (v/v) trypsin/EDTA, processed with primary and secondary antibodies and analyzed by flow cytometry (A, white dot plot). The cells grown in absence of doxicycline did not show any GFP-derived fluorescence or cell surface staining (A, white dot plot).

However, cells exposed to doxicycline (1 µg/ml) were characterized by increased GFP-derived fluorescence (50-100 fold), as well as cell surface staining (10-20 fold), if cells were processed with antibodies (C, pink dot plot). Without antibody processing, GFP-derived fluorescence, but no cell surface staining was detected (B, green dot plot).
FGF2-GFP bound to the cell surface could be removed from the cell surface by trypsin treatment (10 min, 0,125% trypsin/EDTA (v/v), D) since the data obtained were quantified as shown in the following figure 3.7:

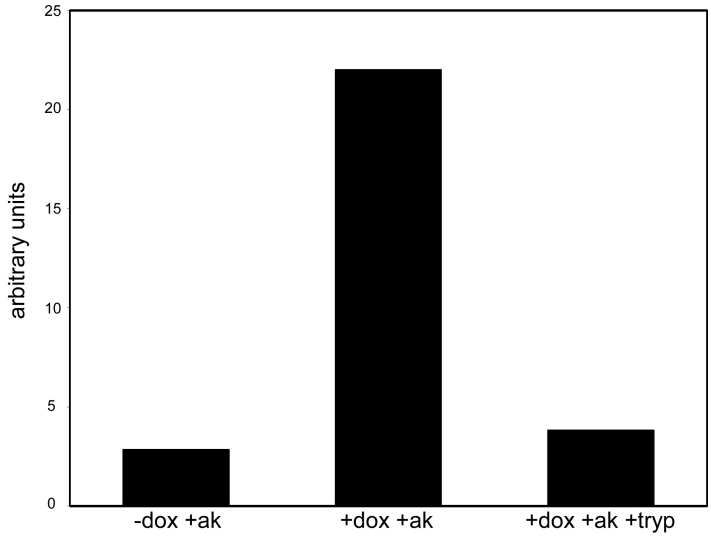

figure 3.7: Quantification of cell surface staining. Mean value of fluorescence detected on the cell surface is shown.

The diagram shows a 7fold increase of the signal for cell surface staining upon doxycyline incubation. When cells were treated with trypsin, the cell surface signal was reduced to background level. Thus, cell surface staining is sensitive to trypsin treatment, which implicates that FGF2-GFP is bound to the cell surface and removable by proteolytic degradation of cell surface proteins.

A second control experiment was conducted to verify that PE-derived fluorescence corresponds to FGF2-GFP bound to the cell surface. Therefore heparin, a low-molecular-weight compound, was used which is competing with heparin sulfate proteoglycans for the binding to FGF2. Addition of heparin to cells should elute FGF2-GFP associated with plasma membrane-localized heparan sulfate proteoglycans.

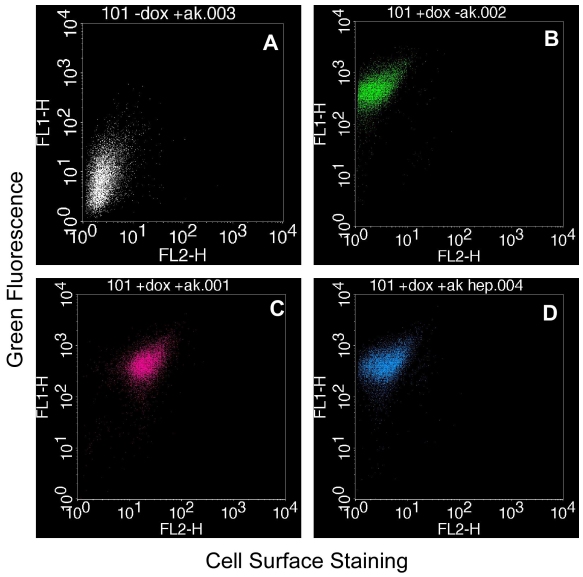

Figure 3.8: Heparin treatment of cells expressing FGF2-GFP reduces the signal for fusion protein bound to the cell surface. Cells were grown on a culture plate (Ø 10 cm) to a confluency of 90%, incubated in absence (panel A) and presence of doxicycline (1µg/ml, 18h, panel B-D), followed by detachment of cells using cell dissociation buffer (CDB). During detachment, Heparin (125µg/ml) was added to CDB (panel D). Cells were then processed without (panel B) and with antibodies (panel A, C; D).

Cells were cultivated on culture plates (∅ 10 cm) to a confluency of about 90% in absence and presence of doxycyline (1 µg/ml), detached from the culture plate using either cell dissociation buffer (Invitrogen) or heparin (125 µg/ml), processed with primary and secondary antibodies and analyzed by flow cytometry (A, white dot plot). The cells grown in absence of doxicycline did not show any GFP-derived fluorescence or cell surface staining (A, white dot plot). However, cells exposed to doxicycline (1 µg/ml) demonstrated an increased GFP-derived fluorescence (50-100 fold), as well as cell surface staining (10-20 fold), if cells were processed with antibodies (C, pink dot plot). Without antibody processing, GFP-derived fluorescence, but no cell surface staining was detected (B, green dot plot). In conclusion, treating cells with heparin (125 µg/ml) during detachment and first antibody incubation removed the cell surface signal demonstrating FGF2-GFP bound to the cell surface since the data obtained were quantified as shown in the following figure 3.9:

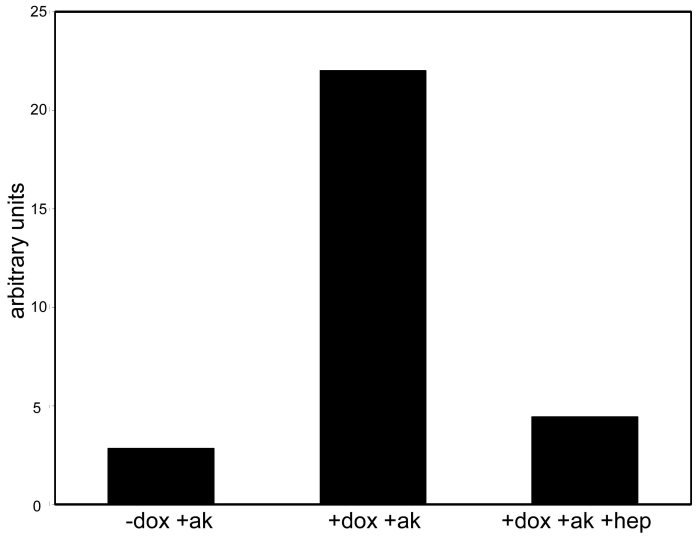

figure 3.9: Quantification of cell surface staining. Mean value of the fluorescence detected on the cell surface is shown.

The diagram displays a 7 fold increase of the cell surface signal after inducing fusion protein expression with doxycyline. When cells were treated with heparin, the signal for cell surface staining was reduced to background level.

3.2.1.2 FGF2-GFP binding capacity to the cell surface

To analyze that the cell surface signal derived from plasma membrane associated FGF2-GFP is limited by the amount of binding sites available, the total binding capacity of $CHO_{FGF2\text{-}GFP}$ cells was analyzed using recombinant His_6-FGF2. This His_6 tagged version of FGF2 was generated based on a PCR product corresponding to the 18 kDa isoform of FGF2 and the vector pET15b (Novagen). Recombinant His6-FGF2 were expressed in *E. coli* BL21 (DE3) cells and purified from a 100000 g supernatant of homogenized cells by using Ni-NTA agarose (Qiagen) according to standard procedures.

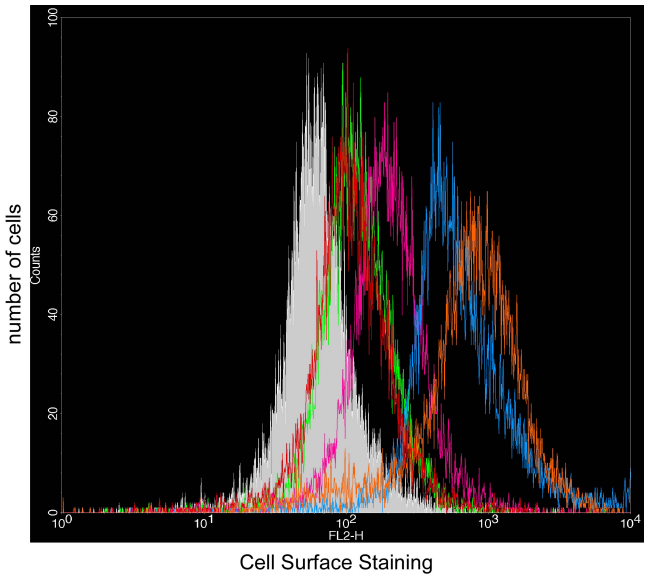

Figure 3.10: Binding capacity of the cell surface as detected in presence of doxycyline.
CHO-$_{FGF2\text{-}GFP}$ cells were cultivated on culture plates (Ø 10 cm) and incubated for 18 h with doxicycline (1µg/ml). The confluent culture dish was then divided into 6 equal samples. 30 min before antibody processing (described above) recombinant FGF2 (His_6-tagged) in different quantities (1ng-red, 10ng-green, 50ng-pink, 100ng-blue, and 500ng-orange) was added to the cells. A FACS analysis was performed after antibody processing.

Therefore, CHO cells were cultivated on culture plates (∅ 10 cm) in presence of doxicycline (1 µg/ml, 18h) to a confluency of about 100% and split into 6 equal samples followed by incubation for 30 min at 4°C with recombinant His_6-FGF2 in different amounts (1ng-red, 10ng-green, 50ng-pink, 100ng-blue, and 500ng-orange). Antibody processing with affinity-purified anti-FGF2 antibodies and PE-coupled secondary antibodies was performed and the samples were analyzed by flow cytometry since the data obtained were quantified as shown in the following figure 3.11:

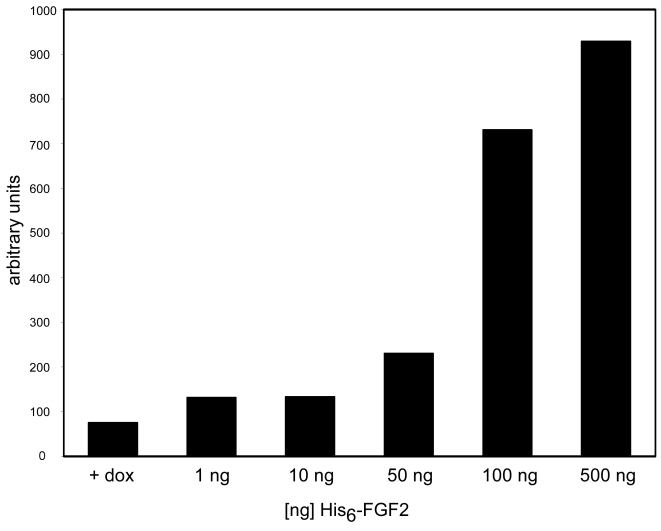

Figure 3.11: Quantification of binding capacity of exogenously added FGF2 compared to secreted, endogenous FGF2.
Mean values as arbitrary units of the fluorescence detected on the cell surface are shown.

Already the addition of minor amounts of His-FGF2 (1ng, 10 ng) to FGF2-GFP secreting cells led to an enhanced signal for cell surface staining, when compared to cells secreting FGF2-GFP without addition of recombinant FGF2. A significantly higher signal for FGF2 derived cell surface staining was obtained by adding higher amounts of recombinant His_6-FGF2 to the samples. The cell surface signal for 500ng His_6-tagged FGF2 was about 10 fold higher when compared to the cell surface signal for secreted endogenous FGF2-GFP. This indicates that the binding capacity of $CHO_{FGF2\text{-}GFP}$ cells for FGF2 is at least 10 times higher than the amount of FGF2-GFP externalized from these cells. Therefore, the secretion signal observed for endogenous FGF2-GFP is not limited by the amount of heparan sulfate proteoglycans available on the cell surface.

3.2.2 Characterization of FGF2-GFP secretion regarding kinetics, unspecific release and sensitivity to ouabain

To study the kinetics of FGF2-GFP export, the following experiment was conducted. $CHO_{FGF2\text{-}GFP}$ cells were cultivated on 6 well plates in presence of doxicycline (1 µg/ml) to a confluency of about 90% for different time periods (6 h, 12 h, 24 h, 48 h, 72)

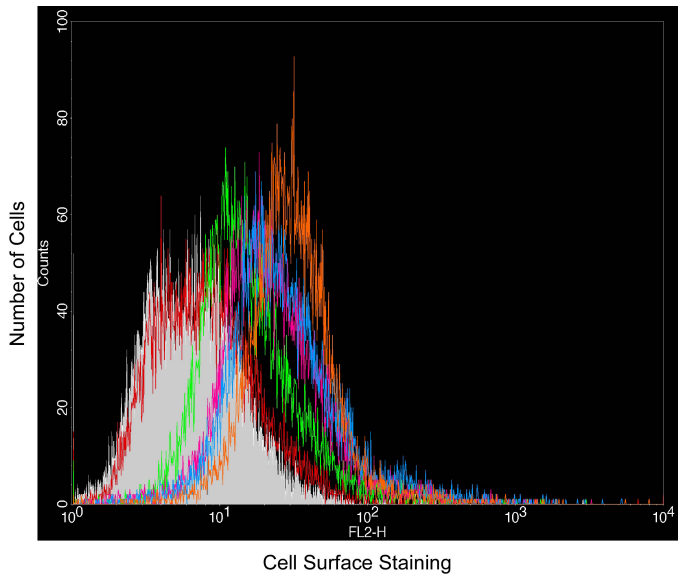

figure 3.12: Kinetics for cell surface staining mediated by FGF2-GFP.
$CHO_{FGF2\text{-}GFP}$ cells were cultivated on culture plates (Ø 10 cm) to a confluency of 90% and incubated with doxicycline (1 µg/ml) for different time periods (6h-red, 12h-green, 24h-pink, 48h-blue, and 72h-orange). After processing with antibodies (1:30 anti-GFP; 1:300 goat anti-rabbit PE coupled) a FACS analysis was performed.

After detachment from the culture plate using CDB, cells were processed with anti-GFP and PE-conjugated goat anti-rabbit antibodies, and analyzed by FACS analysis. To adjust background levels, $CHO_{MCAT/TAM2}$ cells were used as a negative control.

When cells were exposed to doxicycline (1 µg/ml) for 6 h, the signal for FGF2-GFP bound to the cell surface was almost not enhanced, compared to control cells. Incubation of cells with doxycyline for 12 h led to a significant signal for cell surface staining which was further enhanced by prolonging the doxicycline incubation time up to 72 h. The raw data obtained were subjected to a weight curve fit and are representative of two individual experiments.

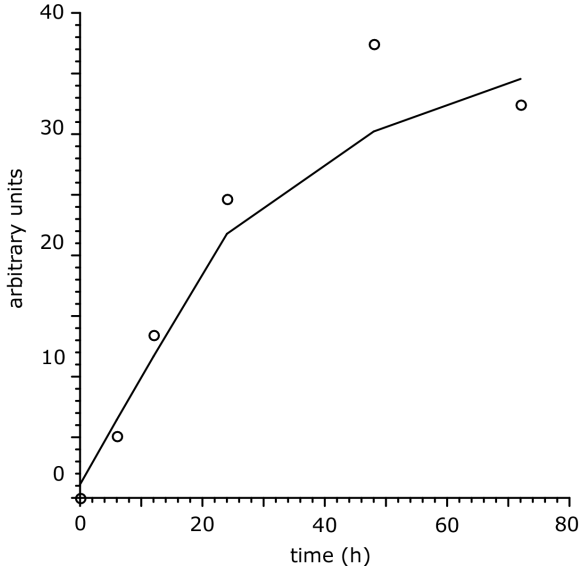

figure 3.13: Kinetic analysis of FGF2-GFP export. $CHO_{FGF2\text{-}GFP}$ cells were grown in the presence of doxicycline for the times indicated followed by FACS processing, including antibody treatment, as described in Materials and Methods. The raw data have been subjected to a weighted curve fit and are representative of two independent experiments.

The amount of secreted FGF2 increases in a linear manner for 48 hours, but the signal reaches saturation levels after an incubation time of 48 h, indicating steady state conditions.

To verify that the signal detected on the cell surface does not reflect unspecifically released material derived from damaged cells but rather secreted FGF2-GFP the following experiments were conducted: Non-induced $CHO_{FGF2\text{-}GFP}$ cells were incubated with a supernatant derived from homogenized $CHO_{FGF2\text{-}GFP}$ cells, which were induced to express the fusion protein.

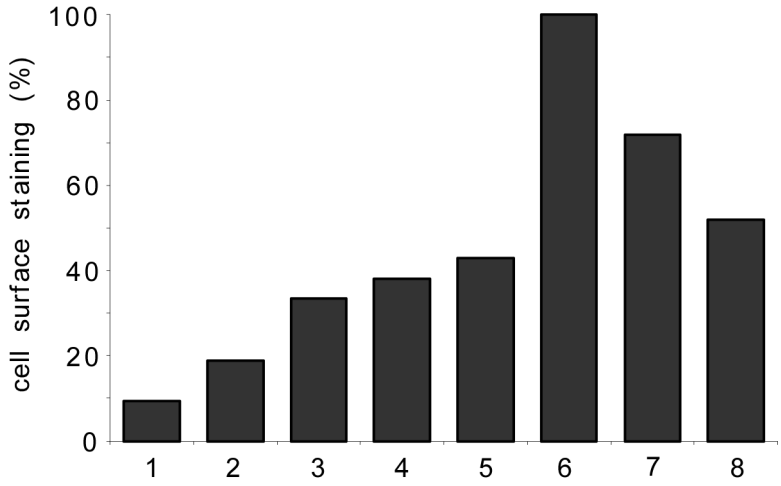

Figure 3.14: Biochemical analysis of FGF2 secretion with regard to unspecific release and sensitivity to ouabain.
$CHO_{FGF2\text{-}GFP}$ cells were grown in the absence of doxicycline followed by the addition of various amounts of a supernatant derived from homogenized $CHO_{FGF2\text{-}GFP}$ cells that were grown on a culture plate (∅ 10 cm) to 100% confluency and incubated for 48 hours in the presence of doxicycline (lanes 1-5). Based on cell number, 0% (lane 1), 2.5% (lane 2), 5% (lane 3), 7.5% (lane 4) and 10% (lane 5) of this supernatant was added to $CHO_{FGF2\text{-}GFP}$ cells grown in the absence of doxicycline. The PE-derived FGF2-GFP cell surface signal was then compared with the corresponding signal of $CHO_{FGF2\text{-}GFP}$ cells grown for 48 hours in the presence of doxicycline (set to 100%, lane 6). Lanes 7 and 8 refer to experiments under the same conditions as those in lane 6 with the exception that during the whole course of the experiment, 1 mM and 5 mM ouabain, respectively, were added to the culture medium. The data are representative of two independent experiments.

Defined amounts of this lysate corresponding to 0, 2.5, 5, 7.5 or 10% of homogenized cells (lanes 1-5) were added to $CHO_{FGF2\text{-}GFP}$ cells not expressing the reporter molecule, followed by detachment, antibody processing and FACS analysis. The observed signal for cell surface staining of the 10% condition accounted for up to 40% of the signal detected for secreted fusion protein exported by $CHO_{FGF2\text{-}GFP}$ cells (lane 6). During all FACS experiments the amount of dead cells was monitored by the addition of propidium iodide (PI), a low molecular weight dye that only enters damaged cells. Typically, about 2-3% of the total cell population was found to be positive for PI. Thus, the population of FGF2-GFP found on the cell surface (lane 6) can not be derived from damaged cells but rather was secreted by a specific transport mechanism.

This conclusion is further substantiated by the observation that the appearance of FGF2-GFP on the cell surface can be partially inhibited (1mM reduced to 70%; 5mM reduced to 55% as compared to wild-type levels) by ouabain (Figure 3.14; lanes 7, 8).

3.2.3 Biochemical analysis of FGF2-GFP secretion

To further characterize the model cell lines, biochemical experiments were conducted to analyze the extracellular localization of the reporter proteins. Cells were exposed

to doxicycline for 48 hours at 37°C in the presence of heparin (125 µg/ml) in order to prevent FGF2 binding to plasma-membrane-associated HSPGs.

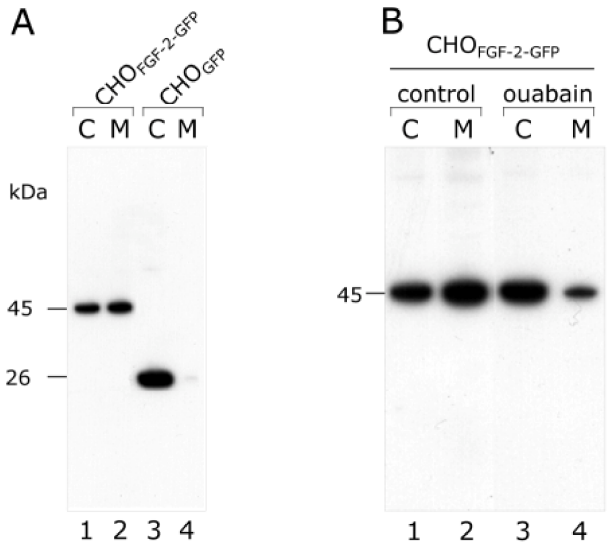

Figure 3.15: Biochemical analysis of FGF2 fusion protein secretion.
The various cell lines indicated were analyzed biochemically with regard to secretion of the reporter molecules (A). Cells were grown on culture plates (Ø 10 cm) in the presence of doxicycline and heparin (125 µg/ml) for 48 hours at 37°C. FGF2-GFP was affinity-purified from detergent cell extracts and the medium by using heparin sepharose. 1% (cells) and 15% (medium) of the eluates were subjected to SDS-PAGE. In case of CHO_{GFP} cells, 1% of both cells and medium were directly subjected to SDS-PAGE (the amount of the medium loaded onto the gel had to be reduced to 1% of the total material because of the high protein concentration). Affinity-purified anti-GFP antibodies were used to detect the reporter molecules. Even after prolonged exposition, no GFP signal could be observed in lane 4. To analyze whether FGF2-GFP is released by a specific mechanism, $CHO_{FGF2\text{-}GFP}$ cells were grown for 48 hours at 37°C in the presence of doxicycline, 125 µmg/ml heparin and 25 µM ouabain, a drug known to inhibit FGF2 export (B). The samples were processed as described for panel A.

After dissociation of cells from the culture plates using cell dissociation buffer, residual cell surface-associated FGF2-GFP was removed from the plasma membrane by heparin and the corresponding cell-free supernatant was combined with the original growth medium. In parallel, detergent extracts from the cellular fractions were prepared. FGF2 fusion proteins were affinity-purified from both the cellular and the medium fractions using heparin sepharose (for more details see Material and Methods, section 2.3.3). FGF2-GFP was then eluted with SDS-containing sample buffer followed by SDS-PAGE and western blot analysis using affinity-purified anti-GFP antibodies and ECL detection as described in section 2.3.2. FGF2-GFP derived from $CHO_{FGF2\text{-}GFP}$ cells was detectable in the supernatant of cultured cells (A, lane 2). Approximately 10% of the total amount of FGF2-GFP fusion protein was found to be secreted. In contrast, GFP could not be detected in the supernatant (A, lane 4) although GFP was found in the total lysate derived form CHO_{GFP} cells (A, lane 3). In a second set of experiments, depicted in panel B, the same biochemical assay as described above was used, however, Ouabain (25 µM) was added to cells exposed to doxicycline (1 µg/ml) and heparin (125 µg/ml) for 48 h

at 37°C. Ouabain, which belongs to the family of G-strophantins (Petersen and Poulsen, 1967), is a glycoside, which blocks the sodium-potassium ATPase (Riehle et al., 1991), and has been shown to partially inhibit the export of FGF2 (Florkiewicz et al., 1998; Dahl et al., 2000). FGF2-GFP secretion from cells incubated with ouabain was significantly reduced when compared to FGF2 secretion without exposure to ouabain. The ratio of the relative amounts of FGF2-GFP in lanes 1 and 2 of panel B (control) is clearly higher than the corresponding ratio of lanes 3 and 4 of panel B (ouabain). Both experiments demonstrate that the export of FGF2-GFP is dependent on the FGF2 part of the fusion protein since GFP is not exported from CHO cells and that the export of FGF2-GFP fusion proteins from CHO cells is partially inhibited by the glycoside ouabain, indicating that FGF2 is secreted by a specific transport mechanism depending on the Na^+/K^+-ATPase.

3.2.4 Analysis of FGF2-GFP secretion by confocal microscopy

To verify the results obtained by FACS analysis using an independent method, experiments based on immunofluorescence confocal microscopy (see Materials and Methods) were conducted. $CHO_{FGF2\text{-}GFP}$ and CHO_{GFP} cells were grown on glass cover slips for 24 hours in absence or presence of doxicycline.

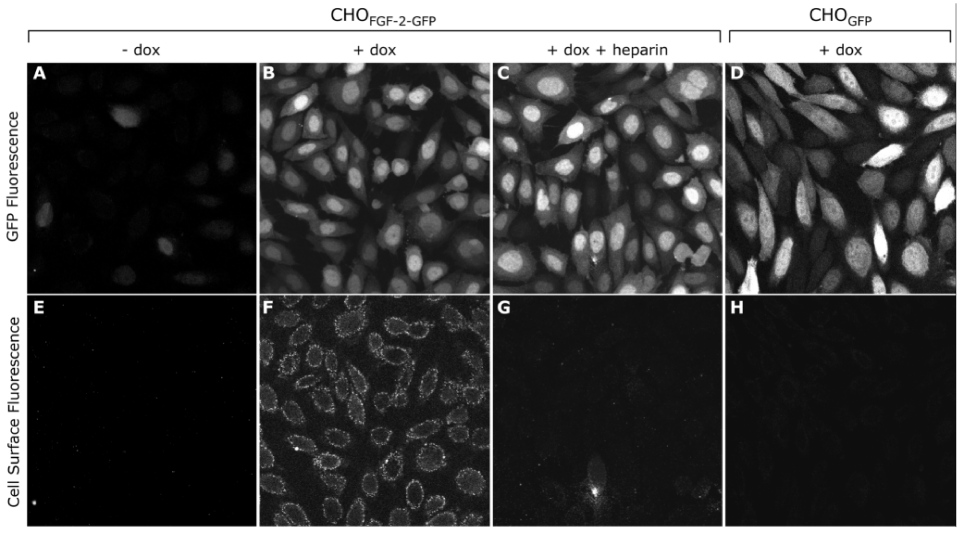

Figure 3.16: Translocation of FGF2-GFP to the surface of the plasma membrane, as determined by confocal microscopy. $CHO_{FGF2\text{-}GFP}$ and CHO_{GFP} cells were grown on glass cover slips for 24 hours at 37°C in the absence or presence of doxicycline. Where indicated, cells were washed with PBS containing 125 µg/ml heparin. Following fixation using 3 % paraformaldehyde, cells were processed with affinity-purified anti-GFP antibodies and secondary antibodies coupled to an Alexa546 fluorophore. The specimens were embedded using Fluoromount G and viewed with a Zeiss LSM 510 confocal microscope. The results shown are representative of four independent experiments.

Samples were washed with PBS or with PBS containing heparin (125 µg/ml) followed by a fixation procedure using paraformaldehyde (3%). Samples were then processed

with affinity-purified anti-GFP antibodies and secondary antibodies coupled to an Alexa546 fluorophore. Finally samples were embedded using Fluoromount G and visualized with a Zeiss LSM 510 confocal microscope.

As shown in figure 3.16, cells were analyzed for GFP fluorescence (A-D) and cell surface staining (E-H). Without addition of doxicycline, GFP-derived fluorescence and cell surface-derived fluorescence was at background levels (A). After induction of expression with doxicycline, FGF2-GFP appeared in the cytoplasm and the nucleus of CHO cells (B), and was also detected in spots on the cell surface (F). Consistent with the FACS experiments shown in figure 3.8, heparin treatment did not influence protein expression as the GFP fluorescence in the cytoplasm and nucleus was not altered (compare B and C). However, the heparin treatment removed FGF2-GFP from the cell surface, resulting in a loss of signal for cell surface staining to background levels (G). CHO cells expressing GFP showed a cytoplasmic fluorescence (D), but cell surface signals were not detected using anti-GFP antibodies (H). These results are fully consistent with the data obtained by FACS analysis.

3.2.5 Secreted biosynthetic FGF2-GFP is targeted to non-lipid raft microdomains

To assess the structural organization of cell-surface-localized FGF2-GFP in more detail, an immunofluorescence confocal microscopy at high magnification was performed using the same protocol as in section 3.2.5.

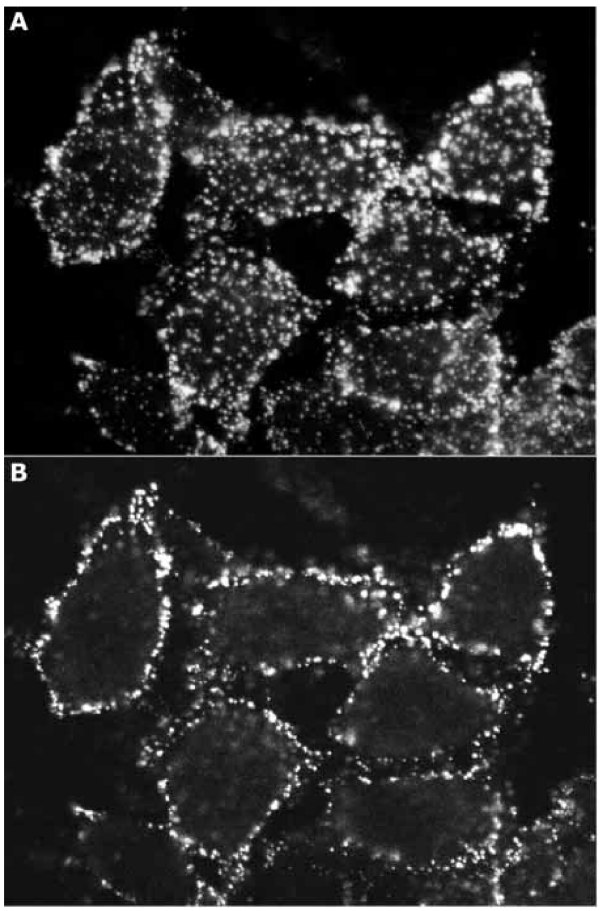

Figure 3.17: Identification of FGF2-GFP-positive microdomains on the extracellular surface of CHO cells.
$CHO_{FGF2\text{-}GFP}$ cells were grown on glass cover slips for 24 h at 37°C in the presence of doxicycline (1 µg/ml). Processing for confocal microscopy was performed as described in the legend of Fig. 3.15. (A) Merged image of 16 confocal planes spanning the whole depth of the cells. (B) A confocal plane close to the bottom of the cells where they are attached to the glass cover slips.

As shown in panel A of figure 3.17 (merged image of 16 confocal planes), FGF2-GFP did not display a homogenous staining of the plasma membrane but rather appeared in bright spots representing distinct microdomains. These microdomains represent structures exclusively localized to the cell surface since sequential scanning of focal planes (one of which is shown in B) revealed the absence of any intracellular staining.

To analyze whether the observed microdomains are related to lipid rafts, the detergent solubility of plasma membrane-associated FGF2-GFP was characterized.

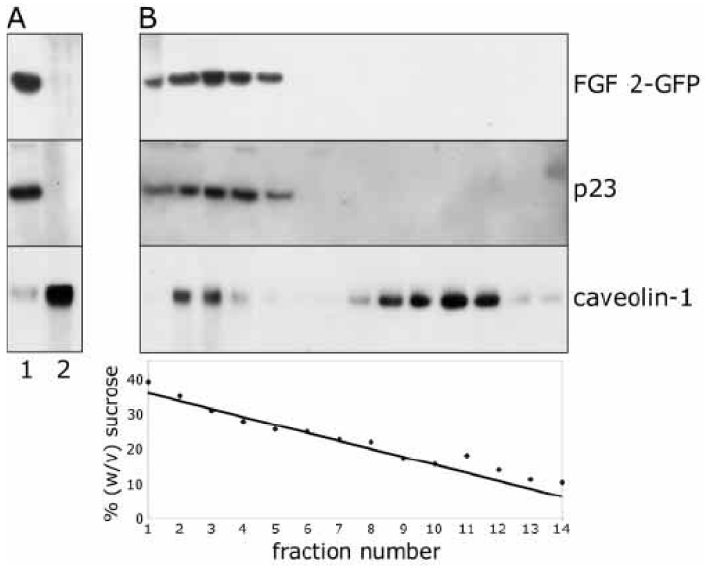

figure 3.18: FGF2-GFP-positive microdomains are distinct from lipid rafts.
$CHO_{FGF2\text{-}GFP}$ cells were grown on culture plates (Ø 15 cm) for 48 h at 37°C in the presence of doxicycline (1 µg/ml). Following a wash procedure using PBS the cells were scraped off the culture plates in a sucrose-containing buffer. Cell breakage was achieved by using a Balch homogenizer followed by differential centrifugation at 1000 g and 5000 g to sediment nuclei and cell debris. The resulting supernatant was loaded on top of a 20% (w/v) sucrose cushion and centrifuged for 60 minutes at 100,000 g in order to collect microsomal membranes freed of cytosolic proteins. The membrane sediment was resuspended in PEN buffer containing 1% (w/v) Triton X-100 at 4°C. While being resuspended several times using a 100 µl tip, the membrane suspension was kept on ice for 30 minutes. The samples were then divided and either subjected to ultracentrifugation in order to sediment detergent-insoluble complexes or adjusted to 40% (w/v) sucrose followed by flotation in a linear sucrose gradient. (A) Detergent-soluble fraction (lane 1), detergent-insoluble fraction (lane 2). (B) 14 fractions of the linear flotation gradient (lanes 1-14) with lane 1 containing the most dense sucrose fraction and lane 14 containing the lightest fraction. In the case of FGF2-GFP and p23 detection, 60% of each fraction was TCA-precipitated and applied to the gel; in the case of caveolin-1, 15% of each fraction was TCA precipitated and applied to the gel.

$CHO_{FGF2\text{-}GFP}$ cells were grown on a culture plate (∅ 15 cm) to a confluency of about 90% and incubated for 48h with doxicycline (1 µg/ml). After washing with PBS, cells were scraped off in sucrose-containing buffer, and were broken using a Balch homogenizer, followed by centrifugation at 1000 g and 5000 g in order to pellet nuclei and cell debris. The supernatant was loaded on top of a 20% (w/v) sucrose cushion and centrifuged for 60 minutes at 100000 g. The sedimented microsomal membranes, freed from cell debris, nuclei and soluble proteins were resuspended in PEN buffer containing Triton X-100 (1%) at 4°C. The samples were divided and either subjected to ultracentrifugation (sedimentation of detergent-insoluble fraction) or adjusted to 40% (w/v) sucrose followed by flotation in a linear sucrose gradient (A). The Golgi-localized transmembrane protein p23 (Sohn et al., 1996) was used as a non-lipid raft marker (Gkantiragas et al., 2001) and the plasma-membrane localized protein caveolin-1 as a classical lipid raft marker (Rothberg et al., 1992; Kurzchalia and Parton, 1999). P23 as well as FGF2-GFP could be detected only in the soluble fraction (lane 1), whereas caveolin-1 was almost exclusively found in the insoluble fraction (lane 2). Moreover, caveolin-1 could be detected in the light fractions, corresponding to about 15% (w/v) sucrose, of the flotation gradient (B). In contrast,

p23 and FGF2-GFP were exclusively localized to the bottom fractions of the gradient demonstrating that the microdomains observed by confocal microscopy were not related to lipid rafts. A formal possibility would be that a potential association of FGF2-GFP with lipid rafts could not be detected because the interaction of FGF2-GFP with cell surface HSPGs is detergent-sensitive which, in turn, would cause FGF2-GFP to appear in the supernatant of detergent-treated membranes. However, as demonstrated in chapter 3.2.4, FGF2-GFP could be affinity-purified from cellular detergent extracts by using heparin-sepharose, a method that mimics the interaction of FGF2 with heparan sulfate proteoglycans (Burgess and Maciag, 1989).

3.2.6 Intercellular spreading of exported biosynthetic FGF2-GFP

With the *in vivo* system developed it was possible to visualize and quantify secreted FGF2-GFP. In order to distinguish a translocation mechanism that involves a soluble intermediate between export and binding to proteoglycans from an integrated process where the export machinery directly delivers FGF2 to the proteoglycan binding site, a FACS and a confocal microscopy experiment were performed.
$CHO_{FGF2\text{-}GFP}$ cells and $CHO_{MCAT/TAM2}$ cells were used for FACS analysis. $CHO_{MCAT/TAM2}$ cells lack the FGF2-GFP reporter construct, which allows for discrimination between both cell lines based on GFP-derived fluorescence. Cells were grown on culture plates (∅ 10 cm) in presence of doxicycline (1 µg/ml, 24 h) to a confluency of about 90%, detached and processed with anti-GFP primary antibodies and PE-coupled secondary antibodies, followed by FACS analysis.

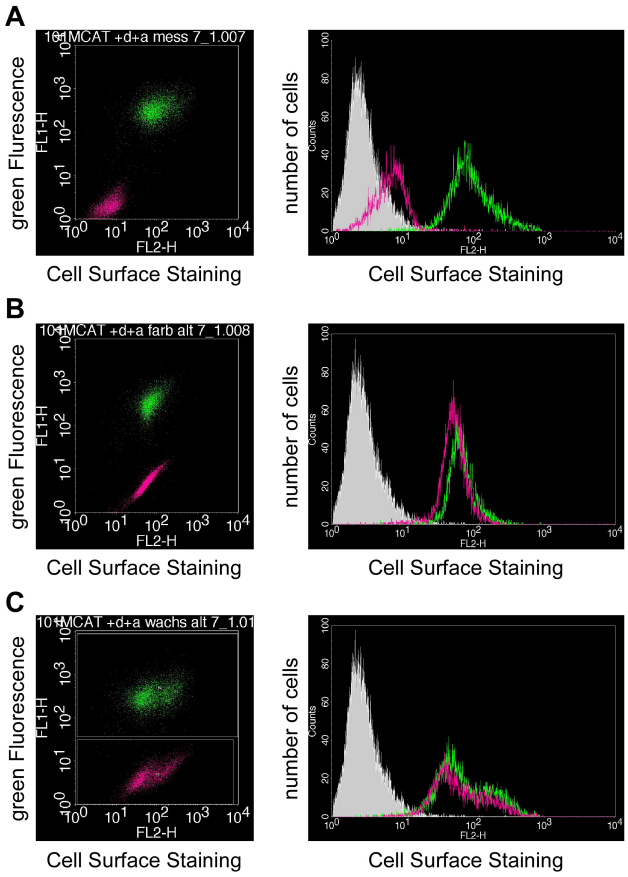

figure 3.19: Intercellular spreading mediated by antibody processing.
Both cell lines $CHO_{MCAT/TAM2}$ and $CHO_{FGF2\text{-}GFP}$ were cultivated separately on culture plates (Ø 10 cm) to a confluency of 60% and incubated with doxicycline for 24 h (1 µg/ml). Cells were processed by antibodies separately and combined prior to FACS analysis (A). Both cell lines were cultivated individually and incubated with doxicycline (1µg/ml). Cells were combined and processed with antibodies prior to FACS analysis (B). Both Cell lines were cultivated in one culture plate in the presence of doxicycline (1µg/ml) at a ratio of 1:1 followed by antibody processing and FACS analysis (C).

When the two different cell lines were cultivated and processed with antibodies separately and combined immediately prior to FACS analysis, a striking difference in cell surface staining for both cell lines was observed (A). When both cell lines were cultivated individually but combined for antibody processing, the signal for cell surface staining of both cell lines was still significantly discriminative (B). However, $CHO_{MCAT/TAM2}$ (pink) and $CHO_{FGF2\text{-}GFP}$ cells (green) did not differ from each other as clearly as in the experimental settings described above. If $CHO_{FGF2\text{-}GFP}$ and $CHO_{MCAT/TAM2}$ cells were cultivated together in a ratio of 1:1, followed by antibody processing, no difference in cell surface staining was detectable (C). This experiment reveals that FGF2-GFP secreted from the expressing cells spread to the cell surface of non-expressing cells.

A similar experiment was performed and analyzed using confocal microscopy to verify the data obtained by FACS analysis.

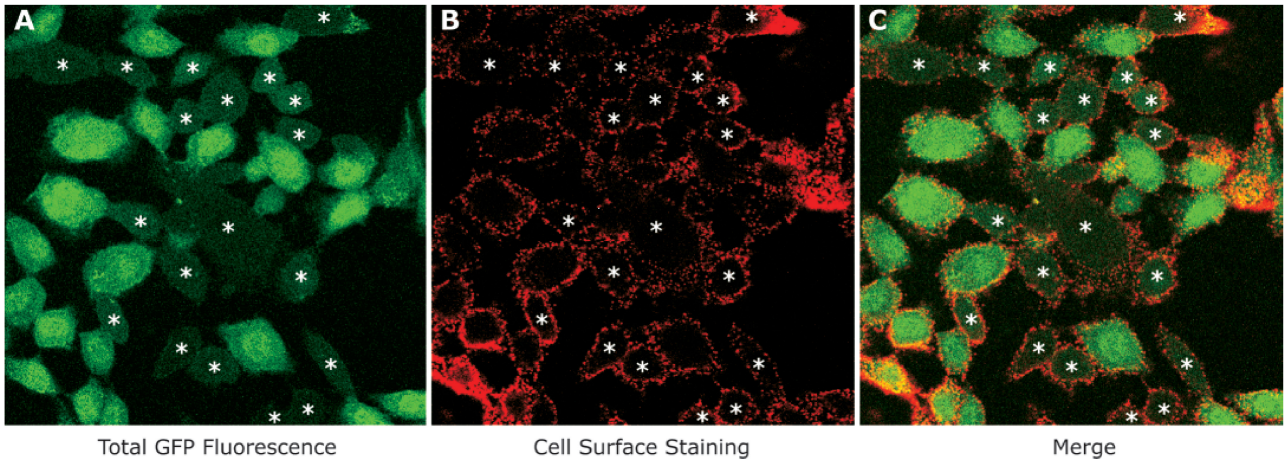

Figure 3.20: Intercellular spreading of secreted FGF2-GFP. $CHO_{FGF2\text{-}GFP}$ and $CHO_{MCAT/TAM2}$ cells were cultured on glass cover slips in a 1:1 ratio. Following incubation for 24 hours at 37°C in the presence of doxicycline, the cells were fixed with PFA and processed with affinity-purified anti-GFP antibodies. Primary antibodies were detected with anti-rabbit IgG antibodies coupled to Alexa546. The specimens were viewed using a Zeiss LSM 510 confocal microscope.

$CHO_{FGF2\text{-}GFP}$ and $CHO_{MCAT/TAM2}$ cells were co-cultivated in presence of doxicycline (1 µg/ml, 24 h, 37°C) in a ratio of 1:1 on cover slips to a confluency of 50-60%. After fixation without permeabilization using paraformaldehyde (3%) the cells were further processed with primary affinity-purified anti-GFP and secondary mouse anti-rabbit IgG antibodies coupled to Alexa546, embedded with Fluoromount G and visualized with a Zeiss LSM 510 confocal microscope. As shown in figure 3.20, $CHO_{MCAT/TAM2}$ cells did not express FGF2-GFP and showed no signal for GFP fluorescence but a cell surface signal was detected due to HSPG associated FGF2-GFP (marked with asterisk). These results implicate that after secretion, FGF2-GFP exists as a soluble intermediate, which can be transferred between cells and clusters on HSPGs accumulating in cell surface microdomains.

3.2.7 Refinement of FACS processings in order to prevent unspecific release

During the preparation for FACS analysis the cells were detached from the culture plates using CDB prior to antibody processing. This procedure might lead to an unspecific release of FGF2-GFP from damaged cells followed by cell surface binding and thus resulting in a falsely increased signal of cell surface staining. Therefore, an advanced FACS procedure was established where the antibody treatment was performed prior to cell detachment. The advantage over the old procedure is that

residual antibodies have been depleted when the cells were detached from the culture plate. Therefore, potential unspecifically released FGF2-GFP did not result in an APC-derived signal for cell surface staining.

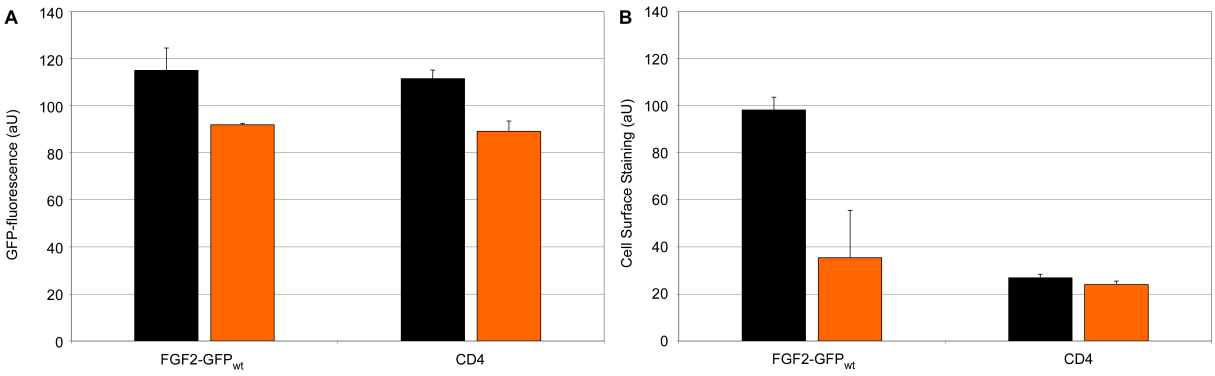

Figure 3.21: Comparison of standard and refined FACS procedure.
A GFP fluorescence. **B** Cell surface staining. $CHO_{FGF2\text{-}GFP}$ and CD4 positive CHO_{GFP} cells were grown on 6 well plates to a confluency of 50% and incubated with doxicycline (1µg/ml) for 16h at 37°C. Cells were either detached from the culture plate using cell dissociation buffer (CDB) prior to antibody staining (black bars) or antibody processing was performed while cells were attached to culture plates (red bars). The antibody treatment was equal for both FACS procedures; the only difference was the time point of cell detachment. The incubation with first antibody was for 1h at 4°C with affinity-purified anti-GFP antibodies followed by an incubation of 30 min at 4°C with a secondary goat anti-rabbit IgG coupled to APC (allophycocyanin).

For the establishment of the advanced FACS assay, $CHO_{FGF2\text{-}GFP}$ and CD4 positive CHO_{GFP} cells were used. In contrast to FGF2 which is secreted as a soluble protein, CD4 is an integral plasma membrane protein. Therefore, these cell lines serve as a control to verify if the accessibility of anti-CD4 antibodies is reduced due to steric hindrance when cells are attached to the culture plate. Therefore, cell lines were grown on 6 well plates to a confluency of 50% in presence of doxicycline (1 µg/ml) for 16h at 37°C. Both cell surface proteins were then detected by using specific antibodies for GFP and CD4. As shown in section 3.2.7, FGF2-GFP is able to spread between membranes. In contrast, CD4 is an integral membrane protein, which is not transferred between cells.

The standard protocol was performed by detaching the cells prior to antibody processing (affinity-purified anti-GFP antibody (1:50) at 4°C for 1h and secondary goat anti-rabbit IgG coupled to APC (1:750) at 4°C for 30 min; black bars). For the advanced FACS protocol, cells were processed with antibodies under the same conditions as described for standard protocol, but cell detachment was performed after antibody processing (red bars). CD4 was detected by an anti CD4 antibody and a secondary goat anti-rabbit antibody coupled to APC.

As shown in figure 3.21 panel A, the signal for GFP-derived fluorescence was slightly reduced using plate-labelling (advance protocol, red bars) compared to labelling in

suspension (standard protocol, black bars). Figure 3.21 panel B displays the signal for FGF2 and CD4 detected on the cell surface of the corresponding cell lines. A significant reduction of signal (approximately 50%) for FGF2-GFP bound to the cell surface was observed when the plate labelling method was used.
The signal for CD4 was constant comparing both labelling procedures, showing that the procedure does not influence the antibody detection of an integral membrane protein. The reduced signal for FGF2-GFP bound to heparan sulfate proteoglycans by using the plate labelling method might be caused by less amounts of unspecifically released fusion protein detectable on the cell surface by antibodies. Moreover, FGF2-GFP bound to the cell surface of cells attached to the culture plate is, potentially due to steric hindrance, less accessible to antibodies, than FGF2-GFP bound to the cell surface of cells in solution. It is most likely that both reasons might lead to the reduction of the signal for FGF2-GFP derived cell surface staining.

3.3 Mutational analysis of FGF2-GFP targeting to its transport machinery

In eukaryotic cells classically secreted proteins and proteins transported across other membranes possess signals that mediate targeting to their transport machineries. This has been reported for peroxisomes, the ER, mitochondria, chloroplasts and the nucleus (Walter et al., 1984; Neupert, 1997; Smith and Schnell, 2001). These signals have been identified and their motifs consist of amino acids mostly present in the N- or C-termini of the protein. In contrast to conventionally secreted proteins, FGF2 does not contain a signal peptide, and is not exported in an ER/Golgi dependent manner but by unconventional means. FGF2 is segregated from cytoplasmatic proteins and therefore must contain a signal which is recognized by a so far unknown translocation machinery.
Therefore, a mutational analysis of the FGF2 open reading frame was conducted in order to find export deficient mutants and mutants which have a defect in binding to HSPGs.

3.3.1 Selection and cloning of FGF2 mutants

To determine the signal mediating unconventional secretion of FGF2, several experimental approaches were chosen in order to isolate mutants defective with regard to FGF2 secretion.
In a first step, a random mutagenesis was conducted, introducing randomly multiple mutations into the open reading frame of FGF2. These mutations were obtained by performing an unbiased PCR using 5 mM $MnCl_2$ leading to more frequently mutated adenines and thymines than cytosines and guanines (Shafikhani et al., 1997). The results from the random mutagenesis were then taken as a basis to further investigate the role of distinct point mutations in secretion. Additionally hydrophobic protein surface residues which are potentially involved in protein-protein interaction were identified by an analysis of the crystal structure and were changed by site-directed mutagenesis. Moreover, residues at the N-terminus of FGF2 are disordered and have not been successfully crystallized. Additionally, amino acids cluster at both protein termini which are responsible for the interaction of FGF2 with heparin (Baird et al., 1988; Li et al., 1994). Therefore, The N- and the C-terminus of FGF2 were stepwise truncated and analyzed with regard to their secretion. In the following sections, the cloning strategies for the four different approaches are demonstrated.

3.3.1.1 Random mutagenesis

In order to randomly introduce single and multiple base substitutions, a low fidelity PCR using pRevTRE2-FGF2-GFP-His_6 as a template was performed, beginning with the start codon of FGF2 and ending with an endogenous *BamH I* restriction site at position 406. Both primers were also complementary to an intrinsic *BamH I* restriction site at position -15 and 406. The cloning strategy is depicted in the following figure 3.22.

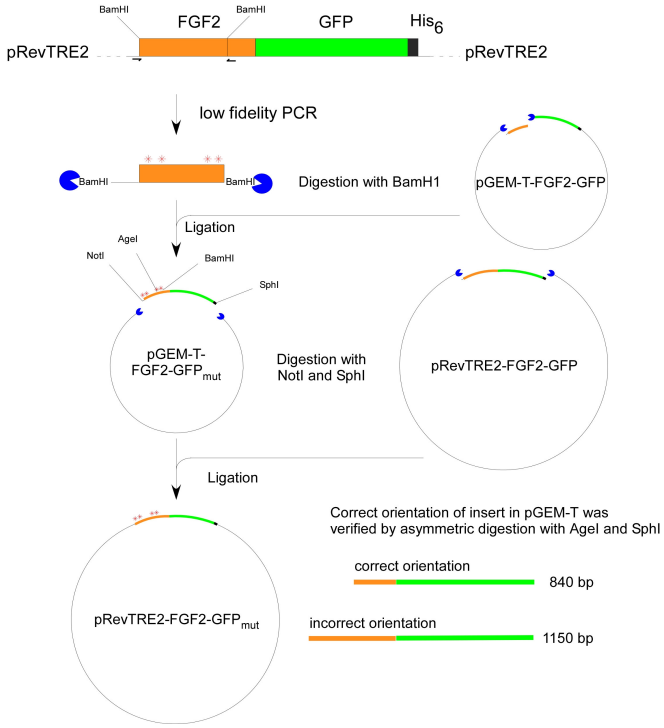

Figure 3.22: schematic overview of the cloning strategy for the introduction of multiple random amino acid changes.

The obtained PCR products were purified by gel extraction to dispose the original vector and primers used. The DNA fragment and pGEM-T-FGF2-GFP were then digested using *BamH I*, followed by ligation. After transformation of E.coli DH5α, DNA was amplified by a mid-scale preparation without selecting single clones in order to receive a subset of different mutants. Mutated FGF2-GFP (FGF2-GFP_{mut}) was then excised from amplified pGEM-T-FGF2-GFP using *Not I* and *Sph I* and ligated into pRevTRE2-FGF2-GFP linearized with the same restriction enzymes. Following transformation, selection of clones and amplification of plasmid DNA, the correct orientation of inserted FGF2-GFP_{mut} was verified by an asymmetric digestion analysis using *Age I* and *Sph I*. Plasmids with correctly orientated FGF2-GFP were finally used for the retroviral transduction of $CHO_{MCAT/TAM2}$ cells. An overview of all mutations obtained is listed in table 3.1.

3.3.1.2 Point mutations

The clones obtained by the random mutagenesis described by a different phenotype regarding stability of the protein, cell surface staining and binding efficiency to heparin where analysed with regard to their multiple mutations, which where then introduced as distinct single mutations in the open reading frame of FGF2.

As a second approach, an analysis of the three-dimensional structure of FGF2 was conducted in collaboration with Dr. Ivo Tews from the group of Prof. Dr. Irmgard Sinning by analyzing FGF2 for surface residues which are potentially involved in protein-protein interactions. Therefore, hydrophobic amino acids, exposed to the protein surface and cysteines responsible for dimerization of FGF2 were chosen as a target for site-directed mutagenesis.

To summarize amino acids changed by site directed, the primary sequence of FGF2 is depicted in figure 3.23 with amino acids changed by site-directed mutagenesis being marked with an asterisk.

```
       *******    **      * *  *   *  *     ** * *       ** * *

1    maagsittlpalpedggsgafppghfkDapkrlyckнggfflrihpdgrvdgvreksdphi

     *  ** ***  * ** ** * *    ** * *   *     * *       *    *

61   klqlqaeergvvsikgvcanrylamkedgrllaskcvtdecffferlesnnyntyrsrky

     *     **  **    *             *

121  tswyvalkrtgqyklgsktgpgqkailflpmsaks
```

Figure 3.23: Primary structure of FGF2.
Amino acids marked with an asterisk were subjected to point mutations.

A detailed list of all amino acid exchanges is provided in table 3.3.

To visualize the location of the mutated amino acids in the three-dimensional structure of FGF2, the following figure 3.24 was generated.

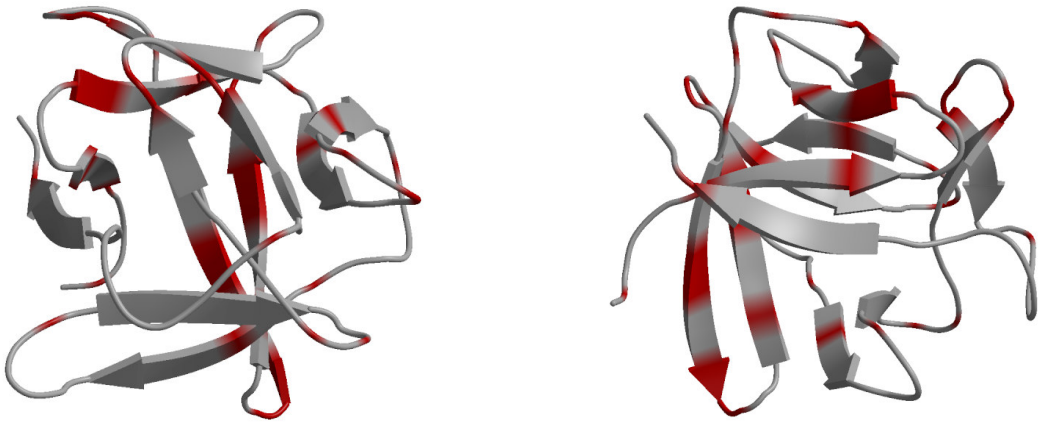

Figure 3.24: Three-dimensional structure of FGF2.
Red areas represent amino acids changed by site-directed mutagenesis of FGF2. Right picture is turned 90° compared to left picture. The picture was created using protein explorer 2.45 beta on the PDB entry domain 1ev2.

The picture was painted using protein explorer software and the PDB entry domain 1ev2. The red areas represent amino acids changes obtained by site-directed mutagenesis of FGF2. As depicted in figure 3.24, most mutations are localized in the β-sheets contributing to the overall structure of FGF2.

The cloning strategy for the generation of point mutations is depicted in the following figure 3.25.

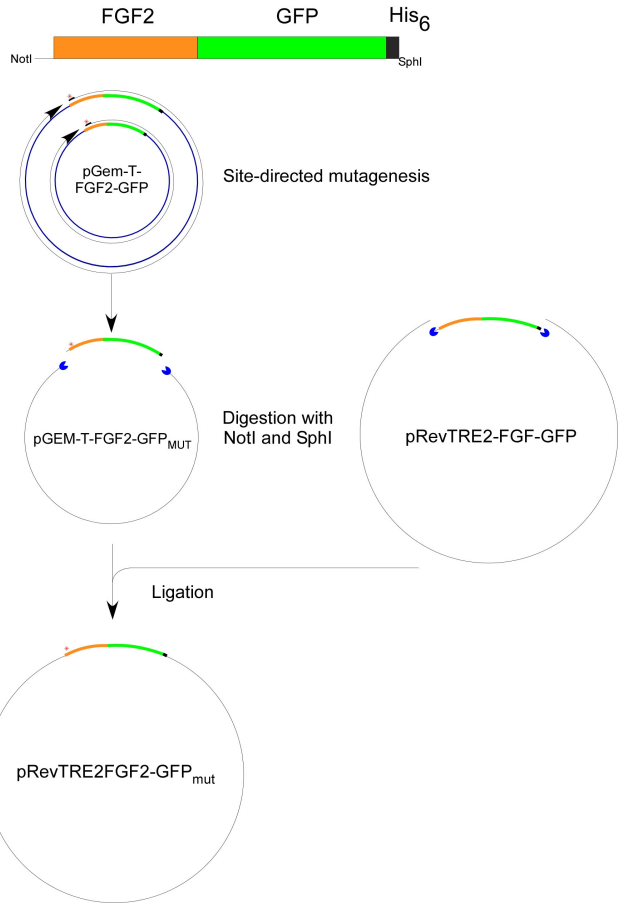

Figure 3.25: schematic overview of the cloning strategy for the introduction of site-directed mutations.

Point mutations were introduced into the open reading frame of FGF2 using the QuickChange Site-Directed Mutagenesis Kit (Stratagene). The PCR reactions were performed according to the manufacturer's instructions using pGEM-T-FGF2-GFP-His_6 as a template and primers containing the desired mutations (see section 2.2.1.2). The primers used are listed in chapter materials and methods, section 2.1.6. After introducing the PCR constructs into DH5α or supercompetent XL-1 blue bacterial cells, clones were selected and plasmid DNA was prepared from bacterial cells. Point-mutated FGF2-GFP was excised from pGEM-T-FGF2-GFP with *Not I* and *Sph I*

and ligated into pRevTRE2-FGF2-GFP-His_6 digested with the same enzymes. Following transformation into DH5α cells, selection of clones, amplification and preparation of plasmid DNA, the insert was sequenced to verify the mutation. Correct constructs were used for retroviral transductions of $CHO_{MCAT/TAM2}$ cells. An overview of all mutations is listed in table 3.3.

3.3.1.3 Truncations

To complete the structural analysis, FGF2 was truncated from both the N-terminus and the C-terminus. The heparin binding sites of FGF2 were identified to cluster at the C-terminus from amino acid 128-138 (Li et al., 1994), as well as at the N-terminus (Baird et al., 1988).

N-terminal Truncation

The first 15 amino acids of FGF2 are part of a flexible region of unknown structure (Eriksson et al., 1991; Plotnikov et al., 1999), which might be potentially involved in protein-protein interactions as it is known for secretory proteins, which do have an N-terminal signal sequence which targets the protein to the transport machinery of the classical secretory pathway. Additionally, the heparin binding sites proposed to be present in the N-terminal region might also play a role in the transport process. It was shown for galectin-1 that binding to its counter-receptor is a prerequisite for its export (Seelenmeyer et al., 2005). To avoid binding of FGF2 to heparan sulfate proteoglycans, heparin binding regions of FGF2 were deleted. Therefore, several truncated versions of FGF2-GFP were generated, lacking the N-terminal 10, 20, 30, 40 and 50 amino acids. The cloning strategy is depicted in the following figure 3.26.

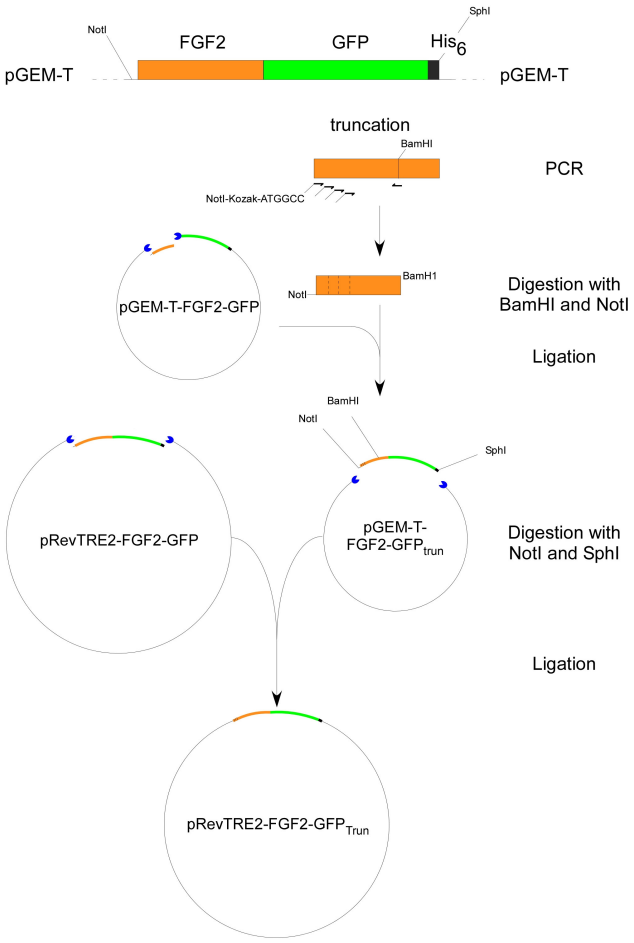

Figure 3.26: schematic overview of the cloning strategy for N-terminal truncations.

In order to obtain the desired truncated DNA fragments of FGF2, PCRs were conducted with two specific primers flanked by a 5´ Not I and a 3` BamH I cleavage site. The Kozak sequence is the consensus sequence for the initiation of translation in vertebrates. This sequence is essential, because it has to be expressed from mammalian CHO cells. The PCR products and pGEM-T-FGF2-GFP were then digested using *Not I* and *BamH I*, followed by ligation, transformation, selection of clones and preparation of plasmid DNA. The FGF2-GFP open reading frame was subsequently excised from pGEM-T-FGF2-GFP using *Not I and Sph I* and ligated with pRevTRE2, linearised by the same restriction enzymes. After verifying the final constructs by DNA sequencing, these vectors were used for retroviral transduction.

3.3.1.4 C-terminal Truncations

The C-terminal truncations were conducted to complete the mutational analysis of FGF2. Since secretion of Galectin-1 depends on its interaction with galactose

containing counter receptors on the cell surface (Seelenmeyer et al., 2005), it is also well possible that secretion of FGF2 depends on its interaction with HSPGs present on the cell surface. The main part of the heparin binding site of FGF2 is localized close to the C-terminus at position 128 – 138 (Li et al., 1994). Therefore, several truncated versions of FGF2-GFP were generated, lacking the C-terminal 10, 20, 30, 40, 50, 60, 70, 90, 100, 110 and 120 amino acids. The cloning strategy is depicted in the following figure 3.27.

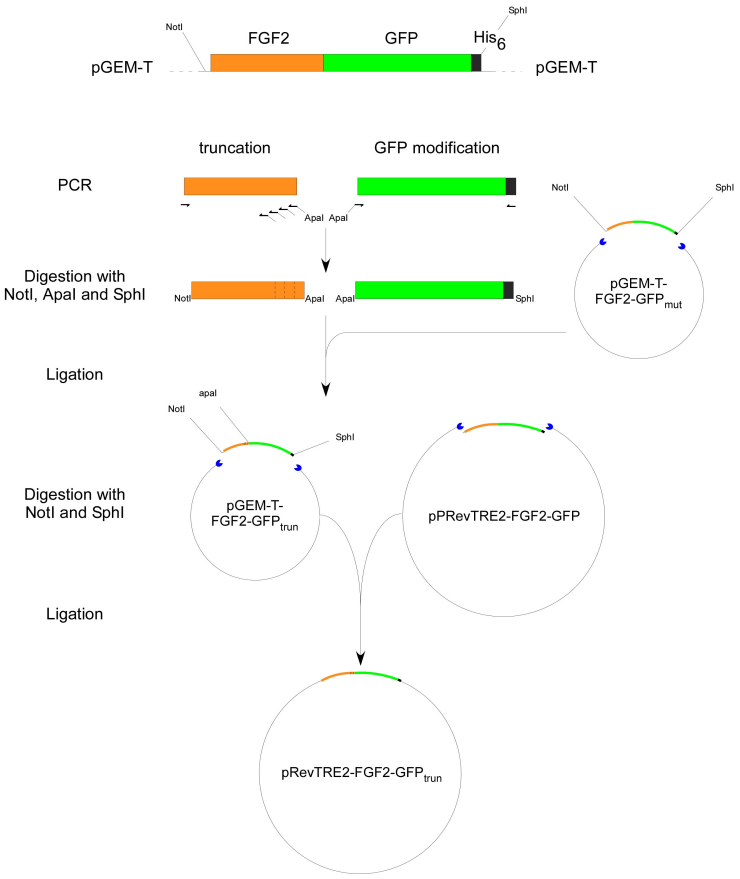

Figure 3.27: schematic overview of cloning strategy for C-terminal truncations.

In order to obtain the desired truncated DNA fragments of FGF2 PCRs were conducted with two specific primers flanked by a 5´ *Not I* and a 3` *Age I* cleavage site. With an additional PCR an Apa I restriction site was introduced to the 5´ end of GFP. The DNA fragments were subsequently digested with *Not I/Apa I* (FGF2) and *Apa I/Sph I* (GFP) and subjected to a triple ligation with pGEM-T-FGF2-GFP cut with *Not I/Sph I*, followed by transformation, selection of clones and preparation of plasmid DNA. The constructs were then verified by sequencing. FGF2-GFP was subsequently excised using *Not I* and *Sph I* and ligated into PRevTRE2 linearised with the same restriction enzymes. These final constructs were used for retroviral transduction of CHO cells.

3.3.2 Characterisation of FGF2 mutants with regard to export efficiency, binding to heparan sulfate proteoglycans *in vivo* and to heparin *in vitro*

All generated FGF2-GFP mutants were characterized regarding export efficiency as well as with regard to their ability to bind to heparin and HSPG by the following *in vivo* and *in vitro* assays.

1. *In vitro* binding assay using heparin beads.
2. *In vivo* binding assay using CHO cells.
3. FACS-based expression and secretion assay.
4. Biochemical secretion assay using a biotin reagent.

In this chapter, wild-type FGF2-GFP was used as a positive and GFP as a negative control to establish the assays described above.

3.3.2.1 In vitro binding of FGF2 using heparin beads

Distinct amino acid clusters are widely distributed over the structure of FGF2 and mediate binding to heparin-derived oligosaccharides (Faham et al., 1996). Therefore an assay using heparin coupled to sepharose beads was developed to analyze mutants with regard to their heparin-binding properties *in vitro*.

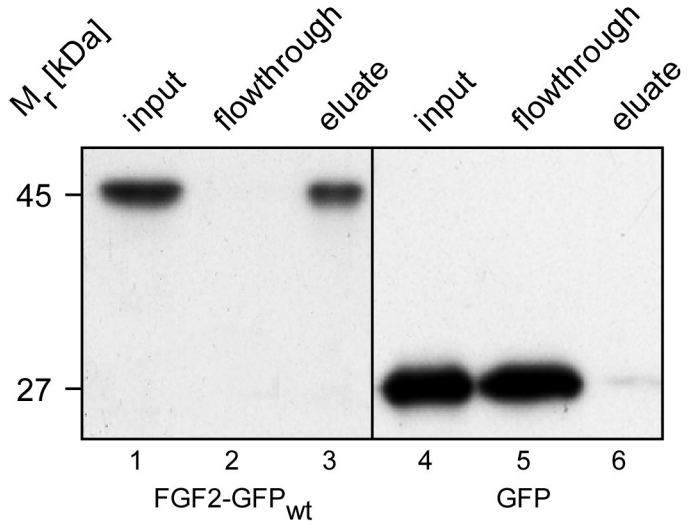

Figure 3.28: *In vitro* binding of FGF2-GFP to heparin beads.
Cell free supernatants prepared from $CHO_{FGF2\text{-}GFP}$ and CHO_{GFP} cells respectively incubated on a culture plate (Ø 15 cm) with doxicycline (1 µg/ml) for 24 h at 37°C, resulting in a confluency of 100% were normalized for GFP fluorescence and incubated with heparin beads for 1h at 4°C. The non-bound fraction was separated and, following extensive washing, bound material was eluted with SDS sample buffer. Input (lane 1; 5%), non-bound material (lane 2; 5%) and bound material (lane 3; 5%) were analyzed by SDS PAGE and Western blotting using affinity-purified anti-GFP antibodies.

$CHO_{FGF2\text{-}GFP}$ and CHO_{GFP} cells were grown on culture plates (∅ 15 cm) in presence of doxicycline (1 µg/ml) for 24 h at 37 °C, resulting in a confluency of about 100%. After washing and detachment, cells were broken up by combining freeze-thaw cycles with sonication and membranes were removed by ultracentrifugation (see Material and Methods, chapter 2.3.6). The obtained cell free supernatants were normalized for GFP-fluorescence and incubated with heparin beads for 1h at 4°C, followed by washing steps in buffer containing Triton X-100 and elution of bound material with SDS-containing sample buffer. Input, flowthrough and eluate were analyzed by SDS-PAGE and Western blotting using anti-GFP antibodies. For more detail see materials and methods, section 2.3.7.

As shown in figure 3.28, the 45 kDa FGF2-GFP_{wt} fusion protein was present in the input (lane 1) and the eluate (lane 3). In the flowthrough fraction (lane 2), representing non-bound material, the protein band representing the fusion protein could not be observed. However, GFP was found in input (lane 4) and flowthrough (lane 5), but not in the eluate (lane 6). These results show that FGF2-GFP binds specifically to heparin *in vitro* mediated by the FGF2 domain and not by the GFP domain of the fusion protein.

3.3.2.2 In vivo binding of FGF2 to CHO cells

CHO cells lack high affinity FGF2 receptors but provide the low affinity receptors heparan sulfate proteoglycans and glycolipids GM_1 on their surface which can be occupied by FGF2. To analyze the cell-binding capacity of mutated FGF2 *in vivo*, an assay was developed where the protein of interest was exogenously added to CHO cells, followed by FACS-based detection and quantification of FGF2-GFP bound to the cell surface.

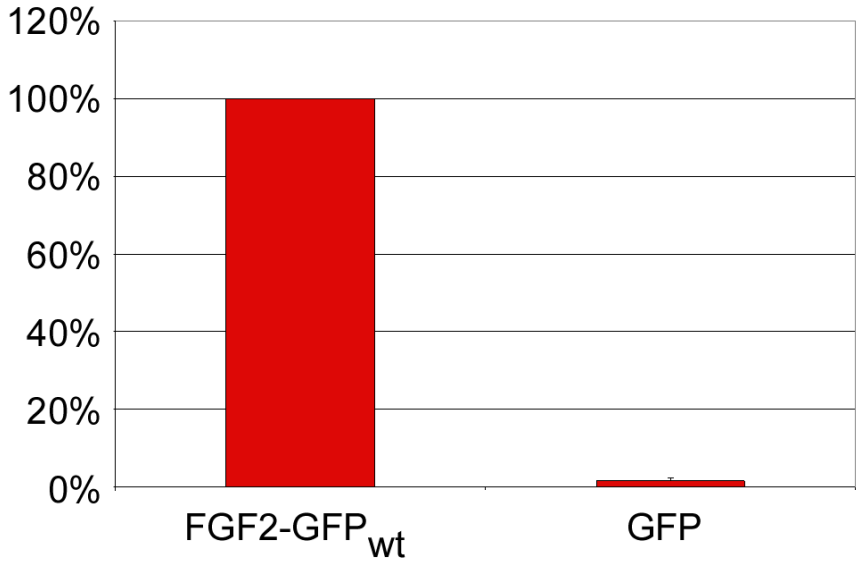

Figure 3.29: *In vivo* binding of the fusion protein to the cell surface of CHO cells.
The FGF2-GFP fusion proteins and GFP respectively were expressed in CHO cells. Cell free supernatants were prepared and normalized for GFP fluorescence. The various supernatants were then incubated with CHO cells for 1h at 4°C to allow cell surface binding. Following treatment with affinity-purified anti-GFP antibodies (1:50) and APC-conjugated secondary antibodies (1:750), cell surface binding was quantified by flow cytometry using a FACSCalibur system from Becton Dickinson (n=3). Cell surface staining of $FGF2\text{-}GFP_{wt}$ was set to 100%.

A cell free supernatant, produced as described in chapter 2.3.6 and normalized for GFP fluorescence (50 GFP units corresponding to about 0,5 µg GFP, Molecular Devices SpectraMax Gemini XS) was diluted 1:10 with growth medium and incubated with $CHO_{MCAT/TAM2}$ cells for 1h at 4°C in order to allow FGF2-GFP fusion proteins to bind to the cell surface. After washing cells with PBS, they were processed for analyzed using a Becton Dickinson FACSCalibur flow cytometry.
As expected, the wild-type form of FGF2-GFP was detectable on the cell surface, because the FGF2 part of the fusion protein binds to heparan sulfate proteoglycans. For GFP alone, as expected a cell surface signal could not be detected.

3.3.2.3 Quantification of FGF2-GFP export by flow cytometry

This described *in vivo* assay (see chapter 3.1) was performed to quantify the amount of expressed and secreted FGF2-GFP fusion protein.

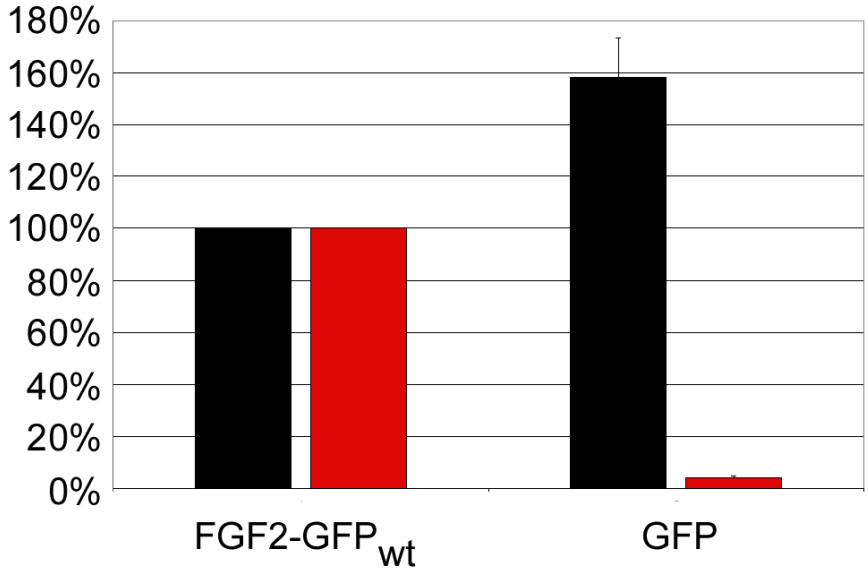

Figure 3.30: Quantitative analysis of secreted proteins from CHO cells employing flow cytometry.
CHO cells were grown on 6-well plates to a final confluency of 60% and induced with doxicycline for 16 h at 37°C to express the proteins indicated. Following removal of the medium, cells were washed and labelled with affinity-purified anti-GFP antibodies and APC-conjugated secondary antibodies while they were still attached to the culture dishes. After detachment of the cells using PBS/EDTA, GFP (expression level; black bars) and APC-derived fluorescence (cell surface; red) were quantified by flow cytometry using a Becton Dickinson FACSCalibur system (n=3). GFP fluorescence and cell surface staining of FGF2-GFP_{wt} was set to 100%.

CHO cells induced to express FGF2-GFP_{wt} and GFP respectively were grown on a 6-well plates to a confluency of about 60 % at 37°C. After a washing step with PBS, cells were processed for FACS analysis as described in materials and methods, section 2.4.2.

The signal for FGF2-GFP expression level (GFP fluorescence, black bars) and cell surface staining (APC derived fluorescence, red bars) was set to 100%, respectively. CHO_{GFP} cells displayed an enhanced GFP fluorescence (160%) when compared to $CHO_{FGF2\text{-}GFPwt}$ cells, indicating a higher expression level of GFP. The signal for cell surface staining of GFP cells was reduced to background levels (5%) when compared to FGF2-GFP.

3.3.2.4 *Biochemical secretion assay using botin to analyze FGF2 export from CHO cells*

This assay was developed to allow a biochemical quantification of FGF2-GFP secretion from CHO cells. Biotin (EZ-link Sulfo-NHS-SS-Biotin; Pierce), a membrane-impermeable low molecular weight reagent was covalently bound to proteins present on the cell surface. The secreted population of FGF2-GFP (bound to plasma membrane-associated heparin sulfate proteoglycans) is therefore well distinguishable from overall expressed fusion protein. After cell lysis biotinylated (extracellular) proteins were separated employing streptavidin beads and analyzed by western blotting.

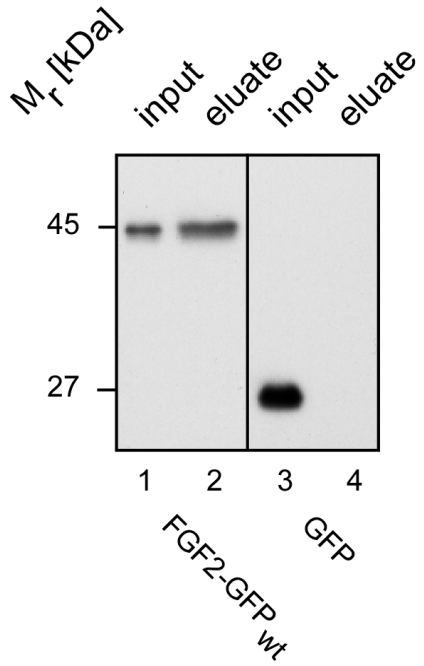

Figure 3.31: Biochemical analysis of FGF2-GFP and GFP export respectively from CHO cells employing cell surface biotinylation.
The indicated proteins were expressed in CHO cells for 16 h at 37°C (6-well plates; 70% confluency). Following removal of the medium, cells were treated with a membrane-impermeable biotinylation reagent. Following detergent-mediated cell lysis biotinylated and nonbiotinylated proteins were separated employing streptavidin beads. Aliquots from the input material (lane 1; 2.5% from total cell lysate) and the biotinylated fraction (lane 2; 50%) were analyzed by SDS-PAGE and Western blotting using affinity-purified anti-GFP antibodies.

FGF2-GFP and GFP were expressed in CHO cells (6 well plates, 70% confluency) by incubation in the presence of doxicycline (1 µg/ml) for 16 h at 37°C. Cells were then treated with a membrane-impermeable biotinylation reagent (EZ-Link Sulfo-NHS-SS-Biotin; Pierce) for 1h at 4°C, followed by cell lysis and affinity-purification using streptavidin beads. For more details see Material and Methods, chapter 2.3.5. The input (2.5% from total cell lysate) as well as proteins eluted from streptavidin

beads (50%) were analyzed by SDS PAGE and western blotting. For FGF2-GFP_{wt} cells, a band was detected in both input (lane 1) and eluate (lane 2). In GFP expressing cells, a signal for GFP could be detected only in the input material (lane 3) but not in the eluate fraction (lane 4). This leads to the conclusion, that FGF2-GFP is secreted and bound to the cell surface. Moreover GFP could not be detected in the eluate, showing that the biotin reagent is not able to cross the plasma membrane.

3.3.3 Analysis of mutants obtained by performing random Mutagenesis

Performing a random mutagenesis of the open reading frame of FGF2 resulted in clones with different subsets of mutated versions of FGF2. 100 distinct mutants were analyzed by flow cytometry regarding FGF2-GFP expression and cell surface staining. 18 from 100 clones were chosen based on altered cell surface staining when compared to wild-type FGF2-GFP. They were also characterized with regard to their ability to bind to heparin.

3.3.3.1 Overview of mutations with regard to their amino acid changes

The low fidelity PCR resulted in randomly distributed mutations within the open reading frame of FGF2. The created mutants are listed with regard to their individual mutations in the following table.

Mutant	Mutations	Number of mutations
25	A3S, E14D, R42H, K61H, V72A, R90K	6
26	G18S, D58G, G89V, R90G, L91F, W123R	6
30	P23S, K55R, E68A, E87D	4
32	G19S, L32Q, R90S, F103L, E105G, N110S	6
63	A20V, R81C	2
71	E14G, F103L	2
151	A2V, T8I, S122G	3
156	E87K, K128E, R129Q	3
193	R81C, L135F	2
201	P13H, F21I, F40L, K55T, L64P, C78S, Y133H	7
210	H59P, E68G, I74T	3
239	A3S, P13L, K61E	3
265	K30E, E67V, C78S	3
284	V77A, N110S	2
315	F21L, R42K, G89V	3
331	D15Y, K35I	2
346	K35R, S56C, N111Y, Y120H	4
365	F39L, V52A, K75I, Q132R	4

Table 3.1: List of mutations for individual clones created by a random mutagenesis.
Abbreviations used are international standards for the identification of amino acids. The first abbreviation is used for the original amino acid present in FGF2, the following number represents the position of the changed amino acid in the sequence of FGF2. The following abbreviation represents the newly generated amino acid.

The assays described in section 3.3.2 were used to analyze the binding ability of the mutants *in vivo* and *in vitro*. The amount of secreted FGF2-GFP was quantified by performing flow cytometry and cell surface biotinylation.

3.3.3.2 *Experimental data for FGF2 mutants not impaired regarding export efficiency and binding to heparin*

In this section, the FGF2 mutants generated by random mutagenesis are depicted which are comparable to wild-type FGF2-GFP with regard to secretion efficiency and binding capability to heparin and heparan sulfate proteoglycans. Moreover, their amino acid changes are shown and a summary of the experimental data is provided. For a detailed view on the assays used, please refer to chapter 3.3.2.

Mutant rM 26 contains 6 amino acid changes: G18S, D58G, G89V, R90G, L91F, W123R.

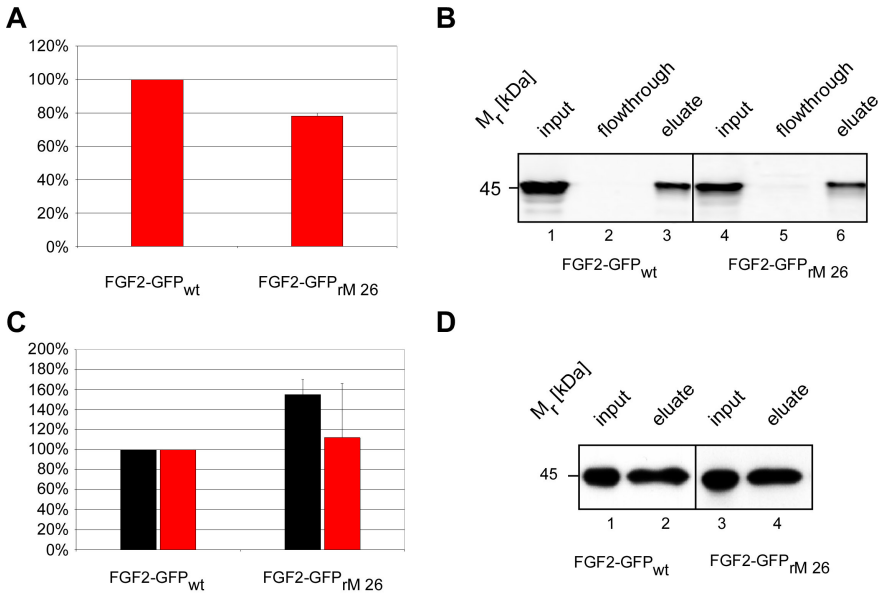

Figure 3.32: Random mutagenesis; 6 amino acid changes: G18S, D58G, G89V, R90G, L91F, W123R **A** FACS analysis of cell free supernatant bound to the surface of $CHO_{MCAT/TAM2}$ cells. Cell surface signal of $FGF2\text{-}GFP_{wt}$ was set to 100%. **B** Binding of cell free supernatant to heparin beads. Cell free supernatant was incubated with heparin beads. Total (input, 10%), non-bound (flowthrough, 10%) and bound material (eluate, 10%) was analyzed by SDS-PAGE and Western blotting. **C** Quantitative analysis of export employing flow cytometry. Expression level (black bars) and secreted protein detected on the cell surface (red bars) is shown. FGF2-GFPwt was set to 100%. **D** Biotinylation assay. Cell surface proteins were labelled with a membrane-impermeable biotin reagent. After cell lysis biotinylated and non-biotinylated proteins were separated by streptavidin beads. Total material (input, 5%) and the biotinylated fraction (eluate, 50%) were analyzed by SDS-PAGE and Western blotting.
All results shown represent an average of at least 3 different experiments. For further details see „Material and Methods“ and explanation of assays in chapter 3.3.2. As a result, this clone does not show any difference to wild-type cells.

As demonstrated in figure 3.32, mutant rM 26 showed a slightly reduced ability to bind *in vivo* to heparan sulfate proteoglycans as compared to wild-type FGF2-GFP (panel A). However, the mutant rM 26 and $FGF\text{-}GFP_{wt}$ showed the same affinity to

heparin *in vitro* (panel B). As demonstrated in panel C, the expression level of FGF2-$GFP_{rM\ 26}$ was enhanced to about 160% ± 10% as compared to FGF2-GFP_{wt}. Additionally, the amount of secreted FGF2-$GFP_{rM\ 26}$ detected on the cell surface was enhanced to about 110% ± 50%. However, the ratio between expressed and secreted protein remained comparable to wild-type protein, indicating unchanged secretion efficiency. The data obtained by flow cytometry was confirmed by the biotinylation assay (panel D).

Mutant rM 63 contains 2 amino acid changes: A20V and R81C

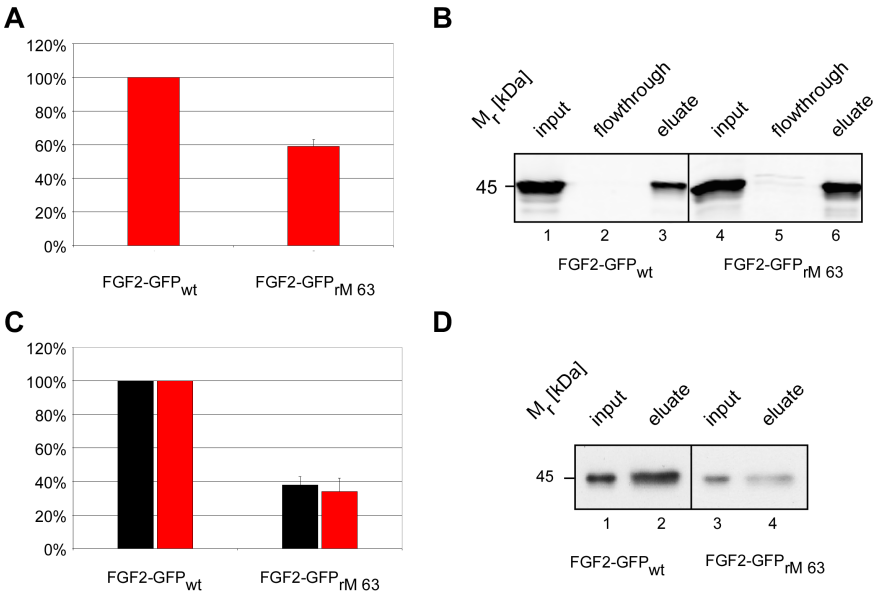

Figure 3.33: Random mutagenesis; 2 amino acid changes: A20V, R81C **A** FACS analysis of cell free supernatant bound to the surface of $CHO_{MCAT/TAM2}$ cells. Cell surface signal of FGF2-GFP_{wt} was set to 100%. **B** Binding of cell free supernatant to heparin beads. Cell free supernatant was incubated with heparin beads. Total (input, 10%), non-bound (flowthrough, 10%) and bound material (eluate, 10%) was analyzed by SDS-PAGE and Western blotting. **C** Quantitative analysis of export employing flow cytometry. Expression level (black bars) and secreted protein detected on the cell surface (red bars) is shown. FGF2-GFPwt was set to 100%. **D** Biotinylation assay. Cell surface proteins were labelled with a membrane-impermeable biotin reagent. After cell lysis biotinylated and non-biotinylated proteins were separated by streptavidin beads. Total material (input, 5%) and the biotinylated fraction (eluate, 50%) were analyzed by SDS-PAGE and Western blotting. All results shown represent an average of at least 3 different experiments. For further details see „Material and Methods“ and explanation of assays in chapter 3.3.2. As a result, this clone does not show any difference to wild-type cells.

As demonstrated in figure 3.33, the mutant rM 63 showed a reduced ability to bind to heparan sulfate proteoglycans *in vivo* (about 60%; panel A), but the affinity to heparin *in vitro* was comparable to FGF2-GFP_{wt}. The expression level and the cell surface staining of FGF2-$GFP_{rM\ 63}$ were reduced (panel C), but the ratio between expressed and secreted protein remained comparable to wild-type protein, indicating unchanged secretion efficiency. The data obtained by flow cytometry was confirmed by the biotinylation assay (panel D). These experiments demonstrate that mutant rM 63

does not differ from wild-type FGF2-GFP with regard to secretion efficiency, affinity to heparin and heparan sulfate proteoglycans.

Mutant rM 151 contains 3 amino acid changes: A2V, T8I and S122G.

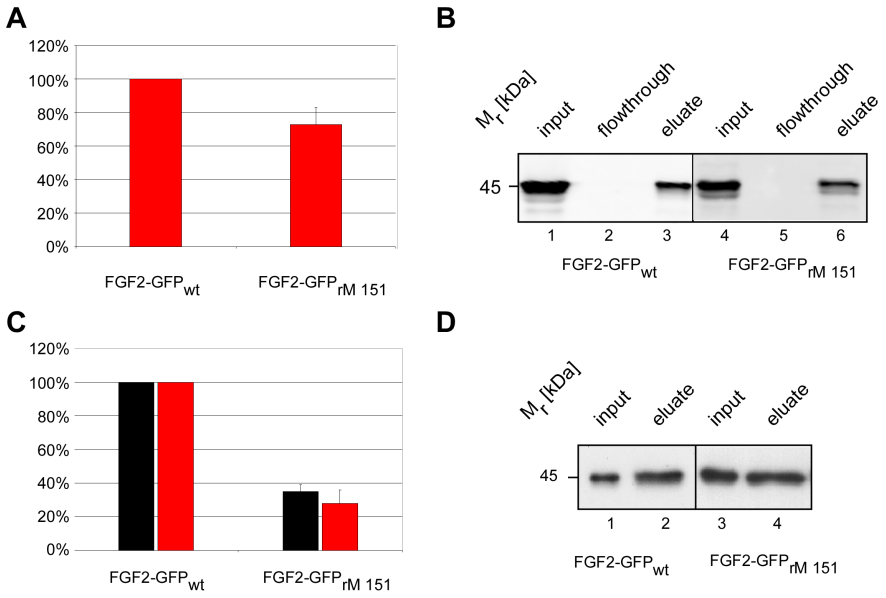

Figure 3.34: Random mutagenesis; 3 amino acid changes: A2V, T8I, S122G **A** FACS analysis of cell free supernatant bound to the surface of $CHO_{MCAT/TAM2}$ cells. Cell surface signal of $FGF2\text{-}GFP_{wt}$ was set to 100%. **B** Binding of cell free supernatant to heparin beads. Cell free supernatant was incubated with heparin beads. Total (input, 10%), non-bound (flowthrough, 10%) and bound material (eluate, 10%) was analyzed by SDS-PAGE and Western blotting. **C** Quantitative analysis of export employing flow cytometry. Expression level (black bars) and secreted protein detected on the cell surface (red bars) is shown. FGF2-GFPwt was set to 100%. **D** Biotinylation assay. Cell surface proteins were labelled with a membrane-impermeable biotin reagent. After cell lysis biotinylated and non-biotinylated proteins were separated by streptavidin beads. Total material (input, 5%) and the biotinylated fraction (eluate, 50%) were analyzed by SDS-PAGE and Western blotting. All results shown represent an average of at least 3 different experiments. For further details see „Material and Methods“ and explanation of assays in chapter 3.3.2. As a result, this clone does not show any difference to wild-type cells.

As demonstrated in figure 3.34, the mutant rM 151 showed a reduced ability to bind to heparan sulfate proteoglycans *in vivo* (about 80%; panel A), but the affinity to heparin *in vitro* was comparable to $FGF2\text{-}GFP_{wt}$. The expression level and the cell surface staining of $FGF2\text{-}GFP_{rM\ 151}$ were reduced (panel C), but the ratio between expressed and secreted protein remained comparable to wild-type protein, indicating unchanged secretion efficiency. The data obtained by flow cytometry was confirmed by the biotinylation assay (panel D). These experiments demonstrate that the mutant rM 151 does not differ from wild-type FGF2-GFP with regard to secretion efficiency, affinity to heparin and heparan sulfate proteoglycans.

Mutant rM 239 contains 3 amino acid changes: A3S, P13L and K61E.

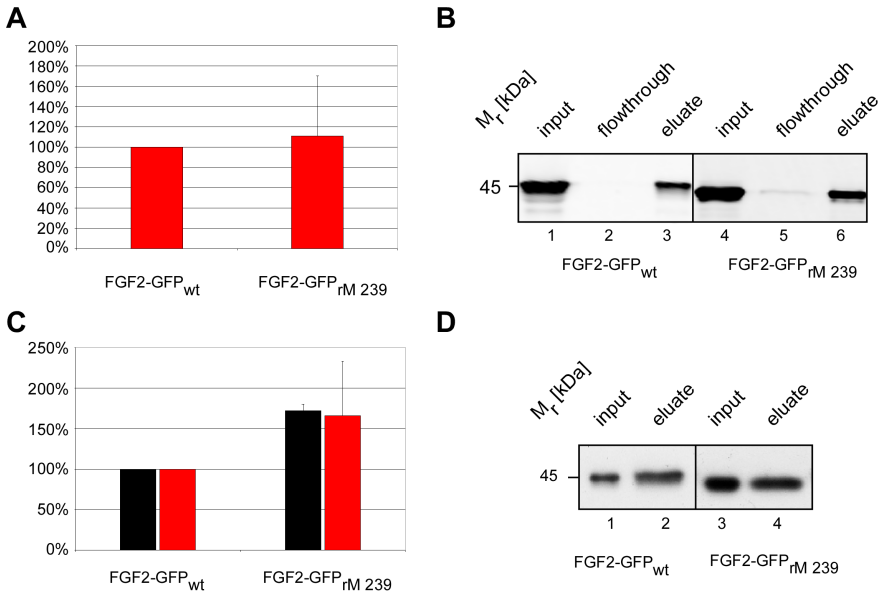

Figure 3.35: Random mutagenesis; 3 amino acid changes: A3S, P13L, K61E **A** FACS analysis of cell free supernatant bound to the surface of $CHO_{MCAT/TAM2}$ cells. Cell surface signal of FGF2-GFPwt was set to 100%. **B** Binding of cell free supernatant to heparin beads. Cell free supernatant was incubated with heparin beads. Total (input, 10%), non-bound (flowthrough, 10%) and bound material (eluate, 10%) was analyzed by SDS-PAGE and Western blotting. **C** Quantitative analysis of export employing flow cytometry. Expression level (black bars) and secreted protein detected on the cell surface (red bars) is shown. FGF2-GFPwt was set to 100%. **D** Biotinylation assay. Cell surface proteins were labelled with a membrane-impermeable biotin reagent. After cell lysis biotinylated and non-biotinylated proteins were separated by streptavidin beads. Total material (input, 5%) and the biotinylated fraction (eluate, 50%) were analyzed by SDS-PAGE and Western blotting. All results shown represent an average of at least 3 different experiments. For further details see „Material and Methods“ and explanation of assays in chapter 3.3.2. As a result, this clone does not show any difference to wild-type cells.

As demonstrated in figure 3.35, the mutant rM 239 showed an enhanced ability to bind to heparan sulfate proteoglycans *in vivo* (about 120%; panel A), but the affinity to heparin *in vitro* was comparable to $FGF2\text{-}GFP_{wt}$. The expression level and the cell surface staining of $FGF2\text{-}GFP_{rM\ 239}$ were also enhanced (panel C), but the ratio between expressed and secreted protein remained comparable to wild-type protein, indicating unchanged secretion efficiency. The data obtained by flow cytometry was confirmed by the biotinylation assay (panel D). These experiments demonstrate that the mutant rM 239 does not differ from wild-type FGF2-GFP with regard to secretion efficiency.

Mutant rM 265 contains 3 amino acid changes: K30E, E67V and C78S.

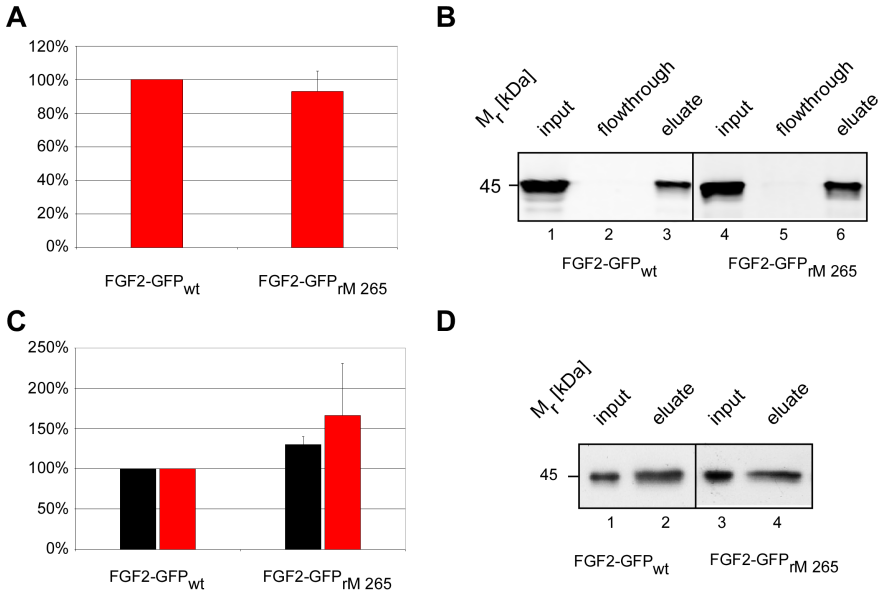

Figure 3.36.: Random mutagenesis; 3 amino acid changes: K30E, E67V, C78S **A** FACS analysis of cell free supernatant bound to the surface of $CHO_{MCAT/TAM2}$ cells. Cell surface signal of FGF2-GFPwt was set to 100%. **B** Binding of cell free supernatant to heparin beads. Cell free supernatant was incubated with heparin beads. Total (input, 10%), non-bound (flowthrough, 10%) and bound material (eluate, 10%) was analyzed by SDS-PAGE and Western blotting. **C** Quantitative analysis of export employing flow cytometry. Expression level (black bars) and secreted protein detected on the cell surface (red bars) is shown. FGF2-GFPwt was set to 100%. **D** Biotinylation assay. Cell surface proteins were labelled with a membrane-impermeable biotin reagent. After cell lysis biotinylated and non-biotinylated proteins were separated by streptavidin beads. Total material (input, 5%) and the biotinylated fraction (eluate, 50%) were analyzed by SDS-PAGE and Western blotting. All results shown represent an average of at least 3 different experiments. For further details see „Material and Methods“ and explanation of assays in chapter 3.3.2. As a result, this clone does not show any difference to wild-type cells.

As demonstrated in figure 3.36, the affinity of $FGF2\text{-}GFP_{rM\ 265}$ to heparan sulfate proteoglycans *in vivo* (panel A) and to heparin *in vitro* (panel B) was comparable to $FGF2\text{-}GFP_{wt}$. The expression level of $FGF2\text{-}GFP_{rM\ 265}$ was enhanced to about 120 % and the signal for secreted fusion protein showed about 160% ± 60% (panel C). The biotinylation assay showed slightly decreased secretion efficiency when compared to $FGF2\text{-}GFP_{wt}$ (panel D). These experiments demonstrate that the mutant rM 265 does not differ from wild-type FGF2-GFP with regard to binding efficiency to heparan sulfate proteoglycans and heparin. The secretion efficiency of $FGF2\text{-}GFP_{rM\ 265}$ was shown to be slightly different as analyzed with both secretion assays. However, since both assays do not detect a significant reduction of secretion efficiency, this clone belongs to the group of mutants showing no phenotype.

Mutant rM 284 contains 2 amino acid changes: V77A, N110S.

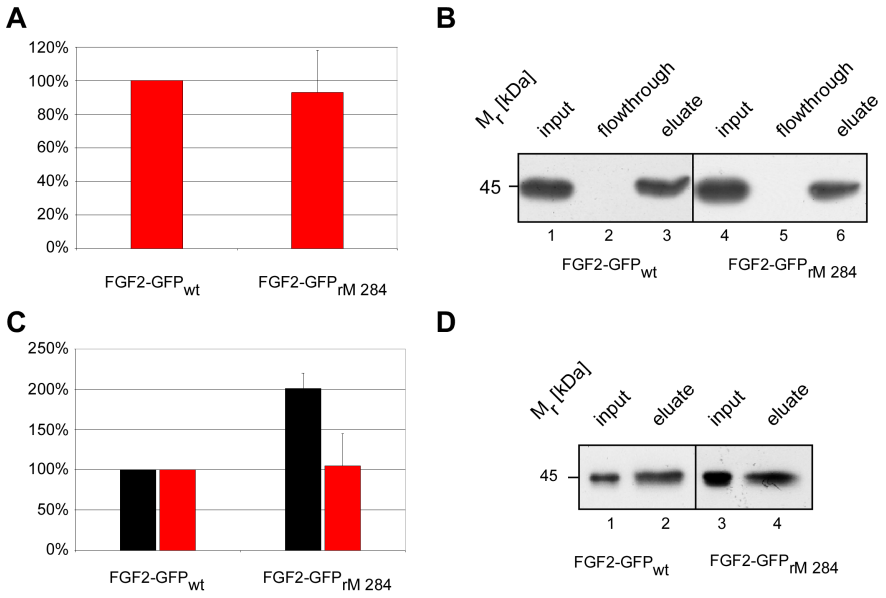

Figure 3.37: Random mutagenesis; 2 amino acid changes: V77A, N110S **A** FACS analysis of cell free supernatant bound to the surface of $CHO_{MCAT/TAM2}$ cells. Cell surface signal of FGF2-GFPwt was set to 100%. **B** Binding of cell free supernatant to heparin beads. Cell free supernatant was incubated with heparin beads. Total (input, 10%), non-bound (flowthrough, 10%) and bound material (eluate, 10%) was analyzed by SDS-PAGE and Western blotting. **C** Quantitative analysis of export employing flow cytometry. Expression level (black bars) and secreted protein detected on the cell surface (red bars) is shown. FGF2-GFPwt was set to 100%. **D** Biotinylation assay. Cell surface proteins were labelled with a membrane-impermeable biotin reagent. After cell lysis biotinylated and non-biotinylated proteins were separated by streptavidin beads. Total material (input, 5%) and the biotinylated fraction (eluate, 50%) were analyzed by SDS-PAGE and Western blotting. All results shown represent an average of at least 3 different experiments. For further details see „Material and Methods“ and explanation of assays in chapter 3.3.2. As a result, this clone does not show any difference to wild-type cells.

As demonstrated in figure 3.37, the affinity of $FGF2\text{-}GFP_{rM\ 284}$ to heparan sulfate proteoglycans *in vivo* (panel A) and to heparin *in vitro* (panel B) was comparable to $FGF2\text{-}GFP_{wt}$. The expression level of $FGF2\text{-}GFP_{rM\ 284}$ was enhanced to about 200 % and the signal for secreted fusion protein showed about 100% ± 50% (panel C). The biotinylation assay confirmed the result obtained by flow cytometry (panel D). These experiments demonstrate that the mutant rM 284 does not differ from wild-type FGF2-GFP with regard to secretion efficiency and binding efficiency to heparan sulfate proteoglycans or heparin. Since both assays do not detect a clear reduction of secretion efficiency, this clone belongs to the group of mutants showing no phenotype.

Mutant rM 315 contains 3 amino acid changes: F21L, R42K and G89V.

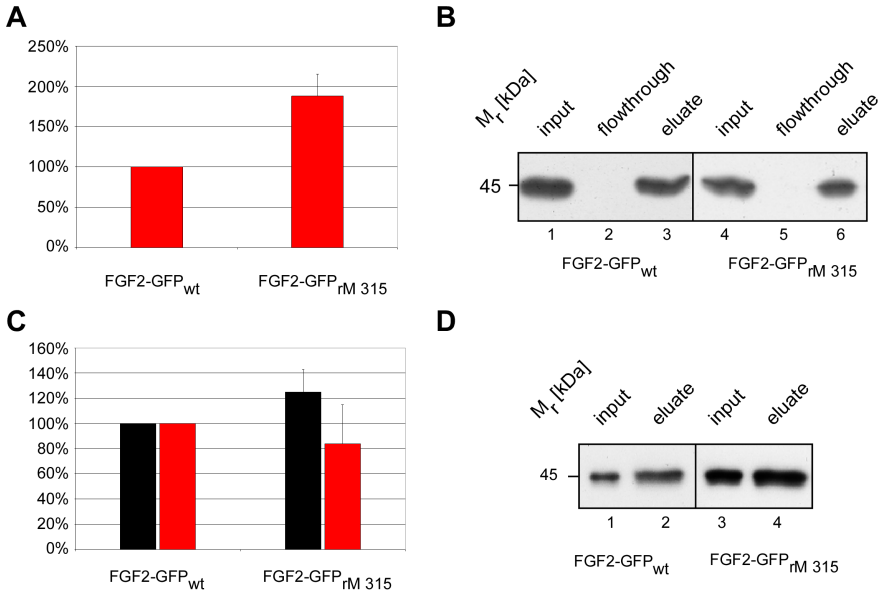

Figure 3.38: Random mutagenesis; 3 amino acid changes: F21L, R42K, G89V **A** FACS analysis of cell free supernatant bound to the surface of $CHO_{MCAT/TAM2}$ cells. Cell surface signal of FGF2-GFPwt was set to 100%. **B** Binding of cell free supernatant to heparin beads. Cell free supernatant was incubated with heparin beads. Total (input, 10%), non-bound (flowthrough, 10%) and bound material (eluate, 10%) was analyzed by SDS-PAGE and Western blotting. **C** Quantitative analysis of export employing flow cytometry. Expression level (black bars) and secreted protein detected on the cell surface (red bars) is shown. FGF2-GFPwt was set to 100%. **D** Biotinylation assay. Cell surface proteins were labelled with a membrane-impermeable biotin reagent. After cell lysis biotinylated and non-biotinylated proteins were separated by streptavidin beads. Total material (input, 5%) and the biotinylated fraction (eluate, 50%) were analyzed by SDS-PAGE and Western blotting. All results shown represent an average of at least 3 different experiments. For further details see „Material and Methods“ and explanation of assays in chapter 3.3.2. As a result, this clone does not show any difference to wild-type cells.

As demonstrated in figure 3.38, the mutant rM 315 showed an enhanced ability to bind to heparan sulfate proteoglycans *in vivo* (about 190%; panel A), but the affinity to heparin *in vitro* was comparable to FGF2-GFP_{wt}. The expression level of FGF2-$GFP_{rM\ 315}$ was enhanced to about 120 % and the signal for secreted fusion protein showed about 80% ± 30% (panel C). The biotinylation assay showed confirmed the result obtained by flow cytometry (panel D). These experiments demonstrate that the mutant rM 315 does not differ from wild-type FGF2-GFP with regard to export efficiency, although the binding efficiency to heparan sulfate proteoglycans is enhanced. Since both secretion assays do not detect a clear reduction of export efficiency, this clone belongs to the group of mutants showing no phenotype.

Mutant rM 331 contains 2 amino acid changes: D15Y and K35I.

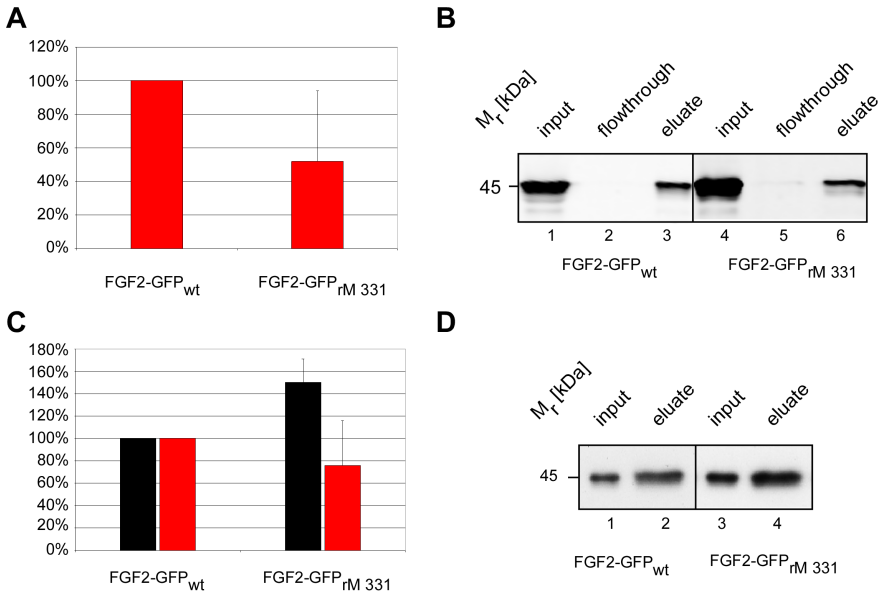

Figure 3.39: Random mutagenesis; 2 amino acid changes: D15Y, K35I **A** FACS analysis of cell free supernatant bound to the surface of $CHO_{MCAT/TAM2}$ cells. Cell surface signal of FGF2-GFPwt was set to 100%. **B** Binding of cell free supernatant to heparin beads. Cell free supernatant was incubated with heparin beads. Total (input, 10%), non-bound (flowthrough, 10%) and bound material (eluate, 10%) was analyzed by SDS-PAGE and Western blotting. **C** Quantitative analysis of export employing flow cytometry. Expression level (black bars) and secreted protein detected on the cell surface (red bars) is shown. FGF2-GFPwt was set to 100%. **D** Biotinylation assay. Cell surface proteins were labelled with a membrane-impermeable biotin reagent. After cell lysis biotinylated and non-biotinylated proteins were separated by streptavidin beads. Total material (input, 5%) and the biotinylated fraction (eluate, 50%) were analyzed by SDS-PAGE and Western blotting. All results shown represent an average of at least 3 different experiments. For further details see „Material and Methods“ and explanation of assays in chapter 3.3.2. As a result, this clone does not show any difference to wild-type cells.

As demonstrated in figure 3.39, the mutant rM 331 showed a reduced ability to bind to heparan sulfate proteoglycans *in vivo* (about 50% ± 50%; panel A), but the affinity to heparin *in vitro* was comparable to $FGF2\text{-}GFP_{wt}$. The expression level of $FGF2\text{-}GFP_{rM\ 331}$ was enhanced to about 150 % and the signal for secreted fusion protein showed about 80% ± 40% (panel C). The biotinylation assay confirmed the result obtained by flow cytometry (panel D). These experiments demonstrate that the mutant rM 331 does not differ from wild-type FGF2-GFP with regard to secretion efficiency and binding efficiency to heparan sulfate proteoglycans or heparin. Since both secretion assays do not detect a clear reduction of secretion efficiency, this clone belongs to the group of mutants showing no phenotype.

Mutant RM 346 contains 4 amino acid changes: K35R, S56C, N111Y and Y120H.

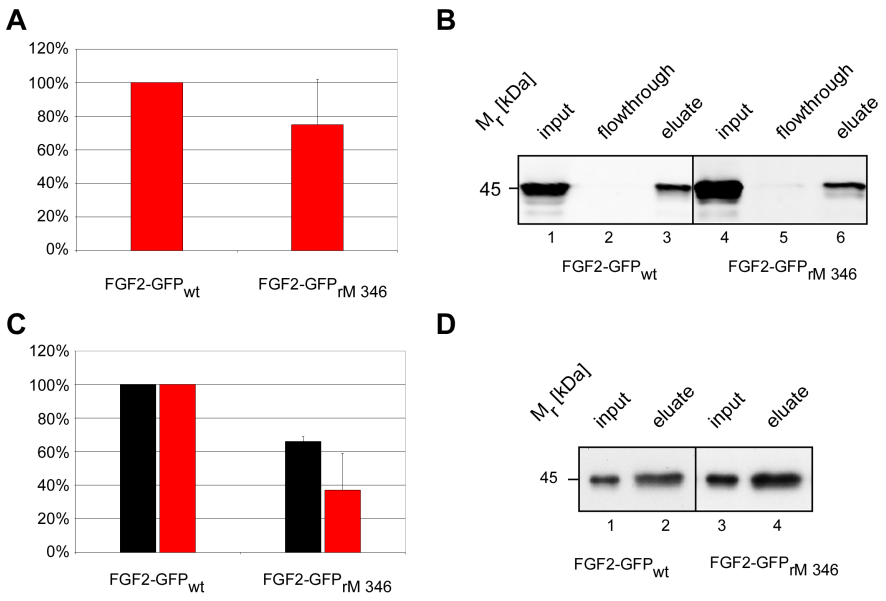

Figure 3.40: Random mutagenesis; 4 amino acid changes: K35R, S56C, N111Y, Y120H **A** FACS analysis of cell free supernatant bound to the surface of $CHO_{MCAT/TAM2}$ cells. Cell surface signal of FGF2-GFPwt was set to 100%. **B** Binding of cell free supernatant to heparin beads. Cell free supernatant was incubated with heparin beads. Total (input, 10%), non-bound (flowthrough, 10%) and bound material (eluate, 10%) was analyzed by SDS-PAGE and Western blotting. **C** Quantitative analysis of export employing flow cytometry. Expression level (black bars) and secreted protein detected on the cell surface (red bars) is shown. FGF2-GFPwt was set to 100%. **D** Biotinylation assay. Cell surface proteins were labelled with a membrane-impermeable biotin reagent. After cell lysis biotinylated and non-biotinylated proteins were separated by streptavidin beads. Total material (input, 5%) and the biotinylated fraction (eluate, 50%) were analyzed by SDS-PAGE and Western blotting.
All results shown represent an average of at least 3 different experiments. For further details see „Material and Methods“ and explanation of assays in chapter 3.3.2. As a result, this clone does not show any difference to wild-type cells.

As demonstrated in figure 3.40, the mutant rM 346 showed a slightly reduced ability to bind to heparan sulfate proteoglycans *in vivo* (about 80% ± 20%; panel A), which is confirmed by the ability to bind to heparin *in vitro* (panel B). The expression level and the cell surface staining of $FGF2\text{-}GFP_{rM\ 346}$ were reduced (panel C), but the ratio between expressed and secreted protein was comparable to wild-type protein, indicating unchanged secretion efficiency. This result could not be confirmed by the biotinylation assay, which showed reduced expression level (lane 3) and less secreted FGF2-GFP fusion protein when compared to wild-type FGF2-GFP (lane 1 and 2; panel D). These experiments demonstrate that the ability of mutant rM 346 to bind to heparin and to heparan sulfate proteoglycans is slightly reduced. However, since both secretion assays fail to detect a clear reduction of secretion efficiency, this clone belongs to the group of mutants showing no phenotype.

Mutant RM 365 contains 4 amino acid changes: K35R, S56C, N111Y and Y120H.

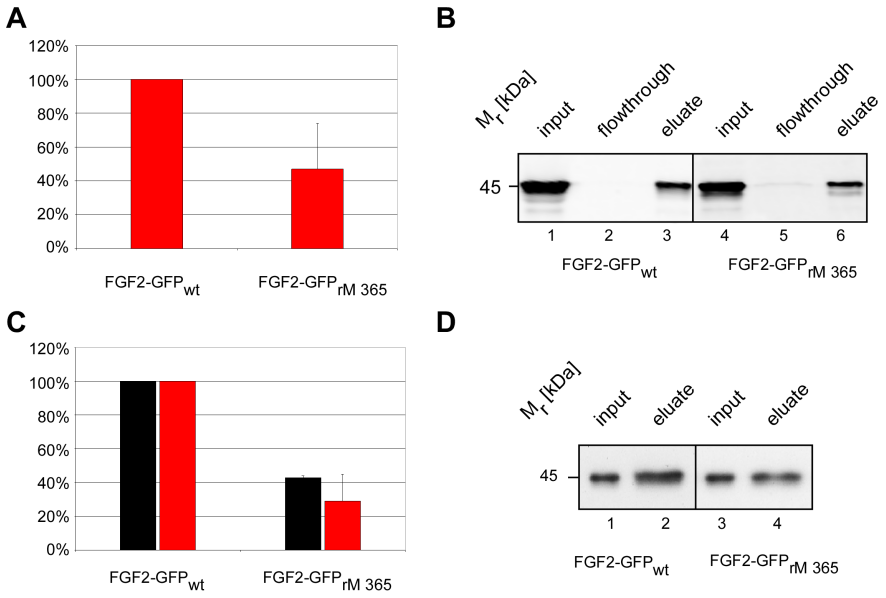

Figure 3.41: Random mutagenesis; 4 amino acid changes: F39L, V52A, K75I, Q132R **A** FACS analysis of cell free supernatant bound to the surface of $CHO_{MCAT/TAM2}$ cells. Cell surface signal of FGF2-GFPwt was set to 100%. **B** Binding of cell free supernatant to heparin beads. Cell free supernatant was incubated with heparin beads. Total (input, 10%), non-bound (flowthrough, 10%) and bound material (eluate, 10%) was analyzed by SDS-PAGE and Western blotting. **C** Quantitative analysis of export employing flow cytometry. Expression level (black bars) and secreted protein detected on the cell surface (red bars) is shown. FGF2-GFPwt was set to 100%. **D** Biotinylation assay. Cell surface proteins were labelled with a membrane-impermeable biotin reagent. After cell lysis biotinylated and non-biotinylated proteins were separated by streptavidin beads. Total material (input, 5%) and the biotinylated fraction (eluate, 50%) were analyzed by SDS-PAGE and Western blotting.
All results shown represent an average of at least 3 different experiments. For further details see „Material and Methods“ and explanation of assays in chapter 3.3.2. As a result, this clone does not show any difference to wild-type cells.

As demonstrated in figure 3.41, the mutant rM 365 showed a reduced ability to bind to heparan sulfate proteoglycans *in vivo* (about 50% ± 30%; panel A), but the affinity to heparin *in vitro* was comparable to FGF2-GFP_{wt} (panel B). The expression level and the cell surface staining of FGF2-$GFP_{rM\ 365}$ were reduced (panel C), but the ratio between expressed and secreted protein remained comparable to wild-type protein, indicating unchanged secretion efficiency. As detected by the biotinylation assay (panel D), the mutant rM 365 shows the same expression level of the fusion protein (lane 3) as compared to FGF2-GFP_{wt} (lane 1). Additionally, the amount of secreted FGF2-$GFP_{rM\ 365}$ (lane 4) is reduced when compared to FGF2-GFP_{wt} (lane 2). Taken these results together, this mutant does not show a secretion deficiency and its binding ability to heparin is not impaired.

The mutants listed in this section do not demonstrate decreased secretion efficiency and reduced affinity to heparin or heparan sulfate proteoglycans when compared to wild-type FGF2-GFP. Therefore, they were termed “no phenotype”.

3.3.3.3 *Experimental data for FGF2 mutants impaired in binding and protein stability*

In this section, FGF2 mutants generated by random mutagenesis are depicted which show reduced affinity to heparin *in vitro* and to heparan sulfate proteoglycans *in vivo*. Additionally, they demonstrate reduced expression levels of intracellular FGF2-GFP fusion protein. Moreover, their amino acid changes are shown and a summary of the experimental data is provided. For a detailed view on the assays used, please refer to chapter 3.3.2.

Mutant rM 25 contains 6 amino acid changes: A3S, E14D, R42H, K61H, V72A and R90K

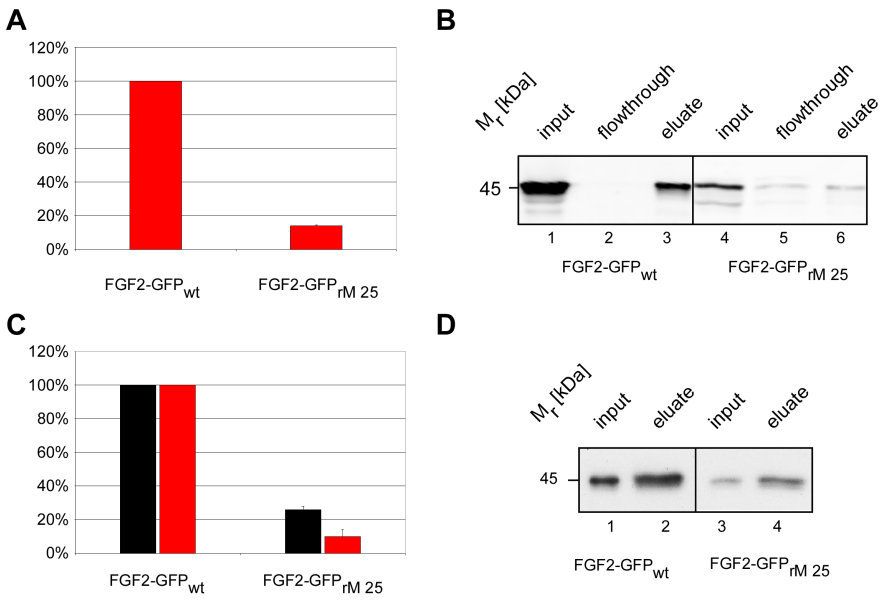

Figure 3.42: Random mutagenesis; 6 amino acid changes: A3S, E14D, R42H, K61H, V72A, R90K **A** FACS analysis of cell free supernatant bound to the surface of $CHO_{MCAT/TAM2}$ cells. Cell surface signal of $FGF2\text{-}GFP_{wt}$ was set to 100%. **B** Binding of cell free supernatant to heparin beads. Cell free supernatant was incubated with heparin beads. Total (input, 10%), non-bound (flowthrough, 10%) and bound material (eluate, 10%) was analyzed by SDS-PAGE and Western blotting. **C** Quantitative analysis of export employing flow cytometry. Expression level (black bars) and secreted protein detected on the cell surface (red bars) is shown. FGF2-GFPwt was set to 100%. **D** Biotinylation assay. Cell surface proteins were labelled with a membrane-impermeable biotin reagent. After cell lysis biotinylated and non-biotinylated proteins were separated by streptavidin beads. Total material (input, 5%) and the biotinylated fraction (eluate, 50%) were analyzed by SDS-PAGE and Western blotting. All results shown represent an average of at least 3 different experiments. For further details see „Material and Methods“ and explanation of assays in chapter 3.3.2. As a result, this clone shows a binding deficiency in both binding assays. Both secretion assays reveal that the reduced signal for secreted FGF2 is resulting from the low amount of expressed reporter protein and the impaired binding ability to heparan sulfate proteoglycans.

As demonstrated in figure 3.42, mutant rM 25 showed a reduced ability to bind to heparan sulfate proteoglycans *in vivo* (panel A) as well as to heparin *in vitro* (panel B) when compared to $FGF2\text{-}GFP_{wt}$. The expression level and cell surface staining of $FGF2\text{-}GFP_{rM\ 25}$ is strongly reduced compared to wild-type FGF2-GFP as shown by flow cytometry (panel C) and biotinylation assay (panel D). The combined data

obtained demonstrate that the mutations of FGF2-GFP$_{rM\ 25}$ cause impaired binding to heparin and heparan sulfate proteoglycans as well as an instable fusion protein.

Mutant rM 30 contains 6 amino acid changes: G18S, D58G, G89V, R90G, L91F and W123R.

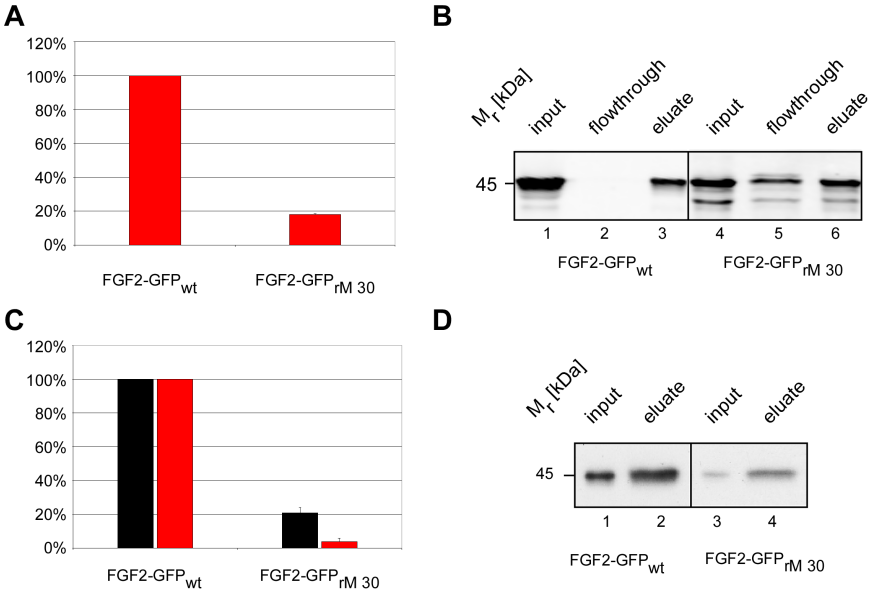

Figure 3.43: Random mutagenesis; 6 amino acid changes: G18S, D58G, G89V, R90G, L91F, W123R **A** FACS analysis of cell free supernatant bound to the surface of CHO$_{MCAT/TAM2}$ cells. Cell surface signal of FGF2-GFP$_{wt}$ was set to 100%. **B** Binding of cell free supernatant to heparin beads. Cell free supernatant was incubated with heparin beads. Total (input, 10%), non-bound (flowthrough, 10%) and bound material (eluate, 10%) was analyzed by SDS-PAGE and Western blotting. **C** Quantitative analysis of export employing flow cytometry. Expression level (black bars) and secreted protein detected on the cell surface (red bars) is shown. FGF2-GFPwt was set to 100%. **D** Biotinylation assay. Cell surface proteins were labelled with a membrane-impermeable biotin reagent. After cell lysis biotinylated and non-biotinylated proteins were separated by streptavidin beads. Total material (input, 5%) and the biotinylated fraction (eluate, 50%) were analyzed by SDS-PAGE and Western blotting. All results shown represent an average of at least 3 different experiments. For further details see „Material and Methods“ and explanation of assays in chapter 3.3.2. As a result, this clone shows a binding deficiency in both binding assays. Both secretion assays reveal that the reduced signal for secreted FGF2 is resulting from the low amount of expressed reporter protein and the impaired binding ability to heparan sulfate proteoglycans.

As demonstrated in figure 3.43, mutant rM 30 showed a reduced ability to bind to heparan sulfate proteoglycans *in vivo* (panel A) as well as to heparin *in vitro* (panel B) when compared to FGF2-GFP$_{wt}$. The expression level and cell surface staining of FGF2-GFP$_{rM\ 30}$ is strongly reduced compared to wild-type FGF2-GFP as shown by flow cytometry (panel C) and biotinylation assay (panel D). The combined data obtained demonstrate that the mutations of FGF2-GFP$_{rM\ 30}$ cause impaired binding to heparin and heparan sulfate proteoglycans as well as an instable fusion protein.

Mutant rM 32 contains 4 amino acid changes: P23S, K55R, E68A, E87D.

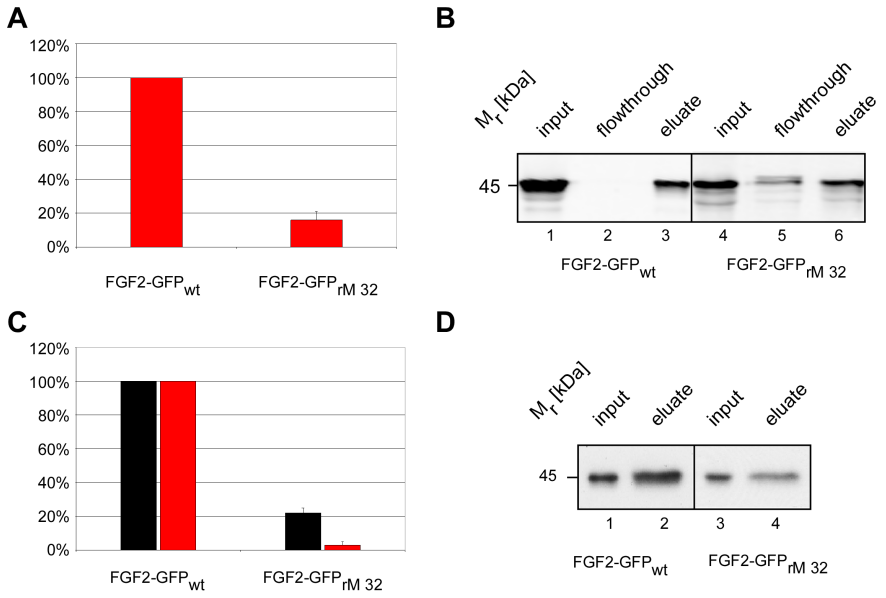

Figure 3.44: Random mutagenesis; 4 amino acid changes: P23S, K55R, E68A, E87D **A** FACS analysis of cell free supernatant bound to the surface of $CHO_{MCAT/TAM2}$ cells. Cell surface signal of $FGF2\text{-}GFP_{wt}$ was set to 100%. **B** Binding of cell free supernatant to heparin beads. Cell free supernatant was incubated with heparin beads. Total (input, 10%), non-bound (flowthrough, 10%) and bound material (eluate, 10%) was analyzed by SDS-PAGE and Western blotting. **C** Quantitative analysis of export employing flow cytometry. Expression level (black bars) and secreted protein detected on the cell surface (red bars) is shown. FGF2-GFPwt was set to 100%. **D** Biotinylation assay. Cell surface proteins were labelled with a membrane-impermeable biotin reagent. After cell lysis biotinylated and non-biotinylated proteins were separated by streptavidin beads. Total material (input, 5%) and the biotinylated fraction (eluate, 50%) were analyzed by SDS-PAGE and Western blotting. All results shown represent an average of at least 3 different experiments. For further details see „Material and Methods“ and explanation of assays in chapter 3.3.2. As a result this clone shows a binding deficiency in both binding assays. Both secretion assays reveal that the reduced signal for secreted FGF2 is resulting from the low amount of expressed reporter protein and the impaired binding ability to heparan sulfate proteoglycans.

As demonstrated in figure 3.44, mutant rM 32 showed a reduced ability to bind to heparan sulfate proteoglycans *in vivo* (panel A) as well as to heparin *in vitro* (panel B) when compared to $FGF2\text{-}GFP_{wt}$. The expression level and cell surface staining of $FGF2\text{-}GFP_{rM\ 32}$ is strongly reduced compared to wild-type FGF2-GFP as shown by flow cytometry (panel C) and biotinylation assay (panel D). The combined data obtained demonstrate that the mutations of $FGF2\text{-}GFP_{rM\ 32}$ cause impaired binding to heparin and heparan sulfate proteoglycans as well as an instable fusion protein.

Mutant rM 71 contains 6 amino acid changes: A3S, E14D, R42H, K61H, V72A and R90K.

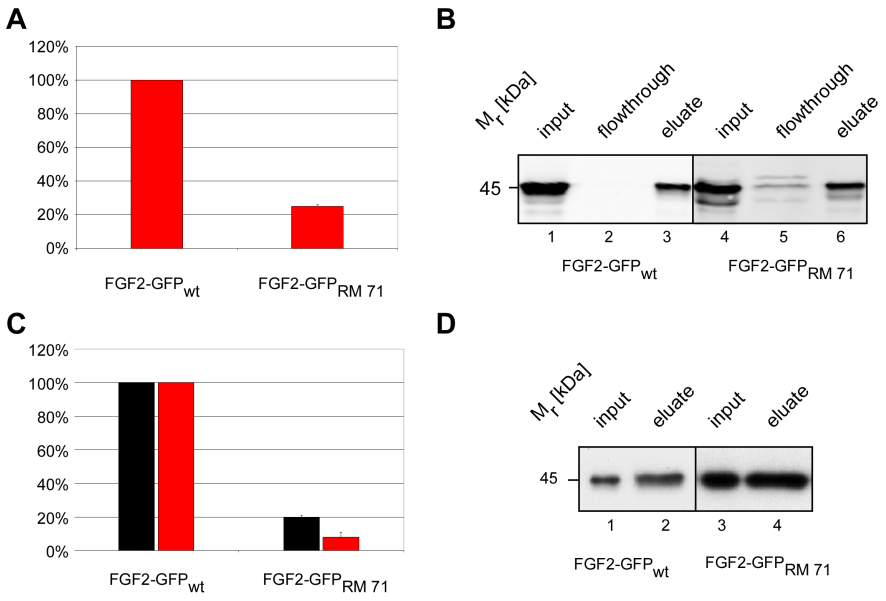

Figure 3.45: Random mutagenesis; 6 amino acid changes: A3S, E14D, R42H, K61H, V72A, R90K **A** FACS analysis of cell free supernatant bound to the surface of $CHO_{MCAT/TAM2}$ cells. Cell surface signal of $FGF2\text{-}GFP_{wt}$ was set to 100%. **B** Binding of cell free supernatant to heparin beads. Cell free supernatant was incubated with heparin beads. Total (input, 10%), non-bound (flowthrough, 10%) and bound material (eluate, 10%) was analyzed by SDS-PAGE and Western blotting. **C** Quantitative analysis of export employing flow cytometry. Expression level (black bars) and secreted protein detected on the cell surface (red bars) is shown. FGF2-GFPwt was set to 100%. **D** Biotinylation assay. Cell surface proteins were labelled with a membrane-impermeable biotin reagent. After cell lysis biotinylated and non-biotinylated proteins were separated by streptavidin beads. Total material (input, 5%) and the biotinylated fraction (eluate, 50%) were analyzed by SDS-PAGE and Western blotting. All results shown represent an average of at least 3 different experiments. For further details see Materials and Methods. As a result, this clone shows a binding deficiency in both binding assays. Both secretion assays reveal that the reduced signal for secreted FGF2 is resulting from the low amount of expressed reporter protein and the impaired binding ability to heparan sulfate proteoglycans.

As demonstrated in figure 3.45, mutant rM 71 showed a reduced ability to bind to heparan sulfate proteoglycans *in vivo* (panel A) as well as to heparin *in vitro* (panel B) when compared to $FGF2\text{-}GFP_{wt}$. The expression level and cell surface staining of $FGF2\text{-}GFP_{rM\ 71}$ is strongly reduced compared to wild-type FGF2-GFP as shown by flow cytometry (panel C) and biotinylation assay (panel D). The combined data obtained demonstrate that the mutations of $FGF2\text{-}GFP_{rM\ 71}$ cause impaired binding to heparin and heparan sulfate proteoglycans as well as an instable fusion protein.

Mutant rM 193 exhibits 2 amino acid changes: R81C and L135F.

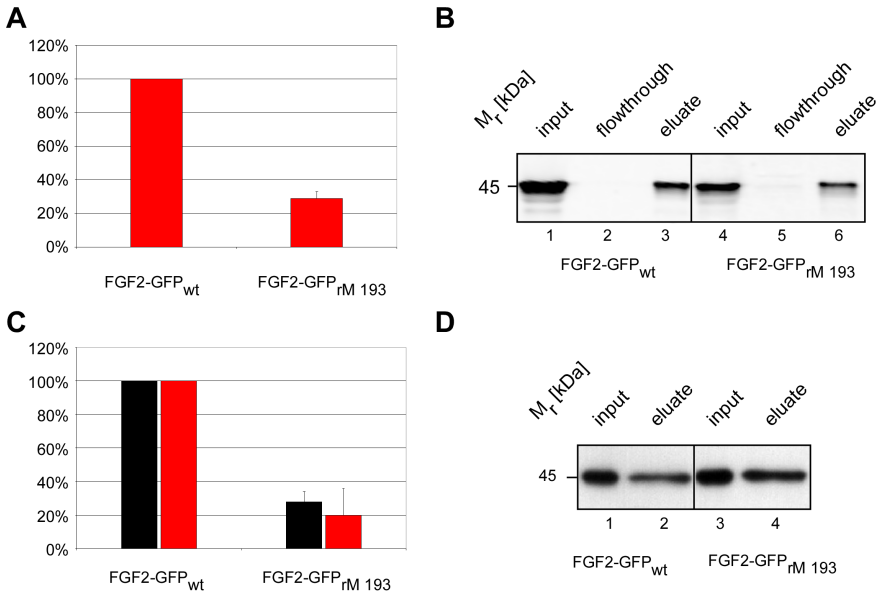

Figure 3.46: Random mutagenesis; 2 amino acid changes: R81C, L135F **A** FACS analysis of cell free supernatant bound to the surface of $CHO_{MCAT/TAM2}$ cells. Cell surface signal of $FGF2\text{-}GFP_{wt}$ was set to 100%. **B** Binding of cell free supernatant to heparin beads. Cell free supernatant was incubated with heparin beads. Total (input, 10%), non-bound (flowthrough, 10%) and bound material (eluate, 10%) was analyzed by SDS-PAGE and Western blotting. **C** Quantitative analysis of export employing flow cytometry. Expression level (black bars) and secreted protein detected on the cell surface (red bars) is shown. FGF2-GFPwt was set to 100%. **D** Biotinylation assay. Cell surface proteins were labelled with a membrane-impermeable biotin reagent. After cell lysis biotinylated and non-biotinylated proteins were separated by streptavidin beads. Total material (input, 5%) and the biotinylated fraction (eluate, 50%) were analyzed by SDS-PAGE and Western blotting. All results shown represent an average of at least 3 different experiments. For further details see Materials and Methods. As a result, this clone shows a binding deficiency in both binding assays Both secretion assays reveal that the reduced signal for secreted FGF2 is resulting from the low amount of expressed reporter protein and the impaired binding ability to heparan sulfate proteoglycans.

As demonstrated in figure 3.46, mutant rM 193 showed a reduced ability to bind to heparan sulfate proteoglycans *in vivo* (panel A) when compared to $FGF2\text{-}GFP_{wt}$, but its affinity to bind to heparin *in vitro* (panel B) was not impaired. The expression level and of $FGF2\text{-}GFP_{rM\ 193}$ is strongly reduced as shown by flow cytometry (panel C), but as detected by the biotinylation assay (panel D), the mutant rM 193 showed the same expression level of fusion protein (lane 3) as compared to $FGF2\text{-}GFP_{wt}$ (lane 1). However, the amount of secreted $FGF2\text{-}GFP_{rM\ 193}$ was comparable to $FGF2\text{-}GFP_{wt}$. Although the combined data obtained are not consistent, $FGF2\text{-}GFP_{rM\ 193}$ shows impaired binding to heparan sulfate proteoglycans and an instable fusion protein.

Mutant rM 201 contains 7 amino acid changes: P13H, F21I, F40L, K55T, L64P, C78S and Y133H.

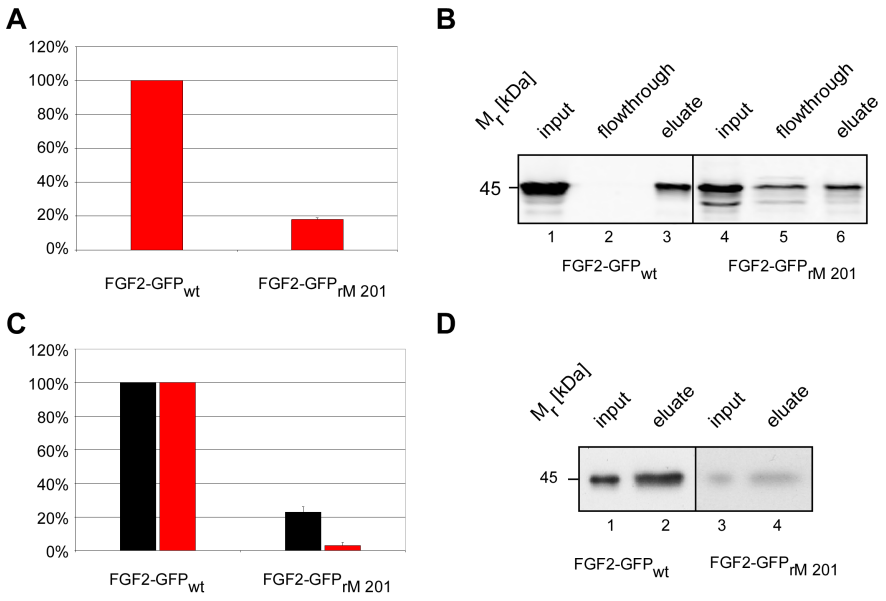

Figure 3.47: Random mutagenesis; 7 amino acid changes: P13H, F21I, F40L, K55T, L64P, C78S, Y133H **A** FACS analysis of cell free supernatant bound to the surface of $CHO_{MCAT/TAM2}$ cells. Cell surface signal of $FGF2\text{-}GFP_{wt}$ was set to 100%. **B** Binding of cell free supernatant to heparin beads. Cell free supernatant was incubated with heparin beads. Total (input, 10%), non-bound (flowthrough, 10%) and bound material (eluate, 10%) was analyzed by SDS-PAGE and Western blotting. **C** Quantitative analysis of export employing flow cytometry. Expression level (black bars) and secreted protein detected on the cell surface (red bars) is shown. FGF2-GFPwt was set to 100%. **D** Biotinylation assay. Cell surface proteins were labelled with a membrane-impermeable biotin reagent. After cell lysis biotinylated and non-biotinylated proteins were separated by streptavidin beads. Total material (input, 5%) and the biotinylated fraction (eluate, 50%) were analyzed by SDS-PAGE and Western blotting. All results shown represent an average of at least 3 different experiments. For further details see Materials and Methods. As a result, this clone shows a binding deficiency in both binding assays. Both secretion assays reveal that the reduced signal for secreted FGF2 is resulting from the low amount of expressed reporter protein.

As demonstrated in figure 3.47, mutant rM 201 showed a reduced ability to bind to heparan sulfate proteoglycans *in vivo* (panel A) as well as to heparin *in vitro* (panel B) when compared to $FGF2\text{-}GFP_{wt}$. The expression level and cell surface staining of $FGF2\text{-}GFP_{rM\ 201}$ is strongly reduced compared to wild-type FGF2-GFP as shown by flow cytometry (panel C) and biotinylation assay (panel D). The combined data obtained demonstrate that the mutations of $FGF2\text{-}GFP_{rM\ 201}$ cause impaired binding to heparin and heparan sulfate proteoglycans as well as an instable fusion protein.

Mutant RM 210 contains 3 amino acid changes: H59P, E68G and I74T.

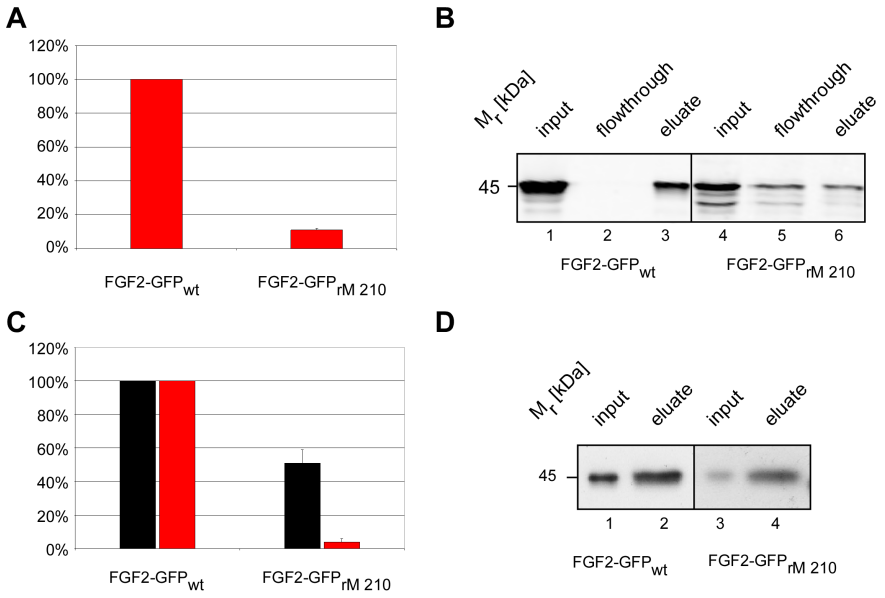

Figure 3.48: Random mutagenesis; 3 amino acid changes: H59P, E68G, I74T **A** FACS analysis of cell free supernatant bound to the surface of $CHO_{MCAT/TAM2}$ cells. Cell surface signal of FGF2-GFPwt was set to 100%. **B** Binding of cell free supernatant to heparin beads. Cell free supernatant was incubated with heparin beads. Total (input, 10%), non-bound (flowthrough, 10%) and bound material (eluate, 10%) was analyzed by SDS-PAGE and Western blotting. **C** Quantitative analysis of export employing flow cytometry. Expression level (black bars) and secreted protein detected on the cell surface (red bars) is shown. FGF2-GFPwt was set to 100%. **D** Biotinylation assay. Cell surface proteins were labelled with a membrane-impermeable biotin reagent. After cell lysis biotinylated and non-biotinylated proteins were separated by streptavidin beads. Total material (input, 5%) and the biotinylated fraction (eluate, 50%) were analyzed by SDS-PAGE and Western blotting. All results shown represent an average of at least 3 different experiments. For further details see Materials and Methods. As a result, this clone shows a binding deficiency in both binding assays. Both secretion assays reveal that the reduced signal for secreted FGF2 is resulting from the low amount of expressed reporter protein.

As demonstrated in figure 3.48, mutant rM 210 showed a reduced ability to bind to heparan sulfate proteoglycans *in vivo* (panel A) as well as to heparin *in vitro* (panel B) when compared to $FGF2\text{-}GFP_{wt}$. The expression level and cell surface staining of $FGF2\text{-}GFP_{rM\ 210}$ is reduced compared to wild-type FGF2-GFP as shown by flow cytometry (panel C) and biotinylation assay (panel D). The combined data obtained demonstrate that the mutations of $FGF2\text{-}GFP_{rM\ 210}$ cause impaired binding to heparin and heparan sulfate proteoglycans as well as an instable fusion protein.

The mutants listed in this section demonstrate an impaired binding to heparin *in vitro* and heparan-sulfate proteoglycans *in vivo*. Additionally, the expression level of the various versions of FGF2-GFP is strongly reduced, indicating a potentionally misfolded proteins which is rapidly degraded or reduced translation rates. As a consequence thereof, these mutants were termed “low expressed and impaired in binding”.

3.3.3.4 *Experimental data for a secretion deficient FGF2 mutant*

The mutant depicted in this section was shown to be secretion deficient using the standard assays described in section 3.3.2.

Mutant rM156 contains 3 amino acid changes: E87K, K128E and R129Q.

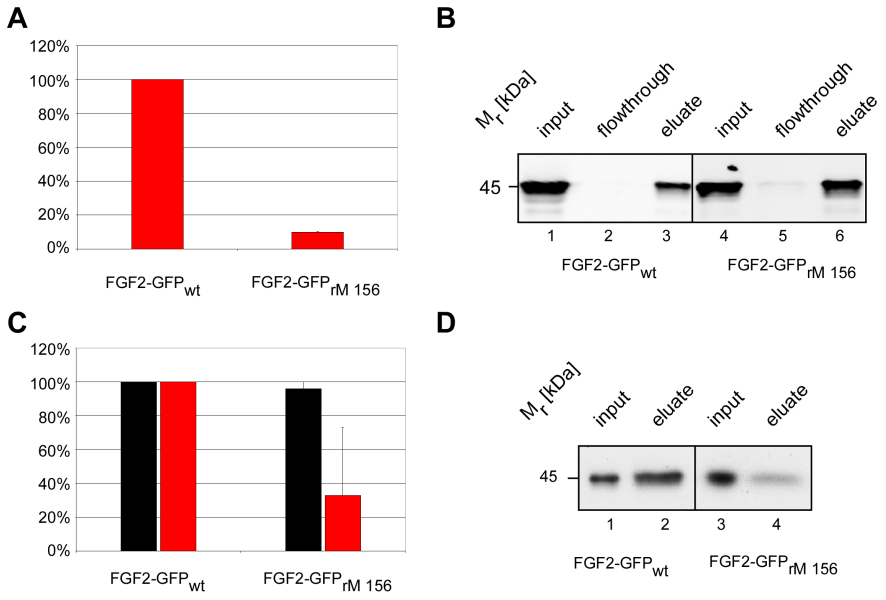

Figure 3.49: Random mutagenesis; 3 amino acid changes: E87K, K128E, R129Q **A** FACS analysis of cell free supernatant bound to the surface of $CHO_{MCAT/TAM2}$ cells. Cell surface signal of $FGF2\text{-}GFP_{wt}$ was set to 100%. **B** Binding of cell free supernatant to heparin beads. Cell free supernatant was incubated with heparin beads. Total (input, 10%), non-bound (flowthrough, 10%) and bound material (eluate, 10%) was analyzed by SDS-PAGE and Western blotting. **C** Quantitative analysis of export employing flow cytometry. Expression level (black bars) and secreted protein detected on the cell surface (red bars) is shown. FGF2-GFPwt was set to 100%. **D** Biotinylation assay. Cell surface proteins were labelled with a membrane-impermeable biotin reagent. After cell lysis biotinylated and non-biotinylated proteins were separated by streptavidin beads. Total material (input, 5%) and the biotinylated fraction (eluate, 50%) were analyzed by SDS-PAGE and Western blotting. All results shown represent an average of at least 3 different experiments. For further details see „Material and Methods“ and explanation of assays in chapter 3.3.2. As a result, this clone shows a reduced signal for protein presented on the cell surface. The result for binding differs. $FGF2\text{-}GFP_{RM156}$ was able to bind to heparin beads in vitro, but could not be bound to the Cell Surface of $CHO_{MCAT/TAM2}$ cells. This clone was subject of further characterizations.

As demonstrated in figure 3.49, the mutant rM156 displayed a constant FGF2-GFP expression level but a reduced signal for secreted FGF2-GFP bound to the cell surface when compared to $FGF2\text{-}GFP_{wt}$ as shown by flow cytometry and cell surface biotinylation, indicating that these mutations influence unconventional secretion of FGF2-GFP. Additionally it was shown that the protein is able to bind *in vitro* to heparin, but its binding *in vivo* to the cell surface of CHO cells is impaired. The combined data obtained for mutant rM 156 are not consistent. It remains elusive if the impaired binding to heparan sulfate proteoglycans results in the reduced amount of secreted FGF2-GFP bound to the cell surface. Therefore, this mutant was characterized in more detail as described in chapter 3.4.2.

3.3.3.5 *Classification of FGF2-GFP mutants obtained by random mutagenesis with regard to secretion efficiency, protein stability and binding to heparin*

The results obtained for the different versions of FGF2-GFP mutants as analyzed by the standard assays are summarized in table 3.2:

classification	Clones
No phenotype	26
	63
	151
	239
	265
	284
	315
	331
	346
	365
Reduced expression level and impaired binding	25
	30
	32
	193
	201
	210
Secretion mutant and impaired in binding	156

Table 3.2: Classifications made for clones created by random mutagenesis.

The results obtained by characterization of mutants generated by random mutagenesis show that most of the generated clones have phenotype characteristics with regard to secretion and heparin binding (10). Additionally mutants with impaired heparin binding ability show low expression levels of FGF2-GFP in the cytosol (7). One mutant was observed, which shows a reduced signal for secreted fusion protein. Strikingly, this fusion protein fails to bind to CHO cells *in vivo*, although binding to heparin beads *in vitro* occurs efficiently. This mutant was further characterized as described in section 3.4.2.

3.3.4 Analysis of mutants obtained by site-directed mutagenesis

In this approach single amino acids of FGF2 were exchanged by site-directed mutagenesis. The mutated amino acids were selected based on the following criteria:

1. Random mutagenesis: Mutants bearing multiple randomly introduced amino acid changes showing an impaired heparin binding ability or altered secretion of FGF2 were further characterized by exchanging every mutated amino acid individually to determine the role of a single amino acid in binding and secretion.

2. Three-dimensional structure: Based on the crystal structure, hydrophobic surface residues of FGF2-GFP were chosen for mutation, which are potentially involved in protein-protein interactions, thus mediating interactions with the translocation machinery.

3. N-terminus: Numerous examples for N-terminal export motifs were shown in the literature. Classical secretory proteins contain an N-terminal signal peptide (Walter et al., 1984) and proteins localized to mitochondria contain an N-terminal cleavable signal sequence (Neupert, 1997). Moreover, it might be possible that co- and/or posttranslational processings of amino acids might be involved in the export process. Side-directed mutations were introduced into the N-terminus to verify if N-terminal residues might be involved in the secretion of FGF2.

4. Dimerization: It has been shown for FGF-1, that the protein is released in an unconventional manner in response to temperature stress as a latent homodimer (Tarantini et al., 1995). Additionally it was shown that dimerization is a prerequisite for FGF2 mediated signalling (Kwan et al., 2001). Therefore two cysteines, potentially mediating dimerization of FGF2 (Kwan et al., 2001), were mutated individually and in combination.

The individual mutations and the criteria for choosing the distinct point mutations are listed in the following table:

Clone	Approach	Clone	Approach
A3V	Random Mutagenesis 25	*E67V*	Random Mutagenesis 265
G4A	N-terminal mutation	*E68A*	Random Mutagenesis 26
S5A	N-terminal mutation	*E68G*	Random Mutagenesis 210
I6T	N-terminal mutation	*R69A*	3-D structure
T7A	N-terminal mutation	*V72A*	Random Mutagenesis 25
T7E	N-terminal mutation	*I74T*	Random Mutagenesis 210
T7D	N-terminal mutation	*K75I*	Random Mutagenesis 365
T8M	Random Mutagenesis 217	*V77A*	Random Mutagenesis 284
E14D	Random Mutagenesis 25	*C78A*	Dimerization
F21I	Random Mutagenesis 201	*N80A*	3-D structure
P23S	Random Mutagenesis	*Y82A*	3-D structure
F26A	3-D structure	*E87K*	Random Mutagenesis 156
K30E	Random Mutagenesis 265	*D88A*	3-D structure
Y33A	3-D structure	*L92A*	3-D structure
F39L	Random Mutagenesis 365	*C96A*	Dimerization
F39A	3-D structure	*F102A*	3-D structure
F40L	Random Mutagenesis 201	*F104A*	3-D structure
R42H	Random Mutagenesis 25	*Y112A*	3-D structure
R53H	3-D structure	*S122A*	3-D structure
K55T	Random Mutagenesis 201	*K128E*	Random Mutagenesis 156
K55R	Random Mutagenesis 26	*R129Q*	Random Mutagenesis 156
H59P	Random Mutagenesis 210	*Q132R*	Random Mutagenesis 365
K61E	Random Mutagenesis 239	*Y133H*	Random Mutagenesis 201
L64P	Random Mutagenesis 201	*Y133A*	3-D structure
Q65A	3-D structure	*S152A*	3-D structure
CC78/96AA	Dimerization		

Table 3.3: Overview of the selection procedure for the construction of point mutations

As listed in table 3.3, 25 point mutations were selected based on the analysis of random mutagenesis, 16 were selected based on crystal structure study, 3 were selected based on their ability to dimerize FGF2 and 6 were chosen based on their location at the N-terminus.

The experimental data for point mutations is shown in the following section, including *in vivo* and *in vitro* binding assays and secretion assays.

3.3.4.1 *Experimental data for mutants showing no phenotype regarding secretion efficiency and affinity to heparin*

In this section, the FGF2 mutants generated by site-directed mutagenesis are depicted which are comparable to wild-type FGF2-GFP with regard to secretion efficiency and binding capability to heparin and heparan sulfate proteoglycans. Moreover, their amino acid changes are shown and a summary of the experimental data is provided. For a detailed view on the assays used, please refer to chapter 3.3.2.

The following mutant contains a mutation at position 3 changing alanine to valine.

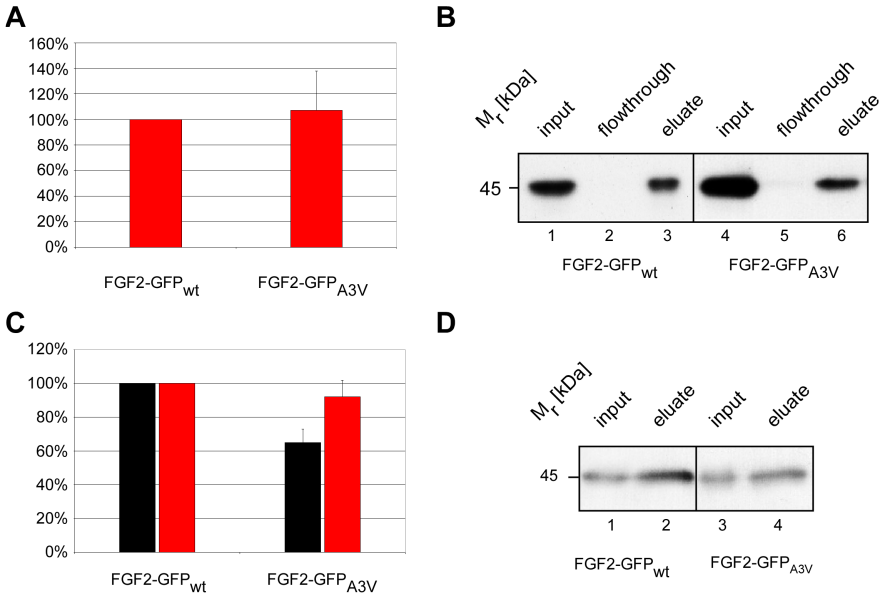

Figure 3.50: Point mutation; amino acid change: A3V **A** FACS analysis of cell free supernatant bound to the surface of $CHO_{MCAT/TAM2}$ cells. cell surface signal of FGF2-GFPwt was set to 100%. **B** Binding of cell free supernatant to heparin beads. Cell free supernatant was incubated with heparin beads. Total (input, 10%), non-bound (flowthrough, 10%) and bound material (eluate, 10%) was analyzed by SDS-PAGE and Western blotting. **C** Quantitative analysis of export employing flow cytometry. Expression level (black bars) and secreted protein detected on the cell surface (red bars) is shown. FGF2-GFPwt was set to 100%. **D** Biotinylation assay. Cell surface proteins were labelled with a membrane-impermeable biotin reagent. After cell lysis biotinylated and non-biotinylated proteins were separated by streptavidin beads. Total material (input, 5%) and the biotinylated fraction (eluate, 50%) were analyzed by SDS-PAGE and Western blotting. All results shown represent an average of at least 3 different experiments. For further details see „Material and Methods“ and explanation of assays in chapter 3.3.2. To summarize the obtained data, this clone does not differ from observations made for wild type FGF2-GFP.

As demonstrated in figure 3.50, the affinities of $FGF2\text{-}GFP_{A3V}$ to heparan sulfate proteoglycans *in vivo* (panel A) and to heparin *in vitro* (panel B) was comparable to those of $FGF2\text{-}GFP_{wt}$. As detected by flow cytometry (panel C), the expression level of $FGF2\text{-}GFP_{A3V}$ was slightly reduced as compared to $FGF2\text{-}GFP_{wt}$, but the amount of secreted fusion protein detected on the cell surface did not vary from wild-type level, in contrast to the result obtained by the biotinylation assay (panel D), which showed slightly reduced secretion efficiency of the mutant when compared to FGF2-

GFP_{wt} cells. However, the combined data obtained for this mutant demonstrate that A3V is not deficient in secretion or impaired in heparin binding and does not show a phenotype which is different from FGF2-GFP_{wt} cells.

The following mutant contains a mutation at position 4, changing glycine to alanine.

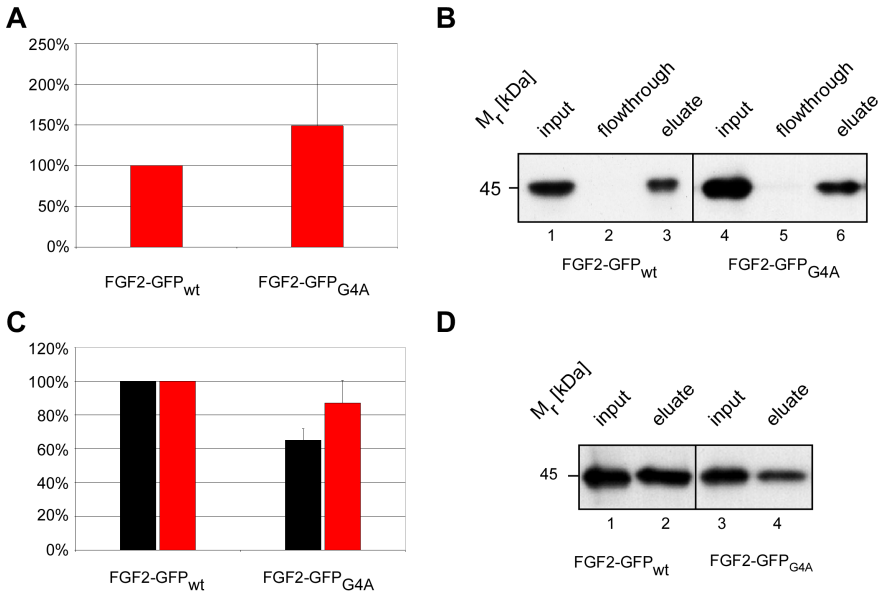

Figure 3.51: Point mutation; amino acid change: G4A **A** FACS analysis of cell free supernatant bound to the surface of $CHO_{MCAT/TAM2}$ cells. Cell surface signal of FGF2-GFPwt was set to 100%. **B** Binding of cell free supernatant to heparin beads. Cell free supernatant was incubated with heparin beads. Total (input, 10%), non-bound (flowthrough, 10%) and bound material (eluate, 10%) was analyzed by SDS-PAGE and Western blotting. **C** Quantitative analysis of export employing flow cytometry. Expression level (black bars) and secreted protein detected on the cell surface (red bars) is shown. FGF2-GFPwt was set to 100%. **D** Biotinylation assay. Cell surface proteins were labelled with a membrane-impermeable biotin reagent. After cell lysis biotinylated and non-biotinylated proteins were separated by streptavidin beads. Total material (input, 5%) and the biotinylated fraction (eluate, 50%) were analyzed by SDS-PAGE and Western blotting. All results shown represent an average of at least 3 different experiments. For further details see „Material and Methods" and explanation of assays in chapter 3.3.2. To summarize the obtained data, this clone does not alter from observations made for wild-type FGF2-GFP.

As demonstrated in figure 3.51, the mutant G4A showed an enhanced ability to bind to heparan sulfate proteoglycans *in vivo* (about 150% ± 100%; panel A), but its affinity to heparin *in vitro* was comparable to FGF2-GFP_{wt} heparin affinity. As detected by flow cytometry (panel C), the expression level of FGF2-GFP_{G4A} was slightly reduced as compared to FGF2-GFP_{wt}, but the amount of secreted fusion protein detected on the cell surface did not vary from wild-type level. The data obtained by flow cytometry were confirmed by the biotinylation assay (panel D). These experiments demonstrate that the mutant G4A does not differ from wild-type FGF2-GFP with regard to secretion efficiency, affinity to heparin and heparan sulfate proteoglycans.

The following mutant contains a mutation at position 5, changing serine to alanine.

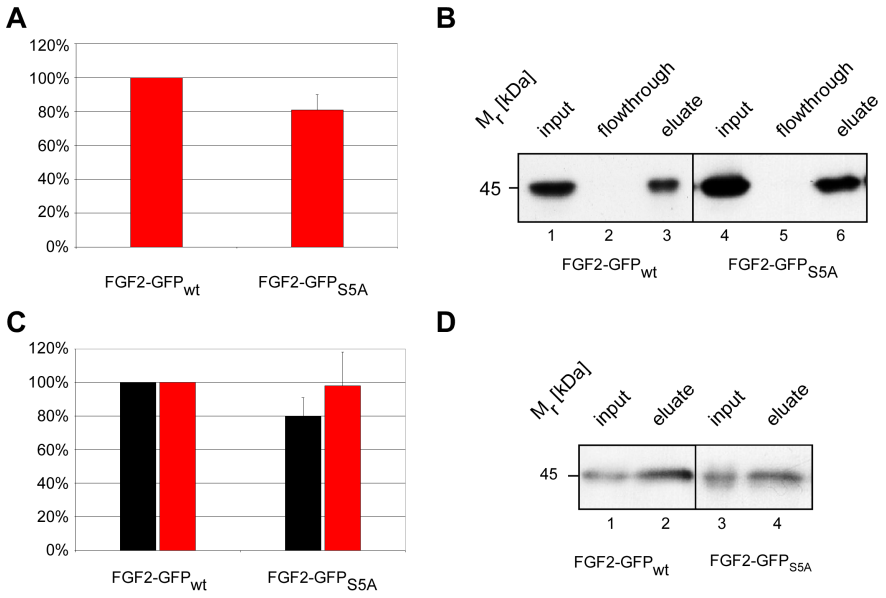

Figure 3.52: Point mutation; amino acid change: S5A **A** FACS analysis of cell free supernatant bound to the surface of $CHO_{MCAT/TAM2}$ cells. Cell surface signal of FGF2-GFPwt was set to 100%. **B** Binding of cell free supernatant to heparin beads. Cell free supernatant was incubated with heparin beads. Total (input, 10%), non-bound (flowthrough, 10%) and bound material (eluate, 10%) was analyzed by SDS-PAGE and Western blotting. **C** Quantitative analysis of export employing flow cytometry. Expression level (black bars) and secreted protein detected on the cell surface (red bars) is shown. FGF2-GFPwt was set to 100%. **D** Biotinylation assay. Cell surface proteins were labelled with a membrane-impermeable biotin reagent. After cell lysis biotinylated and non-biotinylated proteins were separated by streptavidin beads. Total material (input, 5%) and the biotinylated fraction (eluate, 50%) were analyzed by SDS-PAGE and Western blotting. All results shown represent an average of at least 3 different experiments. For further details see „Material and Methods“ and explanation of assays in chapter 3.3.2. To summarize the obtained data, this clone does not alter from observations made for wild-type FGF2-GFP.

As demonstrated in figure 3.52, the affinities of $FGF2\text{-}GFP_{S5A}$ to heparan sulfate proteoglycans *in vivo* (panel A) and to heparin *in vitro* (panel B) was comparable to those of $FGF2\text{-}GFP_{wt}$. As detected by flow cytometry (panel C), the expression level of $FGF2\text{-}GFP_{S5A}$ was slightly reduced as compared to $FGF2\text{-}GFP_{wt}$, but the amount of secreted fusion protein detected on the cell surface did not vary from wild-type level, in contrast to the result obtained by the biotinylation assay (panel D), which showed slightly reduced secretion efficiency of the mutant when compared to $FGF2\text{-}GFP_{wt}$ cells. However, the combined data obtained for this mutant demonstrate that S5A is not deficient in secretion or impaired in heparin binding and does not show a phenotype which is different from $FGF2\text{-}GFP_{wt}$ cells.

The following mutant contains a mutation at position 6, changing isoleucine to alanine.

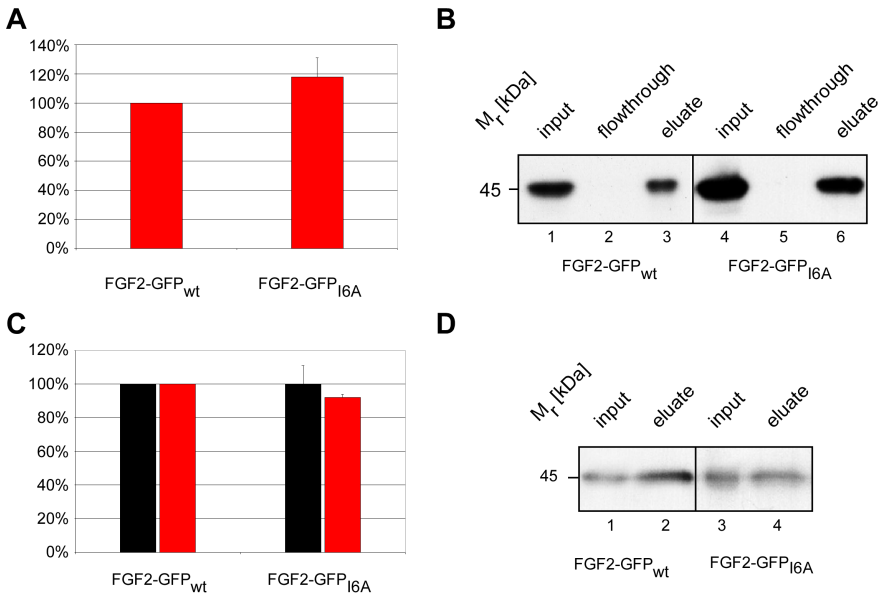

Figure 3.53: Point mutation; amino acid change: I6A **A** FACS analysis of cell free supernatant bound to the surface of $CHO_{MCAT/TAM2}$ cells. Cell surface signal of FGF2-GFPwt was set to 100%. **B** Binding of cell free supernatant to heparin beads. Cell free supernatant was incubated with heparin beads. Total (input, 10%), non-bound (flowthrough, 10%) and bound material (eluate, 10%) was analyzed by SDS-PAGE and Western blotting. **C** Quantitative analysis of export employing flow cytometry. Expression level (black bars) and secreted protein detected on the cell surface (red bars) is shown. FGF2-GFPwt was set to 100%. **D** Biotinylation assay. Cell surface proteins were labelled with a membrane-impermeable biotin reagent. After cell lysis biotinylated and non-biotinylated proteins were separated by streptavidin beads. Total material (input, 5%) and the biotinylated fraction (eluate, 50%) were analyzed by SDS-PAGE and Western blotting. All results shown represent an average of at least 3 different experiments. For further details see „Material and Methods“ and explanation of assays in chapter 3.3.2. To summarize the obtained data, this clone does not alter from observations made for wild-type FGF2-GFP.

As demonstrated in figure 3.53, the affinities of $FGF2\text{-}GFP_{I6A}$ to heparan sulfate proteoglycans *in vivo* (panel A) and to heparin *in vitro* (panel B) was comparable to those of$FGF2\text{-}GFP_{wt}$. As detected by flow cytometry (panel C), both the expression level and the cell surface staining of $FGF2\text{-}GFP_{I6A}$ did not vary from wild-type level, in contrast to the result obtained by the biotinylation assay (panel D), which showed slightly reduced secretion efficiency of the mutant when compared to $FGF2\text{-}GFP_{wt}$ cells. However, the combined data obtained for this mutant demonstrate that I6A is not deficient in secretion or impaired in heparin binding and does not show a phenotype which is different from $FGF2\text{-}GFP_{wt}$ cells.

The following mutant contains a mutation at position 7, changing threonine to alanine.

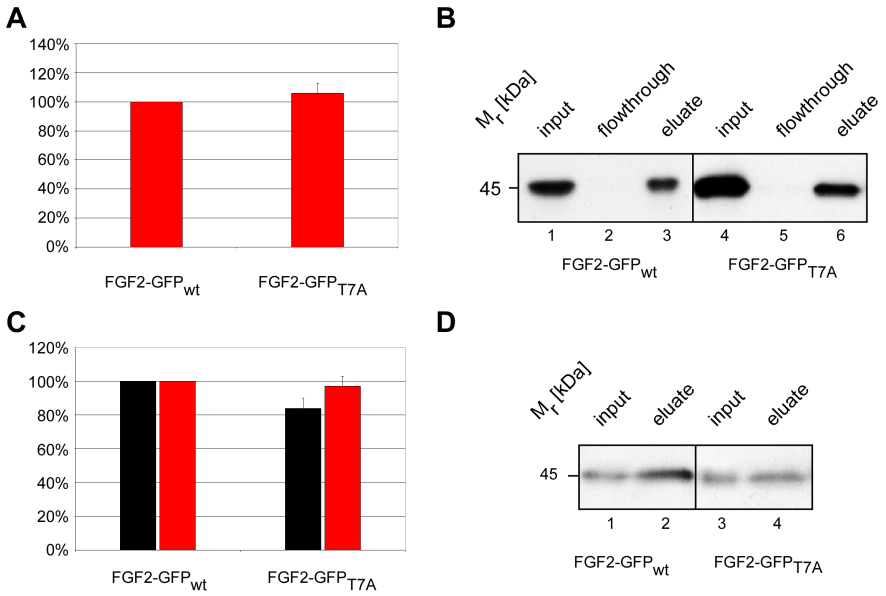

Figure 3.54: Point mutation; amino acid change: T7A **A** FACS analysis of cell free supernatant bound to the surface of $CHO_{MCAT/TAM2}$ cells. Cell surface signal of FGF2-GFPwt was set to 100%. **B** Binding of cell free supernatant to heparin beads. Cell free supernatant was incubated with heparin beads. Total (input, 10%), non-bound (flowthrough, 10%) and bound material (eluate, 10%) was analyzed by SDS-PAGE and Western blotting. **C** Quantitative analysis of export employing flow cytometry. Expression level (black bars) and secreted protein detected on the cell surface (red bars) is shown. FGF2-GFPwt was set to 100%. **D** Biotinylation assay. Cell surface proteins were labelled with a membrane-impermeable biotin reagent. After cell lysis biotinylated and non-biotinylated proteins were separated by streptavidin beads. Total material (input, 5%) and the biotinylated fraction (eluate, 50%) were analyzed by SDS-PAGE and Western blotting. All results shown represent an average of at least 3 different experiments. For further details see „Material and Methods“ and explanation of assays in chapter 3.3.2. To summarize the obtained data, this clone does not alter from observations made for wild-type FGF2-GFP.

As demonstrated in figure 3.54, the affinities of $FGF2\text{-}GFP_{T7A}$ to heparan sulfate proteoglycans *in vivo* (panel A) and to heparin *in vitro* (panel B) was comparable to those of $FGF2\text{-}GFP_{wt}$. As detected by flow cytometry (panel C), both the expression level and the cell surface staining of $FGF2\text{-}GFP_{T7A}$ did not vary from wild-type level, in contrast to the result obtained by the biotinylation assay (panel D), which showed slightly reduced secretion efficiency of the mutant when compared to $FGF2\text{-}GFP_{wt}$ cells. However, the combined data obtained for this mutant demonstrate that T7A is not deficient in secretion or impaired in heparin binding and does not show a phenotype which is different from $FGF2\text{-}GFP_{wt}$ cells.

The following mutant contains a mutation at position 7, changing threonine to glutamic acid.

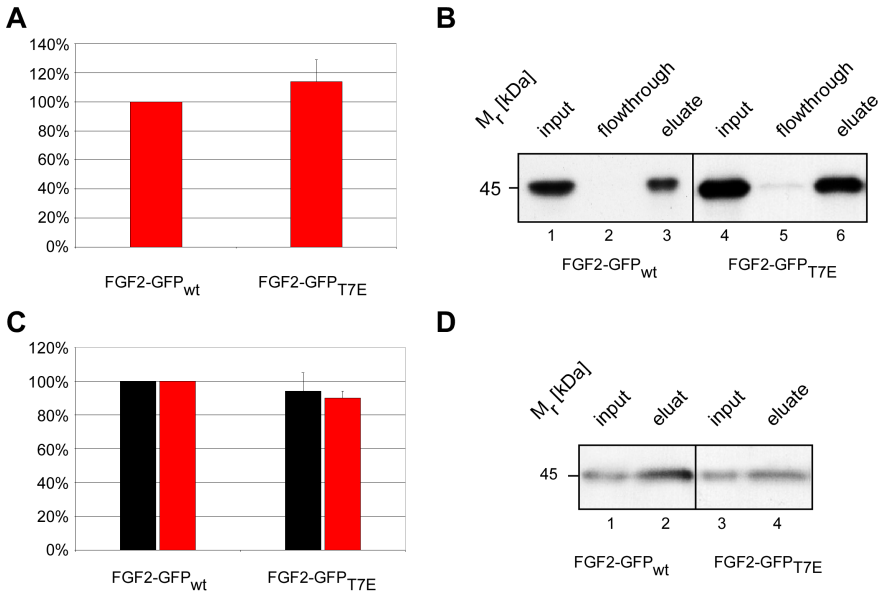

Figure 3.55: Point mutation; amino acid change: T7E **A** FACS analysis of cell free supernatant bound to the surface of $CHO_{MCAT/TAM2}$ cells. Cell surface signal of FGF2-GFPwt was set to 100%. **B** Binding of cell free supernatant to heparin beads. Cell free supernatant was incubated with heparin beads. Total (input, 10%), non-bound (flowthrough, 10%) and bound material (eluate, 10%) was analyzed by SDS-PAGE and Western blotting. **C** Quantitative analysis of export employing flow cytometry. Expression level (black bars) and secreted protein detected on the cell surface (red bars) is shown. FGF2-GFPwt was set to 100%. **D** Biotinylation assay. Cell surface proteins were labelled with a membrane-impermeable biotin reagent. After cell lysis biotinylated and non-biotinylated proteins were separated by streptavidin beads. Total material (input, 5%) and the biotinylated fraction (eluate, 50%) were analyzed by SDS-PAGE and Western blotting. All results shown represent an average of at least 3 different experiments. For further details see „Material and Methods“ and explanation of assays in chapter 3.3.2. To summarize the obtained data, this clone does not alter from observations made for wild-type FGF2-GFP.

As demonstrated in figure 3.55, the affinities of $FGF2\text{-}GFP_{T7E}$ to heparan sulfate proteoglycans *in vivo* (panel A) and to heparin *in vitro* (panel B) was comparable to those of $FGF2\text{-}GFP_{wt}$. As detected by flow cytometry (panel C), both the expression level and the cell surface staining of $FGF2\text{-}GFP_{T7E}$ did not vary from wild-type level, in contrast to the result obtained by the biotinylation assay (panel D), which showed slightly reduced secretion efficiency of the mutant when compared to $FGF2\text{-}GFP_{wt}$ cells. However, the combined data obtained for this mutant demonstrate that T7E is not deficient in secretion or impaired in heparin binding and does not show a phenotype which is different from $FGF2\text{-}GFP_{wt}$ cells.

The following mutant contains a mutation at position 7, changing threonine to aspartic acid.

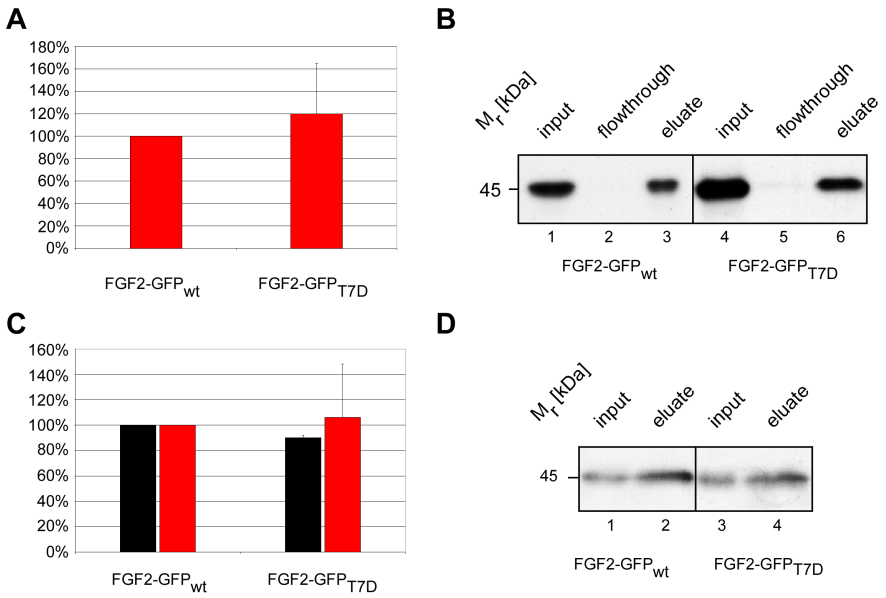

Figure 3.56: Point mutation; amino acid change: T7D **A** FACS analysis of cell free supernatant bound to the surface of $CHO_{MCAT/TAM2}$ cells. Cell surface signal of FGF2-GFPwt was set to 100%. **B** Binding of cell free supernatant to heparin beads. Cell free supernatant was incubated with heparin beads. Total (input, 10%), non-bound (flowthrough, 10%) and bound material (eluate, 10%) was analyzed by SDS-PAGE and Western blotting. **C** Quantitative analysis of export employing flow cytometry. Expression level (black bars) and secreted protein detected on the cell surface (red bars) is shown. FGF2-GFPwt was set to 100%. **D** Biotinylation assay. Cell surface proteins were labelled with a membrane-impermeable biotin reagent. After cell lysis biotinylated and non-biotinylated proteins were separated by streptavidin beads. Total material (input, 5%) and the biotinylated fraction (eluate, 50%) were analyzed by SDS-PAGE and Western blotting. All results shown represent an average of at least 3 different experiments. For further details see „Material and Methods“ and explanation of assays in chapter 3.3.2. To summarize the obtained data, this clone does not alter from observations made for wild-type FGF2-GFP.

As demonstrated in figure 3.56, the affinity of $FGF2\text{-}GFP_{T7D}$ to heparan sulfate proteoglycans *in vivo* (panel A) and its affinity to heparin *in vitro* (panel B) was comparable to $FGF2\text{-}GFP_{wt}$ heparin affinity. As detected by flow cytometry (panel C), both the expression level and the cell surface staining of $FGF2\text{-}GFP_{T7D}$ did not vary from wild-type level. This result was confirmed by performing a biotinylation assay (panel D). The combined data obtained for this mutant demonstrate that T7D is not deficient in secretion or impaired in heparin binding and does not show a phenotype which is different from $FGF2\text{-}GFP_{wt}$ cells.

The following mutant contains a mutation at position 8, changing threonine to methionine.

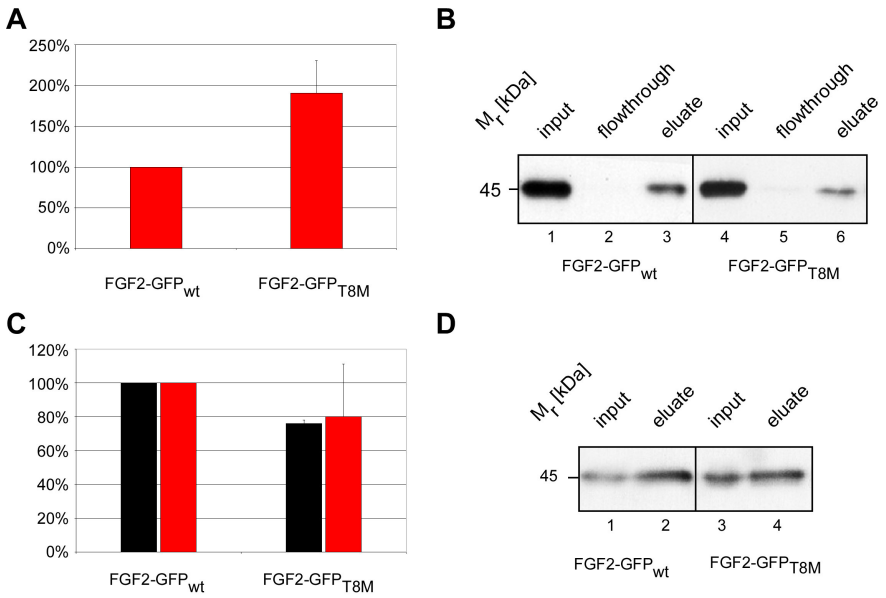

Figure 3.57: Point mutation; amino acid change: T8M **A** FACS analysis of cell free supernatant bound to the surface of $CHO_{MCAT/TAM2}$ cells. Cell surface signal of FGF2-GFPwt was set to 100%. **B** Binding of cell free supernatant to heparin beads. Cell free supernatant was incubated with heparin beads. Total (input, 10%), non-bound (flowthrough, 10%) and bound material (eluate, 10%) was analyzed by SDS-PAGE and Western blotting. **C** Quantitative analysis of export employing flow cytometry. Expression level (black bars) and secreted protein detected on the cell surface (red bars) is shown. FGF2-GFPwt was set to 100%. **D** Biotinylation assay. Cell surface proteins were labelled with a membrane-impermeable biotin reagent. After cell lysis biotinylated and non-biotinylated proteins were separated by streptavidin beads. Total material (input, 5%) and the biotinylated fraction (eluate, 50%) were analyzed by SDS-PAGE and Western blotting. All results shown represent an average of at least 3 different experiments. For further details see „Material and Methods" and explanation of assays in chapter 3.3.2. To summarize the obtained data, this clone does not alter from observations made for wild-type FGF2-GFP.

As demonstrated in figure 3.57, the affinity of $FGF2\text{-}GFP_{T8M}$ to heparan sulfate proteoglycans in vivo (panel A) was enhanced (about 200% ± 40%), but its affinity to heparin *in vitro* (panel B) was comparable to $FGF2\text{-}GFP_{wt}$ heparin affinity. As detected by flow cytometry (panel C), both the expression level and the cell surface staining of $FGF2\text{-}GFP_{T8M}$ did not vary from wild-type level. This result was confirmed by performing the biotinylation assay (panel D). The combined data obtained for this mutant demonstrate that T8M is not deficient in secretion or impaired in heparin binding and does not show a phenotype which is different from $FGF2\text{-}GFP_{wt}$ cells.

The following mutant contains a mutation at position 14, changing glutamic acid to aspartic acid.

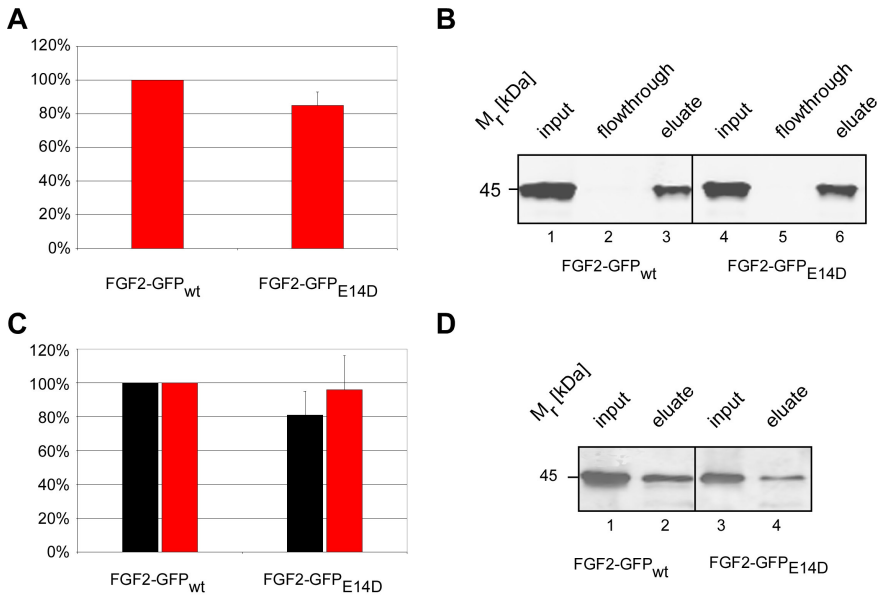

Figure 3.58: Point mutation; amino acid change: E14D **A** FACS analysis of cell free supernatant bound to the surface of $CHO_{MCAT/TAM2}$ cells. Cell surface signal of FGF2-GFPwt was set to 100%. **B** Binding of cell free supernatant to heparin beads. Cell free supernatant was incubated with heparin beads. Total (input, 10%), non-bound (flowthrough, 10%) and bound material (eluate, 10%) was analyzed by SDS-PAGE and Western blotting. **C** Quantitative analysis of export employing flow cytometry. Expression level (black bars) and secreted protein detected on the cell surface (red bars) is shown. FGF2-GFPwt was set to 100%. **D** Biotinylation assay. Cell surface proteins were labelled with a membrane-impermeable biotin reagent. After cell lysis biotinylated and non-biotinylated proteins were separated by streptavidin beads. Total material (input, 5%) and the biotinylated fraction (eluate, 50%) were analyzed by SDS-PAGE and Western blotting. All results shown represent an average of at least 3 different experiments. For further details see „Material and Methods“ and explanation of assays in chapter 3.3.2. To summarize the obtained data, this clone does not alter from observations made for wild-type FGF2-GFP.

As demonstrated in figure 3.58, the affinity of $FGF2\text{-}GFP_{E14D}$ to heparan sulfate proteoglycans *in vivo* (panel A) and its affinity to heparin *in vitro* (panel B) was comparable to $FGF2\text{-}GFP_{wt}$ heparin affinity. As detected by flow cytometry (panel C), both the expression level and the cell surface staining of $FGF2\text{-}GFP_{E14D}$ did not vary from wild-type level. This result was confirmed by performing a biotinylation assay (panel D). The combined data obtained for this mutant demonstrate that E14D is not deficient in secretion or impaired in heparin binding and does not show a phenotype which is different from $FGF2\text{-}GFP_{wt}$ cells.

The following mutant contains a mutation at position 21, changing phenylalanine to isoleucine.

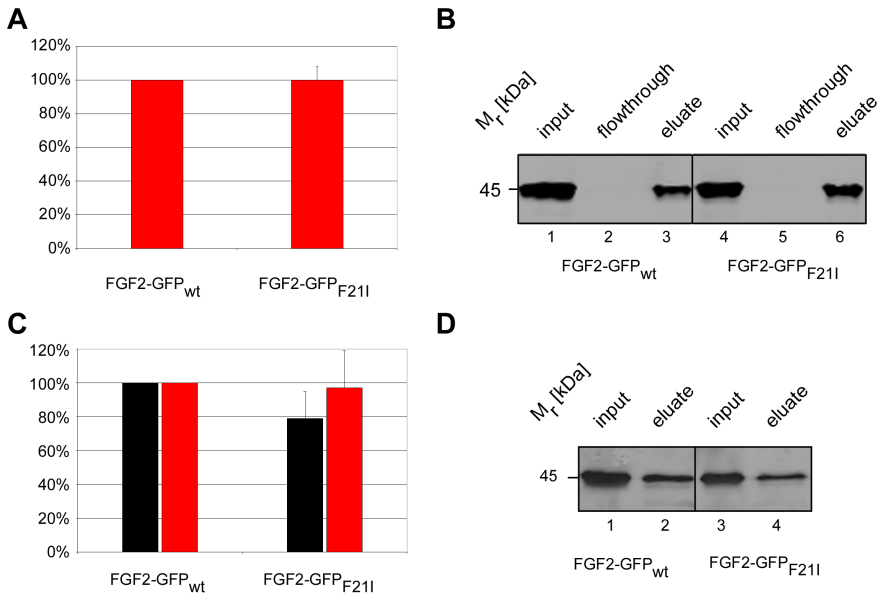

Figure 3.59: Point mutation; amino acid change: F21I **A** FACS analysis of cell free supernatant bound to the surface of $CHO_{MCAT/TAM2}$ cells. Cell surface signal of FGF2-GFPwt was set to 100%. **B** Binding of cell free supernatant to heparin beads. Cell free supernatant was incubated with heparin beads. Total (input, 10%), non-bound (flowthrough, 10%) and bound material (eluate, 10%) was analyzed by SDS-PAGE and Western blotting. **C** Quantitative analysis of export employing flow cytometry. Expression level (black bars) and secreted protein detected on the cell surface (red bars) is shown. FGF2-GFPwt was set to 100%. **D** Biotinylation assay. Cell surface proteins were labelled with a membrane-impermeable biotin reagent. After cell lysis biotinylated and non-biotinylated proteins were separated by streptavidin beads. Total material (input, 5%) and the biotinylated fraction (eluate, 50%) were analyzed by SDS-PAGE and Western blotting. All results shown represent an average of at least 3 different experiments. For further details see „Material and Methods“ and explanation of assays in chapter 3.3.2. To summarize the obtained data, this clone does not alter from observations made for wild-type FGF2-GFP.

As demonstrated in figure 3.59, the affinity of $FGF2\text{-}GFP_{F21I}$ to heparan sulfate proteoglycans *in vivo* (panel A) and its affinity to heparin *in vitro* (panel B) was comparable to $FGF2\text{-}GFP_{wt}$ heparin affinity. As detected by flow cytometry (panel C), both the expression level and the cell surface staining of $FGF2\text{-}GFP_{F21I}$ did not vary from wild-type level. This result was confirmed by performing a biotinylation assay (panel D). The combined data obtained for this mutant demonstrate that F21I is not deficient in secretion or impaired in heparin binding and does not show a phenotype which is different from $FGF2\text{-}GFP_{wt}$ cells.

The following mutant contains a mutation at position 23, changing proline to serine.

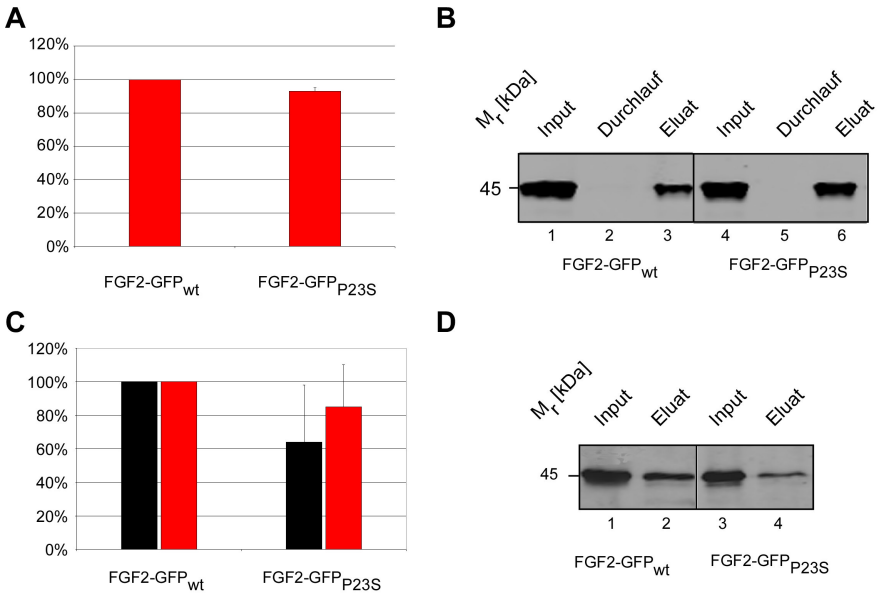

Figure 3.60: Point mutation; amino acid change: P23S **A** FACS analysis of cell free supernatant bound to the surface of $CHO_{MCAT/TAM2}$ cells. Cell surface signal of FGF2-GFPwt was set to 100%. **B** Binding of cell free supernatant to heparin beads. Cell free supernatant was incubated with heparin beads. Total (input, 10%), non-bound (flowthrough, 10%) and bound material (eluate, 10%) was analyzed by SDS-PAGE and Western blotting. **C** Quantitative analysis of export employing flow cytometry. Expression level (black bars) and secreted protein detected on the cell surface (red bars) is shown. FGF2-GFPwt was set to 100%. **D** Biotinylation assay. Cell surface proteins were labelled with a membrane-impermeable biotin reagent. After cell lysis biotinylated and non-biotinylated proteins were separated by streptavidin beads. Total material (input, 5%) and the biotinylated fraction (eluate, 50%) were analyzed by SDS-PAGE and Western blotting. All results shown represent an average of at least 3 different experiments. For further details see „Material and Methods" and explanation of assays in chapter 3.3.2. To summarize the obtained data, this clone does not alter from observations made for wild-type FGF2-GFP.

As demonstrated in figure 3.60, the affinity of $FGF2\text{-}GFP_{P23S}$ to heparan sulfate proteoglycans *in vivo* (panel A) and its affinity to heparin *in vitro* (panel B) was comparable to $FGF2\text{-}GFP_{wt}$ heparin affinity. As detected by flow cytometry (panel C), the expression level of $FGF2\text{-}GFP_{P23S}$ was slightly reduced as compared to $FGF2\text{-}GFP_{wt}$, but the amount of secreted fusion protein detected on the cell surface did not vary from wild-type level, in contrast to the result obtained by the biotinylation assay (panel D), which showed slightly reduced secretion efficiency of the mutant when compared to $FGF2\text{-}GFP_{wt}$. However, the combined data obtained for this mutant demonstrate that P23S is not deficient in secretion or impaired in heparin binding and does not show a phenotype which is different from $FGF2\text{-}GFP_{wt}$ cells.

The following mutant contains a mutation at position 26, changing phenylalanine to alanine.

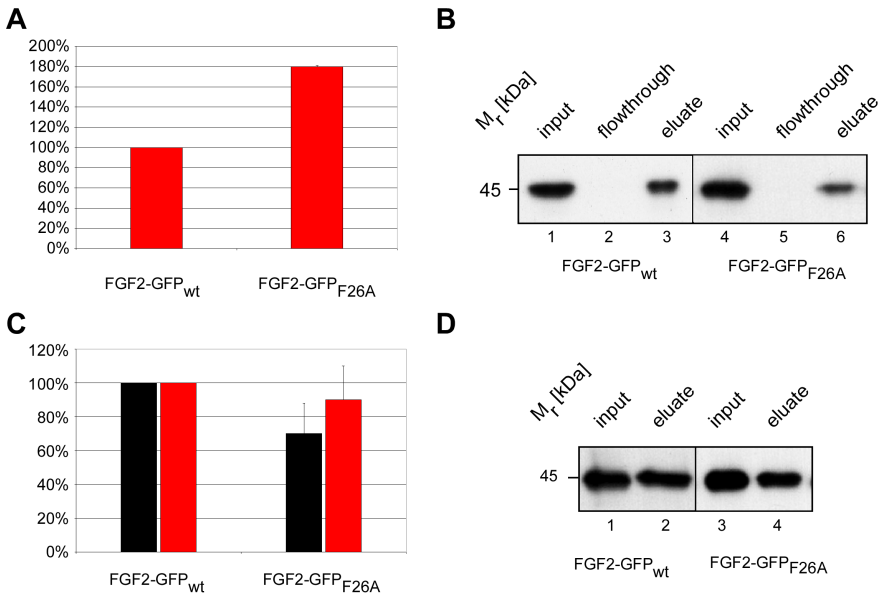

Figure 3.61: Point mutation; amino acid change: F26A **A** FACS analysis of cell free supernatant bound to the surface of $CHO_{MCAT/TAM2}$ cells. Cell surface signal of FGF2-GFPwt was set to 100%. **B** Binding of cell free supernatant to heparin beads. Cell free supernatant was incubated with heparin beads. Total (input, 10%), non-bound (flowthrough, 10%) and bound material (eluate, 10%) was analyzed by SDS-PAGE and Western blotting. **C** Quantitative analysis of export employing flow cytometry. Expression level (black bars) and secreted protein detected on the cell surface (red bars) is shown. FGF2-GFPwt was set to 100%. **D** Biotinylation assay. Cell surface proteins were labelled with a membrane-impermeable biotin reagent. After cell lysis biotinylated and non-biotinylated proteins were separated by streptavidin beads. Total material (input, 5%) and the biotinylated fraction (eluate, 50%) were analyzed by SDS-PAGE and Western blotting. All results shown represent an average of at least 3 different experiments. For further details see „Material and Methods" and explanation of assays in chapter 3.3.2. To summarize the obtained data, this clone does not alter from observations made for wild-type FGF2-GFP.

As demonstrated in figure 3.61, the affinity of $FGF2\text{-}GFP_{F26A}$ to heparan sulfate proteoglycans in vivo (panel A) was enhanced (about 180%), but its affinity to heparin *in vitro* (panel B) was comparable to $FGF2\text{-}GFP_{wt}$ heparin affinity. As detected by flow cytometry (panel C), the expression level of $FGF2\text{-}GFP_{F26A}$ was slightly reduced as compared to $FGF2\text{-}GFP_{wt}$, but the amount of secreted fusion protein detected on the cell surface did not vary from wild-type level. This result was confirmed by performing the biotinylation assay (panel D). The combined data obtained for this mutant demonstrate that F26A is not deficient in secretion or impaired in heparin binding and does not show a phenotype which is different from $FGF2\text{-}GFP_{wt}$ cells.

The following mutant contains a mutation at position 30, changing lysine to glutamic acid.

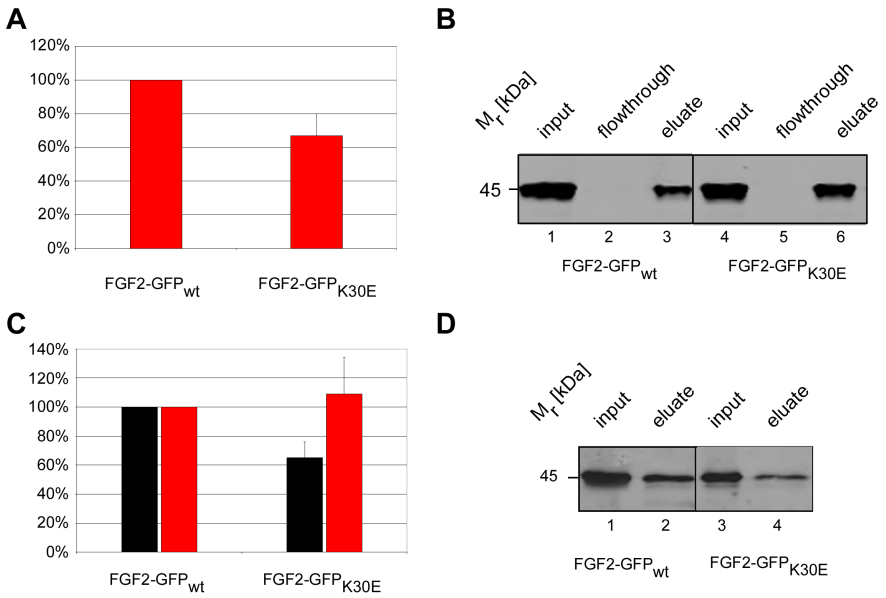

Figure 3.62: Point mutation; amino acid change: K30E **A** FACS analysis of cell free supernatant bound to the surface of $CHO_{MCAT/TAM2}$ cells. Cell surface signal of FGF2-GFPwt was set to 100%. **B** Binding of cell free supernatant to heparin beads. Cell free supernatant was incubated with heparin beads. Total (input, 10%), non-bound (flowthrough, 10%) and bound material (eluate, 10%) was analyzed by SDS-PAGE and Western blotting. **C** Quantitative analysis of export employing flow cytometry. Expression level (black bars) and secreted protein detected on the cell surface (red bars) is shown. FGF2-GFPwt was set to 100%. **D** Biotinylation assay. Cell surface proteins were labelled with a membrane-impermeable biotin reagent. After cell lysis biotinylated and non-biotinylated proteins were separated by streptavidin beads. Total material (input, 5%) and the biotinylated fraction (eluate, 50%) were analyzed by SDS-PAGE and Western blotting. All results shown represent an average of at least 3 different experiments. For further details see „Material and Methods“ and explanation of assays in chapter 3.3.2. To summarize the obtained data, this clone does not alter from observations made for wild-type FGF2-GFP.

As demonstrated in figure 3.62, the affinity of $FGF2\text{-}GFP_{K30E}$ to heparan sulfate proteoglycans *in vivo* (panel A) is reduced (about 60% ± 20%), but its affinity to heparin *in vitro* (panel B) was comparable to $FGF2\text{-}GFP_{wt}$ heparin affinity. As detected by flow cytometry (panel C), the expression level of $FGF2\text{-}GFP_{K30E}$ was slightly reduced as compared to $FGF2\text{-}GFP_{wt}$, but the amount of secreted fusion protein detected on the cell surface did not vary from wild-type level. This result was confirmed by performing the biotinylation assay (panel D). The combined data obtained for this mutant demonstrate that K30E is not deficient in secretion or impaired in heparin binding and does not show a phenotype which is different from $FGF2\text{-}GFP_{wt}$ cells.

The following mutant contains a mutation at position 33, changing tyrosine to alanine.

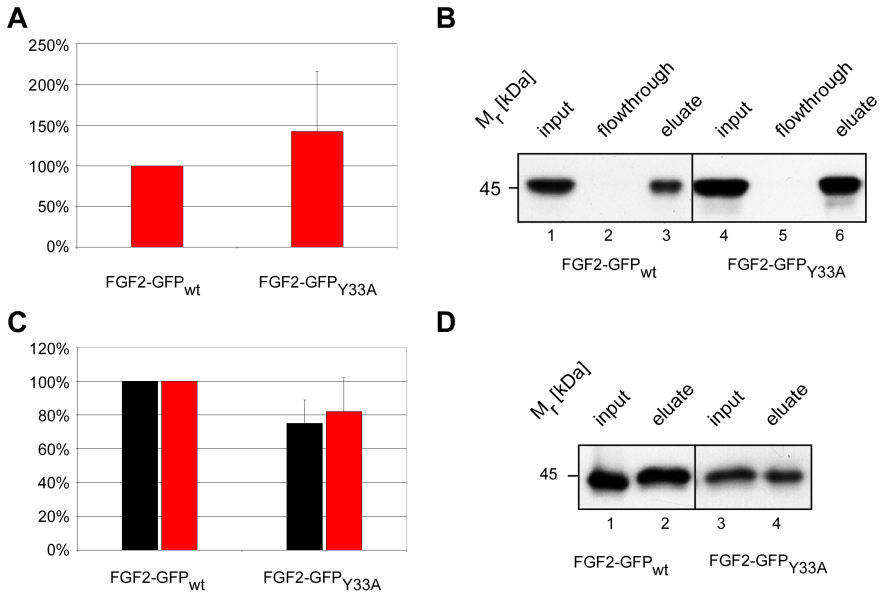

Figure 3.63: Point mutation; amino acid change: Y33A **A** FACS analysis of cell free supernatant bound to the surface of $CHO_{MCAT/TAM2}$ cells. Cell surface signal of FGF2-GFPwt was set to 100%. **B** Binding of cell free supernatant to heparin beads. Cell free supernatant was incubated with heparin beads. Total (input, 10%), non-bound (flowthrough, 10%) and bound material (eluate, 10%) was analyzed by SDS-PAGE and Western blotting. **C** Quantitative analysis of export employing flow cytometry. Expression level (black bars) and secreted protein detected on the cell surface (red bars) is shown. FGF2-GFPwt was set to 100%. **D** Biotinylation assay. Cell surface proteins were labelled with a membrane-impermeable biotin reagent. After cell lysis biotinylated and non-biotinylated proteins were separated by streptavidin beads. Total material (input, 5%) and the biotinylated fraction (eluate, 50%) were analyzed by SDS-PAGE and Western blotting. All results shown represent an average of at least 3 different experiments. For further details see „Material and Methods“ and explanation of assays in chapter 3.3.2. To summarize the obtained data, this clone does not alter from observations made for wild-type FGF2-GFP.

As demonstrated in figure 3.63, the affinity of $FGF2\text{-}GFP_{Y33A}$ to heparan sulfate proteoglycans in vivo (panel A) was enhanced (about 150% ± 60 %), but its affinity to heparin *in vitro* (panel B) was comparable to $FGF2\text{-}GFP_{wt}$ heparin affinity. As detected by flow cytometry (panel C), both the expression level and the cell surface staining of $FGF2\text{-}GFP_{Y33A}$ did not vary from wild-type level. This result was confirmed by performing the biotinylation assay (panel D). The combined data obtained for this mutant demonstrate that Y33A is not deficient in secretion or impaired in heparin binding and does not show a phenotype which is different from $FGF2\text{-}GFP_{wt}$ cells.

The following mutant contains a mutation at position 39, changing phenylalanine to leucine.

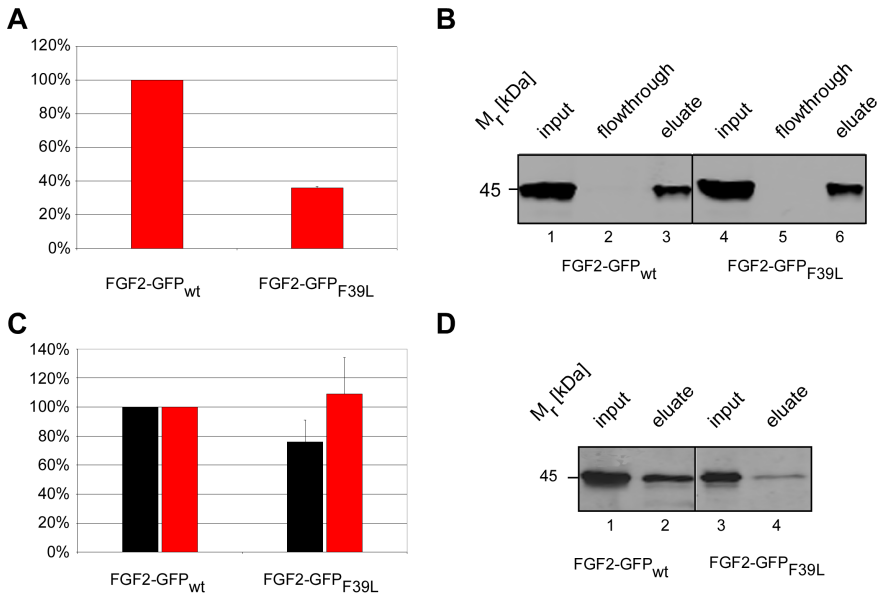

Figure 3.64: Point mutation; amino acid change: F39L **A** FACS analysis of cell free supernatant bound to the surface of $CHO_{MCAT/TAM2}$ cells. Cell surface signal of FGF2-GFPwt was set to 100%. **B** Binding of cell free supernatant to heparin beads. Cell free supernatant was incubated with heparin beads. Total (input, 10%), non-bound (flowthrough, 10%) and bound material (eluate, 10%) was analyzed by SDS-PAGE and Western blotting. **C** Quantitative analysis of export employing flow cytometry. Expression level (black bars) and secreted protein detected on the cell surface (red bars) is shown. FGF2-GFPwt was set to 100%. **D** Biotinylation assay. Cell surface proteins were labelled with a membrane-impermeable biotin reagent. After cell lysis biotinylated and non-biotinylated proteins were separated by streptavidin beads. Total material (input, 5%) and the biotinylated fraction (eluate, 50%) were analyzed by SDS-PAGE and Western blotting. All results shown represent an average of at least 3 different experiments. For further details see „Material and Methods“ and explanation of assays in chapter 3.3.2. To summarize the obtained data, this clone does not alter from observations made for wild-type FGF2-GFP.

As demonstrated in figure 3.64, the affinity of $FGF2\text{-}GFP_{F39L}$ to heparan sulfate proteoglycans *in vivo* (panel A) is reduced (about 40%) but its affinity to heparin *in vitro* (panel B) was comparable to $FGF2\text{-}GFP_{wt}$ heparin affinity. As detected by flow cytometry (panel C), the expression level of $FGF2\text{-}GFP_{F39L}$ was slightly reduced as compared to $FGF2\text{-}GFP_{wt}$, but the amount of secreted fusion protein detected on the cell surface did not vary from wild-type level. The result obtained by the biotinylation assay (panel D) demonstrated slightly reduced secretion efficiency of the mutant when compared to $FGF2\text{-}GFP_{wt}$. The combined data obtained for this mutant demonstrate that F39L is not deficient in secretion or impaired in heparin binding and does not show a phenotype which is different from $FGF2\text{-}GFP_{wt}$ cells.

The following mutant contains a mutation at position 39, changing phenylalanine to alanine.

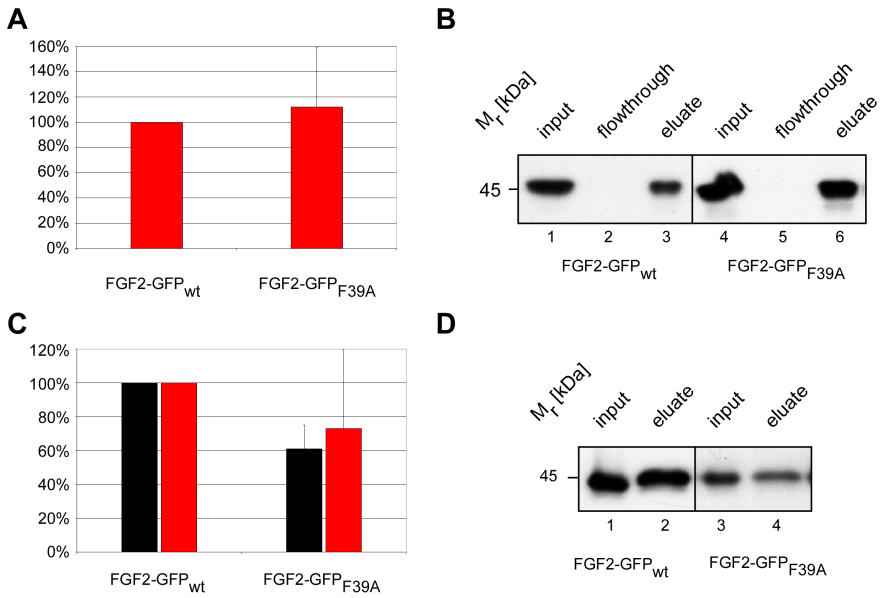

Figure 3.65: Point mutation; amino acid change: F39A **A** FACS analysis of cell free supernatant bound to the surface of $CHO_{MCAT/TAM2}$ cells. Cell surface signal of FGF2-GFPwt was set to 100%. **B** Binding of cell free supernatant to heparin beads. Cell free supernatant was incubated with heparin beads. Total (input, 10%), non-bound (flowthrough, 10%) and bound material (eluate, 10%) was analyzed by SDS-PAGE and Western blotting. **C** Quantitative analysis of export employing flow cytometry. Expression level (black bars) and secreted protein detected on the cell surface (red bars) is shown. FGF2-GFPwt was set to 100%. **D** Biotinylation assay. Cell surface proteins were labelled with a membrane-impermeable biotin reagent. After cell lysis biotinylated and non-biotinylated proteins were separated by streptavidin beads. Total material (input, 5%) and the biotinylated fraction (eluate, 50%) were analyzed by SDS-PAGE and Western blotting. All results shown represent an average of at least 3 different experiments. For further details see „Material and Methods“ and explanation of assays in chapter 3.3.2. To summarize the obtained data, this clone does not alter from observations made for wild-type FGF2-GFP.

As demonstrated in figure 3.65, the affinities of $FGF2\text{-}GFP_{F39A}$ to heparan sulfate proteoglycans *in vivo* (panel A) and heparin *in vitro* (panel B) was comparable to those of $FGF2\text{-}GFP_{wt}$. As detected by flow cytometry (panel C), the expression level of $FGF2\text{-}GFP_{F39A}$ was slightly reduced as compared to $FGF2\text{-}GFP_{wt}$, but the amount of secreted fusion protein detected on the cell surface did not vary from wild-type level. This result was confirmed by performing the biotinylation assay (panel D). The combined data obtained for this mutant demonstrate that F39A is not deficient in secretion or impaired in heparin binding and does not show a phenotype which is different from $FGF2\text{-}GFP_{wt}$ cells.

The following mutant contains a mutation at position 53, changing arginine to histidine.

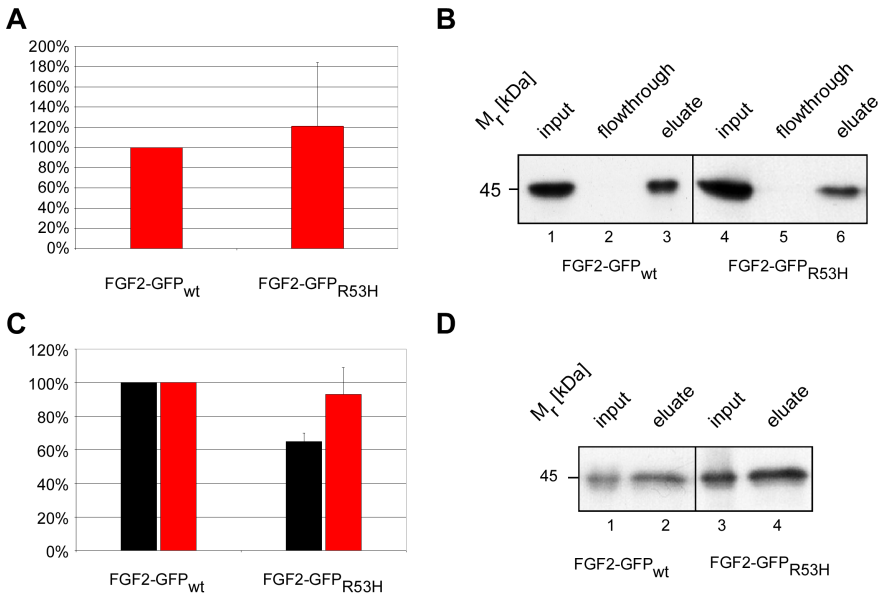

Figure 3.66: Point mutation; amino acid change: R53H **A** FACS analysis of cell free supernatant bound to the surface of $CHO_{MCAT/TAM2}$ cells. Cell surface signal of FGF2-GFPwt was set to 100%. **B** Binding of cell free supernatant to heparin beads. Cell free supernatant was incubated with heparin beads. Total (input, 10%), non-bound (flowthrough, 10%) and bound material (eluate, 10%) was analyzed by SDS-PAGE and Western blotting. **C** Quantitative analysis of export employing flow cytometry. Expression level (black bars) and secreted protein detected on the cell surface (red bars) is shown. FGF2-GFPwt was set to 100%. **D** Biotinylation assay. Cell surface proteins were labelled with a membrane-impermeable biotin reagent. After cell lysis biotinylated and non-biotinylated proteins were separated by streptavidin beads. Total material (input, 5%) and the biotinylated fraction (eluate, 50%) were analyzed by SDS-PAGE and Western blotting. All results shown represent an average of at least 3 different experiments. For further details see „Material and Methods“ and explanation of assays in chapter 3.3.2. To summarize the obtained data, this clone does not alter from observations made for wild-type FGF2-GFP.

As demonstrated in figure 3.66, the affinities of $FGF2\text{-}GFP_{R53H}$ to heparan sulfate proteoglycans *in vivo* (panel A) and to heparin *in vitro* (panel B) was comparable to $FGF2\text{-}GFP_{wt}$ heparin affinity. As detected by flow cytometry (panel C), the expression level of $FGF2\text{-}GFP_{R53H}$ was slightly reduced as compared to $FGF2\text{-}GFP_{wt}$, but the amount of secreted fusion protein detected on the cell surface did not vary from wild-type level. As detected by the biotinylation assay (panel D), the mutant R53H demonstrated an enhanced amount of fusion protein (lane 3) as compared to $FGF2\text{-}GFP_{wt}$ cells (lane 1). However, this mutant does not secrete the fusion protein more efficiently (compare the ration of lane 1 and 2 with the ratio of lane 3 and 4) than wild-type FGF2-GFP cells. The combined data obtained for this mutant demonstrate that R53H is not deficient in secretion or impaired in heparin binding and does not show a phenotype which is different from $FGF2\text{-}GFP_{wt}$ cells.

The following mutant contains a mutation at position 55, changing lysine to threonine.

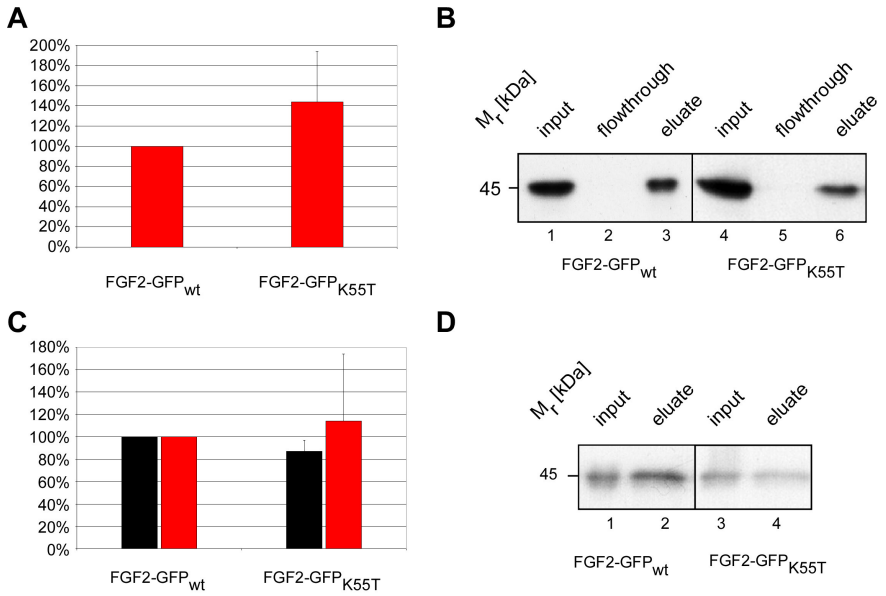

Figure 3.67: Point mutation; amino acid change: K55T **A** FACS analysis of cell free supernatant bound to the surface of $CHO_{MCAT/TAM2}$ cells. Cell surface signal of FGF2-GFPwt was set to 100%. **B** Binding of cell free supernatant to heparin beads. Cell free supernatant was incubated with heparin beads. Total (input, 10%), non-bound (flowthrough, 10%) and bound material (eluate, 10%) was analyzed by SDS-PAGE and Western blotting. **C** Quantitative analysis of export employing flow cytometry. Expression level (black bars) and secreted protein detected on the cell surface (red bars) is shown. FGF2-GFPwt was set to 100%. **D** Biotinylation assay. Cell surface proteins were labelled with a membrane-impermeable biotin reagent. After cell lysis biotinylated and non-biotinylated proteins were separated by streptavidin beads. Total material (input, 5%) and the biotinylated fraction (eluate, 50%) were analyzed by SDS-PAGE and Western blotting. All results shown represent an average of at least 3 different experiments. For further details see „Material and Methods“ and explanation of assays in chapter 3.3.2. To summarize the obtained data, this clone does not alter from observations made for wild-type FGF2-GFP.

As demonstrated in figure 3.67, the affinity of $FGF2\text{-}GFP_{K55T}$ to heparan sulfate proteoglycans in vivo (panel A) was enhanced (about 140% ± 50 %), but its affinity to heparin *in vitro* (panel B) was slightly reduced when compared to $FGF2\text{-}GFP_{wt}$ heparin affinity. As detected by flow cytometry (panel C), both the expression level and the cell surface staining of $FGF2\text{-}GFP_{K55T}$ did not vary from wild-type level, in contrast to the result obtained by the biotinylation assay (panel D), which demonstrated slightly reduced secretion efficiency of the mutant when compared to $FGF2\text{-}GFP_{wt}$ cells. However, the combined data obtained for this mutant demonstrate that K55T is not deficient in secretion or impaired in heparin binding and does not show a phenotype which is different from $FGF2\text{-}GFP_{wt}$ cells.

The following mutant contains a mutation at position 55, changing lysine to arginine.

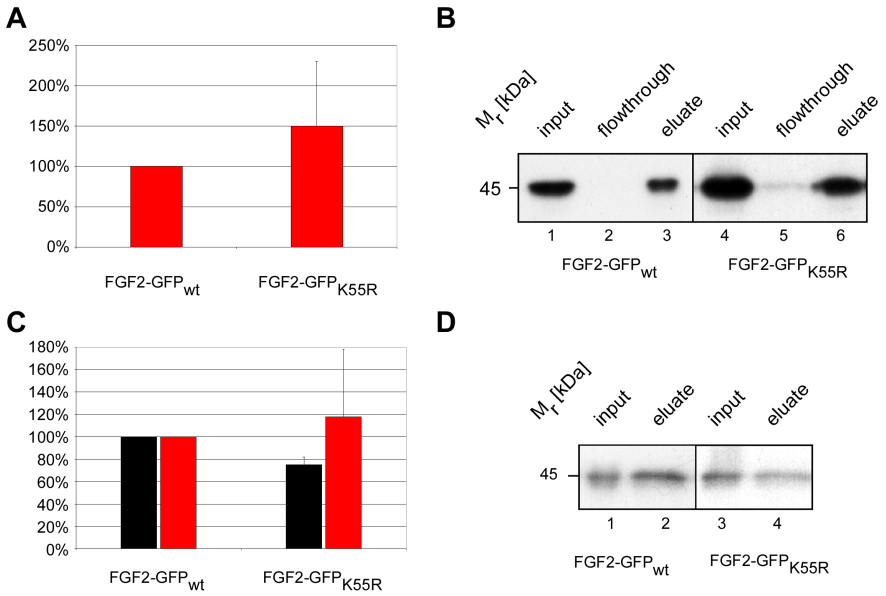

Figure 3.68: Point mutation; amino acid change: K55R **A** FACS analysis of cell free supernatant bound to the surface of $CHO_{MCAT/TAM2}$ cells. Cell surface signal of FGF2-GFPwt was set to 100%. **B** Binding of cell free supernatant to heparin beads. Cell free supernatant was incubated with heparin beads. Total (input, 10%), non-bound (flowthrough, 10%) and bound material (eluate, 10%) was analyzed by SDS-PAGE and Western blotting. **C** Quantitative analysis of export employing flow cytometry. Expression level (black bars) and secreted protein detected on the cell surface (red bars) is shown. FGF2-GFPwt was set to 100%. **D** Biotinylation assay. Cell surface proteins were labelled with a membrane-impermeable biotin reagent. After cell lysis biotinylated and non-biotinylated proteins were separated by streptavidin beads. Total material (input, 5%) and the biotinylated fraction (eluate, 50%) were analyzed by SDS-PAGE and Western blotting. All results shown represent an average of at least 3 different experiments. For further details see „Material and Methods“ and explanation of assays in chapter 3.3.2. To summarize the obtained data, this clone does not alter from observations made for wild-type FGF2-GFP.

As demonstrated in figure 3.68, the affinity of $FGF2\text{-}GFP_{K55R}$ to heparan sulfate proteoglycans in vivo (panel A) was enhanced (about 150% ± 70 %), but its affinity to heparin *in vitro* (panel B) was comparable to $FGF2\text{-}GFP_{wt}$ heparin affinity. As detected by flow cytometry (panel C), both the expression level and the cell surface staining of $FGF2\text{-}GFP_{K55T}$ did not vary from wild-type level, in contrast to the result obtained by the biotinylation assay (panel D), which demonstrated slightly reduced secretion efficiency of the mutant when compared to $FGF2\text{-}GFP_{wt}$ cells. However, the combined data obtained for this mutant demonstrate that K55T is not deficient in secretion or impaired in heparin binding and does not show a phenotype which is different from $FGF2\text{-}GFP_{wt}$ cells.

The following mutant contains a mutation at position 59, changing histidine to proline.

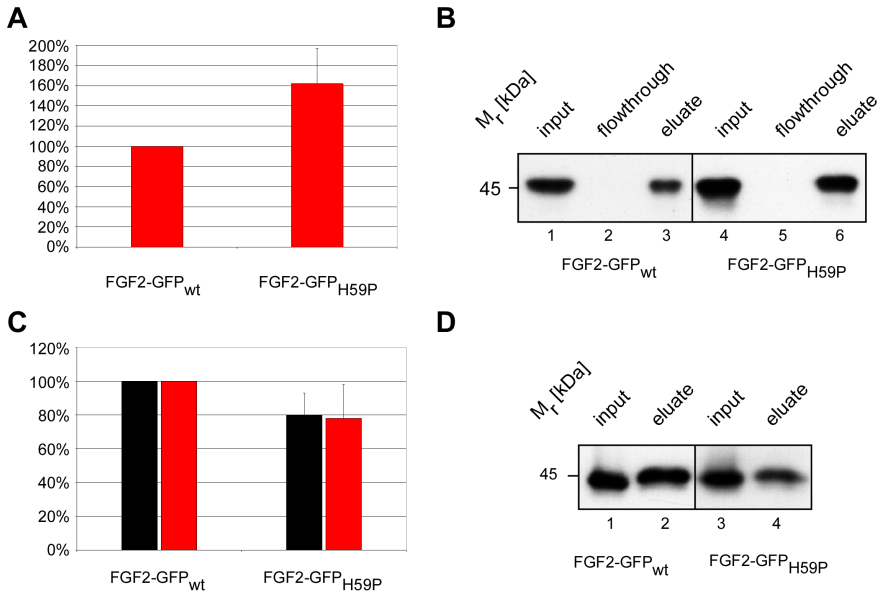

Figure 3.69: Point mutation; amino acid change: H59P **A** FACS analysis of cell free supernatant bound to the surface of $CHO_{MCAT/TAM2}$ cells. Cell surface signal of FGF2-GFPwt was set to 100%. **B** Binding of cell free supernatant to heparin beads. Cell free supernatant was incubated with heparin beads. Total (input, 10%), non-bound (flowthrough, 10%) and bound material (eluate, 10%) was analyzed by SDS-PAGE and Western blotting. **C** Quantitative analysis of export employing flow cytometry. Expression level (black bars) and secreted protein detected on the cell surface (red bars) is shown. FGF2-GFPwt was set to 100%. **D** Biotinylation assay. Cell surface proteins were labelled with a membrane-impermeable biotin reagent. After cell lysis biotinylated and non-biotinylated proteins were separated by streptavidin beads. Total material (input, 5%) and the biotinylated fraction (eluate, 50%) were analyzed by SDS-PAGE and Western blotting. All results shown represent an average of at least 3 different experiments. For further details see „Material and Methods“ and explanation of assays in chapter 3.3.2. To summarize the obtained data, this clone does not alter from observations made for wild-type FGF2-GFP.

As demonstrated in figure 3.69, the affinity of $FGF2\text{-}GFP_{H59P}$ to heparan sulfate proteoglycans in vivo (panel A) was enhanced (about 160% ± 30 %), but its affinity to heparin *in vitro* (panel B) was comparable to $FGF2\text{-}GFP_{wt}$ heparin affinity. As detected by flow cytometry (panel C), both the expression level and the cell surface staining of $FGF2\text{-}GFP_{H59P}$ did not vary from wild-type level, in contrast to the result obtained by the biotinylation assay (panel D), which demonstrated slightly reduced secretion efficiency of the mutant when compared to $FGF2\text{-}GFP_{wt}$ cells. However, the combined data obtained for this mutant demonstrate that the mutant H59P is not deficient in secretion or impaired in heparin binding and does not show a phenotype which is different from $FGF2\text{-}GFP_{wt}$ cells.

The following mutant contains a mutation at position 61, changing lysine to glutamic acid.

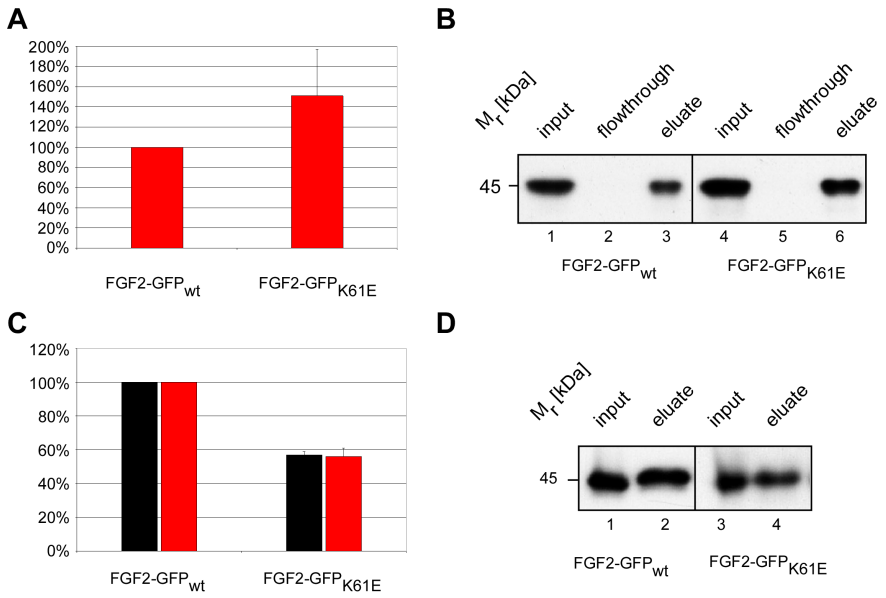

Figure 3.70: Point mutation; amino acid change: K61E **A** FACS analysis of cell free supernatant bound to the surface of $CHO_{MCAT/TAM2}$ cells. Cell surface signal of FGF2-GFPwt was set to 100%. **B** Binding of cell free supernatant to heparin beads. Cell free supernatant was incubated with heparin beads. Total (input, 10%), non-bound (flowthrough, 10%) and bound material (eluate, 10%) was analyzed by SDS-PAGE and Western blotting. **C** Quantitative analysis of export employing flow cytometry. Expression level (black bars) and secreted protein detected on the cell surface (red bars) is shown. FGF2-GFPwt was set to 100%. **D** Biotinylation assay. Cell surface proteins were labelled with a membrane-impermeable biotin reagent. After cell lysis biotinylated and non-biotinylated proteins were separated by streptavidin beads. Total material (input, 5%) and the biotinylated fraction (eluate, 50%) were analyzed by SDS-PAGE and Western blotting. All results shown represent an average of at least 3 different experiments. For further details see „Material and Methods“ and explanation of assays in chapter 3.3.2. To summarize the obtained data, this clone does not alter from observations made for wild-type FGF2-GFP.

As demonstrated in figure 3.70, the affinity of $FGF2\text{-}GFP_{K61E}$ to heparan sulfate proteoglycans in vivo (panel A) was enhanced (about 150% ± 50 %), but its affinity to heparin *in vitro* (panel B) was comparable to $FGF2\text{-}GFP_{wt}$ heparin affinity. As detected by flow cytometry (panel C), both the expression level and the cell surface staining of $FGF2\text{-}GFP_{K61E}$ were reduced to about 60% when compared to $FGF2\text{-}GFP_{wt}$ cells, indicating that this mutation does not have an effect on secretion efficiency. This result was confirmed by the biotinylation assay (panel D). The combined data obtained for this mutant demonstrate that K61E is not deficient in secretion or impaired in heparin binding and does not show a phenotype which is different from $FGF2\text{-}GFP_{wt}$ cells.

The following mutant contains a mutation at position 65, changing glutamine to alanine.

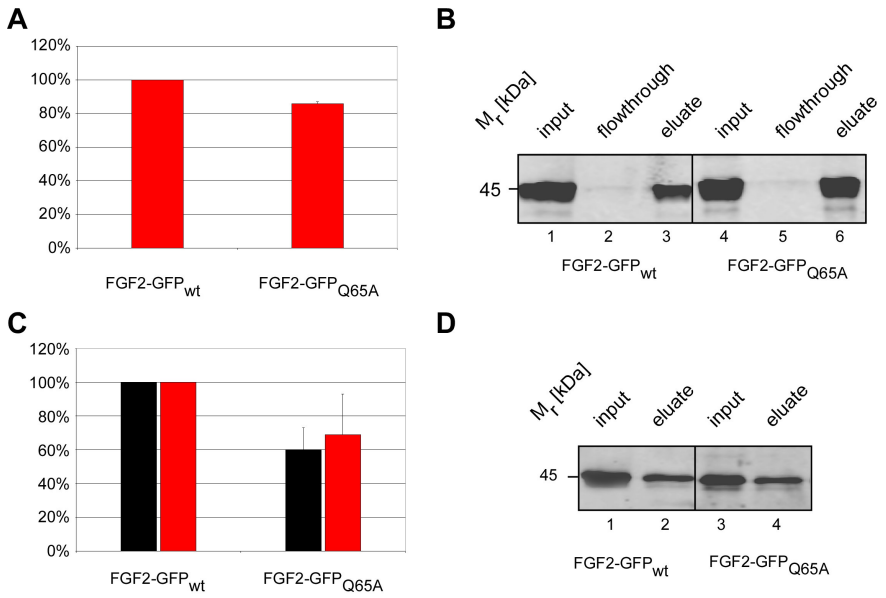

Figure 3.71: Point mutation; amino acid change: Q65A **A** FACS analysis of cell free supernatant bound to the surface of $CHO_{MCAT/TAM2}$ cells. Cell surface signal of FGF2-GFPwt was set to 100%. **B** Binding of cell free supernatant to heparin beads. Cell free supernatant was incubated with heparin beads. Total (input, 10%), non-bound (flowthrough, 10%) and bound material (eluate, 10%) was analyzed by SDS-PAGE and Western blotting. **C** Quantitative analysis of export employing flow cytometry. Expression level (black bars) and secreted protein detected on the cell surface (red bars) is shown. FGF2-GFPwt was set to 100%. **D** Biotinylation assay. Cell surface proteins were labelled with a membrane-impermeable biotin reagent. After cell lysis biotinylated and non-biotinylated proteins were separated by streptavidin beads. Total material (input, 5%) and the biotinylated fraction (eluate, 50%) were analyzed by SDS-PAGE and Western blotting. All results shown represent an average of at least 3 different experiments. For further details see „Material and Methods“ and explanation of assays in chapter 3.3.2. To summarize the obtained data, this clone does not alter from observations made for wild-type FGF2-GFP.

As demonstrated in figure 3.71, the affinities of $FGF2\text{-}GFP_{Q65A}$ to heparan sulfate proteoglycans *in vivo* (panel A) and to heparin *in vitro* (panel B) was comparable to $FGF2\text{-}GFP_{wt}$ heparin affinity. As detected by flow cytometry (panel C), the expression level of $FGF2\text{-}GFP_{Q65A}$ was slightly reduced as compared to $FGF2\text{-}GFP_{wt}$, but the amount of secreted fusion protein detected on the cell surface did not vary from wild-type level. This result was confirmed by the biotinylation assay (panel D). The combined data obtained for this mutant demonstrate that Q65A is not deficient in secretion or impaired in heparin binding and does not show a phenotype which is different from $FGF2\text{-}GFP_{wt}$ cells.

The following mutant contains a mutation at position 67, changing glutamic acid to valine.

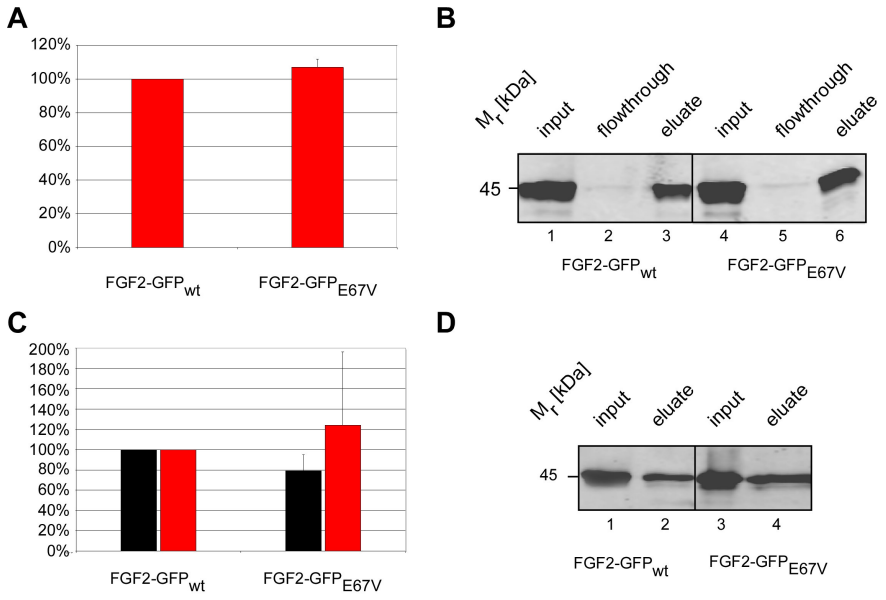

Figure 3.72: Point mutation; amino acid change: E67V **A** FACS analysis of cell free supernatant bound to the surface of $CHO_{MCAT/TAM2}$ cells. Cell surface signal of FGF2-GFPwt was set to 100%. **B** Binding of cell free supernatant to heparin beads. Cell free supernatant was incubated with heparin beads. Total (input, 10%), non-bound (flowthrough, 10%) and bound material (eluate, 10%) was analyzed by SDS-PAGE and Western blotting. **C** Quantitative analysis of export employing flow cytometry. Expression level (black bars) and secreted protein detected on the cell surface (red bars) is shown. FGF2-GFPwt was set to 100%. **D** Biotinylation assay. Cell surface proteins were labelled with a membrane-impermeable biotin reagent. After cell lysis biotinylated and non-biotinylated proteins were separated by streptavidin beads. Total material (input, 5%) and the biotinylated fraction (eluate, 50%) were analyzed by SDS-PAGE and Western blotting. All results shown represent an average of at least 3 different experiments. For further details see „Material and Methods“ and explanation of assays in chapter 3.3.2. To summarize the obtained data, this clone does not alter from observations made for wild-type FGF2-GFP.

As demonstrated in figure 3.72, the affinities of $FGF2\text{-}GFP_{E67V}$ to heparan sulfate proteoglycans *in vivo* (panel A) and to heparin *in vitro* (panel B) was comparable to $FGF2\text{-}GFP_{wt}$ heparin affinity. As detected by flow cytometry (panel C), both the expression level and the cell surface staining of $FGF2\text{-}GFP_{E67V}$ did not vary from wild-type level. This result was confirmed by the biotinylation assay (panel D). The combined data obtained for this mutant demonstrate that E67V is not deficient in secretion or impaired in heparin binding and does not show a phenotype which is different from $FGF2\text{-}GFP_{wt}$ cells.

The following mutant contains a mutation at position 68, changing glutamic acid to alanine.

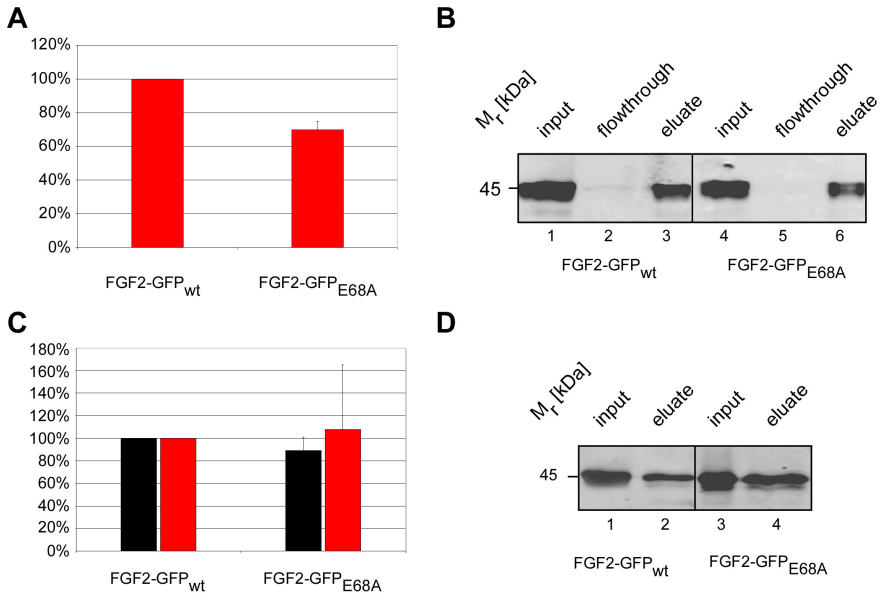

Figure 3.73: Point mutation; amino acid change: E68A **A** FACS analysis of cell free supernatant bound to the surface of $CHO_{MCAT/TAM2}$ cells. Cell surface signal of FGF2-GFPwt was set to 100%. **B** Binding of cell free supernatant to heparin beads. Cell free supernatant was incubated with Heparin beads. Total (input, 10%), non-bound (flowthrough, 10%) and bound material (eluate, 10%) was analyzed by SDS-PAGE and Western blotting. **C** Quantitative analysis of export employing flow cytometry. Expression level (black bars) and secreted protein detected on the cell surface (red bars) is shown. FGF2-GFPwt was set to 100%. **D** Biotinylation assay. Cell surface proteins were labelled with a membrane-impermeable biotin reagent. After cell lysis biotinylated and non-biotinylated proteins were separated by streptavidin beads. Total material (input, 5%) and the biotinylated fraction (eluate, 50%) were analyzed by SDS-PAGE and Western blotting. All results shown represent an average of at least 3 different experiments. For further details see „Material and Methods" and explanation of assays in chapter 3.3.2. To summarize the obtained data, this clone does not alter from observations made for wild-type FGF2-GFP.

As demonstrated in figure 3.73, the affinities of $FGF2\text{-}GFP_{E68A}$ to heparan sulfate proteoglycans *in vivo* (panel A) and to heparin *in vitro* (panel B) was comparable to $FGF2\text{-}GFP_{wt}$ heparin affinity. As detected by flow cytometry (panel C), both the expression level and the cell surface staining of $FGF2\text{-}GFP_{E68A}$ did not vary from wild-type level. This result was confirmed by the biotinylation assay (panel D). The combined data obtained for this mutant demonstrate that E68A is not deficient in secretion or impaired in heparin binding and does not show a phenotype which is different from $FGF2\text{-}GFP_{wt}$ cells.

The following mutant contains a mutation at position 68, changing glutamic acid to glutamine.

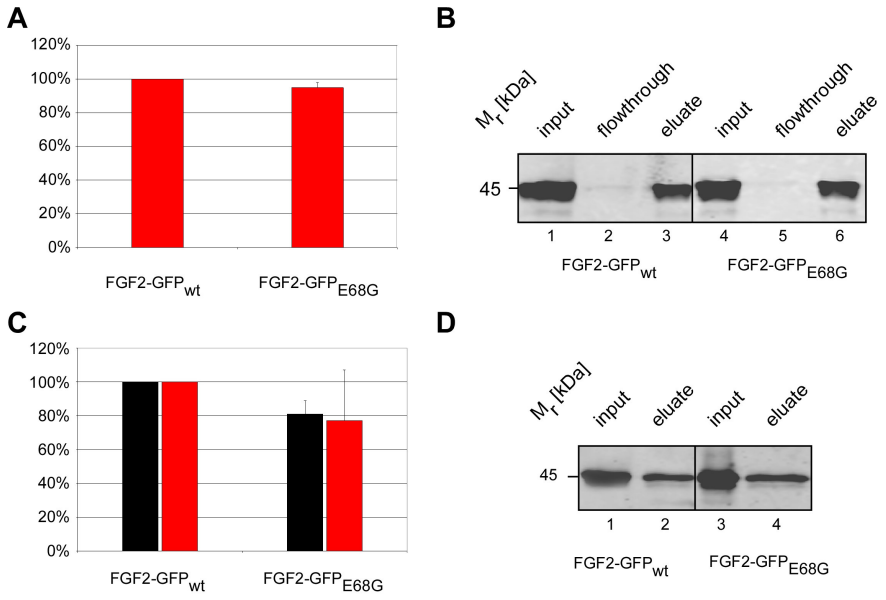

Figure 3.74: Point mutation; amino acid change: E68G **A** FACS analysis of cell free supernatant bound to the surface of $CHO_{MCAT/TAM2}$ cells. Cell surface signal of FGF2-GFPwt was set to 100%. **B** Binding of cell free supernatant to heparin beads. Cell free supernatant was incubated with heparin beads. Total (input, 10%), non-bound (flowthrough, 10%) and bound material (eluate, 10%) was analyzed by SDS-PAGE and Western blotting. **C** Quantitative analysis of export employing flow cytometry. Expression level (black bars) and secreted protein detected on the cell surface (red bars) is shown. FGF2-GFPwt was set to 100%. **D** Biotinylation assay. Cell surface proteins were labelled with a membrane-impermeable biotin reagent. After cell lysis biotinylated and non-biotinylated proteins were separated by streptavidin beads. Total material (input, 5%) and the biotinylated fraction (eluate, 50%) were analyzed by SDS-PAGE and Western blotting. All results shown represent an average of at least 3 different experiments. For further details see „Material and Methods“ and explanation of assays in chapter 3.3.2. To summarize the obtained data, this clone does not alter from observations made for wild-type FGF2-GFP.

As demonstrated in figure 3.74, the affinities of $FGF2\text{-}GFP_{E68G}$ to heparan sulfate proteoglycans *in vivo* (panel A) and to heparin *in vitro* (panel B) was comparable to $FGF2\text{-}GFP_{wt}$ heparin affinity. As detected by flow cytometry (panel C), both the expression level and the cell surface staining of $FGF2\text{-}GFP_{E68G}$ did not vary from wild-type level. This result was confirmed by the biotinylation assay (panel D). The combined data obtained for this mutant demonstrate that E68G is not deficient in secretion or impaired in heparin binding and does not show a phenotype which is different from $FGF2\text{-}GFP_{wt}$ cells.

The following mutant contains a mutation at position 69, changing arginine to alanine.

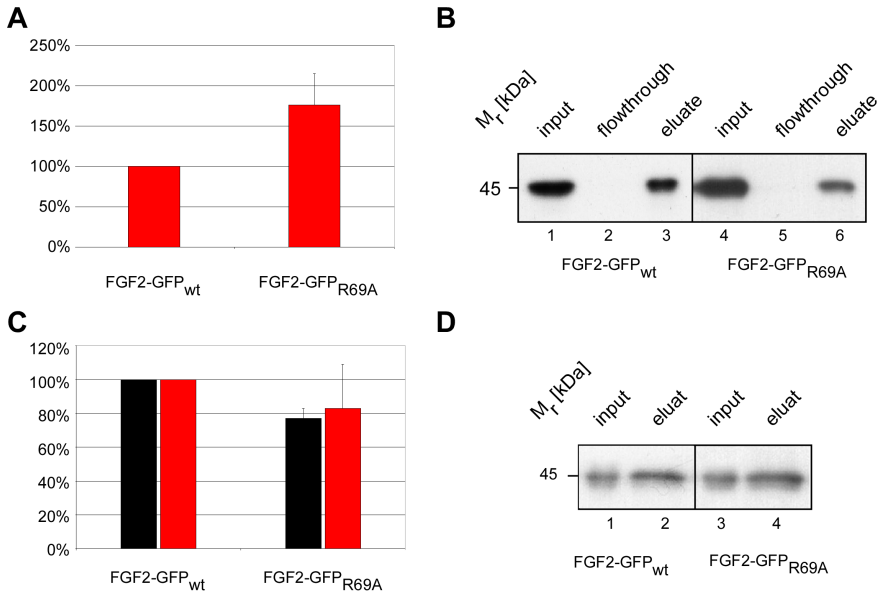

Figure 3.75: Point mutation; amino acid change: R69A **A** FACS analysis of cell free supernatant bound to the surface of $CHO_{MCAT/TAM2}$ cells. Cell surface signal of FGF2-GFPwt was set to 100%. **B** Binding of cell free supernatant to heparin beads. Cell free supernatant was incubated with heparin beads. Total (input, 10%), non-bound (flowthrough, 10%) and bound material (eluate, 10%) was analyzed by SDS-PAGE and Western blotting. **C** Quantitative analysis of export employing flow cytometry. Expression level (black bars) and secreted protein detected on the cell surface (red bars) is shown. FGF2-GFPwt was set to 100%. **D** Biotinylation assay. Cell surface proteins were labelled with a membrane-impermeable biotin reagent. After cell lysis biotinylated and non-biotinylated proteins were separated by streptavidin beads. Total material (input, 5%) and the biotinylated fraction (eluate, 50%) were analyzed by SDS-PAGE and Western blotting. All results shown represent an average of at least 3 different experiments. For further details see „Material and Methods“ and explanation of assays in chapter 3.3.2. To summarize the obtained data, this clone does not alter from observations made for wild-type FGF2-GFP.

As demonstrated in figure 3.75, the affinity of $FGF2\text{-}GFP_{R69A}$ to heparan sulfate proteoglycans in vivo (panel A) was enhanced (about 180% ± 30 %), but its affinity to heparin *in vitro* (panel B) was slightly reduced when compared to $FGF2\text{-}GFP_{wt}$ heparin affinity. As shown by flow cytometry (panel C), both the expression level and the cell surface staining of $FGF2\text{-}GFP_{R69A}$ did not vary from wild-type level. This result was confirmed by the biotinylation assay (panel D). The combined data obtained for this mutant demonstrate that E68G is not deficient in secretion or impaired in heparin binding and does not show a phenotype which is different from $FGF2\text{-}GFP_{wt}$ cells.

The following mutant contains a mutation at position 75, changing lysine to isoleucine.

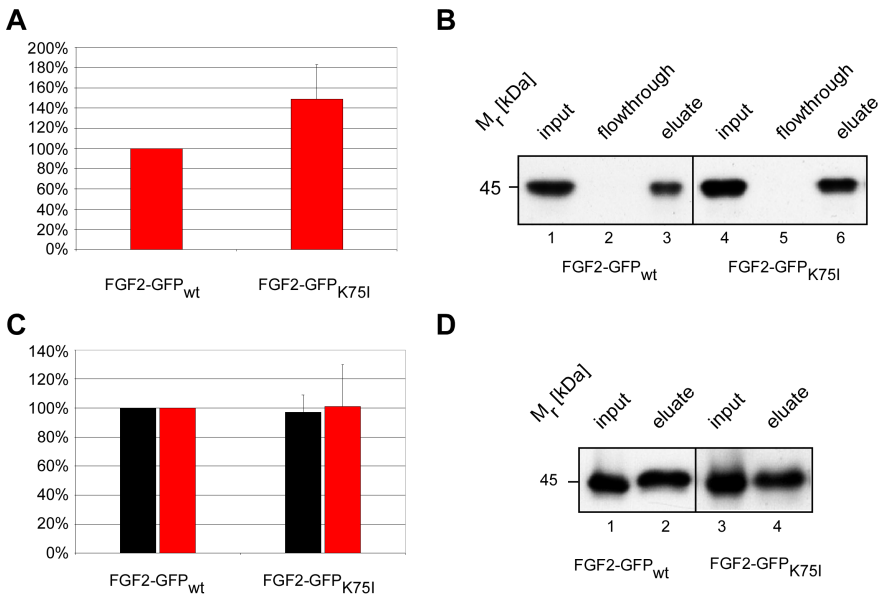

Figure 3.76: Point mutation; amino acid change: K75I **A** FACS analysis of cell free supernatant bound to the surface of $CHO_{MCAT/TAM2}$ cells. Cell surface signal of FGF2-GFPwt was set to 100%. **B** Binding of cell free supernatant to heparin beads. Cell free supernatant was incubated with heparin beads. Total (input, 10%), non-bound (flowthrough, 10%) and bound material (eluate, 10%) was analyzed by SDS-PAGE and Western blotting. **C** Quantitative analysis of export employing flow cytometry. Expression level (black bars) and secreted protein detected on the cell surface (red bars) is shown. FGF2-GFPwt was set to 100%. **D** Biotinylation assay. Cell surface proteins were labelled with a membrane-impermeable biotin reagent. After cell lysis biotinylated and non-biotinylated proteins were separated by streptavidin beads. Total material (input, 5%) and the biotinylated fraction (eluate, 50%) were analyzed by SDS-PAGE and Western blotting. All results shown represent an average of at least 3 different experiments. For further details see „Material and Methods“ and explanation of assays in chapter 3.3.2. To summarize the obtained data, this clone does not alter from observations made for wild-type FGF2-GFP.

As demonstrated in figure 3.76, the affinity of $FGF2\text{-}GFP_{K75E}$ to heparan sulfate proteoglycans in vivo (panel A) was enhanced (about 150% ± 30 %), but its affinity to heparin *in vitro* (panel B) was comparable to $FGF2\text{-}GFP_{wt}$ heparin affinity. As detected by flow cytometry (panel C), both the expression level and the cell surface staining of $FGF2\text{-}GFP_{K75E}$ did not vary from wild-type level. This result was confirmed by the biotinylation assay (panel D). The combined data obtained for this mutant demonstrate that K75E is not deficient in secretion or impaired in heparin binding and does not show a phenotype which is different from $FGF2\text{-}GFP_{wt}$ cells.

The following mutant contains a mutation at position 77, changing valine to alanine.

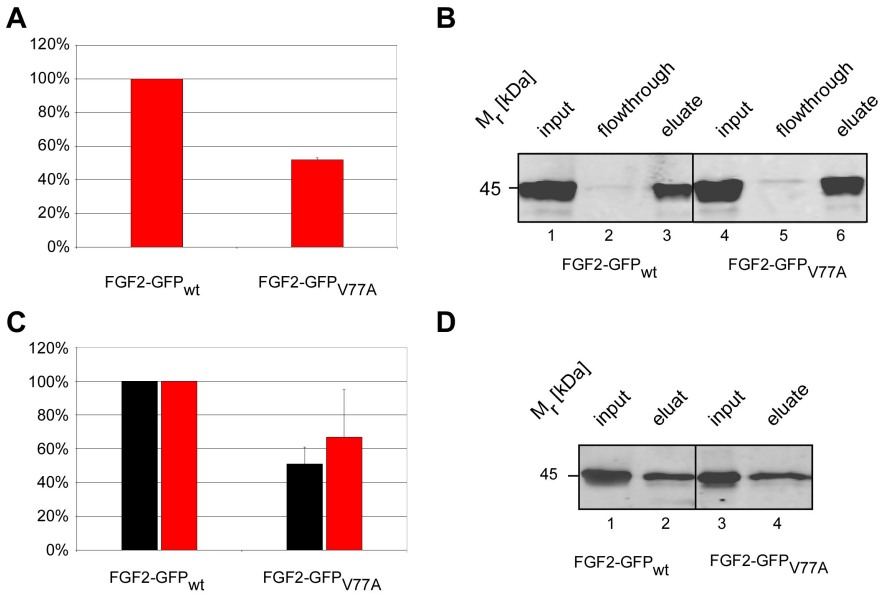

Figure 3.77: Point mutation; amino acid change: V77A **A** FACS analysis of cell free supernatant bound to the surface of $CHO_{MCAT/TAM2}$ cells. Cell surface signal of FGF2-GFPwt was set to 100%. **B** Binding of cell free supernatant to heparin beads. Cell free supernatant was incubated with heparin beads. Total (input, 10%), non-bound (flowthrough, 10%) and bound material (eluate, 10%) was analyzed by SDS-PAGE and Western blotting. **C** Quantitative analysis of export employing flow cytometry. Expression level (black bars) and secreted protein detected on the cell surface (red bars) is shown. FGF2-GFPwt was set to 100%. **D** Biotinylation assay. Cell surface proteins were labelled with a membrane-impermeable biotin reagent. After cell lysis biotinylated and non-biotinylated proteins were separated by streptavidin beads. Total material (input, 5%) and the biotinylated fraction (eluate, 50%) were analyzed by SDS-PAGE and Western blotting. All results shown represent an average of at least 3 different experiments. For further details see „Material and Methods“ and explanation of assays in chapter 3.3.2. To summarize the obtained data, this clone does not alter from observations made for wild-type FGF2-GFP.

As demonstrated in figure 3.77, the affinity of $FGF2\text{-}GFP_{V77A}$ to heparan sulfate proteoglycans *in vivo* (panel A) is reduced (about 50%), but its affinity to heparin *in vitro* (panel B) was comparable to $FGF2\text{-}GFP_{wt}$ heparin affinity. As shown by flow cytometry (panel C), both the expression level and the cell surface staining of $FGF2\text{-}GFP_{V77A}$ was slightly reduced as compared to $FGF2\text{-}GFP_{wt}$. As analyzed by the biotinylation assay (panel D), the mutant V77A did not secrete the fusion protein more efficiently (compare the ration of lane 1 and 2 with the ratio of lane 3 and 4) than wild-type FGF2-GFP cells. The combined data obtained for this mutant demonstrate that V77A is not deficient in secretion or impaired in heparin binding and does not show a phenotype which is different from $FGF2\text{-}GFP_{wt}$ cells.

The following mutant contains a mutation at position 78, changing cysteine to alanine.

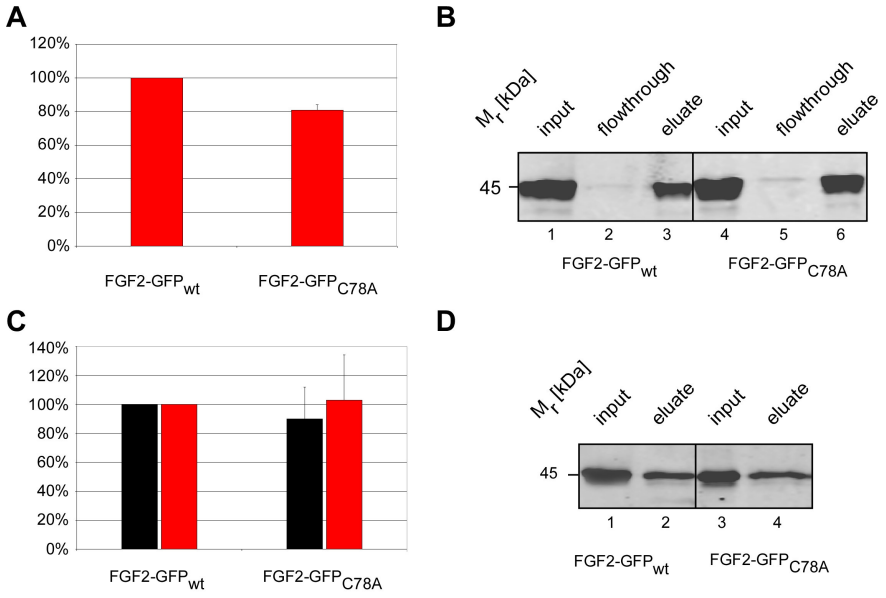

Figure 3.78: Point mutation; amino acid change: C78A **A** FACS analysis of cell free supernatant bound to the surface of $CHO_{MCAT/TAM2}$ cells. Cell surface signal of FGF2-GFPwt was set to 100%. **B** Binding of cell free supernatant to heparin beads. Cell free supernatant was incubated with heparin beads. Total (input, 10%), non-bound (flowthrough, 10%) and bound material (eluate, 10%) was analyzed by SDS-PAGE and Western blotting. **C** Quantitative analysis of export employing flow cytometry. Expression level (black bars) and secreted protein detected on the cell surface (red bars) is shown. FGF2-GFPwt was set to 100%. **D** Biotinylation assay. Cell surface proteins were labelled with a membrane-impermeable biotin reagent. After cell lysis biotinylated and non-biotinylated proteins were separated by streptavidin beads. Total material (input, 5%) and the biotinylated fraction (eluate, 50%) were analyzed by SDS-PAGE and Western blotting. All results shown represent an average of at least 3 different experiments. For further details see „Material and Methods“ and explanation of assays in chapter 3.3.2. To summarize the obtained data, this clone does not alter from observations made for wild-type FGF2-GFP.

As demonstrated in figure 3.78, the affinities of $FGF2\text{-}GFP_{C78A}$ to heparan sulfate proteoglycans *in vivo* (panel A) and to heparin *in vitro* (panel B) was comparable to $FGF2\text{-}GFP_{wt}$ heparin affinity. As detected by flow cytometry (panel C), both the expression level and the cell surface staining of $FGF2\text{-}GFP_{C78A}$ did not vary from wild-type level. This result was confirmed by the biotinylation assay (panel D). The combined data obtained for this mutant demonstrate that C78A is not deficient in secretion or impaired in heparin binding and does not show a phenotype which is different from $FGF2\text{-}GFP_{wt}$ cells.

The following mutant contains a mutation at position 80, changing asparagine to alanine.

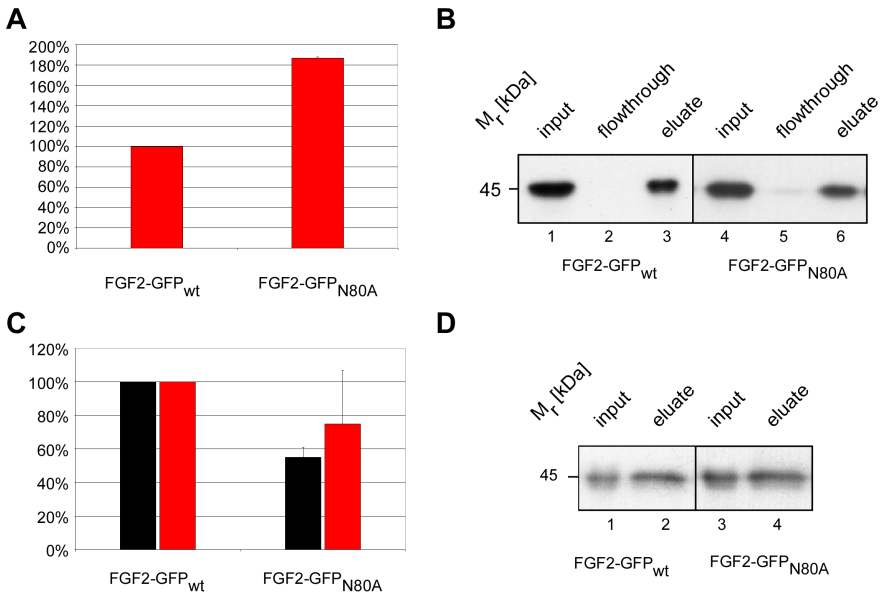

Figure 3.79: Point mutation; amino acid change: N80A **A** FACS analysis of cell free supernatant bound to the surface of $CHO_{MCAT/TAM2}$ cells. Cell surface signal of FGF2-GFPwt was set to 100%. **B** Binding of cell free supernatant to heparin beads. Cell free supernatant was incubated with heparin beads. Total (input, 10%), non-bound (flowthrough, 10%) and bound material (eluate, 10%) was analyzed by SDS-PAGE and Western blotting. **C** Quantitative analysis of export employing flow cytometry. Expression level (black bars) and secreted protein detected on the cell surface (red bars) is shown. FGF2-GFPwt was set to 100%. **D** Biotinylation assay. Cell surface proteins were labelled with a membrane-impermeable biotin reagent. After cell lysis biotinylated and non-biotinylated proteins were separated by streptavidin beads. Total material (input, 5%) and the biotinylated fraction (eluate, 50%) were analyzed by SDS-PAGE and Western blotting. All results shown represent an average of at least 3 different experiments. For further details see „Material and Methods“ and explanation of assays in chapter 3.3.2. To summarize the obtained data, this clone does not alter from observations made for wild-type FGF2-GFP.

As demonstrated in figure 3.79, the affinity of $FGF2\text{-}GFP_{N80A}$ to heparan sulfate proteoglycans *in vivo* (panel A) was enhanced (about 180 %), but its affinity to heparin *in vitro* (panel B) was comparable to $FGF2\text{-}GFP_{wt}$ heparin affinity. As shown by flow cytometry (panel C), the expression level of $FGF2\text{-}GFP_{N80A}$ was slightly reduced as compared to $FGF2\text{-}GFP_{wt}$, but the amount of secreted fusion protein detected on the cell surface did not vary from wild-type level. As analyzed by the biotinylation assay (panel D), the mutant N80A did not secrete the fusion protein more efficiently (compare the ration of lane 1 and 2 with the ratio of lane 3 and 4) than wild-type FGF2-GFP cells. The combined data obtained for this mutant demonstrate that N80A is not deficient in secretion or impaired in heparin binding and does not show a phenotype which is different from $FGF2\text{-}GFP_{wt}$ cells.

The following mutant contains a mutation at position 87, changing glutamic acid to lysine.

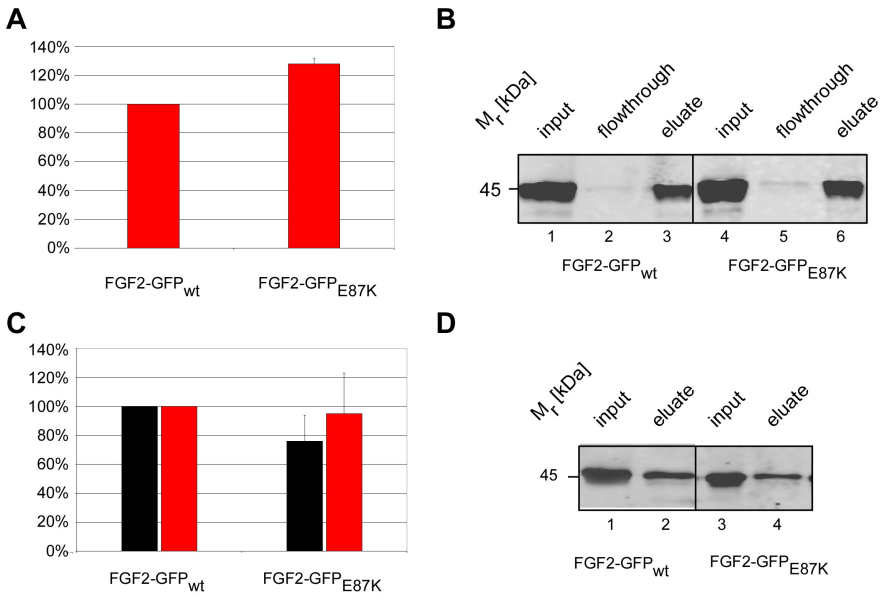

Figure 3.80: Point mutation; amino acid change: E87K **A** FACS analysis of cell free supernatant bound to the surface of $CHO_{MCAT/TAM2}$ cells. Cell surface signal of FGF2-GFPwt was set to 100%. **B** Binding of cell free supernatant to heparin beads. Cell free supernatant was incubated with heparin beads. Total (input, 10%), non-bound (flowthrough, 10%) and bound material (eluate, 10%) was analyzed by SDS-PAGE and Western blotting. **C** Quantitative analysis of export employing flow cytometry. Expression level (black bars) and secreted protein detected on the cell surface (red bars) is shown. FGF2-GFPwt was set to 100%. **D** Biotinylation assay. Cell surface proteins were labelled with a membrane-impermeable biotin reagent. After cell lysis biotinylated and non-biotinylated proteins were separated by streptavidin beads. Total material (input, 5%) and the biotinylated fraction (eluate, 50%) were analyzed by SDS-PAGE and Western blotting. All results shown represent an average of at least 3 different experiments. For further details see „Material and Methods“ and explanation of assays in chapter 3.3.2. To summarize the obtained data, this clone does not alter from observations made for wild-type FGF2-GFP.

As demonstrated in figure 3.80, the affinities of $FGF2\text{-}GFP_{E87K}$ to heparan sulfate proteoglycans *in vivo* (panel A) and to heparin *in vitro* (panel B) was comparable to $FGF2\text{-}GFP_{wt}$ heparin affinity. As detected by flow cytometry (panel C), both the expression level and the cell surface staining of $FGF2\text{-}GFP_{E87K}$ did not vary from wild-type level. This result was confirmed by the biotinylation assay (panel D). The combined data obtained for this mutant demonstrate that E87K is not deficient in secretion or impaired in heparin binding and does not show a phenotype which is different from $FGF2\text{-}GFP_{wt}$ cells.

The following mutant contains a mutation at position 92, changing leucine to alanine

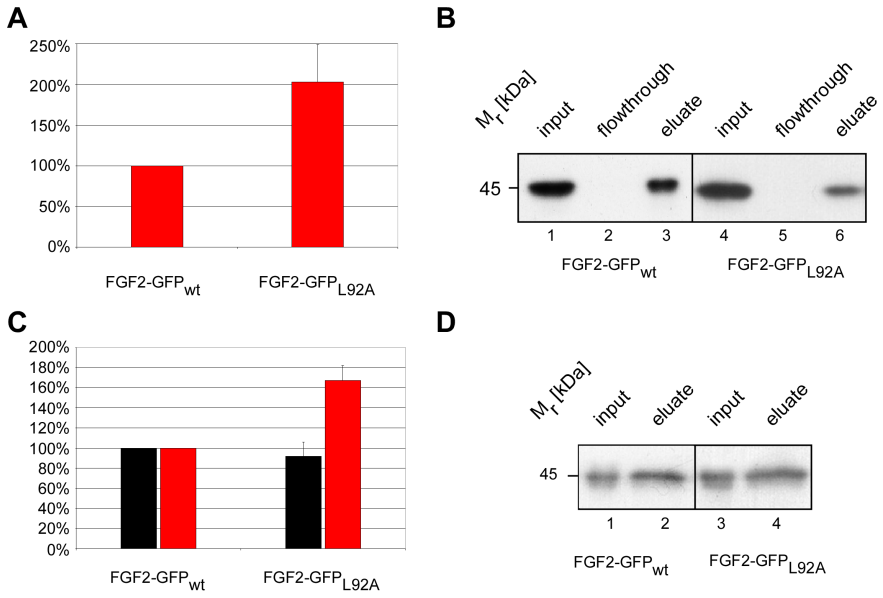

Figure 3.81: Point mutation; amino acid change: L92A **A** FACS analysis of cell free supernatant bound to the surface of $CHO_{MCAT/TAM2}$ cells. Cell surface signal of FGF2-GFPwt was set to 100%. **B** Binding of cell free supernatant to heparin beads. Cell free supernatant was incubated with heparin beads. Total (input, 10%), non-bound (flowthrough, 10%) and bound material (eluate, 10%) was analyzed by SDS-PAGE and Western blotting. **C** Quantitative analysis of export employing flow cytometry. Expression level (black bars) and secreted protein detected on the cell surface (red bars) is shown. FGF2-GFPwt was set to 100%. **D** Biotinylation assay. Cell surface proteins were labelled with a membrane-impermeable biotin reagent. After cell lysis biotinylated and non-biotinylated proteins were separated by streptavidin beads. Total material (input, 5%) and the biotinylated fraction (eluate, 50%) were analyzed by SDS-PAGE and Western blotting. All results shown represent an average of at least 3 different experiments. For further details see „Material and Methods“ and explanation of assays in chapter 3.3.2. To summarize the obtained data, this clone does not alter from observations made for wild-type FGF2-GFP.

As demonstrated in figure 3.81, the affinity of $FGF2\text{-}GFP_{L92A}$ to heparan sulfate proteoglycans *in vivo* (panel A) was enhanced (about 200 % ± 50%), but its affinity to heparin *in vitro* (panel B) was comparable to $FGF2\text{-}GFP_{wt}$ heparin affinity. As analyzed by flow cytometry (panel C), the signal for cell surface staining for $FGF2\text{-}GFP_{L92A}$ was enhanced to about 170% when compared to $FGF2\text{-}GFP_{wt}$, whereas its expression level was shown to be at wild-type levels. However, this result was not confirmed by the biotinylation assay, which demonstrated that mutant L92A did not secrete the fusion protein more efficiently (compare the ration of lane 1 and 2 with the ratio of lane 3 and 4) than wild-type FGF2-GFP cells. Although the data obtained by the secretion assay were inconsistent, L92A is shown to be not deficient in secretion or impaired in heparin binding and does not show a phenotype which is different from $FGF2\text{-}GFP_{wt}$ cells.

The following mutant contains a mutation at position 96, changing cysteine to alanine.

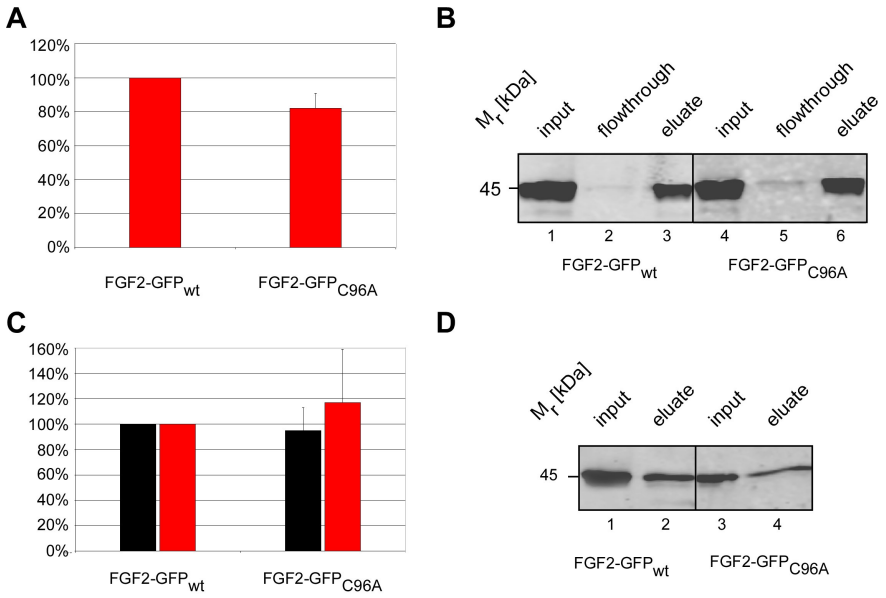

Figure 3.82: Point mutation; amino acid change: C96A **A** FACS analysis of cell free supernatant bound to the surface of $CHO_{MCAT/TAM2}$ cells. Cell surface signal of FGF2-GFPwt was set to 100%. **B** Binding of cell free supernatant to heparin beads. Cell free supernatant was incubated with heparin beads. Total (input, 10%), non-bound (flowthrough, 10%) and bound material (eluate, 10%) was analyzed by SDS-PAGE and Western blotting. **C** Quantitative analysis of export employing flow cytometry. Expression level (black bars) and secreted protein detected on the cell surface (red bars) is shown. FGF2-GFPwt was set to 100%. **D** Biotinylation assay. Cell surface proteins were labelled with a membrane-impermeable biotin reagent. After cell lysis biotinylated and non-biotinylated proteins were separated by streptavidin beads. Total material (input, 5%) and the biotinylated fraction (eluate, 50%) were analyzed by SDS-PAGE and Western blotting. All results shown represent an average of at least 3 different experiments. For further details see „Material and Methods“ and explanation of assays in chapter 3.3.2. To summarize the obtained data, this clone does not alter from observations made for wild-type FGF2-GFP.

As demonstrated in figure 3.82, the affinities of $FGF2\text{-}GFP_{C96A}$ to heparan sulfate proteoglycans *in vivo* (panel A) and to heparin *in vitro* (panel B) was comparable to $FGF2\text{-}GFP_{wt}$ heparin affinity. As detected by flow cytometry (panel C), both the expression level and the cell surface staining of $FGF2\text{-}GFP_{C96A}$ did not vary from wild-type level. This result was confirmed by the biotinylation assay (panel D). The combined data obtained for this mutant demonstrate that C96A is not deficient in secretion or impaired in heparin binding and does not show a phenotype which is different from $FGF2\text{-}GFP_{wt}$ cells.

The following mutant contains a mutation at position 102, changing phenylalanine to alanine.

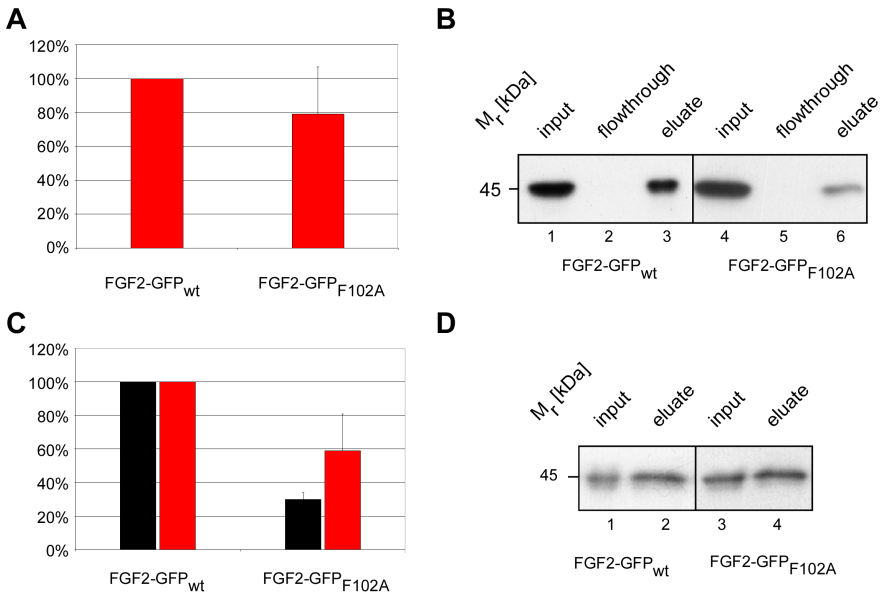

Figure 3.83: Point mutation; amino acid change: F102A **A** FACS analysis of cell free supernatant bound to the surface of $CHO_{MCAT/TAM2}$ cells. Cell surface signal of FGF2-GFPwt was set to 100%. **B** Binding of cell free supernatant to heparin beads. Cell free supernatant was incubated with heparin beads. Total (input, 10%), non-bound (flowthrough, 10%) and bound material (eluate, 10%) was analyzed by SDS-PAGE and Western blotting. **C** Quantitative analysis of export employing flow cytometry. Expression level (black bars) and secreted protein detected on the cell surface (red bars) is shown. FGF2-GFPwt was set to 100%. **D** Biotinylation assay. Cell surface proteins were labelled with a membrane-impermeable biotin reagent. After cell lysis biotinylated and non-biotinylated proteins were separated by streptavidin beads. Total material (input, 5%) and the biotinylated fraction (eluate, 50%) were analyzed by SDS-PAGE and Western blotting. All results shown represent an average of at least 3 different experiments. For further details see „Material and Methods“ and explanation of assays in chapter 3.3.2. To summarize the obtained data, this clone does not alter from observations made for wild-type FGF2-GFP.

As demonstrated in figure 3.83, the affinity of $FGF2\text{-}GFP_{F102A}$ to heparan sulfate proteoglycans in vivo (panel A) was comparable to $FGF2\text{-}GFP_{wt}$. In contrast, its affinity to heparin *in vitro* (panel B) was reduced when compared to $FGF2\text{-}GFP_{wt}$ heparin affinity. As shown by flow cytometry (panel C), both the expression level as well as the signal for cell surface staining for $FGF2\text{-}GFP_{F102A}$ were reduced. This result was not confirmed by the biotinylation assay, which demonstrated that mutant F102A did not secrete the fusion protein more efficiently (compare the ration of lane 1 and 2 with the ratio of lane 3 and 4) than wild-type FGF2-GFP cells. However, the combined data obtained for this mutant demonstrate that F102A is not deficient in secretion or impaired in heparin binding and does not show a phenotype which is different from $FGF2\text{-}GFP_{wt}$ cells.

The following mutant contains a mutation at position 104, changing phenylalanine to alanine.

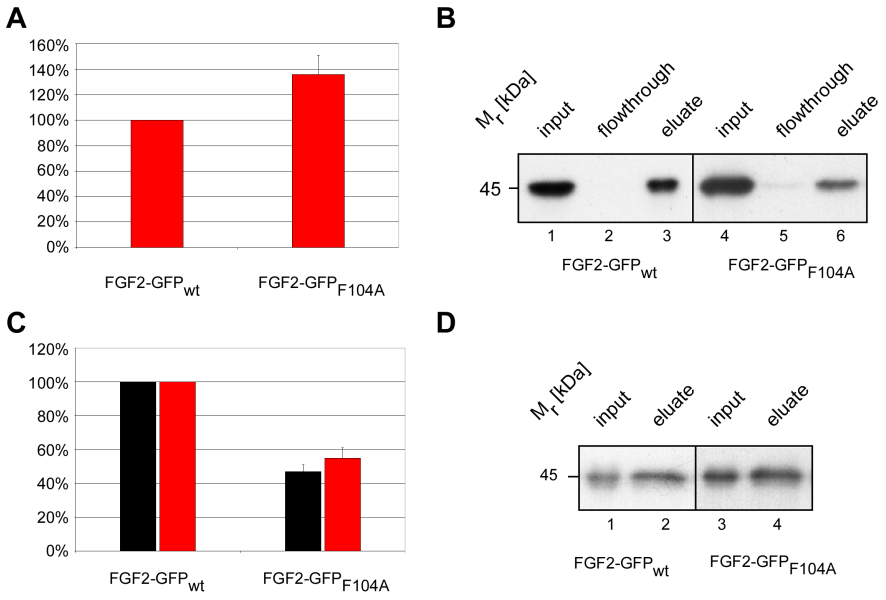

Figure 3.84: Point mutation; amino acid change: F104A **A** FACS analysis of cell free supernatant bound to the surface of $CHO_{MCAT/TAM2}$ cells. Cell surface signal of FGF2-GFPwt was set to 100%. **B** Binding of cell free supernatant to heparin beads. Cell free supernatant was incubated with heparin beads. Total (input, 10%), non-bound (flowthrough, 10%) and bound material (eluate, 10%) was analyzed by SDS-PAGE and Western blotting. **C** Quantitative analysis of export employing flow cytometry. Expression level (black bars) and secreted protein detected on the cell surface (red bars) is shown. FGF2-GFPwt was set to 100%. **D** Biotinylation assay. Cell surface proteins were labelled with a membrane-impermeable biotin reagent. After cell lysis biotinylated and non-biotinylated proteins were separated by streptavidin beads. Total material (input, 5%) and the biotinylated fraction (eluate, 50%) were analyzed by SDS-PAGE and Western blotting. All results shown represent an average of at least 3 different experiments. For further details see „Material and Methods“ and explanation of assays in chapter 3.3.2. To summarize the obtained data, this clone does not alter from observations made for wild-type FGF2-GFP.

As demonstrated in figure 3.84, the affinity of $FGF2\text{-}GFP_{F104A}$ to heparan sulfate proteoglycans in vivo (panel A) was slightly enhanced (140% ± 10 %), whereas its affinity to heparin *in vitro* (panel B) was reduced when compared to $FGF2\text{-}GFP_{wt}$. As shown by flow cytometry (panel C), both the expression level as well as the signal for $FGF2\text{-}GFP_{F104A}$ detected on the cell surface staining were reduced. This result was not confirmed by the biotinylation assay, which demonstrated that mutant F104A did not secrete the fusion protein more efficiently (compare the ration of lane 1 and 2 with the ratio of lane 3 and 4) than wild-type FGF2-GFP cells. However, the combined data obtained for this mutant demonstrate that F104A is not deficient in secretion or impaired in heparin binding and does not show a phenotype which is different from $FGF2\text{-}GFP_{wt}$ cells.

The following mutant contains a mutation at position 112, changing tyrosine to alanine.

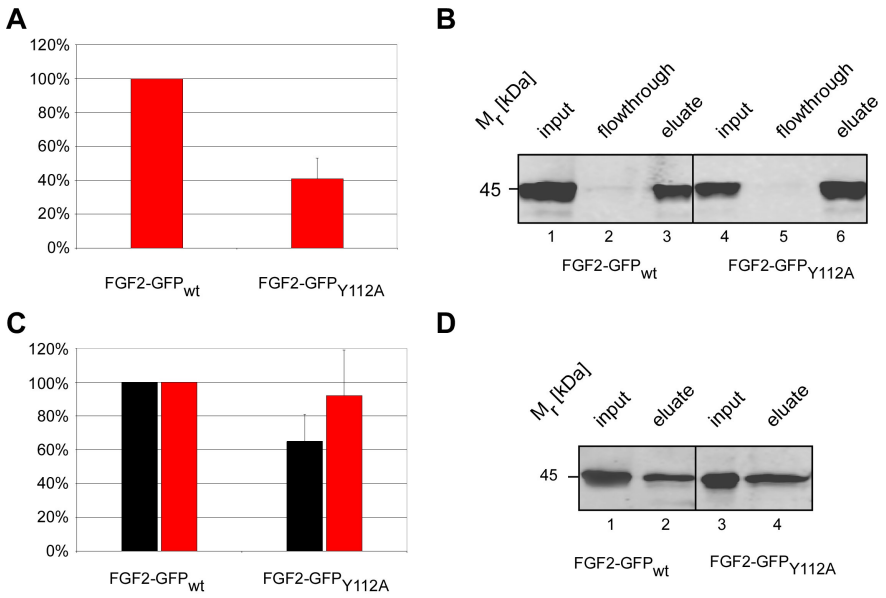

Figure 3.85: Point mutation; amino acid change: Y112A **A** FACS analysis of cell free supernatant bound to the surface of $CHO_{MCAT/TAM2}$ cells. Cell surface signal of FGF2-GFPwt was set to 100%. **B** Binding of cell free supernatant to heparin beads. Cell free supernatant was incubated with heparin beads. Total (input, 10%), non-bound (flowthrough, 10%) and bound material (eluate, 10%) was analyzed by SDS-PAGE and Western blotting. **C** Quantitative analysis of export employing flow cytometry. Expression level (black bars) and secreted protein detected on the cell surface (red bars) is shown. FGF2-GFPwt was set to 100%. **D** Biotinylation assay. Cell surface proteins were labelled with a membrane-impermeable biotin reagent. After cell lysis biotinylated and non-biotinylated proteins were separated by streptavidin beads. Total material (input, 5%) and the biotinylated fraction (eluate, 50%) were analyzed by SDS-PAGE and Western blotting. All results shown represent an average of at least 3 different experiments. For further details see „Material and Methods" and explanation of assays in chapter 3.3.2. To summarize the obtained data, this clone does not alter from observations made for wild-type FGF2-GFP.

As demonstrated in figure 3.85, the affinity of $FGF2\text{-}GFP_{Y112A}$ to heparan sulfate proteoglycans *in vivo* (panel A) is reduced (about 40% ± 10%), but its affinity to heparin *in vitro* (panel B) was comparable to $FGF2\text{-}GFP_{wt}$ heparin affinity. As shown by flow cytometry (panel C), the expression level of $FGF2\text{-}GFP_{Y112A}$ was slightly reduced as compared to $FGF2\text{-}GFP_{wt}$, but the amount of secreted fusion protein detected on the cell surface did not vary from wild-type level. As analyzed by the biotinylation assay (panel D), the mutant Y112A did not secrete the fusion protein more efficiently (compare the ration of lane 1 and 2 with the ratio of lane 3 and 4) than wild-type FGF2-GFP cells. The combined data obtained for this mutant demonstrate that Y112A is not deficient in secretion or impaired in heparin binding and does not show a phenotype which is different from $FGF2\text{-}GFP_{wt}$ cells.

The following mutant contains a mutation at position 122, changing serine to alanine.

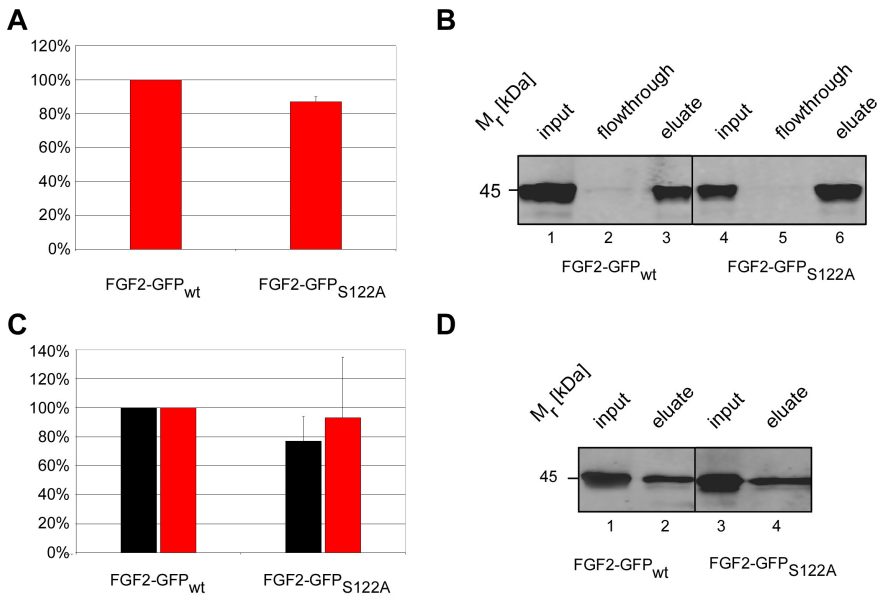

Figure 3.86: Point mutation; amino acid change: S122A **A** FACS analysis of cell free supernatant bound to the surface of $CHO_{MCAT/TAM2}$ cells. Cell surface signal of FGF2-GFPwt was set to 100%. **B** Binding of cell free supernatant to heparin beads. Cell free supernatant was incubated with heparin beads. Total (input, 10%), non-bound (flowthrough, 10%) and bound material (eluate, 10%) was analyzed by SDS-PAGE and Western blotting. **C** Quantitative analysis of export employing flow cytometry. Expression level (black bars) and secreted protein detected on the cell surface (red bars) is shown. FGF2-GFPwt was set to 100%. **D** Biotinylation assay. Cell surface proteins were labelled with a membrane-impermeable biotin reagent. After cell lysis biotinylated and non-biotinylated proteins were separated by streptavidin beads. Total material (input, 5%) and the biotinylated fraction (eluate, 50%) were analyzed by SDS-PAGE and Western blotting. All results shown represent an average of at least 3 different experiments. For further details see „Material and Methods“ and explanation of assays in chapter 3.3.2. To summarize the obtained data, this clone does not alter from observations made for wild-type FGF2-GFP.

As demonstrated in figure 3.86, the affinities of $FGF2\text{-}GFP_{S122A}$ to heparan sulfate proteoglycans *in vivo* (panel A) and to heparin *in vitro* (panel B) was comparable to $FGF2\text{-}GFP_{wt}$ heparin affinity. As detected by flow cytometry (panel C), both the expression level and the cell surface staining of $FGF2\text{-}GFP_{S122A}$ did not vary from wild-type level. This result was confirmed by the biotinylation assay (panel D). The combined data obtained for this mutant demonstrate that S122A is not deficient in secretion or impaired in heparin binding and does not show a phenotype which is different from $FGF2\text{-}GFP_{wt}$ cells.

The following mutant contains a mutation at position 128, changing lysine to glutamic acid.

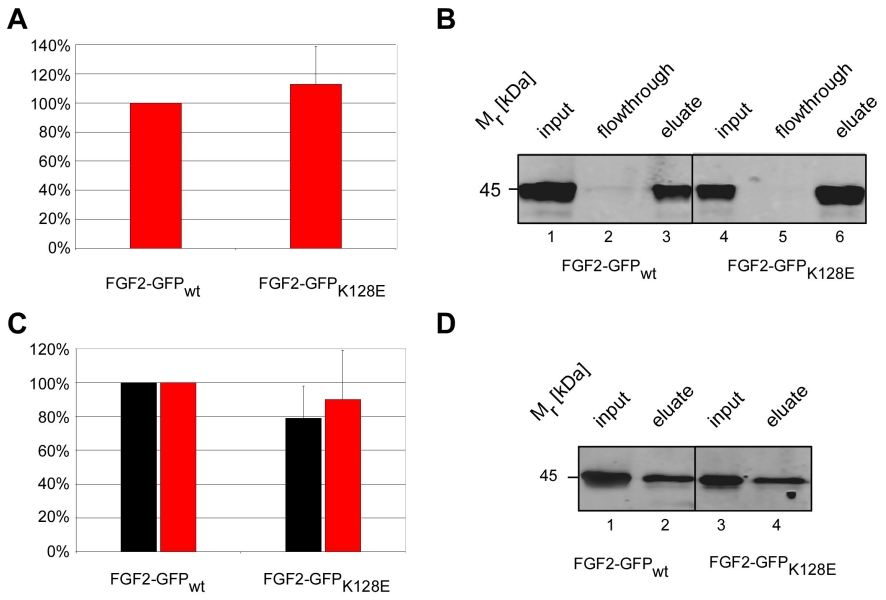

Figure 3.87: Point mutation; amino acid change: K128E **A** FACS analysis of cell free supernatant bound to the surface of $CHO_{MCAT/TAM2}$ cells. Cell surface signal of FGF2-GFPwt was set to 100%. **B** Binding of cell free supernatant to heparin beads. Cell free supernatant was incubated with heparin beads. Total (input, 10%), non-bound (flowthrough, 10%) and bound material (eluate, 10%) was analyzed by SDS-PAGE and Western blotting. **C** Quantitative analysis of export employing flow cytometry. Expression level (black bars) and secreted protein detected on the cell surface (red bars) is shown. FGF2-GFPwt was set to 100%. **D** Biotinylation assay. Cell surface proteins were labelled with a membrane-impermeable biotin reagent. After cell lysis biotinylated and non-biotinylated proteins were separated by streptavidin beads. Total material (input, 5%) and the biotinylated fraction (eluate, 50%) were analyzed by SDS-PAGE and Western blotting. All results shown represent an average of at least 3 different experiments. For further details see „Material and Methods“ and explanation of assays in chapter 3.3.2. To summarize the obtained data, this clone does not alter from observations made for wild-type FGF2-GFP.

As demonstrated in figure 3.87, the affinities of $FGF2\text{-}GFP_{K128E}$ to heparan sulfate proteoglycans *in vivo* (panel A) and to heparin *in vitro* (panel B) was comparable to $FGF2\text{-}GFP_{wt}$ heparin affinity. As detected by flow cytometry (panel C), both the expression level and the cell surface staining of $FGF2\text{-}GFP_{K128E}$ did not vary from wild-type level. This result was confirmed by the biotinylation assay (panel D). The combined data obtained for this mutant demonstrate that K128E is not deficient in secretion or impaired in heparin binding and does not show a phenotype which is different from $FGF2\text{-}GFP_{wt}$ cells.

The following mutant contains a mutation at position 129, changing arginine to glutamine.

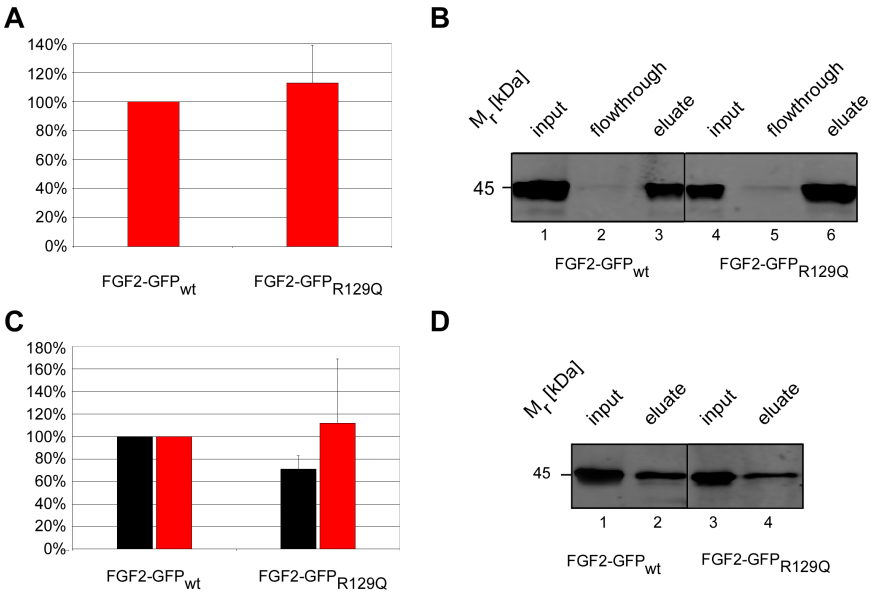

figure 3.88: Point mutation; amino acid change: R129Q **A** FACS analysis of cell free supernatant bound to the surface of $CHO_{MCAT/TAM2}$ cells. Cell surface signal of FGF2-GFPwt was set to 100%. **B** Binding of cell free supernatant to heparin beads. Cell free supernatant was incubated with heparin beads. Total (input, 10%), non-bound (flowthrough, 10%) and bound material (eluate, 10%) was analyzed by SDS-PAGE and Western blotting. **C** Quantitative analysis of export employing flow cytometry. Expression level (black bars) and secreted protein detected on the cell surface (red bars) is shown. FGF2-GFPwt was set to 100%. **D** Biotinylation assay. Cell surface proteins were labelled with a membrane-impermeable biotin reagent. After cell lysis biotinylated and non-biotinylated proteins were separated by streptavidin beads. Total material (input, 5%) and the biotinylated fraction (eluate, 50%) were analyzed by SDS-PAGE and Western blotting. All results shown represent an average of at least 3 different experiments. For further details see „Material and Methods“ and explanation of assays in chapter 3.3.2. To summarize the obtained data, this clone does not alter from observations made for wild-type FGF2-GFP.

As demonstrated in figure 3.88, the affinities of $FGF2\text{-}GFP_{R129Q}$ to heparan sulfate proteoglycans *in vivo* (panel A) and to heparin *in vitro* (panel B) was comparable to $FGF2\text{-}GFP_{wt}$ heparin affinity. As detected by flow cytometry (panel C), both the expression level and the cell surface staining of $FGF2\text{-}GFP_{R129Q}$ did not vary from wild-type level. This result was confirmed by the biotinylation assay (panel D). The combined data obtained for this mutant demonstrate that R129Q is not deficient in secretion or impaired in heparin binding and does not show a phenotype which is different from $FGF2\text{-}GFP_{wt}$ cells.

The following mutant contains a mutation at position 132, changing glutamine to arginine.

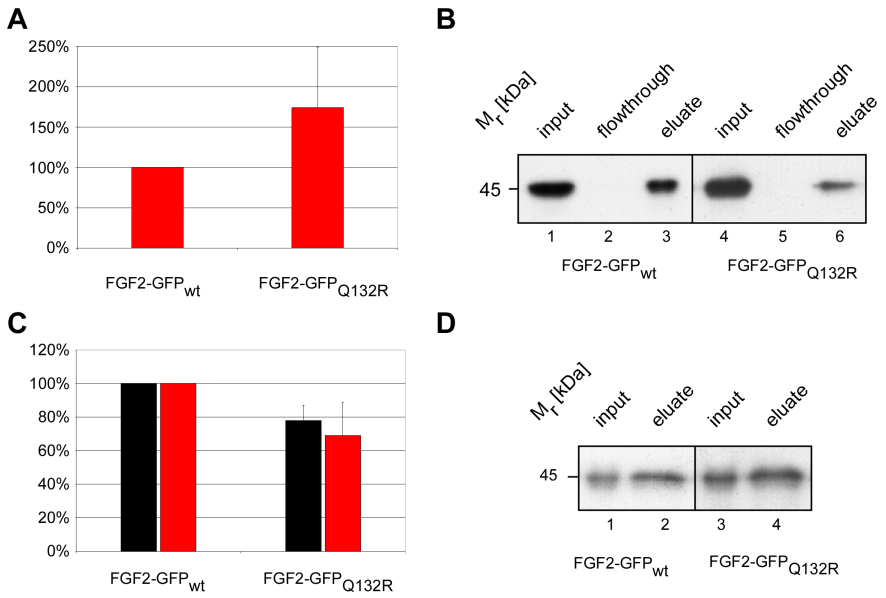

Figure 3.89: Point mutation; amino acid change: Q132R **A** FACS analysis of cell free supernatant bound to the surface of $CHO_{MCAT/TAM2}$ cells. Cell surface signal of FGF2-GFPwt was set to 100%. **B** Binding of cell free supernatant to heparin beads. Cell free supernatant was incubated with heparin beads. Total (input, 10%), non-bound (flowthrough, 10%) and bound material (eluate, 10%) was analyzed by SDS-PAGE and Western blotting. **C** Quantitative analysis of export employing flow cytometry. Expression level (black bars) and secreted protein detected on the cell surface (red bars) is shown. FGF2-GFPwt was set to 100%. **D** Biotinylation assay. Cell surface proteins were labelled with a membrane-impermeable biotin reagent. After cell lysis biotinylated and non-biotinylated proteins were separated by streptavidin beads. Total material (input, 5%) and the biotinylated fraction (eluate, 50%) were analyzed by SDS-PAGE and Western blotting. All results shown represent an average of at least 3 different experiments. For further details see „Material and Methods“ and explanation of assays in chapter 3.3.2. To summarize the obtained data, this clone does not alter from observations made for wild-type FGF2-GFP.

As demonstrated in figure 3.89, the affinity of $FGF2\text{-}GFP_{Q132R}$ to heparan sulfate proteoglycans in vivo (panel A) was enhanced (170% ± 80 %), whereas its affinity to heparin *in vitro* (panel B) was reduced when compared to $FGF2\text{-}GFP_{wt}$. As shown by flow cytometry (panel C), both the expression level as well as the signal for $FGF2\text{-}GFP_{Q132R}$ detected on the cell surface staining were reduced. This result was not confirmed by the biotinylation assay (panel D), which demonstrated that mutant Q132R did not secrete the fusion protein more efficiently than wild-type FGF2-GFP cells. However, the combined data obtained for this mutant demonstrate that Q132R is not deficient in secretion or impaired in heparin binding and does not show a phenotype which is different from $FGF2\text{-}GFP_{wt}$ cells.

The following mutant contains a mutation at position 133, changing tyrosine to histidine.

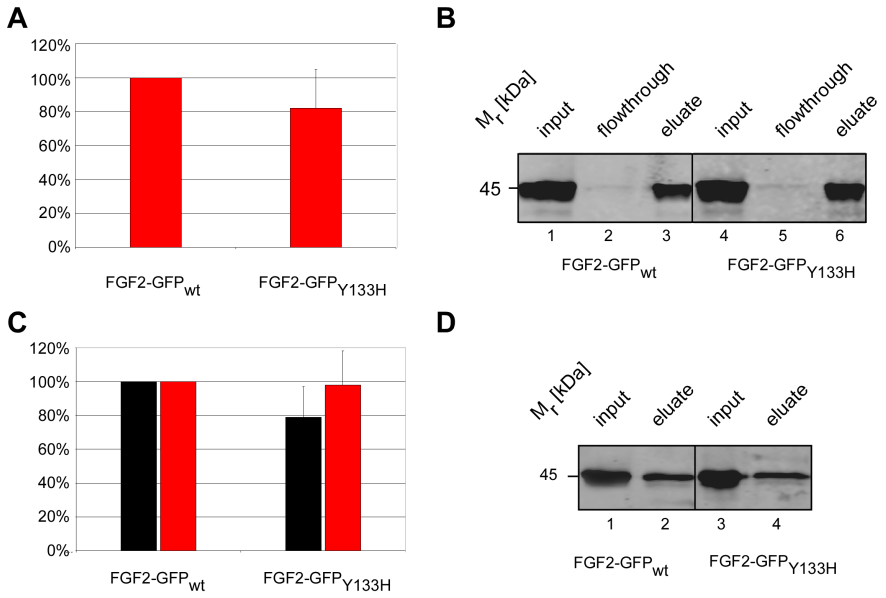

Figure 3.90: Point mutation; amino acid change: Y133H **A** FACS analysis of cell free supernatant bound to the surface of $CHO_{MCAT/TAM2}$ cells. Cell surface signal of FGF2-GFPwt was set to 100%. **B** Binding of cell free supernatant to heparin beads. Cell free supernatant was incubated with heparin beads. Total (input, 10%), non-bound (flowthrough, 10%) and bound material (eluate, 10%) was analyzed by SDS-PAGE and Western blotting. **C** Quantitative analysis of export employing flow cytometry. Expression level (black bars) and secreted protein detected on the cell surface (red bars) is shown. FGF2-GFPwt was set to 100%. **D** Biotinylation assay. Cell surface proteins were labelled with a membrane-impermeable biotin reagent. After cell lysis biotinylated and non-biotinylated proteins were separated by streptavidin beads. Total material (input, 5%) and the biotinylated fraction (eluate, 50%) were analyzed by SDS-PAGE and Western blotting. All results shown represent an average of at least 3 different experiments. For further details see „Material and Methods" and explanation of assays in chapter 3.3.2. To summarize the obtained data, this clone does not alter from observations made for wild-type FGF2-GFP.

As demonstrated in figure 3.90, the affinities of $FGF2\text{-}GFP_{Y133H}$ to heparan sulfate proteoglycans *in vivo* (panel A) and to heparin *in vitro* (panel B) was comparable to $FGF2\text{-}GFP_{wt}$ heparin affinity. As detected by flow cytometry (panel C), both the expression level and the cell surface staining of $FGF2\text{-}GFP_{Y133H}$ did not vary from wild-type level. This result was confirmed by the biotinylation assay (panel D). The combined data obtained for this mutant demonstrate that Y133H is not deficient in secretion or impaired in heparin binding and does not show a phenotype which is different from $FGF2\text{-}GFP_{wt}$ cells.

The following mutant contains a mutation at position 133, changing tyrosine to arginine.

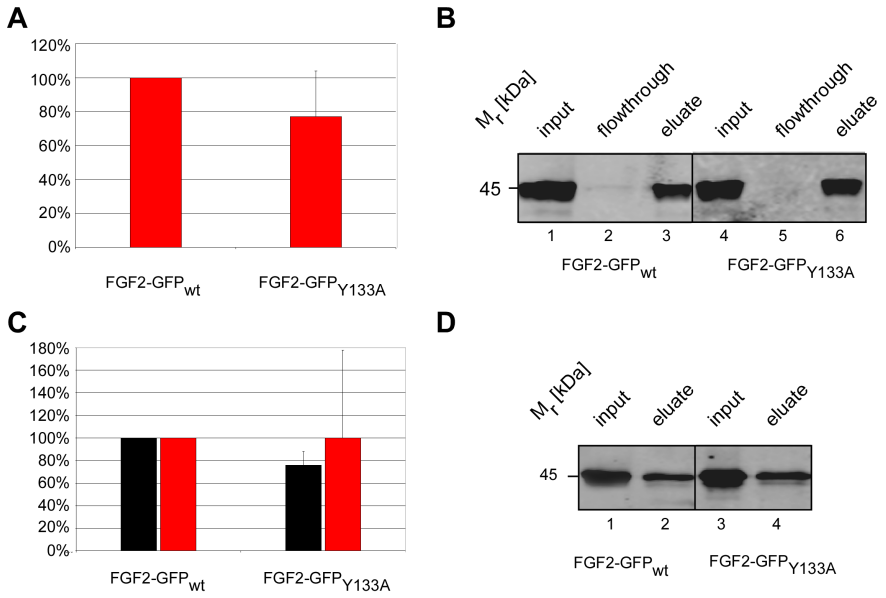

Figure 3.91: Point mutation; amino acid change: Y133A **A** FACS analysis of cell free supernatant bound to the surface of $CHO_{MCAT/TAM2}$ cells. Cell surface signal of FGF2-GFPwt was set to 100%. **B** Binding of cell free supernatant to heparin beads. Cell free supernatant was incubated with heparin beads. Total (input, 10%), non-bound (flowthrough, 10%) and bound material (eluate, 10%) was analyzed by SDS-PAGE and Western blotting. **C** Quantitative analysis of export employing flow cytometry. Expression level (black bars) and secreted protein detected on the cell surface (red bars) is shown. FGF2-GFPwt was set to 100%. **D** Biotinylation assay. Cell surface proteins were labelled with a membrane-impermeable biotin reagent. After cell lysis biotinylated and non-biotinylated proteins were separated by streptavidin beads. Total material (input, 5%) and the biotinylated fraction (eluate, 50%) were analyzed by SDS-PAGE and Western blotting. All results shown represent an average of at least 3 different experiments. For further details see „Material and Methods“ and explanation of assays in chapter 3.3.2. To summarize the obtained data, this clone does not alter from observations made for wild-type FGF2-GFP.

As demonstrated in figure 3.91, the affinities of $FGF2\text{-}GFP_{Y133A}$ to heparan sulfate proteoglycans *in vivo* (panel A) and to heparin *in vitro* (panel B) was comparable to $FGF2\text{-}GFP_{wt}$ heparin affinity. As detected by flow cytometry (panel C), both the expression level and the cell surface staining of $FGF2\text{-}GFP_{Y133A}$ did not vary from wild-type level. This result was confirmed by the biotinylation assay (panel D). The combined data obtained for this mutant demonstrate that Y133A is not deficient in secretion or impaired in heparin binding and does not show a phenotype which is different from $FGF2\text{-}GFP_{wt}$ cells.

The following mutant contains a mutation at position 152, changing serine to arginine.

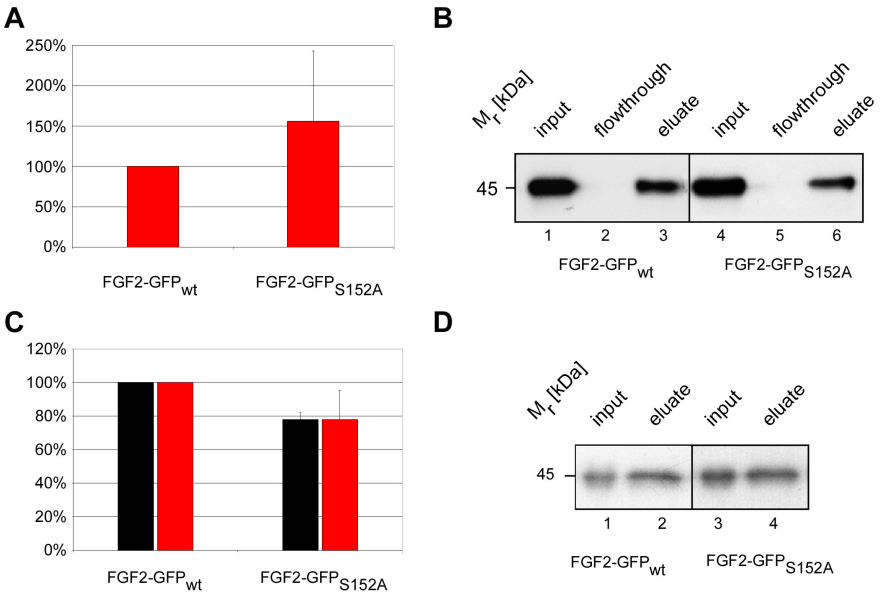

Figure 3.92: Point mutation; amino acid change: S152A **A** FACS analysis of cell free supernatant bound to the surface of $CHO_{MCAT/TAM2}$ cells. Cell surface signal of FGF2-GFPwt was set to 100%. **B** Binding of cell free supernatant to heparin beads. Cell free supernatant was incubated with heparin beads. Total (input, 10%), non-bound (flowthrough, 10%) and bound material (eluate, 10%) was analyzed by SDS-PAGE and Western blotting. **C** Quantitative analysis of export employing flow cytometry. Expression level (black bars) and secreted protein detected on the cell surface (red bars) is shown. FGF2-GFPwt was set to 100%. **D** Biotinylation assay. Cell surface proteins were labelled with a membrane-impermeable biotin reagent. After cell lysis biotinylated and non-biotinylated proteins were separated by streptavidin beads. Total material (input, 5%) and the biotinylated fraction (eluate, 50%) were analyzed by SDS-PAGE and Western blotting. All results shown represent an average of at least 3 different experiments. For further details see „Material and Methods“ and explanation of assays in chapter 3.3.2. To summarize the obtained data, this clone does not alter from observations made for wild-type FGF2-GFP.

As demonstrated in figure 3.92, the affinity of $FGF2\text{-}GFP_{S152A}$ to heparan sulfate proteoglycans in vivo (panel A) was enhanced (about 150% ± 90 %), but its affinity to heparin *in vitro* (panel B) was comparable to $FGF2\text{-}GFP_{wt}$ affinity. As detected by flow cytometry (panel C), both the expression level and the cell surface staining of $FGF2\text{-}GFP_{S152A}$ did not vary from wild-type level. This result was confirmed by the biotinylation assay (panel D). The combined data obtained for this mutant demonstrate that S152A is not deficient in secretion or impaired in heparin binding and does not show a phenotype which is different from $FGF2\text{-}GFP_{wt}$ cells.

To summarize, 43 mutants were shown to be comparable to $FGF2\text{-}GFP_{wt}$ cells, regarding their secretion efficiency, protein stability, affinity to heparan sulfate proteoglycans and to heparin. Therefore, they were termed “no phenotype”

3.3.4.2 *Experimental data for FGF2 mutants showing a reduced expression level of FGF2-GFP*

In this section, the FGF2-GFP mutants generated by site-directed mutagenesis are depicted which demonstrate a reduced expression level, suggesting that the protein might be misfolded and rapidly degraded or that its translation rates are reduced. Moreover, their amino acid changes are shown and a summary of the experimental data is provided. For a detailed view on the assays used, please refer to chapter 3.3.2.

The following mutant contains a mutation at position 40, changing phenylalanine to leucine.

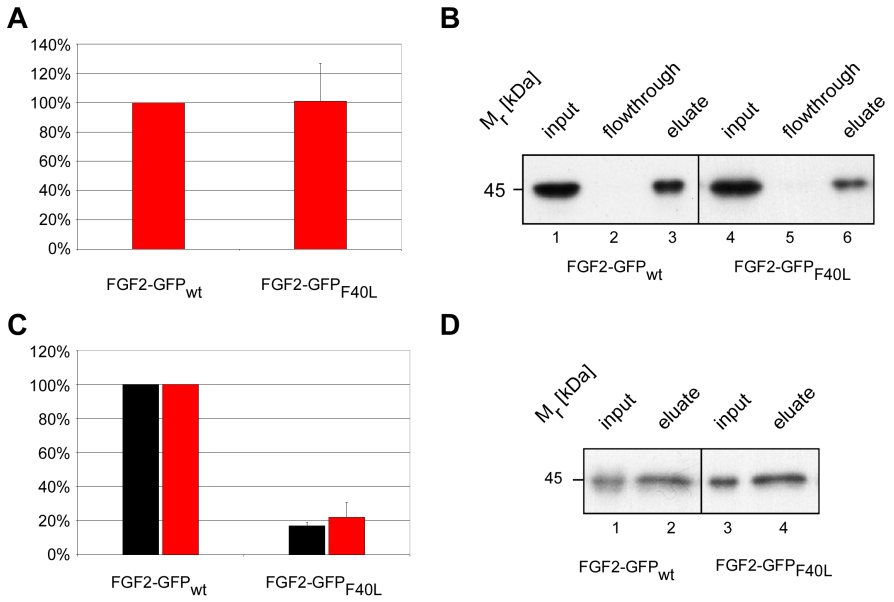

figure 3.93: Point mutation; amino acid change: F40L **A** FACS analysis of cell free supernatant bound to the surface of $CHO_{MCAT/TAM2}$ cells. Cell surface signal of FGF2-GFPwt was set to 100%. **B** Binding of cell free supernatant to heparin beads. Cell free supernatant was incubated with heparin beads. Total (input, 10%), non-bound (flowthrough, 10%) and bound material (eluate, 10%) was analyzed by SDS-PAGE and Western blotting. **C** Quantitative analysis of export employing flow cytometry. Expression level (black bars) and secreted protein detected on the cell surface (red bars) is shown. FGF2-GFPwt was set to 100%. **D** Biotinylation assay. Cell surface proteins were labelled with a membrane-impermeable biotin reagent. After cell lysis biotinylated and non-biotinylated proteins were separated by streptavidin beads. Total material (input, 5%) and the biotinylated fraction (eluate, 50%) were analyzed by SDS-PAGE and Western blotting. All results shown represent an average of at least 3 different experiments. For further details see „Material and Methods“ and explanation of assays in chapter 3.3.2. To summarize the obtained data, the mutated protein is instable in the cytoplasm, but its affinities to heparin and HSPGs are comparable to wild-type FGF2-GFP.

As demonstrated in figure 3.93, the affinity of $FGF2\text{-}GFP_{F40L}$ to heparan sulfate proteoglycans in vivo (panel A) was comparable to $FGF2\text{-}GFP_{wt}$. In contrast, its affinity to heparin *in vitro* (panel B) was reduced when compared to $FGF2\text{-}GFP_{wt}$. As detected by flow cytometry (panel C), the expression level of the mutated fusion protein is strongly reduced to under 20% of wild-type level. The signal for FGF2-

GFP_{F40L} bound to the cell surface is reduced to the same amount as it was shown for the expression level of this mutant, suggesting that the secretion efficiency is not reduced, since the ratio of fusion protein expression to secretion remains constant in comparison to FGF2-GFP_{wt}. This result is confirmed by the biotinylation assay (panel D).

The following mutant contains a mutation at position 42, changing arginine to histidine.

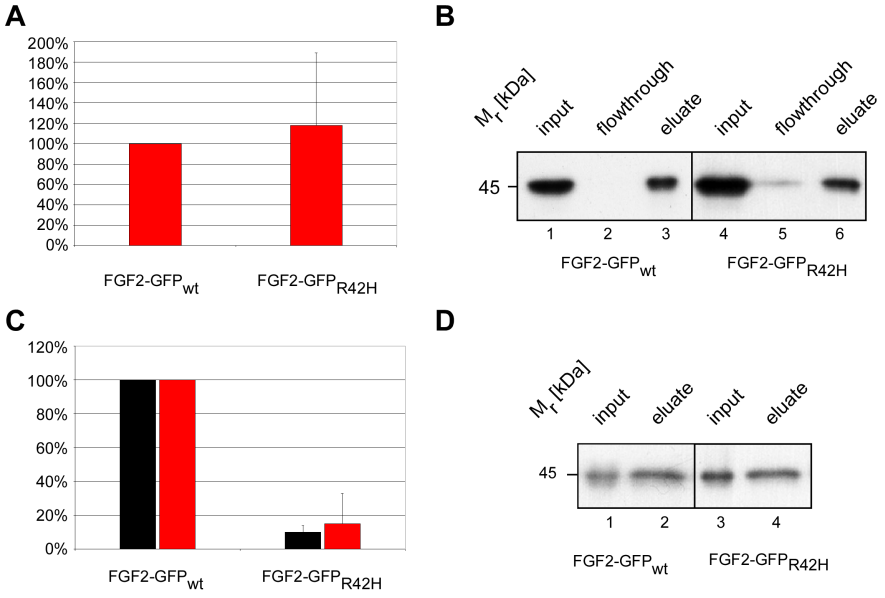

Figure 3.94: Point mutation; amino acid change: R42H **A** FACS analysis of cell free supernatant bound to the surface of $CHO_{MCAT/TAM2}$ cells. Cell surface signal of FGF2-GFPwt was set to 100%. **B** Binding of cell free supernatant to heparin beads. Cell free supernatant was incubated with heparin beads. Total (input, 10%), non-bound (flowthrough, 10%) and bound material (eluate, 10%) was analyzed by SDS-PAGE and Western blotting. **C** Quantitative analysis of export employing flow cytometry. Expression level (black bars) and secreted protein detected on the cell surface (red bars) is shown. FGF2-GFPwt was set to 100%. **D** Biotinylation assay. Cell surface proteins were labelled with a membrane-impermeable biotin reagent. After cell lysis biotinylated and non-biotinylated proteins were separated by streptavidin beads. Total material (input, 5%) and the biotinylated fraction (eluate, 50%) were analyzed by SDS-PAGE and Western blotting. All results shown represent an average of at least 3 different experiments. For further details see „Material and Methods“ and explanation of assays in chapter 3.3.2. To summarize the obtained data, the mutated protein is instable in the cytoplasm, but is, concerning binding characteristics, comparable to wild-type FGF2-GFP.

As demonstrated in figure 3.94, the affinities of FGF2-GFP_{R42H} to heparan sulfate proteoglycans *in vivo* (panel A) and to heparin *in vitro* (panel B) was comparable to FGF2-GFP_{wt} heparin affinity. As detected by flow cytometry (panel C), the expression level of the mutated fusion protein is strongly reduced to under 20% of wild-type level. The signal for FGF2-GFP_{R42H} bound to the cell surface is reduced to the same amount as it was shown for the expression level of this mutant, suggesting that the secretion efficiency is not reduced, since the ratio of fusion protein expression to secretion remains constant in comparison to FGF2-GFP_{wt}. This result is confirmed by the biotinylation assay (panel D).

The following mutant contains a mutation at position 72, changing valine to alanine.

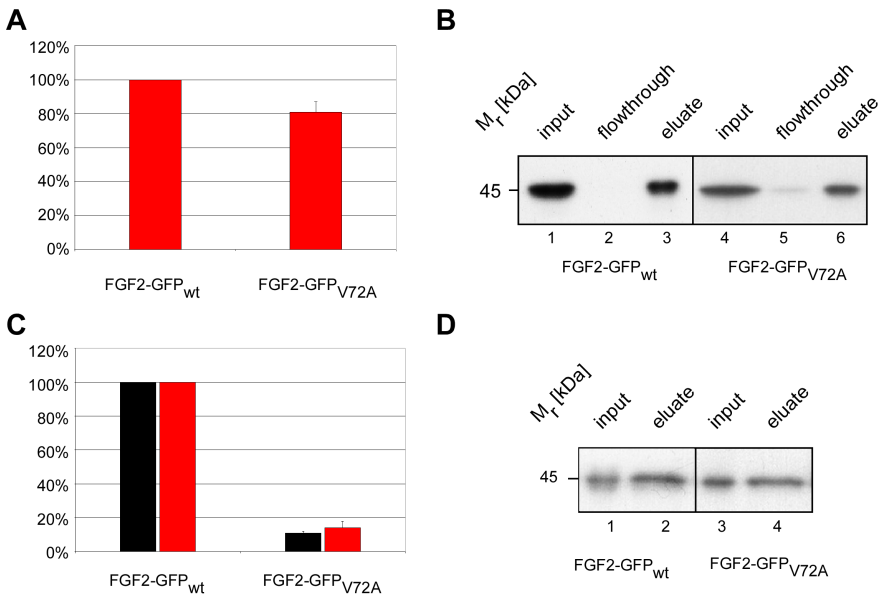

Figure 3.95: Point mutation; amino acid change: V72A **A** FACS analysis of cell free supernatant bound to the surface of $CHO_{MCAT/TAM2}$ cells. Cell surface signal of FGF2-GFPwt was set to 100%. **B** Binding of cell free supernatant to heparin beads. Cell free supernatant was incubated with heparin beads. Total (input, 10%), non-bound (flowthrough, 10%) and bound material (eluate, 10%) was analyzed by SDS-PAGE and Western blotting. **C** Quantitative analysis of export employing flow cytometry. Expression level (black bars) and secreted protein detected on the cell surface (red bars) is shown. FGF2-GFPwt was set to 100%. **D** Biotinylation assay. Cell surface proteins were labelled with a membrane-impermeable biotin reagent. After cell lysis biotinylated and non-biotinylated proteins were separated by streptavidin beads. Total material (input, 5%) and the biotinylated fraction (eluate, 50%) were analyzed by SDS-PAGE and Western blotting. All results shown represent an average of at least 3 different experiments. For further details see „Material and Methods“ and explanation of assays in chapter 3.3.2. To summarize the obtained data, the mutated protein is instable in the cytoplasm, but is, concerning binding characteristics, comparable to wild-type FGF2-GFP.

As demonstrated in figure 3.95, the affinities of $FGF2\text{-}GFP_{V72A}$ to heparan sulfate proteoglycans *in vivo* (panel A) and to heparin *in vitro* (panel B) was comparable to $FGF2\text{-}GFP_{wt}$ heparin affinity. As detected by flow cytometry (panel C), the expression level of the mutated fusion protein is strongly reduced to under 20% of wild-type level. The signal for $FGF2\text{-}GFP_{V72A}$ bound to the cell surface is reduced to the same amount as it was shown for the expression level of this mutant, suggesting that the secretion efficiency is not reduced, since the ratio of fusion protein expression to secretion remains constant in comparison to $FGF2\text{-}GFP_{wt}$. This result is confirmed by the biotinylation assay (panel D).

The three mutants listed in this section demonstrate reduced expression level of the various versions of FGF2-GFP, indicating either rapid degradation due to misfolded proteins or less expressed fusion protein. Therefore, it is questionable if a quantification of the amount of secreted FGF2-GFP is possible. The affinities to heparin and to heparan sulfate proteoglycans are not impaired. As a consequence thereof, these mutants were termed “instable protein”.

3.3.4.3 *Experimental data for FGF2 mutants impaired in protein stability, binding to heparin and to heparan sulfate proteoglycans*

In this section, the FGF2-GFP mutants generated by site-directed mutagenesis are depicted which demonstrate an instable intracellular fusion protein, an impaired binding to heparin and to heparan sulfate proteoglycans. Moreover, their amino acid changes are shown and a summary of the experimental data is provided. For a detailed view on the assays used, please refer to chapter 3.3.2.

The following mutant contains a mutation at position 64, changing leucine to proline.

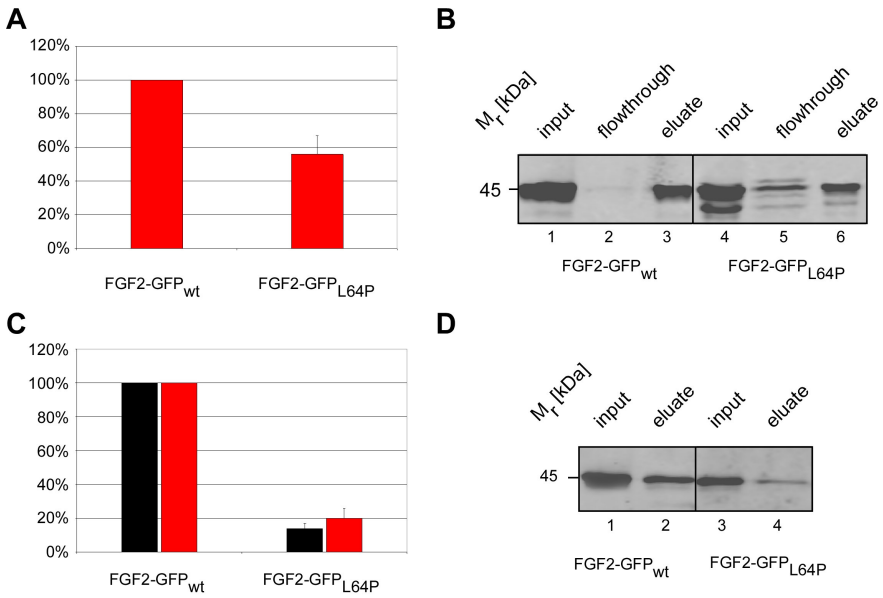

Figure 3.96: Point mutation; amino acid change: L64P **A** FACS analysis of cell free supernatant bound to the surface of $CHO_{MCAT/TAM2}$ cells. Cell surface signal of FGF2-GFPwt was set to 100%. **B** Binding of cell free supernatant to heparin beads. Cell free supernatant was incubated with heparin beads. Total (input, 10%), non-bound (flowthrough, 10%) and bound material (eluate, 10%) was analyzed by SDS-PAGE and Western blotting. **C** Quantitative analysis of export employing flow cytometry. Expression level (black bars) and secreted protein detected on the cell surface (red bars) is shown. FGF2-GFPwt was set to 100%. **D** Biotinylation assay. Cell surface proteins were labelled with a membrane-impermeable biotin reagent. After cell lysis biotinylated and non-biotinylated proteins were separated by streptavidin beads. Total material (input, 5%) and the biotinylated fraction (eluate, 50%) were analyzed by SDS-PAGE and Western blotting. All results shown represent an average of at least 3 different experiments. For further details see „Material and Methods“ and explanation of assays in chapter 3.3.2. To summarize the obtained data, the mutated protein is instable in the cytoplasm, and is, concerning binding characteristics, reduced compared to wild-type FGF2-GFP.

As demonstrated in figure 3.96, the affinities of $FGF2\text{-}GFP_{L64P}$ to heparan sulfate proteoglycans *in vivo* and to heparin *in vitro* were reduced. As detected by flow cytometry (panel C), the expression level of the mutated fusion protein is strongly reduced to under 20% of wild-type level. The signal for $FGF2\text{-}GFP_{L64P}$ bound to the cell surface is reduced to the same amount as it was shown for the expression level of this mutant. The secretion efficiency is not reduced, since the ratio of fusion protein expression to secretion remains constant in comparison to $FGF2\text{-}GFP_{wt}$ cells. This result is confirmed by the biotinylation assay (panel D).

The following mutant contains a mutation at position 74, changing isoleucine to threonine.

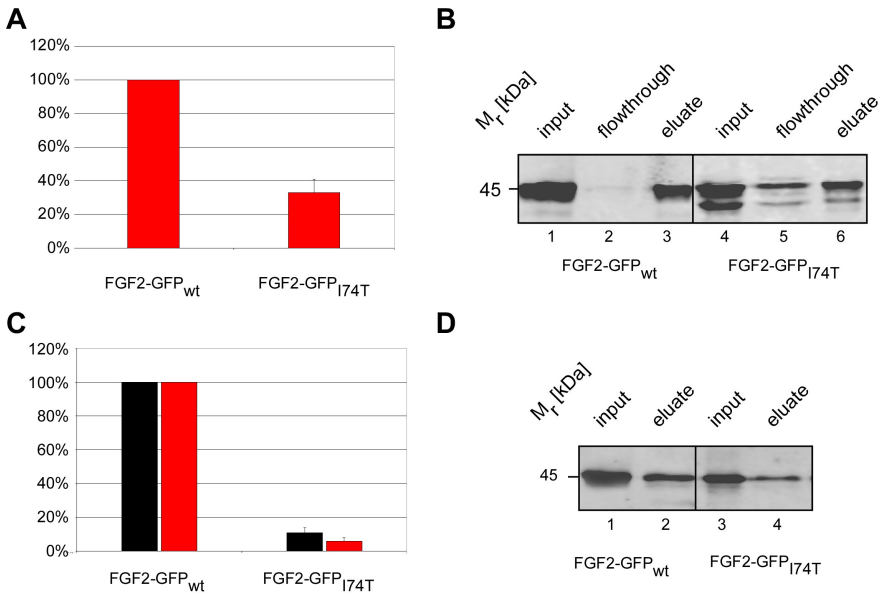

Figure 3.97: Point mutation; amino acid change: I74T **A** FACS analysis of cell free supernatant bound to the surface of $CHO_{MCAT/TAM2}$ cells. Cell surface signal of FGF2-GFPwt was set to 100%. **B** Binding of cell free supernatant to heparin beads. Cell free supernatant was incubated with heparin beads. Total (input, 10%), non-bound (flowthrough, 10%) and bound material (eluate, 10%) was analyzed by SDS-PAGE and Western blotting. **C** Quantitative analysis of export employing flow cytometry. Expression level (black bars) and secreted protein detected on the cell surface (red bars) is shown. FGF2-GFPwt was set to 100%. **D** Biotinylation assay. Cell surface proteins were labelled with a membrane-impermeable biotin reagent. After cell lysis biotinylated and non-biotinylated proteins were separated by streptavidin beads. Total material (input, 5%) and the biotinylated fraction (eluate, 50%) were analyzed by SDS-PAGE and Western blotting. All results shown represent an average of at least 3 different experiments. For further details see „Material and Methods“ and explanation of assays in chapter 3.3.2. To summarize the obtained data, the mutated protein is instable in the cytoplasm, and is, concerning binding characteristics, reduced compared to wild-type FGF2-GFP.

As demonstrated in figure 3.97, the affinities of $FGF2\text{-}GFP_{I74T}$ to heparan sulfate proteoglycans *in vivo* and to heparin *in vitro* were reduced. As detected by flow cytometry (panel C), the expression level of the mutated fusion protein is strongly reduced to under 20% of wild-type level. The signal for $FGF2\text{-}GFP_{I74T}$ bound to the cell surface is reduced to the same amount as it was shown for the expression level of this mutant. The secretion efficiency is not reduced, since the ratio of fusion protein expression to secretion remains constant in comparison to $FGF2\text{-}GFP_{wt}$ cells. This result is confirmed by the biotinylation assay (panel D).

The following mutant contains a mutation at position 82, changing tyrosine to alanine.

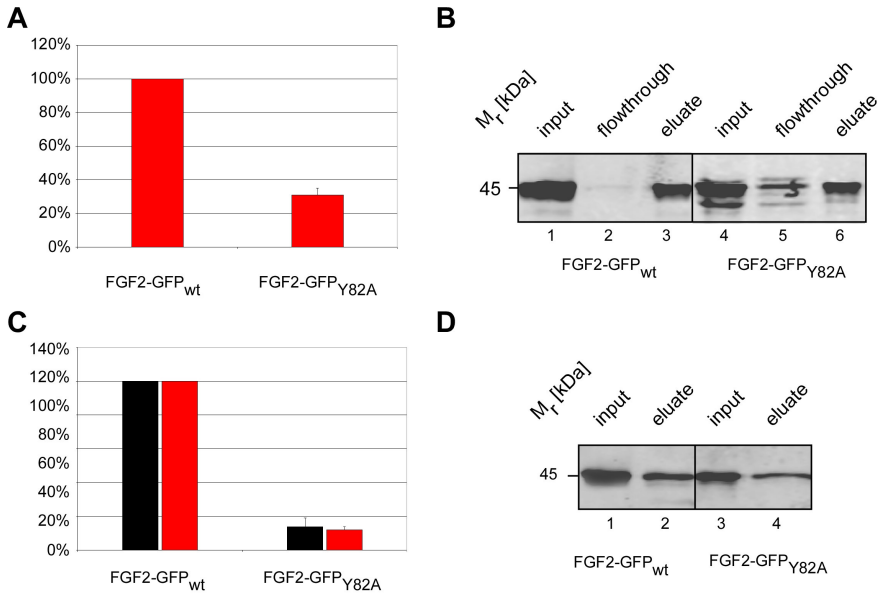

Figure 3.98: Point mutation; amino acid change: Y82A **A** FACS analysis of cell free supernatant bound to the surface of $CHO_{MCAT/TAM2}$ cells. Cell surface signal of FGF2-GFPwt was set to 100%. **B** Binding of cell free supernatant to heparin beads. Cell free supernatant was incubated with heparin beads. Total (input, 10%), non-bound (flowthrough, 10%) and bound material (eluate, 10%) was analyzed by SDS-PAGE and Western blotting. **C** Quantitative analysis of export employing flow cytometry. Expression level (black bars) and secreted protein detected on the cell surface (red bars) is shown. FGF2-GFPwt was set to 100%. **D** Biotinylation assay. Cell surface proteins were labelled with a membrane-impermeable biotin reagent. After cell lysis biotinylated and non-biotinylated proteins were separated by streptavidin beads. Total material (input, 5%) and the biotinylated fraction (eluate, 50%) were analyzed by SDS-PAGE and Western blotting. All results shown represent an average of at least 3 different experiments. For further details see „Material and Methods“ and explanation of assays in chapter 3.3.2. To summarize the obtained data, the mutated protein is instable in the cytoplasm, and is, concerning binding characteristics, reduced compared to wild-type FGF2-GFP.

As demonstrated in figure 3.98, the affinities of $FGF2\text{-}GFP_{Y82A}$ to heparan sulfate proteoglycans *in vivo* and to heparin *in vitro* were reduced. As detected by flow cytometry (panel C), the expression level of the mutated fusion protein is strongly reduced to under 20% of wild-type level. The signal for $FGF2\text{-}GFP_{Y82A}$ bound to the cell surface is reduced to the same amount as it was shown for the expression level of this mutant. The secretion efficiency is not reduced, since the ratio of fusion protein expression to secretion remains constant in comparison to $FGF2\text{-}GFP_{wt}$ cells. This result is confirmed by the biotinylation assay (panel D).

The following mutant contains a mutation at position 88, changing aspartic acid to alanine.

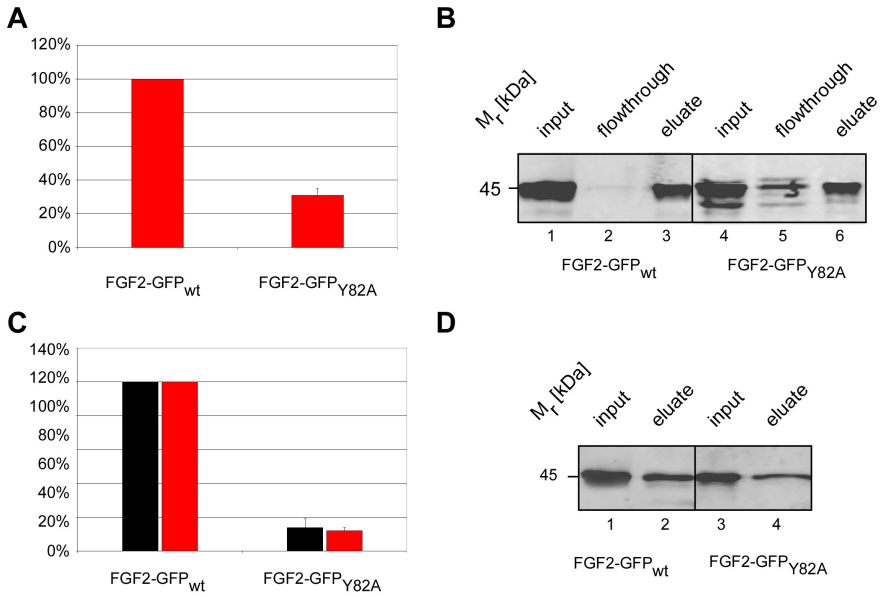

Figure 3.99: Point mutation; amino acid change: D88A **A** FACS analysis of cell free supernatant bound to the surface of $CHO_{MCAT/TAM2}$ cells. Cell surface signal of FGF2-GFPwt was set to 100%. **B** Binding of cell free supernatant to heparin beads. Cell free supernatant was incubated with heparin beads. Total (input, 10%), non-bound (flowthrough, 10%) and bound material (eluate, 10%) was analyzed by SDS-PAGE and Western blotting. **C** Quantitative analysis of export employing flow cytometry. Expression level (black bars) and secreted protein detected on the cell surface (red bars) is shown. FGF2-GFPwt was set to 100%. **D** Biotinylation assay. Cell surface proteins were labelled with a membrane-impermeable biotin reagent. After cell lysis biotinylated and non-biotinylated proteins were separated by streptavidin beads. Total material (input, 5%) and the biotinylated fraction (eluate, 50%) were analyzed by SDS-PAGE and Western blotting. All results shown represent an average of at least 3 different experiments. For further details see „Material and Methods“ and explanation of assays in chapter 3.3.2. To summarize the obtained data, the mutated protein is instable in the cytoplasm, and is, concerning binding characteristics, reduced compared to wild-type FGF2-GFP.

As demonstrated in figure 3.99, the affinities of $FGF2\text{-}GFP_{D88A}$ to heparan sulfate proteoglycans *in vivo* and to heparin *in vitro* were reduced. As detected by flow cytometry (panel C), the expression level of the mutated fusion protein is strongly reduced to under 20% of wild-type level. The signal for $FGF2\text{-}GFP_{D88A}$ bound to the cell surface is reduced to the same amount as it was shown for the expression level of this mutant. The secretion efficiency is not reduced, since the ratio of fusion protein expression to secretion remains constant in comparison to $FGF2\text{-}GFP_{wt}$ cells. This result is confirmed by the biotinylation assay (panel D).

The mutants listed in this section demonstrate an impaired binding to heparin *in vitro* and to heparan-sulfate proteoglycans *in vivo*. Additionally, the expression level of the various versions of FGF2-GFP is strongly reduced, indicating either rapid degradation due to misfolded proteins or reduced expression of the fusion protein. Therefore, it is questionable if a quantification of the amount of secreted FGF2-GFP is possible. As a consequence thereof, these mutants were termed “instable protein and impaired in binding”.

3.3.4.4 *Experimental data for a double cysteine FGF2 mutant potentially deficient in secretion*

The following mutant displays two altered amino acid at position 78 and 96, changing two cysteines to two alanines.

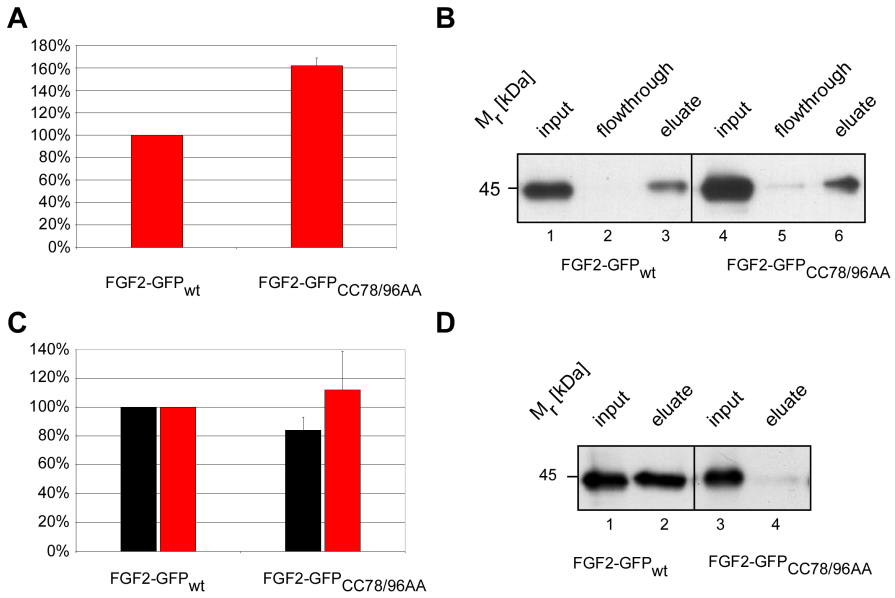

figure 3.100: Point mutation; amino acid changes: CC78/96AA **A** FACS analysis of cell free supernatant bound to the surface $CHO_{MCAT/TAM2}$ cells. Cell surface signal of FGF2-GFPwt was set to 100%. **B** Binding of cell free supernatant to heparin beads. Cell free supernatant was incubated with heparin beads. Total (input, 10%), non-bound (flowthrough, 10%) and bound material (eluate, 10%) was analyzed by SDS-PAGE and Western blotting. **C** Quantitative analysis of export employing flow cytometry. Expression level (black bars) and secreted protein detected on the cell surface (red bars) is shown. FGF2-GFPwt was set to 100%. **D** Biotinylation assay. Cell surface proteins were labelled with a membrane-impermeable biotin reagent. After cell lysis biotinylated and non-biotinylated proteins were separated by streptavidin beads. Total material (input, 5%) and the biotinylated fraction (eluate, 50%) were analyzed by SDS-PAGE and Western blotting. All results shown represent an average of at least 3 different experiments. For further details see „Material and Methods“ and explanation of assays in chapter 3.3.2. This double mutant is positive for both binding in vivo and in vitro. The FACS assay shows a secreted population of FGF2 present on the cell surface staining. In contrast to this observation, the amount of secreted protein as detected by biotinylation is significantly reduced compared to wild-type FGF2-GFP.

As demonstrated in figure 3.100, the affinity of $FGF2\text{-}GFP_{CC78/96AA}$ to heparan sulfate proteoglycans *in vivo* (panel A) and to heparin *in vitro* (panel B) was comparable to $FGF2\text{-}GFP_{wt}$ heparin affinity. Results obtained by flow cytometry show that expression level and cell surface staining are not reduced when compared to wild-type FGF2-GFP. Strikingly, biotinylation of cell surface proteins results in a significantly reduced streptavidin-bound fraction of mutated protein, indicating a reduction in secretion of $FGF2\text{-}GFP_{CC78/96AA}$. However, this discrepancy between FACS analysis and cell surface biotinylation remains unclear.

3.3.4.5 *Overview of mutants obtained by point mutation with regard to secretion efficiency, affinity to heparin and protein stability*

The generated mutants were analyzed by standard assays as previously described in chapter 3.3.2. As a result, the observations made are listed in the following table:

Mutant	Classification	Mutant	Classification
A3V	No Phenotype	*E67V*	No Phenotype
G4A	No Phenotype	*E68A*	No Phenotype
S5A	No Phenotype	*E68G*	No Phenotype
I6T	No Phenotype	*R69A*	No Phenotype
T7A	No Phenotype	*V72A*	Instable Protein
T7E	No Phenotype	*I74T*	Instable Protein / Impaired Binding
T7D	No Phenotype	*K75I*	No Phenotype
T8M	No Phenotype	*V77A*	No Phenotype
E14D	No Phenotype	*C78A*	No Phenotype
F21I	No Phenotype	*N80A*	No Phenotype
P23S	No Phenotype	*Y82A*	Instable Protein / Impaired Binding
F26A	No Phenotype	*E87K*	No Phenotype
K30E	No Phenotype	*D88A*	Instable Protein / Impaired Binding
Y33A	No Phenotype	*L92A*	No Phenotype
F39L	No Phenotype	*C96A*	No Phenotype
F39A	No Phenotype	*F102A*	No Phenotype
F40L	Instable Protein	*F104A*	No Phenotype
R42H	Instable Protein	*Y112A*	No Phenotype
R53H	No Phenotype	*S122A*	No Phenotype
K55T	No Phenotype	*K128E*	No Phenotype
K55R	No Phenotype	*R129Q*	No Phenotype
H59P	No Phenotype	*Q132R*	No Phenotype
K61E	No Phenotype	*Y133H*	No Phenotype
L64P	Instable Protein / Impaired Binding	*Y133A*	No Phenotype
Q65A	No Phenotype	*S152A*	No Phenotype
CC78/96AA	Negative in Biotinylation		

Table 3.4: Overview of classifications made for point mutations with regard to secretion and heparin binding ability.

The results obtained by characterization of point mutations showed that most of the generated clones are comparable to FGF2-GFP_{wt} with regard to protein stability, secretion efficiency and affinity to heparin or heparan sulfate proteoglycans (44).

Additionally, mutants showing reduced expression levels of FGF2-GFP in the cytosol (7) also mainly demonstrate an impaired binding ability of their fusion protein to heparin and heparan sulfate proteoglycans (4). Moreover, a mutant (CC78/96AA) was observed, which displayed a reduced signal for secreted fusion protein present on the surface as detected by cell surface biotinylation, but this could not be confirmed by flow cytometry and will be further characterized in our laboratory.

3.3.5 Truncations of N- and C-Terminus

In order to elucidate a potential export motif that might be present at the very ends of FGF2, both the N- and C-terminus were truncated.

3.3.5.1 Functional analysis of FGF2 mutants with N-terminal Truncations

Although the crystal structure of FGF2 has been resolved in 1991 (Ago et al., 1991), the disordered N-terminal residues of FGF2 remain of unknown structure. Additionally a small heparin binding region appears to be present at the N-terminus at position 20-40 (Baird et al., 1988; Ogura et al., 1999). To investigate the effect of the flexible region and the N-terminal heparin binding sites with regard to unconventional secretion of FGF2, up to 50 amino acids from the N-terminus were systematically deleted in steps of 10 amino acids. After stably introducing the cDNA into the genome of CHO cells, the cells were analyzed regarding export efficiency of FGF2. An overview of the mutants is listed in the following table 3.4.

Mutant	Truncation
ΔN10-FGF2	10 amino acids from N-terminus deleted
ΔN20-FGF2	20 amino acids from N-terminus deleted
ΔN30-FGF2	30 amino acids from N-terminus deleted
ΔN40-FGF2	40 amino acids from N-terminus deleted
ΔN50-FGF2	50 amino acids from N-terminus deleted

Table 3.5: overview of N-terminal truncations.

The N-terminal truncations of FGF2-GFP were analyzed with regard to secretion efficiency, fusion protein stability, affinity to heparin and to heparan sulfate proteoglycans. Moreover, a summary of the experimental data is provided. For a detailed view on the assays used, please refer to chapter 3.3.2.

Truncation ΔN-10-FGF2-GFP lacks the N-terminal 10 amino acids.

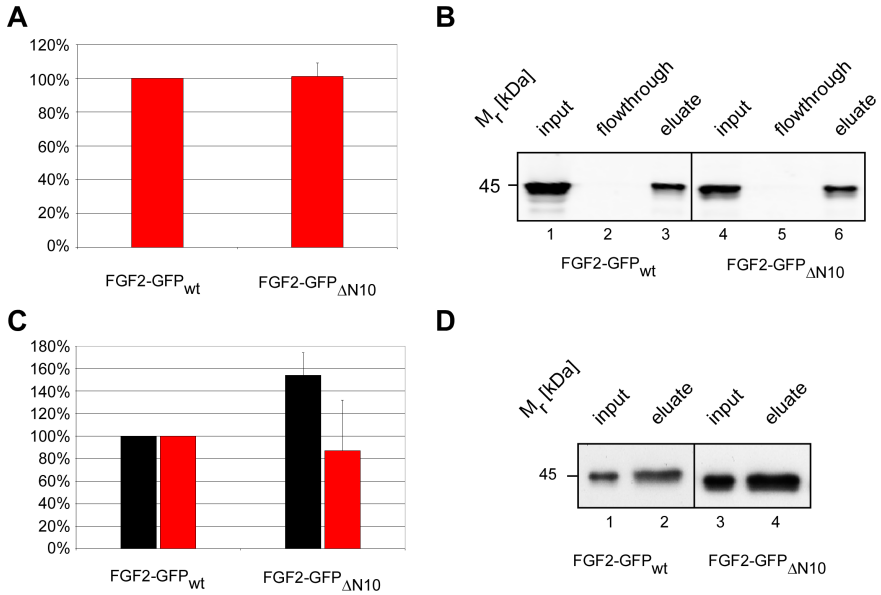

Figure 3.101: N-terminal truncations; 10 amino acids form the N-terminus deleted **A** FACS analysis of cell free supernatant bound to the surface of $CHO_{MCAT/TAM2}$ cells. Cell surface signal of FGF2-GFPwt was set to 100%. **B** Binding of cell free supernatant to heparin beads. Cell free supernatant was incubated with heparin beads. Total (input, 10%), non-bound (flowthrough, 10%) and bound material (eluate, 10%) was analyzed by SDS-PAGE and Western blotting. **C** Quantitative analysis of export employing flow cytometry. Expression level (black bars) and secreted protein detected on the cell surface (red bars) is shown. FGF2-GFPwt was set to 100%. **D** Biotinylation assay. Cell surface proteins were labelled with a membrane-impermeable biotin reagent. After cell lysis biotinylated and non-biotinylated proteins were separated by streptavidin beads. Total material (input, 5%) and the biotinylated fraction (eluate, 50%) were analyzed by SDS-PAGE and Western blotting. All results shown represent an average of at least 3 different experiments. For further details see „Material and Methods“ and explanation of assays in chapter 3.3.2. To summarize the obtained data, this truncation does not differ from observations made for wild-type FGF2-GFP.

As demonstrated in figure 3.101, the affinities of ΔN-10-FGF2-GFP to heparan sulfate proteoglycans *in vivo* (panel A) and to heparin *in vitro* (panel B) was comparable to $FGF2\text{-}GFP_{wt}$ heparin affinity. As shown by flow cytometry, the expression level of the truncated fusion protein was enhanced to about 150 % as compared to wild-type FGF2-GFP. The signal for the secreted truncated version of the fusion protein bound to the cell surface was comparable to the amount of secreted cell surface associated $FGF2\text{-}GFP_{wt}$. (panel C). The biotinylation assay showed that the secretion efficiency is not reduced, since the ratio of fusion protein expression to secretion remains constant in comparison to $FGF2\text{-}GFP_{wt}$ cells. The combined data obtained for this mutant demonstrate that ΔN-20-FGF2-GFP is not deficient in secretion or impaired in heparin binding and does not show a phenotype which is different from $FGF2\text{-}GFP_{wt}$ cells.

Truncation ΔN-20-FGF2-GFP lacks the N-terminal 20 amino acids.

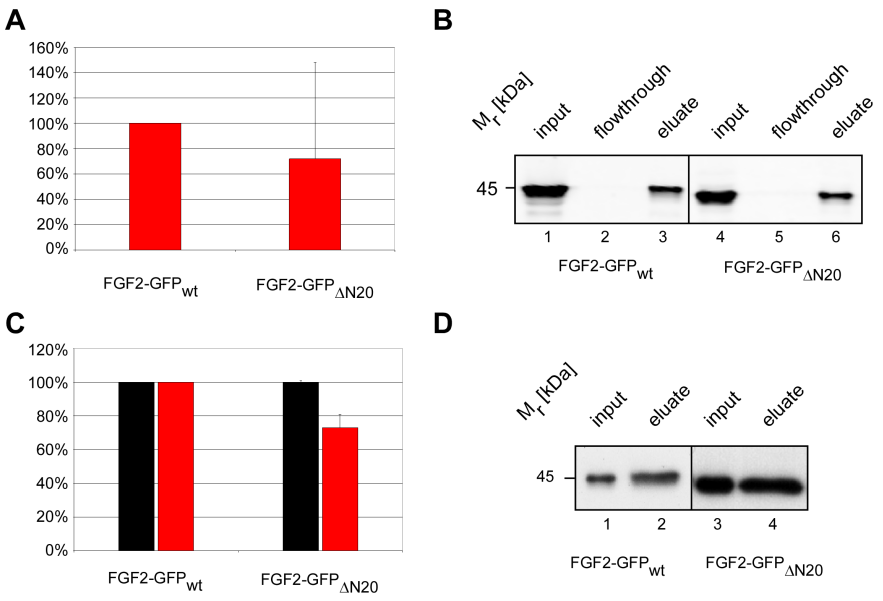

Figure 3.102: N-terminal Truncations; 20 amino acids form the N-terminus deleted **A** FACS analysis of cell free supernatant bound to the surface of $CHO_{MCAT/TAM2}$ cells. Cell surface signal of FGF2-GFPwt was set to 100%. **B** Binding of cell free supernatant to heparin beads. Cell free supernatant was incubated with heparin beads. Total (input, 10%), non-bound (flowthrough, 10%) and bound material (eluate, 10%) was analyzed by SDS-PAGE and Western blotting. **C** Quantitative analysis of export employing flow cytometry. Expression level (black bars) and secreted protein detected on the cell surface (red bars) is shown. FGF2-GFPwt was set to 100%. **D** Biotinylation assay. Cell surface proteins were labelled with a membrane-impermeable biotin reagent. After cell lysis biotinylated and non-biotinylated proteins were separated by streptavidin beads. Total material (input, 5%) and the biotinylated fraction (eluate, 50%) were analyzed by SDS-PAGE and Western blotting. All results shown represent an average of at least 3 different experiments. For further details see „Material and Methods“ and explanation of assays in chapter 3.3.2. To summarize the obtained data, this truncation does not alter from observations made for wild-type FGF2-GFP.

As demonstrated in figure 3.102, the affinities of ΔN-20-FGF2-GFP to heparan sulfate proteoglycans *in vivo* (panel A) and to heparin *in vitro* (panel B) was comparable to $FGF2\text{-}GFP_{wt}$ heparin affinity. As detected by flow cytometry (panel C), both the expression level and the cell surface staining of the truncated version of FGF2-GFP did not vary from wild-type level. This result was confirmed by the biotinylation assay (panel D). The combined data obtained for this mutant demonstrate that ΔN-20-FGF2-GFP is not deficient in secretion or impaired in heparin binding and does not show a phenotype which is different from $FGF2\text{-}GFP_{wt}$ cells.

Truncation ΔN-30-FGF2-GFP lacks the N-terminal 30 amino acids.

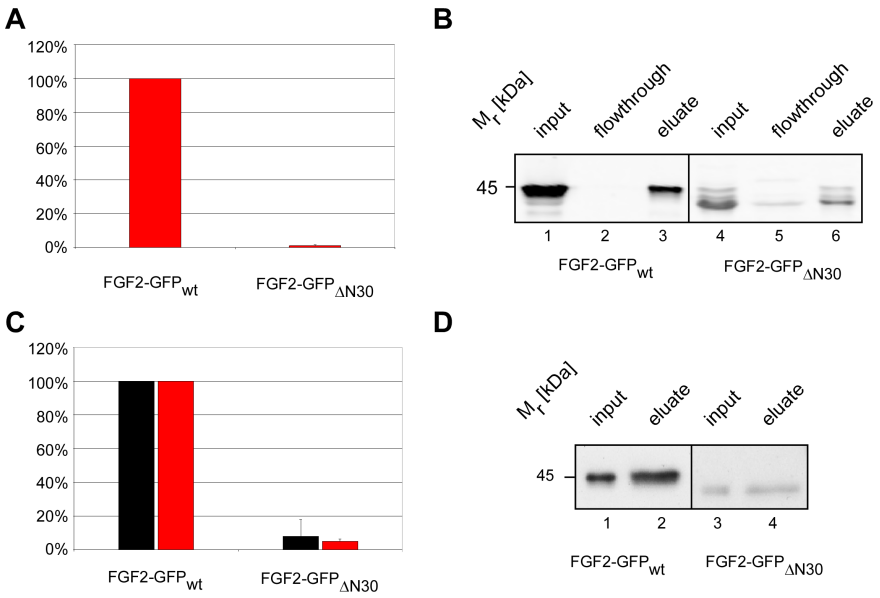

Figure 3.103: N-terminal Truncations;30 amino acids form the N-terminus deleted **A** FACS analysis of cell free supernatant bound to the surface of $CHO_{MCAT/TAM2}$ cells. Cell surface signal of FGF2-GFPwt was set to 100%. **B** Binding of cell free supernatant to heparin beads. Cell free supernatant was incubated with heparin beads. Total (input, 10%), non-bound (flowthrough, 10%) and bound material (eluate, 10%) was analyzed by SDS-PAGE and Western blotting. **C** Quantitative analysis of export employing flow cytometry. Expression level (black bars) and secreted protein detected on the cell surface (red bars) is shown. FGF2-GFPwt was set to 100%. **D** Biotinylation assay. Cell surface proteins were labelled with a membrane-impermeable biotin reagent. After cell lysis biotinylated and non-biotinylated proteins were separated by streptavidin beads. Total material (input, 5%) and the biotinylated fraction (eluate, 50%) were analyzed by SDS-PAGE and Western blotting. All results shown represent an average of at least 3 different experiments. For further details see „Material and Methods“ and explanation of assays in chapter 3.3.2. To summarize the obtained data, this truncation shows a total loss of binding in vivo and in vitro. Additionally, the expression level is significantly reduced compared to $FGF2\text{-}GFP_{wt}$.

As demonstrated in figure 3.103, the affinities of ΔN-30-FGF2-GFP to heparan sulfate proteoglycans *in vivo* (panel A) and to heparin *in vitro* (panel B) was lost by truncating 30 N-terminal amino acids. Moreover, as detected by flow cytometry (panel C), both the expression level and the cell surface staining of the truncated version of FGF2-GFP were reduced to less than 10%. This result was confirmed by the biotinylation assay (panel D). The combined data obtained for this mutant demonstrate that ΔN-30-FGF2-GFP is the binding to heparin or heparan sulfate proteoglycans is strongly impaired and that its expression is heavily reduced.

Truncation ΔN-40-FGF2-GFP lacks the N-terminal 40 amino acids.

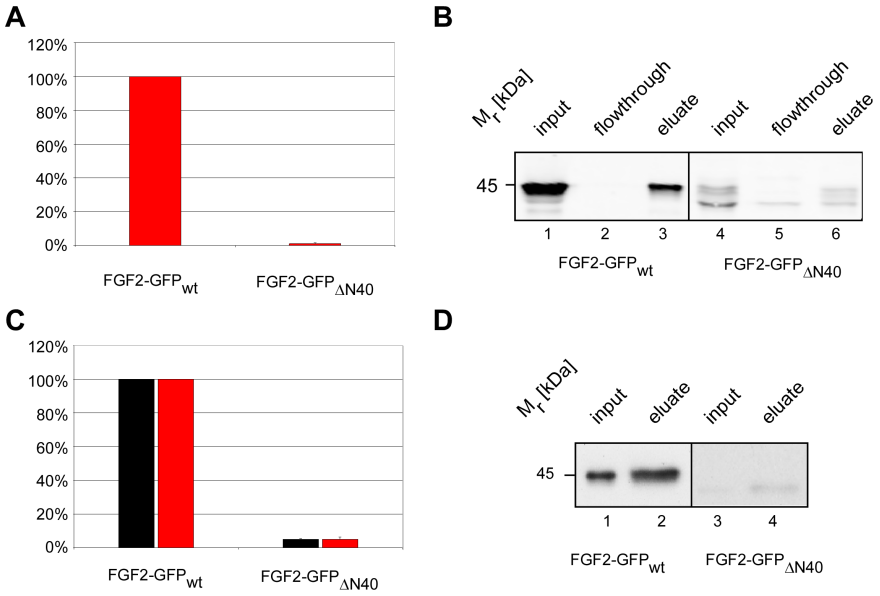

Figure 3.104: N-terminal Truncations; 40 amino acids form the N-terminus deleted **A** FACS analysis of cell free supernatant bound to the surface of CHO $CHO_{MCAT/TAM2}$ cells. Cell surface signal of FGF2-GFPwt was set to 100%. **B** Binding of cell free supernatant to heparin beads. Cell free supernatant was incubated with heparin beads. Total (input, 10%), non-bound (flowthrough, 10%) and bound material (eluate, 10%) was analyzed by SDS-PAGE and Western blotting. **C** Quantitative analysis of export employing flow cytometry. Expression level (black bars) and secreted protein detected on the cell surface (red bars) is shown. FGF2-GFPwt was set to 100%. **D** Biotinylation assay. Cell surface proteins were labelled with a membrane-impermeable biotin reagent. After cell lysis biotinylated and non-biotinylated proteins were separated by streptavidin beads. Total material (input, 5%) and the biotinylated fraction (eluate, 50%) were analyzed by SDS-PAGE and Western blotting. All results shown represent an average of at least 3 different experiments. For further details see „Material and Methods“ and explanation of assays in chapter 3.3.2. To summarize the obtained data, this truncation shows a total loss of binding in vivo and in vitro. Additionally, the expression level is significantly reduced compared to $FGF2\text{-}GFP_{wt}$.

As demonstrated in figure 3.104, the affinities of ΔN-40-FGF2-GFP to heparan sulfate proteoglycans *in vivo* (panel A) and to heparin *in vitro* (panel B) was lost by truncating 40 N-terminal amino acids. Moreover, as detected by flow cytometry (panel C), both the expression level and the cell surface staining of the truncated version of FGF2-GFP were reduced to less than 10%. This result was confirmed by the biotinylation assay (panel D). The combined data obtained for this mutant demonstrate that ΔN-40-FGF2-GFP is the binding to heparin or heparan sulfate proteoglycans is strongly impaired and that its expression is heavily reduced.

Truncation ΔN-50-FGF2-GFP lacks the N-terminal 50 amino acids.

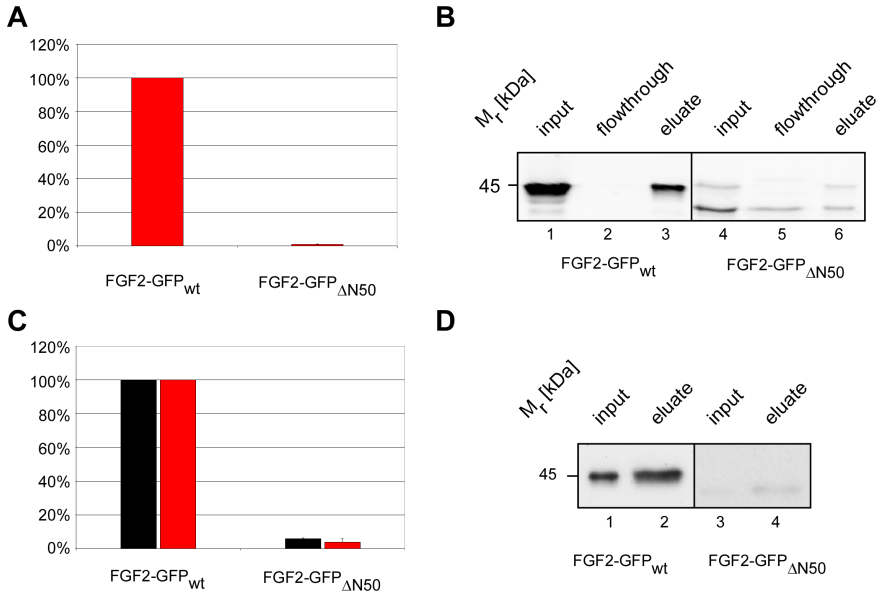

Figure 3.105: N-terminal Truncations; 50 amino acids form the N-terminus deleted **A** FACS analysis of cell free supernatant bound to the surface of $CHO_{MCAT/TAM2}$ cells. Cell surface signal of FGF2-GFPwt was set to 100%. **B** Binding of cell free supernatant to heparin beads. Cell free supernatant was incubated with heparin beads. Total (input, 10%), non-bound (flowthrough, 10%) and bound material (eluate, 10%) was analyzed by SDS-PAGE and Western blotting. **C** Quantitative analysis of export employing flow cytometry. Expression level (black bars) and secreted protein detected on the cell surface (red bars) is shown. FGF2-GFPwt was set to 100%. **D** Biotinylation assay. Cell surface proteins were labelled with a membrane-impermeable biotin reagent. After cell lysis biotinylated and non-biotinylated proteins were separated by streptavidin beads. Total material (input, 5%) and the biotinylated fraction (eluate, 50%) were analyzed by SDS-PAGE and Western blotting. All results shown represent an average of at least 3 different experiments. For further details see „Material and Methods“ and explanation of assays in chapter 3.3.2. To summarize the obtained data, this truncation shows a total loss of binding in vivo and in vitro. Additionally, the expression level is significantly reduced compared to $FGF2\text{-}GFP_{wt}$.

As demonstrated in figure 3.105, the affinities of ΔN-50-FGF2-GFP to heparan sulfate proteoglycans *in vivo* (panel A) and to heparin *in vitro* (panel B) was lost by truncating 50 N-terminal amino acids. Moreover, as detected by flow cytometry (panel C), both the expression level and the cell surface staining of the truncated version of FGF2-GFP were reduced to less than 10%. This result was confirmed by the biotinylation assay (panel D). The combined data obtained for this mutant demonstrate that ΔN-50-FGF2-GFP is the binding to heparin or heparan sulfate proteoglycans is strongly impaired and that its expression is heavily reduced.

The data obtained allows the classification of truncations with regard to export efficiency of their fusion protein, stability of the fusion protein and its binding affinity to heparin and to heparan sulfate proteoglycans.

Mutant	Classification
ΔN10	No Phenotype
ΔN20	No Phenotype
ΔN30	Instable Protein / Impaired in binding
ΔN40	Instable Protein / Impaired in binding
ΔN50	Instable Protein / Impaired in binding

Table 3.6: Overview of classifications mad for truncations

The first 20 amino acids, featuring the flexible region of FGF2, did not have any impact on export efficiency of FGF2. Deleting more than 20 amino acids from the N-terminus led to a reduced expression level of the fusion protein, as indicated by the low signal for GFP-fluorescence observed in the FACS analysis, suggesting an instable fusion protein which might be incorrectly folded and therefore rapidly degraded or synthesized with lower translation rates as FGF2-GFP_{wt}. Additionally, the truncated versions of FGF2-GPF with more than 20 deleted residues showed an impaired ability to bind to CHO cells *in vivo* and to heparin *in vitro*.

3.3.5.2 *Functional analysis of FGF2 mutants with C-terminal Truncations*

FGF2 binding to heparin is mediated by amino acids distributed throughout the protein (Wong and Burgess, 1998). Strikingly, a heparin binding cluster of 10 amino acids (position 128-138) (Li et al., 1994; Ogura et al., 1999) is found to be present at the C-terminus. It has been reported that a basic cluster around the amino acid asparagine at position 102 might mediate binding to heparin as well (Faham et al., 1996). Therefore, FGF2 was systematically truncated from the C-terminus in steps of 10 amino acids up to a deletion of 119 amino acids.

Mutant	Truncation
C_{wt}	Serves as wt control
$C_{1\text{-}146}$	9 aa form C-terminus deleted
$C_{1\text{-}136}$	19 aa form C-terminus deleted
$C_{1\text{-}126}$	29 aa form C-terminus deleted
$C_{1\text{-}116}$	39 aa form C-terminus deleted
$C_{1\text{-}106}$	49 aa form C-terminus deleted
$C_{1\text{-}96}$	59 aa form C-terminus deleted
$C_{1\text{-}86}$	69 aa form C-terminus deleted
$C_{1\text{-}66}$	89 aa form C-terminus deleted
$C_{1\text{-}56}$	99 aa form C-terminus deleted
$C_{1\text{-}46}$	109 aa form C-terminus deleted
$C_{1\text{-}36}$	119 aa form C-terminus deleted

Table 3.7: overview for C-terminal truncations

The cells were analyzed regarding export efficiency, fusion protein stability, binding to heparin *in vitro* and to heparan sulfate proteoglycans *in vivo*.

C_{wt} – wild-type control

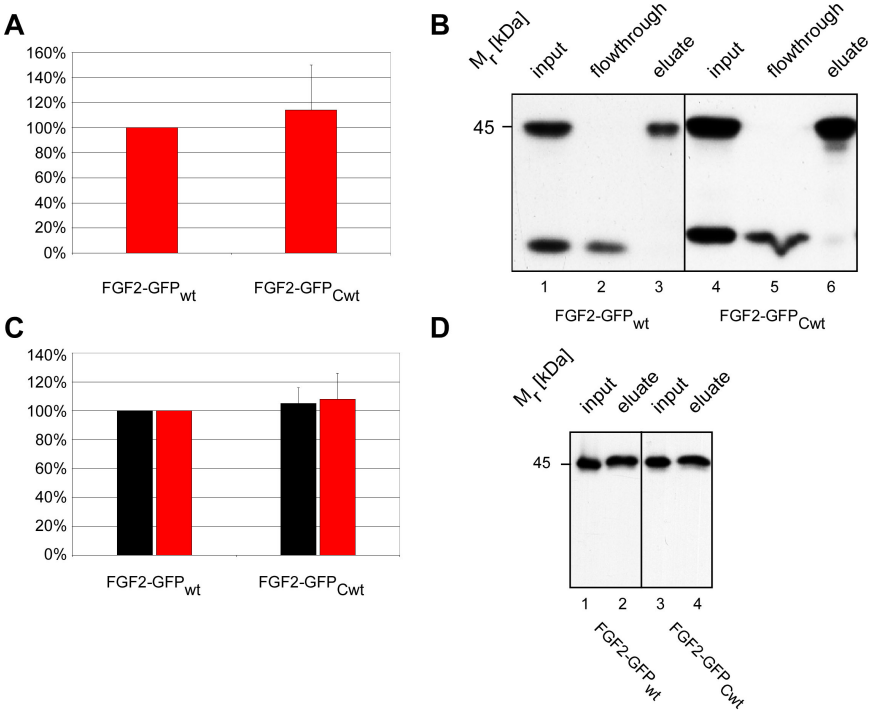

Figure 3.106: C-terminal Truncations; 2 amino acids as linker between FGF2 and GFP; serves as wt-control **A** FACS analysis of cell free supernatant bound to the surface of $CHO_{MCAT/TAM2}$ cells. Cell surface signal of FGF2-GFPwt was set to 100%. **B** Binding of cell free supernatant to heparin beads. Cell free supernatant was incubated with heparin beads. Total (input, 10%), non-bound (flowthrough, 10%) and bound material (eluate, 10%) was analyzed by SDS-PAGE and Western blotting. **C** Quantitative analysis of export employing flow cytometry. Expression level (black bars) and secreted protein detected on the cell surface (red bars) is shown. FGF2-GFPwt was set to 100%. **D** Biotinylation assay. Cell surface proteins were labelled with a membrane-impermeable biotin reagent. After cell lysis biotinylated and non-biotinylated proteins were separated by streptavidin beads. Total material (input, 5%) and the biotinylated fraction (eluate, 50%) were analyzed by SDS-PAGE and Western blotting. All results shown represent an average of at least 3 different experiments. For further details see „Material and Methods“ and explanation of assays in chapter 3.3.2. To summarize the obtained data, this truncation does not alter from observations made for wild-type FGF2-GFP.

The addition of two amino acids as a linker between FGF2-GFP did not influence unconventional secretion and binding to heparin and CHO cells as compared to wild-type FGF2-GFP. Therefore, this clone C_{wt} was used as a positive control for the analysis of all C-terminal truncations.

$C_{1\text{-}146}$ – Deletion of 9 amino acids from the C-terminus

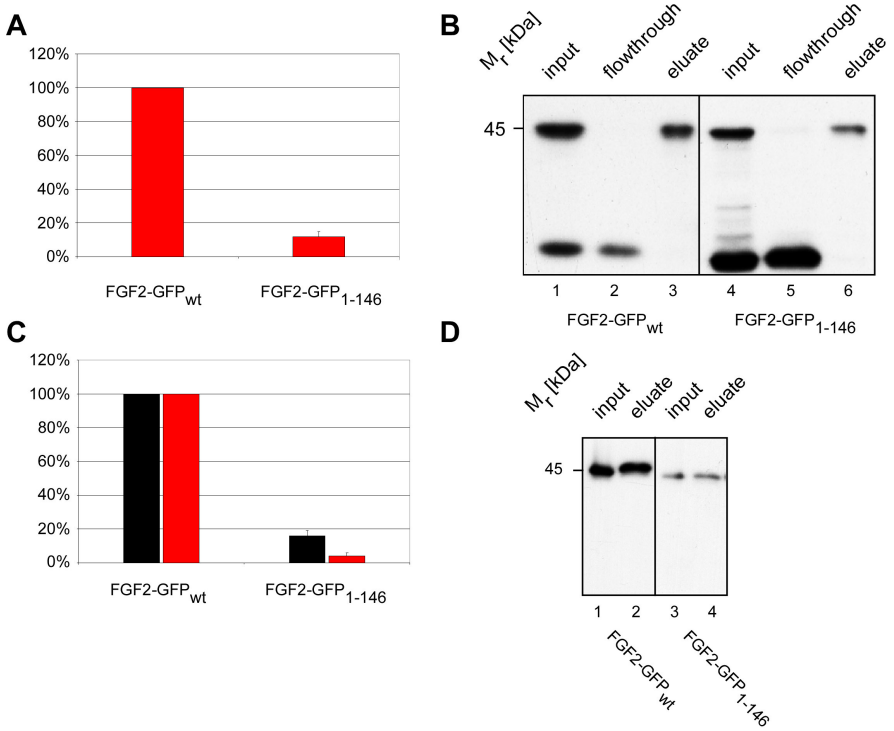

Figure 3.107: C-terminal Truncations; 9 amino acids form the C-terminus deleted **A** FACS analysis of cell free supernatant bound to the surface of $CHO_{MCAT/TAM2}$ cells. Cell surface signal of FGF2-GFPwt was set to 100%. **B** Binding of cell free supernatant to heparin beads. Cell free supernatant was incubated with heparin beads. Total (input, 10%), non-bound (flowthrough, 10%) and bound material (eluate, 10%) was analyzed by SDS-PAGE and Western blotting. **C** Quantitative analysis of export employing flow cytometry. Expression level (black bars) and secreted protein detected on the cell surface (red bars) is shown. FGF2-GFPwt was set to 100%. **D** Biotinylation assay. Cell surface proteins were labelled with a membrane-impermeable biotin reagent. After cell lysis biotinylated and non-biotinylated proteins were separated by streptavidin beads. Total material (input, 5%) and the biotinylated fraction (eluate, 50%) were analyzed by SDS-PAGE and Western blotting. All results shown represent an average of at least 3 different experiments. For further details see „Material and Methods“ and explanation of assays in chapter 3.3.2. To summarize the obtained data, this truncation shows a binding deficiency in vivo. In contrast, the truncated protein binds in vitro quantitatively to heparin beads. The expression level is significantly reduced, indicating rapid degradation of the protein.

Deleting 9 amino acids from the C-terminus led to a significant reduction of the ability to bind to HSPGs present on $CHO_{MCAT/TAM2}$ cells. In contrast, binding to heparin beads *in vitro* was not impaired. The expression level of the truncated protein was significantly reduced, indicating a rapid degradation in the cytoplasm or lowered translation rates. Extracellular protein bound to the plasma membrane was not detectable by FACS analysis due to reduced amount of fusion protein present in the cytoplasm. The biotinylation of cell surface protein showed minor amounts of fusion protein bound to the cell surface as it could be eluted from streptavidin beads using SDS-containing sample buffer.

$C_{1\text{-}136}$ – Deletion of 19 amino acids from the C-terminus

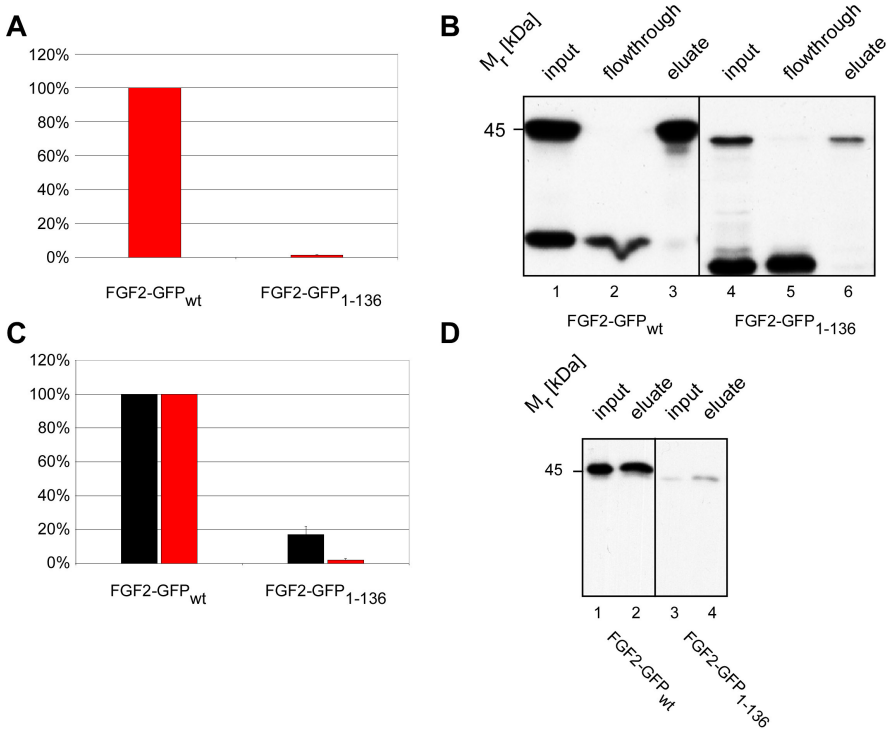

Figure 3.108: C-terminal Truncations; 19 amino acids form the C-terminus deleted **A** FACS analysis of cell free supernatant bound to the surface of $CHO_{MCAT/TAM2}$ cells. Cell surface signal of FGF2-GFPwt was set to 100%. **B** Binding of cell free supernatant to heparin beads. Cell free supernatant was incubated with heparin beads. Total (input, 10%), non-bound (flowthrough, 10%) and bound material (eluate, 10%) was analyzed by SDS-PAGE and Western blotting. **C** Quantitative analysis of export employing flow cytometry. Expression level (black bars) and secreted protein detected on the cell surface (red bars) is shown. FGF2-GFPwt was set to 100%. **D** Biotinylation assay. Cell surface proteins were labelled with a membrane-impermeable biotin reagent. After cell lysis biotinylated and non-biotinylated proteins were separated by streptavidin beads. Total material (input, 5%) and the biotinylated fraction (eluate, 50%) were analyzed by SDS-PAGE and Western blotting. All results shown represent an average of at least 3 different experiments. For further details see „Material and Methods“ and explanation of assays in chapter 3.3.2. To summarize the obtained data, this truncation shows a binding deficiency in vivo. In contrast, the truncated protein binds in vitro quantitatively to heparin beads. The expression level is significantly reduced, indicating rapid degradation of the protein.

Deleting 19 amino acids from the C-terminus led to a significant reduction of the ability to bind to HSPGs present on $CHO_{MCAT/TAM2}$ cells. In contrast, binding to heparin beads *in vitro* was not impaired. The expression level of the truncated protein was significantly reduced, indicating a rapid degradation in the cytoplasm or lowered translation rates. Extracellular protein bound to the plasma membrane was not detectable by FACS analysis due to reduced amount of fusion protein present in the cytoplasm. The biotinylation of cell surface protein showed minor amounts of fusion protein bound to the cell surface as it could be eluted from streptavidin beads using SDS-containing sample buffer.

$C_{1\text{-}126}$ – Deletion of 29 amino acids from the C-terminus

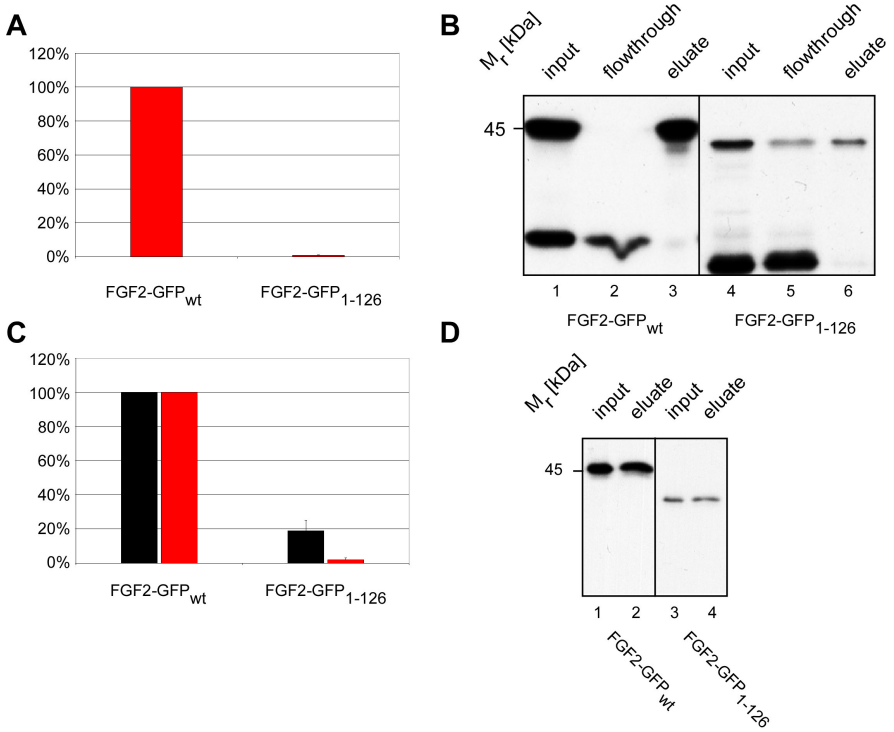

Figure 3.109: C-terminal Truncations; 29 amino acids form the C-terminus deleted **A** FACS analysis of cell free supernatant bound to the surface of $CHO_{MCAT/TAM2}$ cells. Cell surface signal of FGF2-GFPwt was set to 100%. **B** Binding of cell free supernatant to heparin beads. Cell free supernatant was incubated with heparin beads. Total (input, 10%), non-bound (flowthrough, 10%) and bound material (eluate, 10%) was analyzed by SDS-PAGE and Western blotting. **C** Quantitative analysis of export employing flow cytometry. Expression level (black bars) and secreted protein detected on the cell surface (red bars) is shown. FGF2-GFPwt was set to 100%. **D** Biotinylation assay. Cell surface proteins were labelled with a membrane-impermeable biotin reagent. After cell lysis biotinylated and non-biotinylated proteins were separated by streptavidin beads. Total material (input, 5%) and the biotinylated fraction (eluate, 50%) were analyzed by SDS-PAGE and Western blotting. All results shown represent an average of at least 3 different experiments. For further details see „Material and Methods“ and explanation of assays in chapter 3.3.2. To summarize the obtained data, this truncation shows a binding deficiency in vivo. The protein binds in vitro to heparin beads, but not as quantitative as truncations described earlier. The expression level is significantly reduced.

Deleting 29 amino acids from the C-terminus led to a significant reduction of the ability to bind to HSPGs present on $CHO_{MCAT/TAM2}$ cells. This fusion protein showed, in contrast to less truncated versions of FGF2-GFP, an impaired affinity to heparin. Only 60% of the input fraction was eluted from heparin beads, whereas 40% were present in the non-bound flowthrough fraction. The expression level of the truncated protein was significantly reduced, indicating a rapid degradation in the cytoplasm. Extracellular protein bound to the plasma membrane was not detectable by FACS analysis due to reduced amount of fusion protein present in the cytoplasm. The biotinylation of cell surface protein showed minor amounts of fusion protein bound to the cell surface as it could be eluted from streptavidin beads using SDS-containing sample buffer.

$C_{1\text{-}116}$ – Deletion of 39 amino acids from the C-terminus

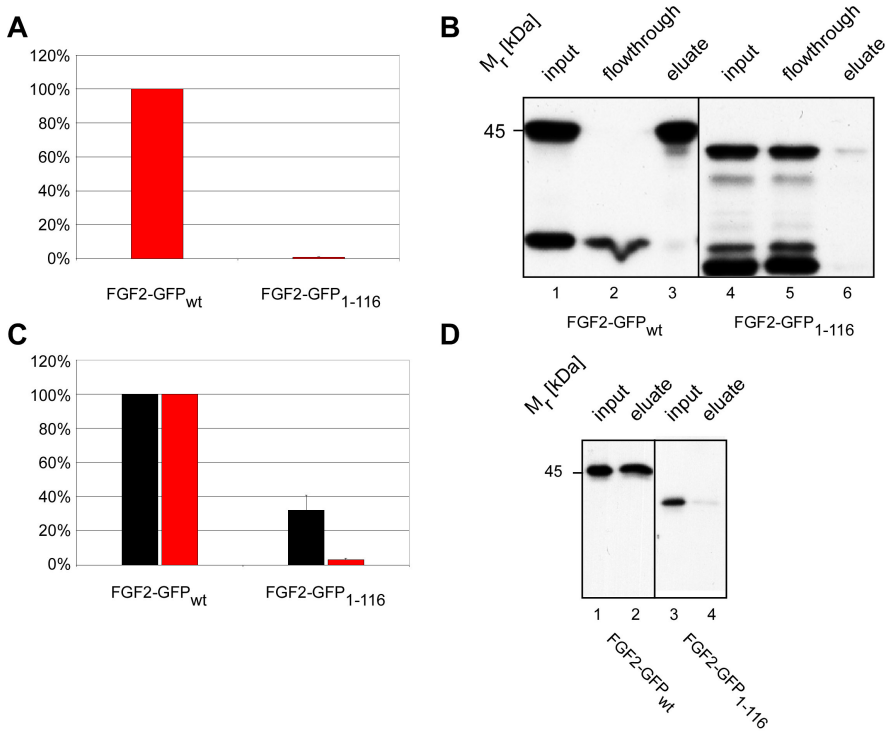

Figure 3.110: C-terminal Truncations; 39 amino acids form the C-terminus deleted **A** FACS analysis of cell free supernatant bound to the surface of $CHO_{MCAT/TAM2}$ cells. Cell surface signal of FGF2-GFPwt was set to 100%. **B** Binding of cell free supernatant to heparin beads. Cell free supernatant was incubated with heparin beads. Total (input, 10%), non-bound (flowthrough, 10%) and bound material (eluate, 10%) was analyzed by SDS-PAGE and Western blotting. **C** Quantitative analysis of export employing flow cytometry. Expression level (black bars) and secreted protein detected on the cell surface (red bars) is shown. FGF2-GFPwt was set to 100%. **D** Biotinylation assay. Cell surface proteins were labelled with a membrane-impermeable biotin reagent. After cell lysis biotinylated and non-biotinylated proteins were separated by streptavidin beads. Total material (input, 5%) and the biotinylated fraction (eluate, 50%) were analyzed by SDS-PAGE and Western blotting. All results shown represent an average of at least 3 different experiments. For further details see „Material and Methods“ and explanation of assays in chapter 3.3.2. To summarize the obtained data, this truncation shows a binding deficiency in vivo. The protein binds in vitro marginally to heparin beads, the majority of the protein is not able to bind in vitro. The expression level is significantly reduced.

Deleting 39 amino acids from the C-terminus led to a significant reduction of the ability to bind to HSPGs present on $CHO_{MCAT/TAM2}$ cells. This fusion protein showed, in contrast to less truncated versions of FGF2-GFP, an impaired affinity to heparin. Only minor amount of fusion protein was found in the input fraction, whereas a vast majority was found in the non-bound flowthrough fraction. The expression level of the truncated protein was significantly reduced, indicating a rapid degradation in the cytoplasm. Extracellular protein bound to the plasma membrane was not detectable by FACS analysis due to reduced amount of fusion protein present in the cytoplasm. The biotinylation of cell surface protein showed almost no fusion protein bound to the cell surface as it could be eluted only in minor amounts from streptavidin beads using SDS-containing sample buffer.

C_{1-106} – Deletion of 49 amino acids from the C-terminus

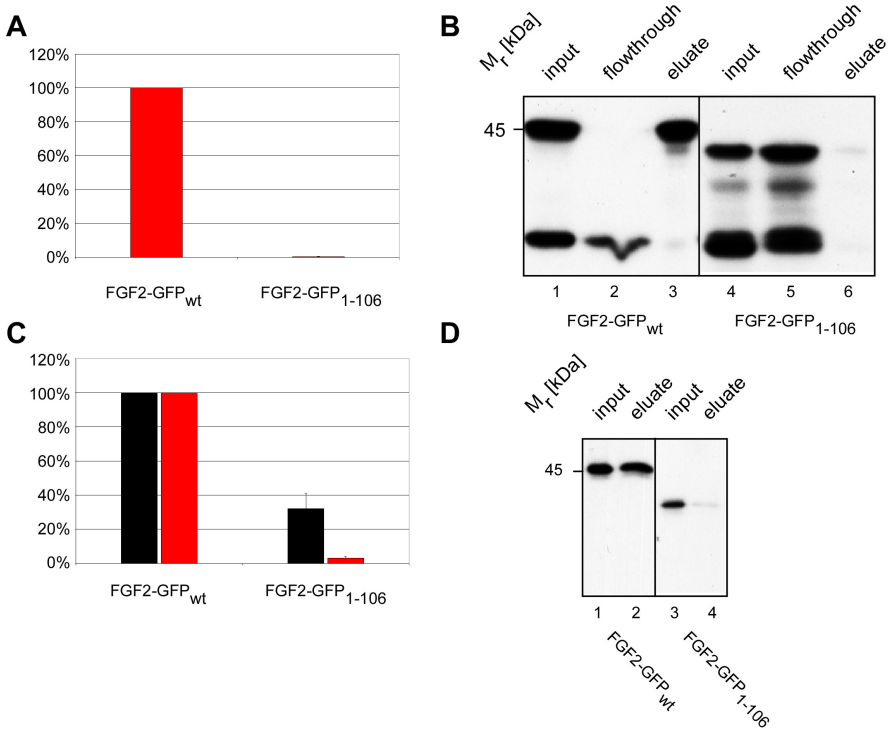

Figure 3.111: C-terminal Truncations; 49 amino acids form the C-terminus deleted **A** FACS analysis of cell free supernatant bound to the surface of $CHO_{MCAT/TAM2}$ cells. Cell surface signal of FGF2-GFPwt was set to 100%. **B** Binding of cell free supernatant to heparin beads. Cell free supernatant was incubated with heparin beads. Total (input, 10%), non-bound (flowthrough, 10%) and bound material (eluate, 10%) was analyzed by SDS-PAGE and Western blotting. **C** Quantitative analysis of export employing flow cytometry. Expression level (black bars) and secreted protein detected on the cell surface (red bars) is shown. FGF2-GFPwt was set to 100%. **D** Biotinylation assay. Cell surface proteins were labelled with a membrane-impermeable biotin reagent. After cell lysis biotinylated and non-biotinylated proteins were separated by streptavidin beads. Total material (input, 5%) and the biotinylated fraction (eluate, 50%) were analyzed by SDS-PAGE and Western blotting. All results shown represent an average of at least 3 different experiments. For further details see „Material and Methods“ and explanation of assays in chapter 3.3.2. To summarize the obtained data, this truncation shows a binding deficiency in vivo. The protein binds in vitro marginally to heparin beads, the majority of the protein is not able to bind in vitro. The expression level is significantly reduced.

Deleting 49 amino acids from the C-terminus led to a significant reduction of the ability to bind to HSPGs present on $CHO_{MCAT/TAM2}$ cells. This fusion protein showed, in contrast to less truncated versions of FGF2-GFP, an impaired affinity to heparin. Only minor amount of fusion protein was found in the input fraction, whereas a vast majority was found in the non-bound flowthrough fraction. The affinity of FGF2 to heparin is reduced when compared to C_{1-116}.The expression level of the truncated protein was significantly reduced, indicating a rapid degradation in the cytoplasm. Extracellular protein bound to the plasma membrane was not detectable by FACS analysis due to the reduced amount of fusion protein present in the cytoplasm. The biotinylation of cell surface protein showed almost no fusion protein bound to the cell surface as it could be eluted only in minor amounts from streptavidin beads using SDS-containing sample buffer.

$C_{1\text{-}96}$ – Deletion of 59 amino acids from the C-terminus

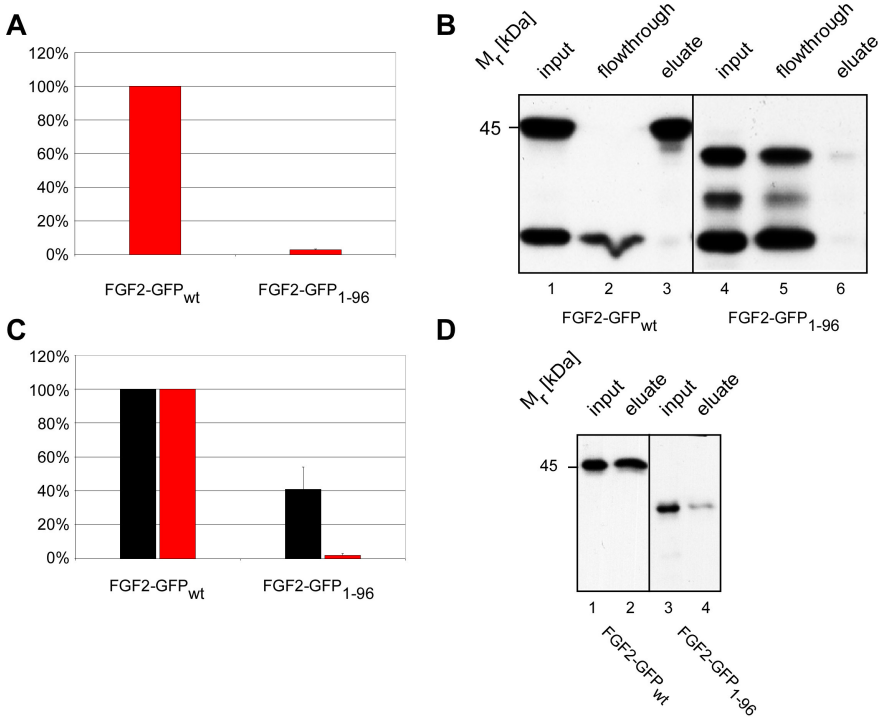

Figure 3.112: C-terminal Truncations; 59 amino acids form the C-terminus deleted **A** FACS analysis of cell free supernatant bound to the surface of $CHO_{MCAT/TAM2}$ cells. Cell surface signal of FGF2-GFPwt was set to 100%. **B** Binding of cell free supernatant to heparin beads. Cell free supernatant was incubated with heparin beads. Total (input, 10%), non-bound (flowthrough, 10%) and bound material (eluate, 10%) was analyzed by SDS-PAGE and Western blotting. **C** Quantitative analysis of export employing flow cytometry. Expression level (black bars) and secreted protein detected on the cell surface (red bars) is shown. FGF2-GFPwt was set to 100%. **D** Biotinylation assay. Cell surface proteins were labelled with a membrane-impermeable biotin reagent. After cell lysis biotinylated and non-biotinylated proteins were separated by streptavidin beads. Total material (input, 5%) and the biotinylated fraction (eluate, 50%) were analyzed by SDS-PAGE and Western blotting. All results shown represent an average of at least 3 different experiments. For further details see „Material and Methods“ and explanation of assays in chapter 3.3.2. To summarize the obtained data, this truncation shows a binding deficiency in vivo. The protein binds in vitro marginally to heparin beads, the majority of the protein is not able to bind in vitro. The expression level is significantly reduced.

Deleting 59 amino acids from the C-terminus led to a significant reduction of the ability to bind to HSPGs present on $CHO_{MCAT/TAM2}$ cells. This fusion protein showed, in contrast to less truncated versions of FGF2-GFP, an impaired affinity to heparin. Only minor amount of fusion protein was found in the input fraction, whereas a vast majority was found in the non-bound flowthrough fraction. The affinity of FGF2 to heparin is reduced when compared to $C_{1\text{-}106}$.The expression level of the truncated protein was significantly reduced, indicating a rapid degradation in the cytoplasm. Extracellular protein bound to the plasma membrane was not detectable by FACS analysis due to the reduced amount of fusion protein present in the cytoplasm. The biotinylation of cell surface protein showed almost no fusion protein bound to the cell surface as it could be eluted only in minor amounts from streptavidin beads using SDS-containing sample buffer.

C_{1-86} – Deletion of 69 amino acids from the C-terminus

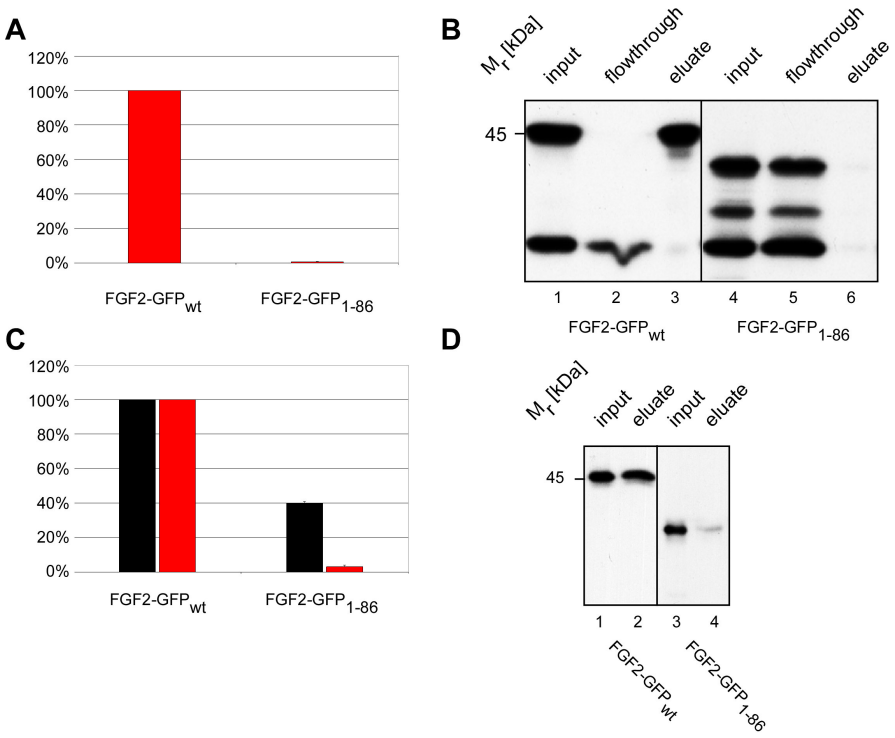

Figure 3.113: C-terminal Truncations; 69 amino acids form the C-terminus deleted **A** FACS analysis of cell free supernatant bound to the surface of $CHO_{MCAT/TAM2}$ cells. Cell surface signal of FGF2-GFPwt was set to 100%. **B** Binding of cell free supernatant to heparin beads. Cell free supernatant was incubated with heparin beads. Total (input, 10%), non-bound (flowthrough, 10%) and bound material (eluate, 10%) was analyzed by SDS-PAGE and Western blotting. **C** Quantitative analysis of export employing flow cytometry. Expression level (black bars) and secreted protein detected on the cell surface (red bars) is shown. FGF2-GFPwt was set to 100%. **D** Biotinylation assay. Cell surface proteins were labelled with a membrane-impermeable biotin reagent. After cell lysis biotinylated and non-biotinylated proteins were separated by streptavidin beads. Total material (input, 5%) and the biotinylated fraction (eluate, 50%) were analyzed by SDS-PAGE and Western blotting. All results shown represent an average of at least 3 different experiments. For further details see „Material and Methods“ and explanation of assays in chapter 3.3.2. To summarize the obtained data, this truncation shows a binding deficiency in vivo. From this point of degradation, the protein also fails to bind to heparin beads in vivo. The expression level is significantly reduced.

Deleting 69 amino acids from the C-terminus led to a significant reduction of the ability to bind to HSPGs present on $CHO_{MCAT/TAM2}$ cells. A deletion of 69 amino acids results in a total loss of the ability for FGF2-GFP to bind to heparin *in vitro*. Less truncated versions of the fusion protein were still able, although partly in minor amounts, to bind to heparin. It was not possible to detect the fusion protein in the input fraction, but truncated FGF2-GFP was found exclusively in the non-bound flowthrough fraction. The expression level of this truncated protein was significantly reduced as compared to wild-type level, indicating a rapid degradation in the cytoplasm. Extracellular protein bound to the plasma membrane was not detectable by FACS analysis due to reduced amount of fusion protein present in the cytoplasm. The biotinylation of cell surface protein showed almost no fusion protein bound to the cell surface as it could be eluted only in minor amounts from streptavidin beads using SDS-containing sample buffer.

$C_{1\text{-}66}$ – Deletion of 89 amino acids from the C-terminus

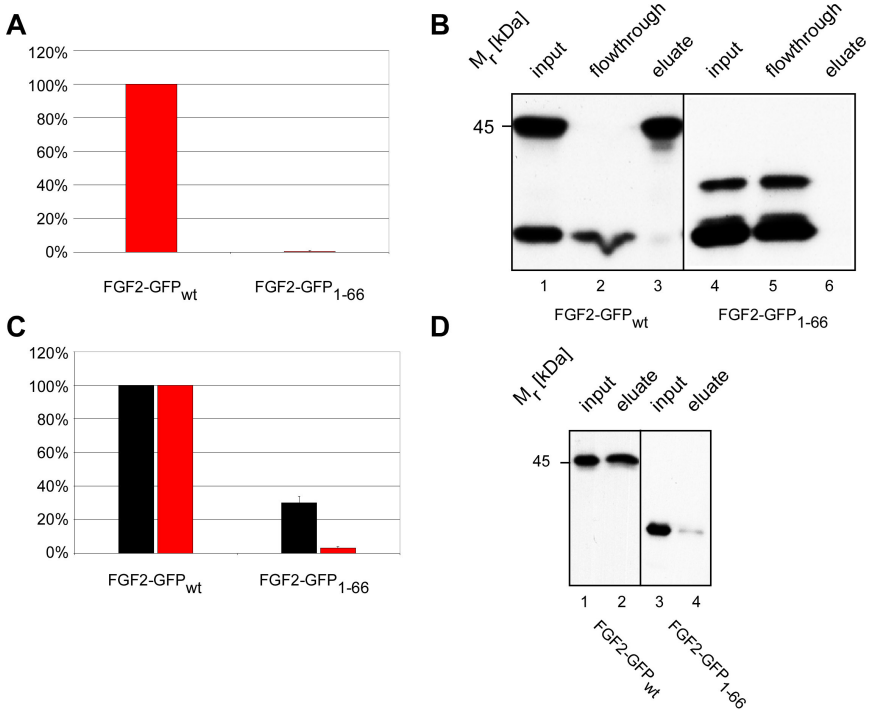

Figure 3.114: C-terminal Truncations; 89 amino acids form the C-terminus deleted **A** FACS analysis of cell free supernatant bound to the surface of $CHO_{MCAT/TAM2}$ cells. Cell surface signal of FGF2-GFPwt was set to 100%. **B** Binding of cell free supernatant to heparin beads. Cell free supernatant was incubated with heparin beads. Total (input, 10%), non-bound (flowthrough, 10%) and bound material (eluate, 10%) was analyzed by SDS-PAGE and Western blotting. **C** Quantitative analysis of export employing flow cytometry. Expression level (black bars) and secreted protein detected on the cell surface (red bars) is shown. FGF2-GFPwt was set to 100%. **D** Biotinylation assay. Cell surface proteins were labelled with a membrane-impermeable biotin reagent. After cell lysis biotinylated and non-biotinylated proteins were separated by streptavidin beads. Total material (input, 5%) and the biotinylated fraction (eluate, 50%) were analyzed by SDS-PAGE and Western blotting. All results shown represent an average of at least 3 different experiments. For further details see „Material and Methods“ and explanation of assays in chapter 3.3.2. To summarize the obtained data, this truncation shows a binding deficiency in vivo. From this point of degradation, the protein also fails to bind to heparin beads in vivo. The expression level is significantly reduced.

Deleting 89 amino acids from the C-terminus led to a significant reduction of the ability to bind to HSPGs present on $CHO_{MCAT/TAM2}$ cells. In the assay for binding of FGF2-GFP to bind to heparin *in vitro*, it was not possible to detect fusion protein in the eluate fraction, but truncated FGF2-GFP was found exclusively in the non-bound flowthrough fraction. The expression level of this truncated protein was significantly reduced as compared to wild-type level, indicating a rapid degradation in the cytoplasm. Extracellular protein bound to the plasma membrane was not detectable by FACS analysis due to reduced amount of fusion protein present in the cytoplasm. The biotinylation of cell surface protein showed almost no fusion protein bound to the cell surface as it could be eluted only in minor amounts from streptavidin beads using SDS-containing sample buffer.

C_{1-56} – Deletion of 99 amino acids from the C-terminus

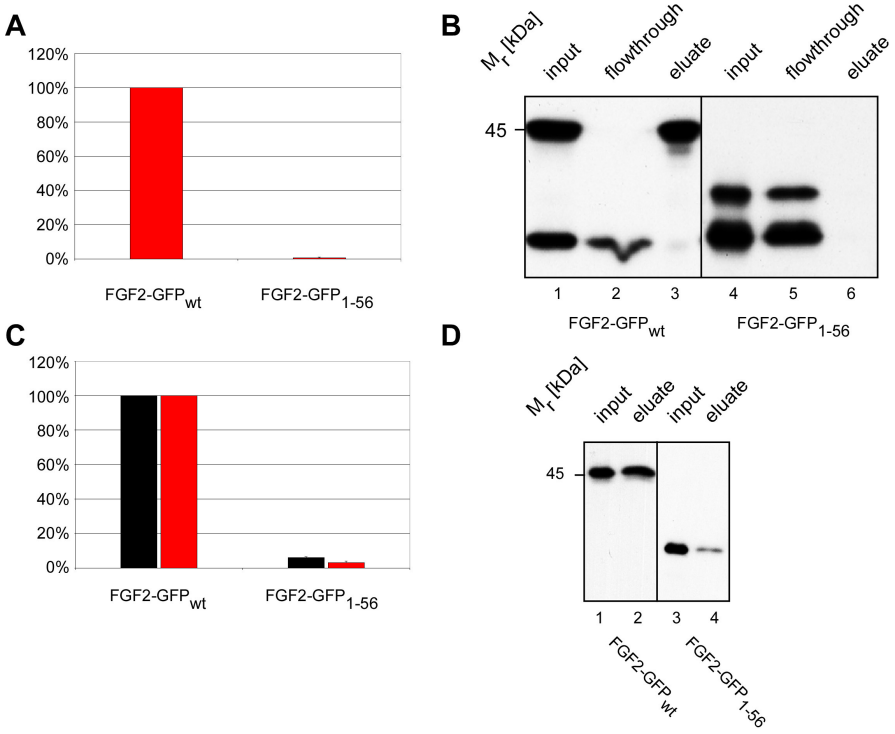

Figure 3.115: C-terminal Truncations; 99 amino acids form the C-terminus deleted **A** FACS analysis of cell free supernatant bound to the surface of $CHO_{MCAT/TAM2}$ cells. Cell surface signal of FGF2-GFPwt was set to 100%. **B** Binding of cell free supernatant to heparin beads. Cell free supernatant was incubated with heparin beads. Total (input, 10%), non-bound (flowthrough, 10%) and bound material (eluate, 10%) was analyzed by SDS-PAGE and Western blotting. **C** Quantitative analysis of export employing flow cytometry. Expression level (black bars) and secreted protein detected on the cell surface (red bars) is shown. FGF2-GFPwt was set to 100%. **D** Biotinylation assay. Cell surface proteins were labelled with a membrane-impermeable biotin reagent. After cell lysis biotinylated and non-biotinylated proteins were separated by streptavidin beads. Total material (input, 5%) and the biotinylated fraction (eluate, 50%) were analyzed by SDS-PAGE and Western blotting. All results shown represent an average of at least 3 different experiments. For further details see „Material and Methods“ and explanation of assays in chapter 3.3.2. To summarize the obtained data, this truncation shows a binding deficiency in vivo. From this point of degradation, the protein also fails to bind to heparin beads in vivo. The expression level is significantly reduced.

Deleting 99 amino acids from the C-terminus led to a significant reduction of the ability to bind to HSPGs present on $CHO_{MCAT/TAM2}$ cells. In the assay for binding of FGF2-GFP to bind to heparin *in vitro*, it was not possible to detect fusion protein in the eluate fraction, but truncated FGF2-GFP was found exclusively in the non-bound flowthrough fraction. The expression level of this truncated protein was significantly reduced as compared to wild-type level, indicating a rapid degradation in the cytoplasm. Extracellular protein bound to the plasma membrane was not detectable by FACS analysis due to reduced amount of fusion protein present in the cytoplasm. The biotinylation of cell surface protein showed almost no fusion protein bound to the cell surface as it could be eluted only in minor amounts from streptavidin beads using SDS-containing sample buffer.

C_{1-46} – Deletion of 109 amino acids from the C-terminus

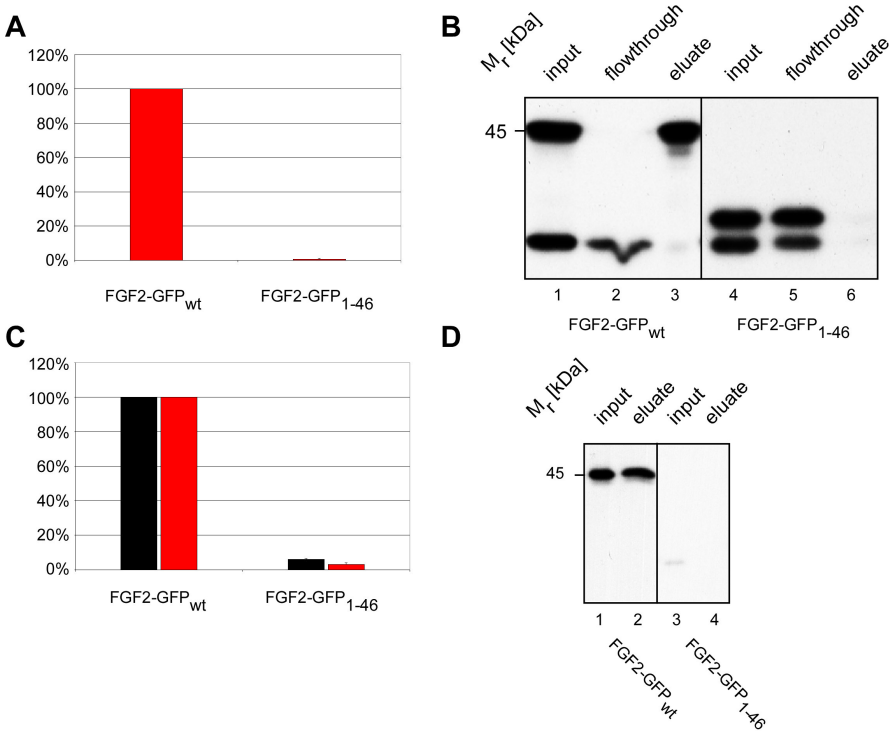

Figure 3.116: C-terminal Truncations; 109 amino acids form the C-terminus deleted **A** FACS analysis of cell free supernatant bound to the surface of $CHO_{MCAT/TAM2}$ cells. Cell surface signal of FGF2-GFPwt was set to 100%. **B** Binding of cell free supernatant to heparin beads. Cell free supernatant was incubated with heparin beads. Total (input, 10%), non-bound (flowthrough, 10%) and bound material (eluate, 10%) was analyzed by SDS-PAGE and Western blotting. **C** Quantitative analysis of export employing flow cytometry. Expression level (black bars) and secreted protein detected on the cell surface (red bars) is shown. FGF2-GFPwt was set to 100%. **D** Biotinylation assay. Cell surface proteins were labelled with a membrane-impermeable biotin reagent. After cell lysis biotinylated and non-biotinylated proteins were separated by streptavidin beads. Total material (input, 5%) and the biotinylated fraction (eluate, 50%) were analyzed by SDS-PAGE and Western blotting. All results shown represent an average of at least 3 different experiments. For further details see „Material and Methods“ and explanation of assays in chapter 3.3.2. To summarize the obtained data, this truncation shows a binding deficiency in vivo. From this point of degradation, the protein also fails to bind to heparin beads in vivo. The expression level is significantly reduced.

Deleting 109 amino acids from the C-terminus led to a significant reduction of the ability to bind to HSPGs present on $CHO_{MCAT/TAM2}$ cells. In the assay for binding of FGF2-GFP to bind to heparin *in vitro*, it was not possible to detect fusion protein in the eluate fraction, but truncated FGF2-GFP was found exclusively in the non-bound flowthrough fraction. The expression level of this truncated protein was significantly reduced as compared to wild-type level, indicating a rapid degradation in the cytoplasm. Extracellular protein bound to the plasma membrane was not detectable by FACS analysis due to reduced amount of fusion protein present in the cytoplasm. The biotinylation of cell surface protein showed almost no fusion protein bound to the cell surface as it could be eluted only in minor amounts from streptavidin beads using SDS-containing sample buffer.

C_{1-36} – Deletion of 119 amino acids from the C-terminus

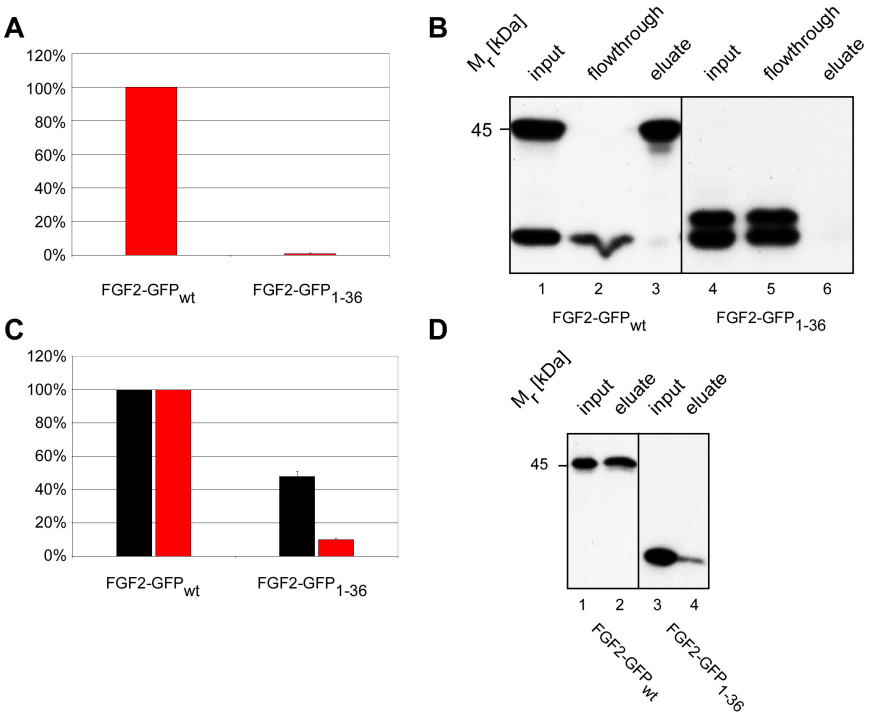

Figure 3.117: C-terminal Truncations; 119 amino acids form the C-terminus deleted **A** FACS analysis of cell free supernatant bound to the surface of $CHO_{MCAT/TAM2}$ cells. Cell surface signal of FGF2-GFPwt was set to 100%. **B** Binding of cell free supernatant to heparin beads. Cell free supernatant was incubated with heparin beads. Total (input, 10%), non-bound (flowthrough, 10%) and bound material (eluate, 10%) was analyzed by SDS-PAGE and Western blotting. **C** Quantitative analysis of export employing flow cytometry. Expression level (black bars) and secreted protein detected on the cell surface (red bars) is shown. FGF2-GFPwt was set to 100%. **D** Biotinylation assay. Cell surface proteins were labelled with a membrane-impermeable biotin reagent. After cell lysis biotinylated and non-biotinylated proteins were separated by streptavidin beads. Total material (input, 5%) and the biotinylated fraction (eluate, 50%) were analyzed by SDS-PAGE and Western blotting. All results shown represent an average of at least 3 different experiments. For further details see „Material and Methods“ and explanation of assays in chapter 3.3.2. To summarize the obtained data, this truncation shows a binding deficiency in vivo. From this point of degradation, the protein also fails to bind to heparin beads in vivo. The expression level is slightly enhanced compared to other truncations. Extracellular protein bound to the plasma membrane is not detectable via flow cytometry but in minor amounts with cell surface biotinylation.

Deleting 119 amino acids from the C-terminus led to a significant reduction of the ability to bind to HSPGs present on $CHO_{MCAT/TAM2}$ cells. In the assay for binding of FGF2-GFP to bind to heparin *in vitro*, it was not possible to detect fusion protein in the eluate fraction, but truncated FGF2-GFP was found exclusively in the non-bound flowthrough fraction. The expression level of this truncated protein was significantly reduced as compared to wild-type level, indicating a rapid degradation in the cytoplasm. Extracellular protein bound to the plasma membrane was not detectable by FACS analysis due to reduced amount of fusion protein present in the cytoplasm. The biotinylation of cell surface protein showed almost no fusion protein bound to the cell surface as it could be eluted only in minor amounts from streptavidin beads using SDS-containing sample buffer.

The results obtained by the functional characterization of FGF2 mutants with C-terminal truncation are listed in the flowing table:

Mutant	Classification
C_{wt}	Wild-type
C_{1-146}	Instable Protein / impaired *in vivo* binding
C_{1-136}	Instable Protein / impaired *in vivo* binding
C_{1-126}	Instable Protein / impaired *in vivo* and *in vitro* binding
C_{1-116}	Instable Protein / impaired *in vivo* and *in vitro* binding
C_{1-106}	Instable Protein / impaired *in vivo* and *in vitro* binding
C_{1-96}	Instable Protein / impaired *in vivo* and *in vitro* binding
C_{1-86}	Instable Protein / Binding deficient
C_{1-66}	Instable Protein / Binding deficient
C_{1-56}	Instable Protein / Binding deficient
C_{1-46}	Instable Protein / Binding deficient
C_{1-36}	Instable Protein / Binding deficient

Table 3.8: Overview of classifications made for C-terminal truncations

As a summary, the C-terminus is crucial for both stability of the protein and ability to bind to heparin and HSPGs. The wild-type control, bearing a linker of two amino acids between FGF2 and GFP, showed phenotype characteristics and is used as a positive control. All truncations characterized, showed instability of the fusion protein present in the cytoplasm. Moreover all truncated proteins were not able to bind to HSPGs present on the cell surface. In contrast, the ability to bind to heparin *in vitro* was influenced by the number of deleted amino acids. Deleting up to 19 amino acids from the C-terminus had no effect on the *in vitro* binding to heparin, but truncation of 29 amino acids led to a reduced binding affinity to heparin beads *in vitro*. Proportional to the stepwise deletion of 10 amino acids, the truncated versions of FGF2 lost their affinity to heparin *in vitro*. Expanding truncations to 69 amino acids resulted in a total loss of FGF2 affinity for heparin beads. The data collected during the analysis of C-terminal truncations showed that the C-terminus is necessary to sustain protein stability. This data indicates that binding of FGF2 to heparan sulfate proteoglycans might be a prerequisite for FGF2 secretion. Therefore it has to be elucidated if the truncations are not secreted into the media of CHO cells expressing the truncated versions of FGF2-GFP.

3.4 Characterization of FGF2-GFP mutants differing from wild-type as identified by the screening procedure

After finishing screening of all mutants generated, some of them demonstrated a noticeable difference from wild-type characteristics. The C-terminal truncations did not bind to heparan sulfate proteoglycans present on the cell surface of CHO cells and were impaired to bind to heparin. Since secretion of Galectin-1 is dependent of binding to its counter receptor (Seelenmeyer et al., 2005), it has to be analyzed if the same is true for FGF2. Therefore it has to be elucidated, if the C-terminal truncations are not secreted from CHO cells. The mutant rM 156 showed a reduced secretion of the fusion protein as analyzed by flow cytometry and cell surface biotinylation. The data obtained for binding of rM 156 to heparin and to HSPGs are controversy, because the mutant was able to bind to heparin, but not to HSPGs present on the cell surface. For the dimerization mutant 53, bearing two mutated cysteines at position 78 and 96, the secretion assays demonstrated a controversary signal for export efficiency of the fusion protein. A reduced signal for secreted fusion protein was detected as analyzed by cell surface biotinylation. In contrast, wild-type levels for secreted fusion protein were observed by flow cytometry.
Mutant rM 156 and the C-terminal truncations were analyzed in more detail as described in the following chapters.

3.4.1 Analysis of C-terminal truncations with regard to unconventional secretion

The assays used to quantify the amount of secreted FGF2-GFP detect only cell surface bound fusion protein. During the mutagenesis analysis it was shown that C-terminally truncated versions of FGF2-GFP are not able to bind to the cell surface and are thus not detectable by flow cytometry or cell surface biotinylation, even if export took place. To analyze if these mutants, deficient in binding to the cell surface are also deficient in secretion, conditioned growth medium was applied to immune-precipitation in order to detect extracellularly localized soluble fusion protein.

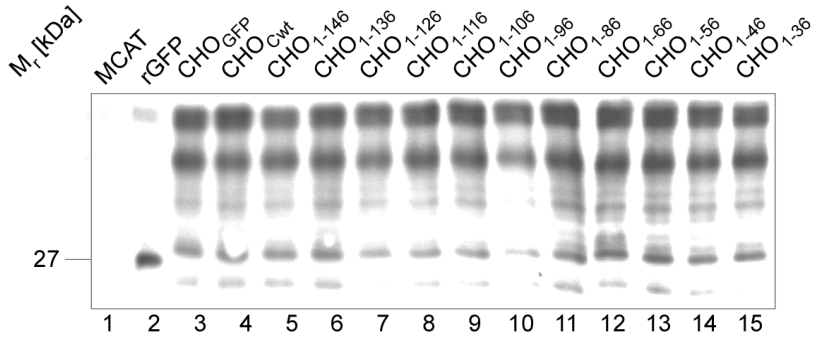

Figure 3.118: analysis of export employing medium immunoprecipitation. The fusion proteins indicated were expressed in CHO cells (lines 3-15) for 48 h at 37°C (6-well plates; 70% confluency). $CHO_{MCAT/TAM2}$ cells without and with addition of recombinant GFP to the medium were used as a control (line 1 and 2). The medium was removed and subjected to immunoprecipitation using affinity-purified anti-GFP antibodies.

C-terminal truncations were expressed in CHO cells by incubation in with doxicycline (1 µg/ml) for 48 h at 37°C (6-well plates; 70% confluency). Additionally recombinant GFP was exogenously added to MCAT cells. The growth medium was removed and the cells were washed once with PBS. Medium and PBS wash buffer were combined and subjected to immunoprecipitation using affinity-purified anti-GFP antibodies. As shown in figure

Exogenously added recombinant GFP was immunoprecipitated from the medium of MCAT cells (lane 2). GFP from expressing CHO_{GFP} cells was not detectable in the medium. Additionally, C-terminal truncations were not immunoprecipitated from the growth medium.

Since the fusion proteins were neither detected in the cell culture medium nor in the cell surface, it can be concluded that C-terminal truncations of FGF2 prevent its secretion.

3.4.2 Characterization of mutant rM 156

The mutant 156 generated by random mutagenesis showed a reduced secretion as detected by FACS analysis and biotinylation assay (see figure 3.38). Another characteristic of this mutant was its ability to bind *in vitro* to heparin beads, but its failure to bind *in vivo* to HSPGs of the cell surface. However, although the fusion protein was not able to bind to the cell surface, a significant signal was detected if it was applied *in vitro* to heparin beads.

A set of experiments was conducted in order to confirm the results obtained by the screening procedure and to fully characterize this mutant with regard to protein degradation and potentially secreted FGF2 failed to bind to the cell surface. In order

to immuno-precipitate the potential population, which is not bound to the cell surface, but present in the medium, the cell surface biotinylation assay was modified. It was enhanced by using heparin beads on growth medium from secreting cells in order to detect the population which was not bound to the cell surface. A degradation experiment over time and at different temperatures was conducted, to exclude that the reduced signal for the unconventional secretion is mediated by protein degradation.

Additionally, individual mutations of clone rM156 were subjected to a detailed analysis to detect if the potential defect of this mutant is caused by combination of the mutations or by a single amino acid. The point mutations used were the following: Mutant 36, bearing a mutation at position 87 changing glutamic acid to lysine (E to K), mutant 45, mutated at position 128 changing lysine to glutamic acid (K to E) and mutant 46, changing arginine to glutamine (R to Q) at position 129.

3.4.2.1 Quantification of secretion employing FACS Analysis

In order to reproduce the results from the screening, the amount of expressed and secreted fusion protein was quantified using flow cytometry under the same conditions as during screening process.

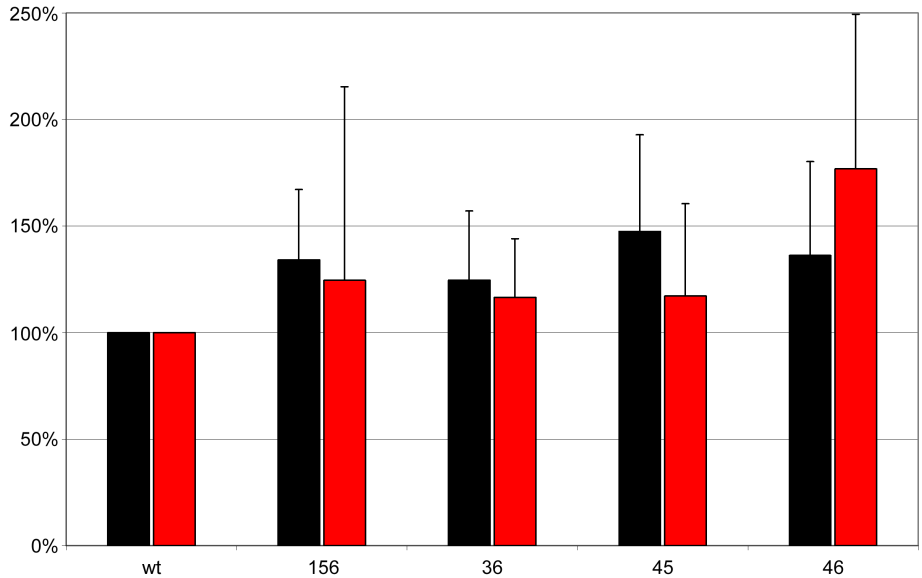

Figure 3.119: FACS analysis. All Experiments performed as described during screening process and set as average of 13 experiments. FGF2-GFPwt was set to 100%. Clone 156 and point mutation 36 (E87K), 45 (K128E) and 46 (R129Q) were depicted in relation to FGF2-GFP$_{wt}$.Black bars represent GFP fluorescence, red bars indicate the cell surface staining as measured by antibody staining.

The experiment was performed under the same conditions as described for the screening. The result shown in figure 3.119 displays the average of 13 experiments. It was not possible to reproduce the signal for cell surface staining in mutant rM156 as described for the screening in section 3.3.3.4. The single mutations did not display an altered signal for extracellular FGF2-GFP compared to the screening.

3.4.2.2 Biotinylation of surface proteins to assess the amount of secreted FGF2

In order to confirm the result obtained by cell surface biotinylation during screening, this assay was also repeated as described previously. As stated, this mutant displays an impaired binding to CHO cells. Therefore the signal for secreted FGF2-GFP has to be analyzed as a combined signal from cell surface associated FGF2 and soluble FGF2, which is not able to bind to CHO cells. In order to detect potential fusion protein, not associated with the cell surface, medium from secreting cells was targeted to heparin beads in order to fish the soluble population. The signal for both, biotinylated cell surface associated and heparin bound soluble FGF2-GFP represented the overall signal for secreted fusion protein.

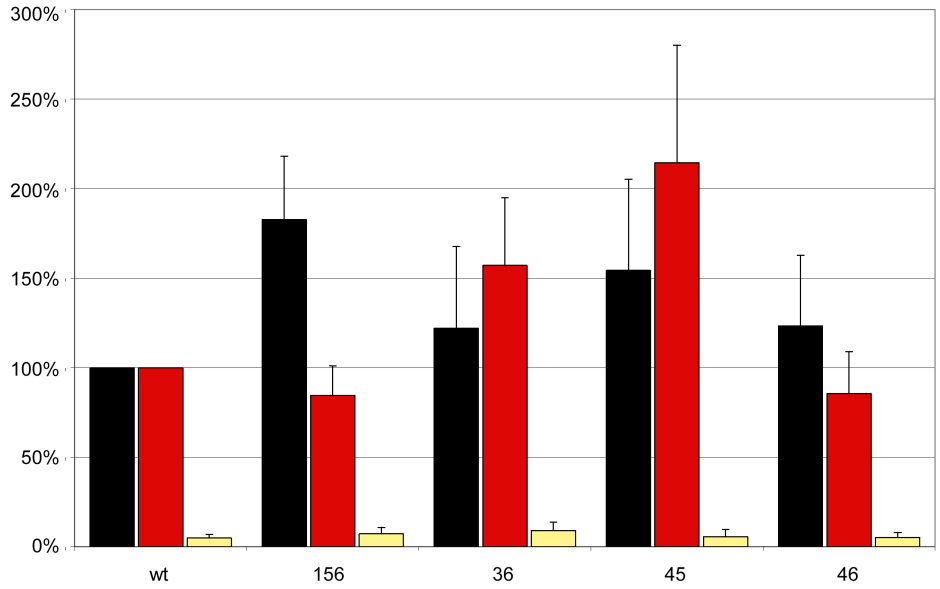

Figure 3.120: Quantification of FGF2-GFP fusion protein export of from CHO cells employing cell surface biotinylation and heparin binding from cell culture supernatants. The fusion proteins indicated were expressed in CHO cells for 16 h at 37°C (6-well plates; 70% confluency). The medium was removed and subjected to binding to heparin beads. Cell surfaces were treated with a membrane-impermeable biotinylation reagent. Following detergent mediated cell lysis, biotinylated and non-biotinylated proteins were separated employing streptavidin beads. Aliquots from the input material (black bars, 2.5%), the biotinylated fraction (red bars, 50%) were analyzed by SDS-PAGE. Additionally the medium was subjected to heparin beads (1h, 4°C) in order to bind extracellular, non-bound FGF2-GFP to the beads. The protein was eluted from the beads using SDS-sample buffer and the eluate (yellow bars, 50%) was also analyzed by SDS-PAGE, followed by Western blotting using affinity-purified anti-GFP antibodies. Primary antibodies were then detected with Alexa 680-coupled anti-rabbit secondary antibodies. Signals for FGF2-GFP fusion proteins were quantified using a LI-COR Odyssey imaging system. For further details, see Material and Methods.

The experiment was conducted as described previously for the screening. Additionally to the biotinylation of cell surface proteins, the medium was subjected to heparin beads (1h, 4°C) to bind secreted but non-bound material. The result depicted in figure 3.120 displays an average of four individual experiments. Strikingly and in contrast to the result obtained during the screening process, the signal for secreted fusion protein, bound to the cell surface was not reduced. Moreover, as a positive control, the mutants obtained by site-directed mutagenesis 36, 45 and 46 displayed a comparable level of biotinylated protein as detected during screening process. Additionally, it was not possible, to bind neither FGF2-GFP_{wt} nor mutated proteins from the medium using heparin beads, indicating that secreted fusion protein was completely bound to heparan sulfate proteoglycans present on the cell surface. The *in vivo* binding assay made use of FGF2-GFP present in a cell free supernatant derived from CHO cells expressing the fusion proteins, whereas biotinylation assay detected secreted, endogenous FGF2-GFP associated with the plasma membrane. This might explain the difference in the result of both assays, because the translocation process might also directly mediate binding, thereby changing affinity of FGF2 to heparan sulfate proteoglycans.

3.4.2.3 Degradation experiment

The interpretation of the results obtained for mutant rM 156 would be further complicated if the signal is getting lost due to degradation of the fusion protein. Therefore an analysis was conducted to quantify the amount of degraded fusion proteins for FGF2-GFPwt and the mutated versions of FGF2-GFP as indicated in the following figure 3.121.

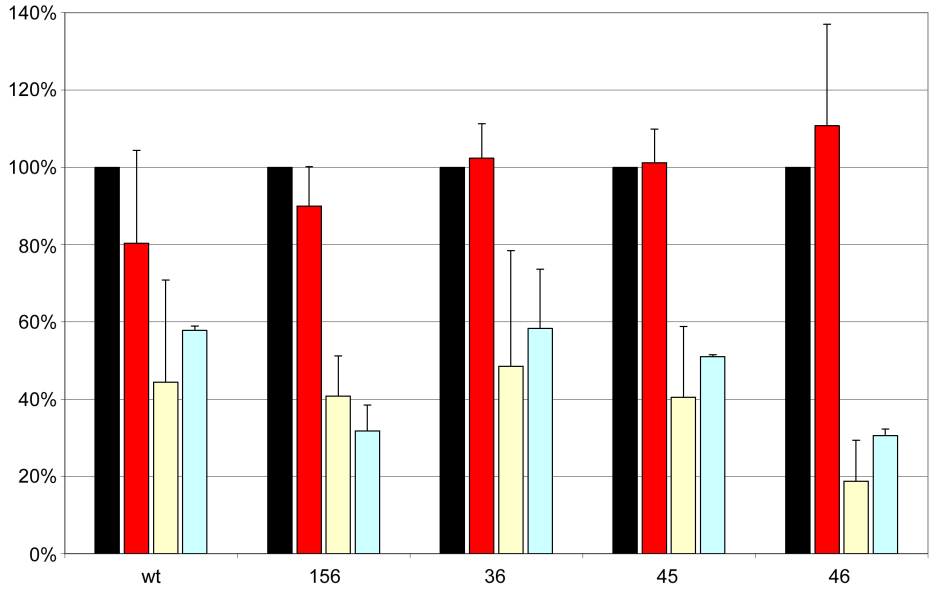

Figure 3.121: Stability of FGF2-GFP fusion proteins in conditioned media derived from CHO cells. The fusion proteins indicated were expressed in CHO cells for 16 h at 37°C (6-well plates; 70% confluency). From each cell line, a cell-free supernatant was prepared. Normalized amounts (GFP fluorescence) were incubated in conditioned medium derived from CHO cells for the times indicated followed by binding to heparin beads. The samples were analyzed by SDS-PAGE and Western blotting using antibodies directed against GFP. Black bar: input (no heparin binding, 10%); lane 2: no incubation (binding to heparin beads, 10%); lane 3: incubation for 24 h at 4°C (binding to heparin beads, 10%); lane 4: incubation for 24 h at 37°C (binding to heparin beads, 10%). For further details, see Material and Methods

The assay was performed using cell free supernatant, for the generation see Material and Methods, chapter 2.3.6. After normalizing the amount of protein (GFP fluorescence), the cell free supernatant was incubated in conditioned medium derived from CHO cells for 24 h at 4°C and 37°C. The solution was then subjected to heparin beads (1 h, 4°C) in order to precipitate FGF2-GFP from the medium. FGF2-GFP bound to heparin was eluted from beads using SDS sample buffer, followed by SDS-PAGE and Western blotting.

When comparing the signal for input (black bar) and non pre-incubated FGF2-GFP bound to heparin beads (red bar), there was no difference detectable, indicating quantitative binding to heparin beads and elution of FGF2-GFP from the beads.

After an incubation of the fusion protein for 24 h at 4°C (Yellow bars), the signal for wild-type and mutated protein, was significantly reduced. 50% of the input material could be detected for wt protein and mutants 156, 36 and 45. This result showed that the fusion protein was degraded in 24 h at 4°C, but protein derived from mutants was degraded to the same amount compared to wild-type protein. The mutations did not have an influence on the stability of the fusion protein. But mutant 46 was an exception, showing a signal reduced to 20% when compared to wild-type for its fusion protein detectable after 24 h at 4°C. Therefore, the mutation R to Q at position 129 affected the stability of the fusion protein. Incubating the proteins at 37°C for 24

h (light blue bars) did not result in a higher degradation when compared to incubation at 4°C for 24 h.

This experiment displayed that FGF2-GFP was degraded independently from mutations and temperature. In all assays, FGF2-GFP$_{wt}$ is compared with a specific mutant. Since in the case for rM 156, mutants and FGF2-GFP$_{wt}$ were degraded to the same extent, a quantification of the secreted fraction, bound to the cell surface was possible.

3.4.2.4 Binding efficiency to HSPGs of FGF2-GFP$_{wt}$, rM 156 and clone 36

The mutant rM 156 was tested during the screening process to be negative for binding to HSPGs present on the cell surface of CHO cells. In contrast, it was able to bind *in vitro* to heparin beads. To probe the binding efficiency of the mutants rM 156 and point mutation 36, an experiment was conducted where cell free supernatant was normalized, subjected to CHO$_{MCAT/TAM2}$ cells cells and incubated at 37°C or 4°C for 1 h or 16h. The detection of cell surface associated fusion protein occurred by flow cytometry.

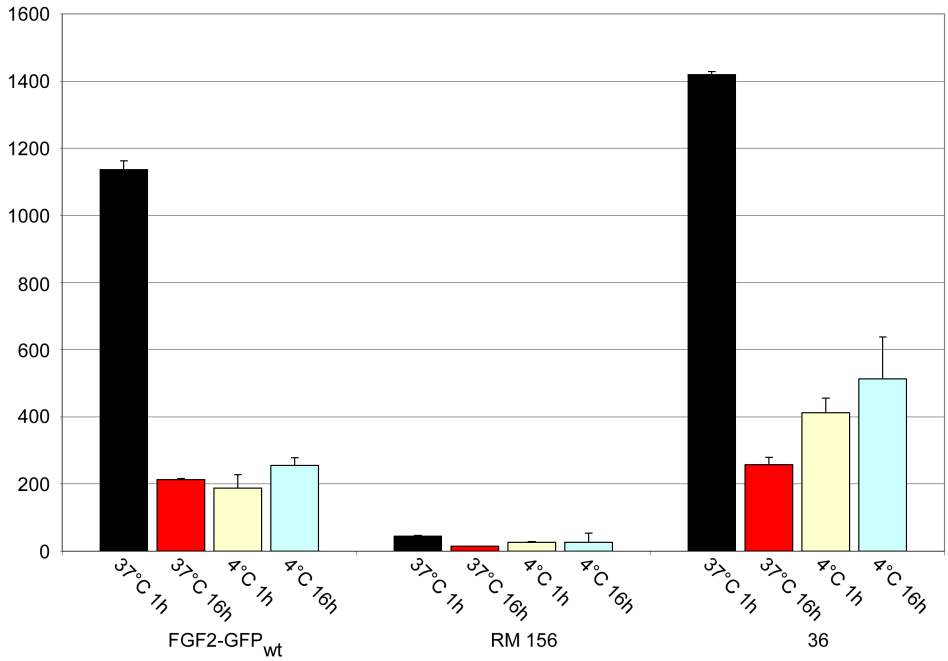

Figure 3.122: Analysis of FGF2 binding efficiency of various FGF2-GFP fusion proteins based on binding to CHO cells**.** The various fusion proteins indicated were expressed in CHO cells. Cell-free supernatants were prepared and normalized by GFP fluorescence. The supernatants indicated were then incubated with CHO cells for the time and temperature indicated to allow cell surface binding. Following treatment with affinity-purified anti-GFP antibodies and APC-conjugated secondary antibodies, cell surface binding was quantified by flow cytometry.

The assay was performed with cell free supernatant, for generation see Material and Methods. After normalizing the amount of protein (GFP fluorescence), the cell free supernatant was incubated for different time periods and at different temperatures with $CHO_{MCAT/TAM2}$ cells to allow binding of the fusion proteins to heparan sulfate proteoglycans present on the cell surface. Cells were then processed with antibodies and prepared for FACS analysis, as described previously. FGF2-GFP_{wt} displayed a signal of about 1150 arbitrary units, when incubated at 37°C for 1 h (black bars). Shifting the temperature to 4°C led to a reduced signal for FGF2-GFP_{wt} bound to the cell surface as compared to incubation at 37°C, indicating that the binding of the fusion protein to the cell surface is temperature sensitive, since only 15% of the fusion protein bind to the cell surface at 4°C. Extending incubation time of cell free supernatant with $CHO_{MCAT/TAM2}$ cells led to a reduced signal as well. The reduced amount of fusion protein bound to the cell surface after incubation of 16 h at 37°C may result from degradation of FGF2-GFP. The reduced signal for FGF2-GFP after an incubation of 16 h at 4°C was observed, again probably because of the fusion proteins sensitivity to temperature. Binding of the fusion protein to HSPGs is impaired at 4°C. This observation was also made for mutant 35, although the ability to bind to HSPGs at 4°C is slightly enhanced. In contrast to wild-type protein, cell surface staining could not be detected with flow cytometry for the mutant rM 156, indicating a total loss of binding ability to HSPGs. Another formal possibility would be a higher degree of degradation, but as shown in figure 3.121, a difference between degradation rates of FGF2-GFP_{wt} and mutant rM 156 was not observed.

4 Discussion

Most secretory proteins are exported by eukaryotic cells using an ER/Golgi-dependent pathway which is well characterized on the molecular level. This classical secretory pathway starts with the recognition of an hydrophobic signal sequence present at the N-terminus of a secretory protein (Walter et al., 1984), followed by cotranslational insertion into the lumen of the endoplasmatic reticulum (ER) (Rapoport et al., 1996). In the ER the protein is modified and packaged into vesicles which are targeted to the Golgi apparatus. Following fusion of the vesicles with the membrane, the protein is released into the Golgi where it is further modified (Hille et al., 1984; Abeijon and Hirschberg, 1992). It is then transported from cis- to trans-direction along the various Golgi cisternae. Secretory vesicles bud off the trans-Golgi membrane and travel along the cytoskeleton to the plasma membrane (Goodson et al., 1997) with which the vesicles fuse (Rothman, 1990; Pelham, 1996), thereby releasing their cargo into the extracellular space (Pelham, 1996).

A number of proteins which are not secreted by the ER/Golgi dependent secretory pathway were also found to be present in the extracellular space, leading to the postulation of an ER/Golgi independent export, which was termed unconventional secretion. These proteins lack a classical signal sequence (Muesch et al., 1990) and are not glycosylated despite bearing multiple consensus sequences (Hughes et al., 1992). Additionally, those proteins cannot be found to be present in compartments of the classical export route. Furthermore, their externalization is not blocked by inhibitors of the classical secretory pathway such as brefeldin A and monensin (Rubartelli et al., 1990; Florkiewicz et al., 1995). The first proteins to be described as secreted in an unconventional manner were interleukin-1β, galectins and FGF2. Meanwhile, it was demonstrated that not only cytokines (Interleukins, MIF and thioredoxin), lectins (galectin-1 and galectin-3) and growth factors (fibroblast growth factors) are unconventionally secreted, but also viral proteins (HIV tat, FV bet and HSV VP22), *Leishmania* hydrophilic acylated surface protein B (HASPB) and homeodomain-containing transcription factors (reviewed in Nickel et al. 2003).

The molecular machinery mediating unconventional secretion of these proteins has

yet to be reported. However, it has been demonstrated that the proteins do not share a common pathway, but are rather secreted individually involving different, but maybe similar molecular machineries.
Proteins, exported by unconventional means are of high biomedical relevance. The pro-angiogenic growth factor FGF2 is released by tumour cells to establish growth and spreading through metastases by neovascularization of the tumour. By elucidating the molecular machinery, it would be possible to develop or find inhibitors which specifically block secretion of FGF2 without affecting viable non-tumour cells, thus providing a potent tool in the therapy of tumours.

In the present thesis, a robust *in vivo* system was established which made use of genetically modified CHO cell lines expressing various mutated versions of FGF2-GFP in a doxicycline-dependent manner.

4.1 Generation of CHO cells expressing FGF2-GFP in a doxicycline-dependent manner as a tool for the analysis of FGF2 secretion

In order to analyze unconventional secretion of the 18 kDa isoform of FGF2, a model cell line based on CHO (*Chinese hamster ovary*) cells was generated. CHO cells are generally well suited for the characterization of FGF2, because they lack high affinity FGF receptors (FGFR) with tyrosine kinase activity (Rusnati et al., 2002), thus avoiding autocrine and paracrine induction of biological activities (proliferation, differentiation and others). However, they express low-affinity receptors like heparan sulfate proteoglycans (HSPG) and glycolipids (e.g. GM_1) to which FGF2 binds over its heparin binding motifs. Different CHO clones were generated from precursor cells ($CHO_{MCAT/TAM2}$) to express the reporter proteins FGF2-GFP and GFP, termed $CHO_{FGF2\text{-}GFP}$ and CHO_{GFP}, respectively in a doxicycline-dependent manner as described in section 3.1. These cells were characterized regarding regulation of doxicycline-dependent expression using different cell biological and biochemical methods.
The genetic information for FGF2-GFP was introduced into the genome of CHO cells by retroviral transduction. To verify the retroviral insertion of FGF2-GFP and GFP

cDNA into the genome of CHO cells, a PCR analysis was performed, using genomic DNA extracted from cultured CHO cells as a template. PCR constructs were analyzed by agarose gel electrophoresis and found to be detected with the correct size (figure 3.3), providing evidence for a stable integration of both reporter constructs. The cell lines were characterized using biochemical and cell biological assays in order to demonstrate the functional expression of the reporter proteins. A western blot analysis using affinity-purified anti-GFP antibodies was used to verify doxicycline-dependent expression of FGF2-GFP (45 kDa) and GFP (26 kDa) respectively, showing protein expression only in the presence of doxicycline. In absence of the antibiotic, the reporter proteins could not be detected. Thus, the expression of the reporter proteins is under the control of the transactivator, which was introduced into the CHO cells in the second step of the generation of these model cell lines (see material and methods). This result was confirmed by flow cytometry and fluorescence microscopy (figure 3.4). However, FGF2-GFP showed a prominent nuclear staining as shown by confocal microscopy. The observation of nuclear located FGF2 is discussed controversially in the literature. It was shown that the 18 kDa isoform resides in the cytoplasm, whereas the high molecular isoforms of FGF2 (22-35 kDa) possess a nuclear localization sequence (NLS) at their extended N-terminus, which targets the proteins to the nucleus (Renko et al., 1990).

Like other polypeptides, such as insulin and interleukin-1, 18 kDa FGF2 can translocate into the nucleus after internalization (Bouche et al., 1987) where it is able to up-regulate the synthesis of ribosomal RNA (Baldin et al., 1990). The nuclear translocation was also shown to be independent of lysosomes and microtubules (Ishihara et al., 1993). Interestingly, nuclear translocation of FGF2 was dramatically inhibited by heparinase treatment or in heparin-deficient Chinese hamster ovary cells, suggesting that heparan sulfate proteoglycans of the cell surface are involved in the internalization of exogenous 18 kDa FGF2. Moreover, it was proposed that FGF2 possesses an unconventional bipartite nuclear localization signal (NLS) at its C-terminus, containing two small clusters of basic amino acid residues separated by a hydrophobic region containing eight amino acids, which directs the protein to the nucleus (Hsia et al., 2003). Another reason for the nuclear localization might be that fusion of GFP to FGF2 leads to the nuclear localization, because both proteins might possess one part of a bipartite NLS which is completed after fusion of both proteins, targeting FGF2-GFP to the nucleus. This presumption is supported by the

observation that FGF2-GFP was found to be present in the nucleus of corneal endothelial cells (Choi et al., 2000). Another possible explanation for the nuclear localization of FGF2-GFP would be that the fixation process for confocal microscopy leads to an artificial nuclear staining. This was shown for the unconventional secretory protein vp22. Its nuclear localization was shown to be an artificial effect of the fixation procedure used to analyze cells expressing vp22 employing confocal microscopy (Lundberg and Johansson, 2001). This hypothesis is supported by the observation that cells processed for live-imaging by confocal microscopy do not demonstrate a nuclear FGF2-GFP staining (recent data from our laboratory).

The characterized cells express MCAT (mouse cationic amino acid transporter), which enables retroviral transduction with reporter proteins to analyze the mechanism of unconventionally secreted proteins. In our laboratory, these cells were used to analyze unconventional secretion of *Leishmania* HASPB, galectin-1 and FGF2. The model cell line expressing FGF2 in a doxicycline-dependent manner served as a tool for the development of an efficient model system, which allows for the molecular analysis of unconventional secretion of FGF2 *in vivo*.

4.2 Establishing an in vivo system to analyze unconventional secretion of FGF2

The model cell line $CHO_{FGF2\text{-}GFP}$ was used to develop an experimental system for the analysis of unconventional secretion of FGF2. This system makes use of heparan sulfate proteoglycans (HSPG) present on the cell surface (Burgess and Maciag, 1989; Thompson et al., 1994; Brucato et al., 2002) to which FGF2 is able to bind upon secretion. Extracellularly localized, cell surface associated FGF2-GFP can be detected with specific antibodies and the amount of FGF2-GFP bound to heparan sulfate proteoglycans can be quantified employing flow cytometry.

4.2.1 FGF2-GFP is localized on the cell surface of CHO cells

The binding of secreted FGF2-GFP to plasma membrane-associated heparan sulfate proteoglycans was verified by performing an anti-GFP or anti-FGF2 antibody processing of cells under native conditions, followed by detection of first antibodies

with fluorophore-coupled secondary antibodies (Phycoerythrin or allophycocyanin). The processed cells were then analyzed by flow cytometry to quantify the amount of secreted fusion protein.

The experiments shown in section 3.2.1 demonstrate that a cell surface signal was only detectable if cells were cultured in presence of doxicycline. A cell surface signal could not be detected in the absence of doxicycline incubation, indicating the monospecificity of the antibodies used. Furthermore, these experiments provide evidence that the artificial fusion of GFP to FGF2 does not result in a difference of its binding properties to HSPGs. This result was confirmed by a biochemical assay, where secreted FGF2-GFP was set into relation to intracellular FGF2-GFP. Extracellular FGF2-GFP was released from the cell surface by heparin and subjected to heparin sepharose in order to precipitate secreted FGF2. Intracellular FGF2-GFP was obtained by cell lysis. Cell lysate and heparin sepharose was then incubated with SDS-containing buffer and applied to SDS-PAGE, FGF2-GFP was detected by anti-GFP antibodies. In case for GFP, the supernatant and cell lysate were directly applied to SDS-PAGE and Western blot using anti-GFP antibodies. These experiments demonstrate that the translocation over the plasma membrane is dependent on the FGF2 part of the fusion protein, since GFP alone could not be detected to be cell surface associated.

4.2.2 Characterization of FGF2-GFP localization on the cell surface

To evaluate that the signal detected on the cell surface derives from FGF2-GFP bound to HSPGs, two experiments were conducted. In the first experiment, trypsin was added prior to analysis by flow cytometry. Proteins on the surface were degraded by trypsin, leaving intracellular proteins intact. As shown in the experiment (figure 3.6), the FGF2-GFP derived signal for cell surface staining is reduced to autofluorescence level, indicating that antibody-detected FGF2-GFP is present on the cell surface and can be degraded by the protease trypsin. In a second experiment (figure 3.8), heparin was added to cells expressing FGF2-GFP, in order to specifically remove FGF2-GFP from the cell surface. Since heparin competes with HSPGs for the binding to FGF2, an excess of soluble heparin removes FGF2 from the cell surface. This experiment demonstrated that the signal for FGF2-GFP on the cell surface was almost quantitatively reduced to autofluorescence level. The results

obtained by FACS analysis were confirmed by performing confocal microscopy (figure 3.16). The experiments provide evidence that FGF2-GFP detected by flow cytometry or confocal microscopy is indeed a population of secreted protein bound to HSPGs of the cell surface. Furthermore it could be shown that FGF2 artificially fused to GFP is fully functional for unconventional secretion and binding to HSPGs present on the cell surface.

4.2.3 Functional characterization of the translocation mechanism

Before 1991, FGF2 was suggested to be released unspecifically from injured or dead cells which have lost membrane integrity and release FGF2 in an uncontrolled manner (McNeil et al., 1989). In 1991, Mignatti et al. proposed for the first time that FGF2 might not be released by injured cells but that it is rather secreted by a novel secretion mechanism, which was suggested to be independent from the classical secretory pathway (Mignatti and Rifkin, 1991). This proposal was confirmed later by different research groups, one of them also identifying the Na^+/K^+-ATPase as a potential component of the translocation machinery (Florkiewicz et al., 1998; Dahl et al., 2000). Unfortunately, no further investigations have been made to elucidate other components of the translocation machinery. However, evidence is accumulating that FGF2 is specifically released by a yet unknown mechanism. Multiple experiments were performed in order to functionally characterize the translocation mechanism of FGF2 secretion.

4.2.3.1 Kinetics of the translocation process of FGF2

To analyze the kinetics of FGF2-secretion from CHO cells, the cells were induced to express FGF2-GFP for increasing periods of time, leading to higher amounts of fusion protein expressed (section 3.2.3). The resulting cell surface staining was determined and a linear increase of extracellular FGF2-GFP was observed up to an incubation time of 48 h. Cells expressing the proteins for longer periods of time did not show a higher signal for secreted FGF2. The saturation of the signal after 48 h of doxicycline treatment might be due to limited binding capacities for FGF2-GFP on the plasma membrane or because the steady state level was reached, in which secretion

and endocytosis/degradation are in equilibrium. The observed time-dependency leads to the conclusion that the translocation of FGF2-GFP is a controlled mechanism.

4.2.3.2 Binding capacity of FGF2 for binding to heparan sulfate proteoglycans present on the cell surface of FGF2-GFP

The following experiment was performed to determine the capacity of FGF2 to bind to heparan sulfate proteoglycans present on the cell surface of CHO cells (. For this purpose, cells were incubated in absence of doxicycline and different amounts of recombinant FGF2 were added to the medium. Subsequently, cell surface-associated FGF2 was detected by affinity-purified anti-FGF2 antibodies and quantified by flow cytometry (figure 3.10). The signal for cell surface staining increased linearly up to an addition of a maximal concentration of 500 ng recombinant FGF2 to the medium, indicating that the maximal binding capacity of heparan sulfate proteoglycans of the cell surface for FGF2 was not reached. The signal from exogenously added recombinant FGF2 was set in a direct relation to the signal for endogenous expressed and secreted FGF2-GFP bound to the cell surface. It was 10 times higher than the signal for biosynthetic, secreted FGF2. The concentration of endogenous FGF2 detected on the cell surface can be calculated to less than 1 ng when compared with exogenous added recombinant FGF2. This experiment demonstrates that the amount of expressed and unconventionally secreted protein alone is not able to saturate the heparan sulfate proteoglycan binding sites present on the cell surface. Therefore, the saturation observed after 48 h in the kinetic studies did not represent low binding capacities but rather an equilibrium between endocytosis/degradation and secretion of FGF2.

4.2.3.3 Unspecifically released FGF2-GFP does not contribute to the cell surface signal

The contribution of unspecifically released FGF2-GFP from dead or damaged cells to the signal detected on the cell surface was investigated by the following experiment

(section 3.2.3). A membrane-free supernatant was obtained by homogenization of FGF2-GFP expressing cells employing sonication. This supernatant was then incubated with cells not expressing the fusion protein in order to allow binding of FGF2-GFP to the cell surface. The signal for cell surface staining of endogenous, secreted FGF2-GFP was shown to be twice as high as the amount equivalent to the material released from 10% completely lysed cells. The amount of dead cells was monitored by propidium iodide (PI), a low molecular dye, which enters cells with disrupted plasma membranes and accumulates in the nucleus by intercalating into DNA (Crissman et al., 1976). The typical amount of PI positive cells was found to be 2-3%, indicating that the signal observed on the cell surface from FGF2-GFP secreting cells does not derive from FGF2-GFP unspecifically released by dead cells. The performed experiments provide evidence that the cell surface signal as detected by FACS analysis is derived from controlled secretion of FGF2-GFP.

4.2.3.4 Inhibition of FGF2 secretion by ouabain

The glycoside ouabain is a known inhibitor of unconventional secretion of FGF2 (Trudel et al., 2000). It was shown to interact with the α-subunit of the Na^+/K^+-ATPase which has been suggested to be a part of the translocation machinery of FGF2 export (Florkiewicz et al., 1998; Dahl et al., 2000). Therefore, an *in vivo* experiment based on flow cytometry was performed and ouabain was added in low concentrations (1-5 µM) to the medium of FGF2-GFP expressing CHO cells (figure 3.14). The addition of ouabain resulted in up to 50% decrease of FGF2 export. Accordingly, a biochemical assay was performed (figure 3.15) and it was observed that addition of 25 µM ouabain also resulted in reduced amounts of secreted FGF2. These experiments indicate that the FACS-based signal detected for unconventionally secreted FGF2 results from a regulated translocation in which the Na^+/K^+-ATPase might be involved.

4.2.4 Intercellular spreading of FGF2-GFP

The biological activity of FGF2 is mediated by both autocrine and paracrine mechanisms (Bechtner et al., 1992; Okada-Ban et al., 2000). Therefore FGF2 has to

be able to spread from the producing cell to the target cell on which FGF2 is bound to receptors in order to execute its biological activity. By employing confocal microscopy, it was demonstrated that FGF2-GFP populations are able to spread from one cell to another cell in close proximity (Engling et al., 2002). $CHO_{MCAT/TAM2}$ cells were used to simulate cells which are not able to express and secrete FGF2-GFP (figure 3.20). These cells were cultivated together with $CHO_{FGF2\text{-}GFP}$ cells and incubated with doxicycline to induce FGF2-GFP expression. By comparing the intracellular GFP-derived signal, FGF2-GFP expressing cells ($CHO_{FGF2\text{-}GFP}$) were distinguishable from cells not expressing FGF2-GFP ($CHO_{MCAT/TAM2}$). Both populations were analyzed for FGF2-GFP cell surface localization. $CHO_{MCAT/TAM2}$ cells, although not expressing FGF2-GFP were shown to be positive for cell surface localized fusion protein and therefore it must be derived from FGF2-GFP expressing $CHO_{FGF2\text{-}GFP}$ cells. The spreading of FGF2-GFP from expressing to non-expressing cells implicates that at least a part of the secreted material is probably released into the medium and is able to bind to any cell resulting in a homogenous cell surface staining of both cell lines. This result was confirmed by flow cytometry using the same experimental setup (figure 3.19). FGF2-GFP derived cell surface staining was found to be homogenous for both cell lines when cultivated together on one culture plate. A small, but significant difference of FGF2-GFP derived cell surface staining was observed by flow cytometry when cell populations were cultivated separately on two culture plates and combined for FACS processing and analysis. Cell surface derived signals for both populations were found to be separated, when the populations were cultivated and processed separately. This result indicates that cells have to be in contact either during cultivatation or procession in order to enable FGF2-GFP spreading.

4.2.5 Refinement of FACS processing in order to prevent unspecific release of FGF2-GFP

By performing flow cytometry, FGF2-GFP bound to the cell surface is detected with antibodies directed against GFP. It is not possible to differentiate secreted FGF2-GFP from fusion protein which is released from cells in an uncontrolled fashion. Addition of doxicycline to cell cultures leads to an overexpression of FGF2-GFP and if those cells are injured or dead and lose plasma membrane integrity, they would release major amounts of fusion protein into the medium which subsequently binds to

the cell surface, resulting in an unspecific signal for secreted FGF2-GFP. As discussed in section 4.2.3.3, the amount of unspecifically released FGF2-GFP does not contribute significantly to the signal for secreted FGF2-GFP bound to the cell surface. However, the processing for FACS analysis was improved in a way that cell damage and uncontrolled release of fusion protein is further reduced. Formerly, cells were detached from the culture plates and antibody processing was performed in suspension. In contrast, by improving the procedure, cells were not detached prior to antibody processing and centrifuged during washing steps, but remained attached to the culture plate while treated with both primary and secondary antibodies. To verify if this improvement results in a signal reduced by the amount of unspecifically released FGF2-GFP, a control experiment was conducted, where FGF2-GFP expressing and CD4/GFP expressing cell lines were compared with regard to the FACS procedure (figure 3.21). The GFP fluorescence of both cell lines remained constant independently of the procedure. In contrast, cell surface staining was observed to be different. FGF2-GFP expressing cells showed a significantly reduced cell surface signal of about 40% when antibody processing was conducted on the culture plate as compared to the signal observed for cells processed in suspension. The cell surface signal detected for the plasma membrane protein CD4 remained constant for both procedures. Therefore about 60% of the signal for FGF2-GFP on the cell surface of cells processed in solution might originate either from unspecifically released fusion protein or steric hindrance due to the attachment of cells to the culture plate which might also prevent complete detection of the fusion protein bound to heparan sulfate proteoglycans. This can be excluded for the transmembrane protein CD4, which is equally well detected by flow cytometry, independent of the procedure used. However, steric hindrance can not be excluded to be the reason for the reduced signal detected for FGF2-GFP when cells were processed while being attached to the culture plate, since FGF2-GFP is bound to large heparan sulfate proteoglycan structures and therefore might not be well accessible for anti-GFP antibodies. It has to be assumed that a combination of both possibilities lead to the reduction of the signal for secreted FGF2-GFP. This procedure was then used to further analyze the secretion of FGF2.

4.3 Biosynthetic FGF2-GFP is localized to non-lipid raft microdomains following translocation

The experimental system described was used in order to study the fate of biosynthetic (i.e. endogenous) FGF2-GFP following translocation to the extracellular compartment. FGF2-GFP was shown to accumulate in large macromolecular clusters that appear as bright spots on the cell surface (Engling et al., 2002). FGF2-GFP association with these structures is mediated by HSPGs as heparin treatment causes a loss of FGF2-GFP staining on the cell surface. In order to investigate as to whether FGF2 export and deposition in HSPG-containing microdomains are tightly linked processes, we analyzed the mode of delivery of FGF2-GFP to HSPGs following its externalization. FGF2-GFP was shown to spread between different populations of cultured cells. Moreover, FGF2-GFP prepared as a cell-free supernatant from homogenized $CHO_{FGF2\text{-}GFP}$ cells can associate with non-expressing cells, thereby forming morphologically similar microdomains on their surfaces. In conclusion, FGF2 externalization and deposition in cell surface microdomains do not occur through an integrated process that would restrict cell surface deposition to FGF2-secreting cells. Rather it appears likely that is released as a soluble intermediate which eventually accumulates in HSPG-containing protein clusters. These data are consistent with our finding that the FGF2 binding capacity mediated by HSPGs does not influence the balance of intracellular FGF2 versus extracellular HSPG-bound FGF2. Rather, the cell surface signal detected provides a precise measure of FGF2 externalization which is not limited by the availability of HSPGs. Therefore, the FGF2 export machinery is rate-limiting under the conditions applied. The presence of FGF2-GFP in discrete microdomains on the cell surface implied that these structures might represent protein complexes involved in FGF2 signal transduction. In this context, Davy et al. reported that FGF2 signalling originates from caveolae-like lipid rafts on the cell surface (Davy et al., 2000). A functional FGF2 signal transduction complex consists of FGF2, HSPGs, the co-receptor GM_1 and high-affinity FGF receptors (Rusnati et al., 2002). CHO wild-type cells do synthesize HSPGs and GM_1, however, they do not express high-affinity FGF receptors (Rusnati et al., 2002). Therefore, it was interesting to study the biophysical properties of the FGF2-GFP-positive microdomains observed on the cell surface of CHO cells. Based on detergent solubility combined with flotation experiments in sucrose gradients (figure 3.18), we

can exclude that the FGF2-positive clusters observed are related to lipid rafts. Therefore, initial binding of FGF2 to HSPGs does not result in the correct targeting to caveolae-like lipid rafts where FGF2 signalling is initiated. Rather, FGF receptors are required to direct the core complex of FGF2 signalling to lipid rafts. Accordingly, upon doxicycline-induced FGF2-GFP expression and externalization, $CHO_{FGF2\text{-}GFP}$ cells do not appear to be significantly stimulated with respect to cell proliferation. Therefore, the large FGF2-GFP- and HSPG-containing cell surface clusters appear to represent signalling complex precursors that, in the presence of high affinity FGF receptors, are converted into functional signalling complexes. This transition appears to be accompanied by a targeting of the FGF2 signalling complex to caveolae-like lipid rafts (Engling et al., 2002).

4.4 Screening of FGF2 mutants to elucidate targeting motifs for unconventional secretion

In order to elucidate a potential motif which targets FGF2 to its transport machinery for unconventional secretion, a mutational analysis was conducted, altering multiple and distinct single amino acids as well as truncating the N- and C-termini of FGF2.
It was demonstrated for galectin-1 that its secretion depends on their β-galactoside binding motifs (Seelenmeyer et al., 2005). FGF2 secretion was reconstituted by an *in vitro* experiment that uses inside-out vesicle derived from the plasma membrane of CHO cells. In contrast, FGF2 does not demonstrate membrane translocation when inside-out vesicles were generated from CHO cells treated with sodium chlorite (Schäfer et al., 2004). Sodium chlorite competes with sulfate ions for binding to the ATP-sulfyrulase, thereby inhibiting the generation of heparan sulfates (Baeuerle and Huttner, 1986; Klaassen and Boles, 1997; Safaiyan et al., 1999). Because of the observations made, a focus of the mutational analysis was to generate FGF2 mutants that are deficient in heparin binding and to verify if these mutants are secretion deficient. In order to be able to asses the impact of FGF2 mutations, model cell lines based on CHO cells, transduced with a mutated version of FGF2 cDNA and thus expressing the fusion proteins in a doxicycline-dependent manner were generated. To assess secretion efficiency of the FGF2 mutants generated, two read-out systems were used to monitor the secretion of FGF2.

1) FACS-based secretion assay.
   This assay was described in great detail in the first part of this thesis. It not only allows quantification of FGF2 which binds upon secretion to cell surface associated heparan sulfate proteoglycans, but additionally monitors protein expression by quantification of intracellular GFP fluorescence. This enables to normalize FGF2-GFP secretion for protein expression.

2) Biochemical secretion assay employing cell surface biotinylation.
   This assay enables assessment of the amount of extracellular FGF2-GFP bound to the cell surface of CHO cells. A membrane-impermeable biotinylation reagent was used to label proteins associated with the extracellular side of the plasma membrane. Cells were subsequently lysed and biotin-labelled proteins were purified by using immobilized streptavidin. The secreted biotinylated and the intracellular non-biotinylated populations were analyzed by SDS-PAGE and Western blotting, enabling the quantification of the secreted population in comparison to the overall amount of protein expressed by CHO cells.

Two read-out systems for binding efficiency were used to verify if FGF2-mutants are able to bind to heparin and heparan sulfate proteoglycans in order to employ secretion assays, since both assays detect secreted FGF2-GFP that is bound to heparan sulfate proteoglycans of the plasma membrane. Most importantly, these binding assays were performed in order to identify mutants deficient in heparin binding to verify if FGF2 secretion depends on the interaction of FGF2 with its low affinity receptors present on the outer leaflet of the plasma membrane.

3) *In vitro* binding of FGF2 to heparin.
   This *in vitro* assay was developed to assess the heparin binding capability of FGF2 mutants. Therefore, soluble FGF2-GFP was obtained by disrupting fusion protein expressing cells (see preparation of cell free supernatant in material and methods, section 2.3.6) which was subsequently incubated with heparin beads. The amount of heparin-bound fusion protein was then compared to the overall amount of FGF2-GFP.

Binding to low molecular heparin *in vitro* does not reflect the conditions present in the extracellular space *in vivo*, because FGF2 binds to proteoglycans from which multiple different heparan sulfate side chains originate (23 different disaccharides are known to be present in heparin or heparan sulfates), which were proposed to bind FGF2 with different affinities (Guimond and Turnbull, 1999).

4) *In vivo* binding of FGF2-GFP to heparan sulfate proteoglycans.
   This *in vivo* assay was developed to monitor the binding efficiency of mutated versions of FGF2 to heparan sulfate proteoglycans present on the cell surface of CHO cells. Soluble FGF2-GFP, prepared as described in section 2.3.6, was added to the culture medium of CHO cells to allow binding of the fusion protein to the cell surface. Subsequently, heparan sulfate associated FGF2-GFP was quantified by flow cytometry.

These assays were used to characterize more than one hundred FGF2 mutants obtained by random mutagenesis, site-directed mutagenesis and N- as well as C-terminal truncations.

4.4.1 Characterization of FGF2 mutants obtained by random mutagenesis

In order to elucidate a transport motif directing FGF2 to its export machinery, a random mutagenesis of FGF2-GFP was performed to be able to hit a broad range of amino acids. The cloning strategy, as depicted in figure 3.22, was based on an intrinsic BamH I restriction site in the open reading frame (ORF) of FGF2. Therefore a low fidelity PCR was performed only with the 406 N-terminal nucleotides and not with the complete FGF2-GFP open reading frame, resulting in different FGF2 mutants that demonstrated randomly distributed multiple amino acid changes and an unaltered GFP. The number of individual mutations generated in one open reading frame of FGF2 varied from two to seven (see table 3.1). Finally, 18 different CHO cell pools were generated which express different FGF2 mutants in a doxicycline-dependent manner. These cell pools were subsequently characterized with regard to unconventional secretion and heparin binding capability using the four read-out systems introduced in section 3.3.2. The analysis of these pools showed that 55% of mutants with multiple amino acid changes did not differ in secretion efficiency, protein

stability and heparin binding properties as compared to wild-type protein. About 40% demonstrated significantly reduced secretion of the mutated versions of FGF2. These FGF2 mutants also displayed impaired binding efficiency to heparin as well as to heparan sulfate proteoglycans and decreased protein stability. The ratio of expressed FGF2-GFP to secreted fusion protein is similar for both mutant and wild-type cells, indicating that the mutant cells are still able to secrete FGF2. However, it is questionable if instable FGF2-GFP is efficiently targeted to the export machinery, thus resulting in a reduced signal for secretion efficiency. The reason for the protein instability of these mutants may be due to changes of amino acids which are essential for the correct folding of FGF2. Misfolded proteins are quickly degraded in the cytosol by the ubiquitin-proteasome system (Hendil and Hartmann-Petersen, 2004), providing a quality control for the cell. The reason for impaired binding capacity of these mutants is that correct folding of the protein is a prerequisite for FGF2 to bind to heparin (Seddon et al., 1991). Another possible explanation would be that a heparin-binding region was hit by mutations, but that mutation of one amino acid of this region is not sufficient for causing complete heparin binding deficiency of FGF2. Additionally, heparin binding of FGF2 has been proposed not to be mediated by one distinct heparin-binding motif but that binding occurs by several regions localized at the N- and C-terminus of FGF2 (Baird et al., 1988; Li et al., 1994). By screening the clones obtained by random mutagenesis, only one mutant (rM 156) demonstrated a stable fusion protein and secreted the mutated version of FGF2 less efficiently as compared to wild-type cells, but showed a controversial result for heparin and HSPG-binding efficiency, since this mutant was able to bind to heparin *in vitro*, but failed to bind *in vivo* to heparan sulfate proteoglycans. This mutant was analyzed in more detail and will be discussed in section 4.4.5.

4.4.2 Characterization of FGF2 mutants obtained by site-directed mutagenesis

The point mutations were chosen based on the following criteria and appropriate amino acid changes were introduced into the open reading frame of FGF2 by site-directed mutagenesis:

1) Three-dimensional structure

   The crystal structure of FGF2 was screened for hydrophobic amino acids exposed to the protein surface as these are potential sites for interactions with other proteins.

2) Random mutagenesis

   Point mutations were introduced based on the results obtained by analyzing the random mutagenesis (section 4.4.1), choosing mutants showing altered secretion efficiency and binding capability when compared to wild-type FGF2. Multiple amino acid changes in one protein were individually introduced into FGF2 by site-directed mutagenesis in order to determine the effect of a single amino acid exchange with regard to the effect on FGF2 secretion and binding efficiency.

3) Dimerization

   It has been shown for FGF1, that the protein is released in an unconventional manner in response to temperature stress as a latent homodimer (Tarantini et al., 1995). Additionally it was shown that dimerization is a prerequisite for FGF2 mediated signalling (Kwan et al., 2001). Therefore two cysteines, mediating dimerization of FGF2 (C78 and C96) were mutated individually and in combination.

4) N-terminus

   N-terminal signal sequences targeting a protein to its translocation machinery are well described in the literature and might be involved in the unconventional secretion of FGF2 as well. Secretory proteins contain an N-terminal signal peptide (Walter et al., 1984), peroxisomal proteins have a peroxisomal targeting sequence at their N-terminus and C-terminus (Johnson and Olsen, 2001) and proteins are targeted for the import into mitochondria by N-terminal cleavable signal sequences (Neupert, 1997). The N-terminal amino acids of FGF2 are disordered and of unknown structure and a potential export signal based on the three-dimensional structure was not discovered.

In general, mutations were introduced by changing the original amino acid to alanine. Alanine is a small, uncharged hydrophobic amino acid and removes polar interactions at the respective position, thereby preventing association with potential interaction partners of the translocation machinery. N-terminal threonines were

substituted by alanine in order to remove the consensus site for phosphorylation. To rescue a potential secretion defect based on phosphorylation, threonine was also exchanged to aspartic acid or glutamic acid which are known to mimic phosphorylation (Maciejewski et al., 1995; Lu and Ou, 2002).

Following cloning of point mutations, the various constructs were stably integrated into the genome of $CHO_{MCAT/TAM2}$ cells using a retroviral gene transfer system (please refer to section 3.1). Cells transduced with the different reporter constructs were sorted via FACS to generate cell pools expressing the mutated fusion proteins in a doxicycline-dependent manner. These pools were characterized with regard to unconventional secretion and binding efficiency to heparin and HSPGs employing the four read-out systems described in section 4.3. The analysis of the cells revealed that about 84% (43 out of 51) of the characterized mutants did not differ in both secretion and heparin binding efficiency as compared to wild-type cells. Additionally, 14% of the generated mutants were found to be instable and impaired in binding to heparin *in vitro* and HSPGs *in vivo*. Only the mutant, which was mutated at two cysteine residues to prevent dimerization of FGF2, was observed to have reduced secretion efficiency when compared to wild-type fusion protein. Interestingly, the results obtained for this mutant by cell surface biotinylation and FACS analysis were not consistent. The biochemical assay showed significantly reduced secretion efficiency whereas the FACS-based assay did not display a difference as compared to wild-type levels. The reason for this discrepancy has to be investigated, but it appears possible that FGF2 possesses a different accessibility to heparan sulfate side-chains of proteoglycans. One could envisable that FGF2 binds to heparan sulfates side-chains more in proximity to the plasma membrane as well as due to the large structure of HSPGs to side-chains in distance to the plasma membrane and exposed to the medium. A possible explanation would be that antibodies used for FACS analysis only detect FGF2 bound to heparan sulfates side-chains exposed to the medium, whereas FGF2 bound to heparan sulfates in proximity to the plasma membrane is not detected, because antibodies might not have access to those side-chains due to steric hindrance. In contrast, biotin as a small low molecular compound might be able to penetrate into heparan sulfate proteoglycans and therefore detect the population of FGF2 bound to heparan sulfates present in close proximity to the plasma membrane. As discussed in section 4.3, FGF2 is secreted from the cell and

probably exists as a soluble intermediate which binds to heparin sulfate side-chains of proteoglycans. FGF2 might first occupy easy accessible heparin sulfate side-chains that are exposed to the medium. After saturation of these side-chains, FGF2 binds to heparan sulfate side-chains closer to the plasma membrane. If the dimerization mutant secretes FGF2-GFP less efficiently as compared to wild-type cells, the fusion protein might be mainly localized to exposed heparan sulfate side-chains and the signal for cell surface associated FGF2 analyzed by flow cytometry would therefore remain unchanged due to its accessibility to the antibody. However, since less protein is secreted and is associated with inner heparan sulfate side-chains, the signal for FGF2 exported by the dimerization mutant and detected by biotinylation would be reduced in comparison to the wild-type. A possible explanation for the reduced secretion efficiency of a dimerization mutant might be that the dimerization status of FGF2 is somehow monitored by the putative translocation machinery and since secretion efficiency is reduced, dimerization appears to be a prerequisite for FGF2 secretion. This was observed for FGF1 since it was reported that dimerization plays an important role for the secretion of the growth factor (Jackson et al., 1992). In contrast to FGF2 dimerization, the FGF1 homodimer was shown to be formed in the presence of Cu^{2+} ions by disulfide bonds (Engleka and Maciag, 1992). Consequently, the dimer form is reverted to the monomer form in the presence of reducing agents such as dithiothreitol. Mutations of the cysteine residues involved in dimerization (Cys 30) inhibited the FGF1 secretion in response to heat shock (Jackson et al., 1995; Tarantini et al., 1995). Additionally, FGF1 dimerization is required for and induced by the formation of a multiprotein complex consisting of FGF1, the p40 domain of synaptogamin 1 (Syt-1) and S100A13 (Landriscina et al., 2001a). This complex is thought to be a prerequisite for FGF1 export (Landriscina et al., 2001b). Despite the differences between FGF1 and FGF2 regarding their mode of dimerization, it appears possible that the necessity of dimer formation before secretion might be a common property of FGF export.

4.4.3 Characterization of N-terminally truncated versions of FGF2

N-terminal truncations of FGF2 were performed for reasons which were already explained in section 4.3.2. They were generated by performing a PCR on FGF2-GFP wild-type cDNA using specific primers, thereby truncating N-terminal nucleotides.

$CHO_{MCAT/TAM2}$ cells were retrovirally transduced with truncated versions of the reporter construct, followed by sorting of cell pools expressing the mutated fusion proteins in a doxicycline-dependent manner (for generation of cell lines refer to section 3.1). These pools were characterized with regard to unconventional secretion and binding efficiency to heparin and HSPGs employing the four read-out systems described in section 3.3.2. The analysis of these truncations revealed that deleting the first 20 amino acids form the N-terminus of FGF2 does not result in a different secretion efficiency and binding capacity to heparin when compared to wild-type FGF2. However, truncating more than 20 amino acids at the N-terminus resulted in decreased protein stability and heparin binding capability. These mutants appear to ineffectively secrete the truncated versions of FGF2-GFP, as demonstrated by the signal for FGF2-GFP detected on the cell surface by employing FACS analysis and biotinylation (section 3.3.5.1). However it is questionable if instable proteins, probably partially misfolded, are targeted efficiently to the transport machinery. From these results it has to be concluded, that the first 20 amino acids, which are part of a region of unknown structure are not involved in the transport process of FGF2. As already known from the literature, amino acids located from position 20 to 30 contribute to heparin binding (Baird et al., 1988; Heath et al., 1991). However, deletion of these amino acids does not lead to a block of heparin binding, because an additional heparin binding site remains which lies in the C-terminal part of FGF2 (Li et al., 1994).

4.4.4 Characterization of C-terminally truncated versions of FGF2

We were able in our laboratory to identify galectin counter receptors (i.e. β-galactoside-containing cell surface glycolipids and/or glycoproteins) as essential components of the overall process of galectin-1 secretion (Seelenmeyer et al., 2005). 26 single-site mutations were identified that cause both binding deficiency to counter receptors and export deficiency (Seelenmeyer et al., 2005). These data provide a potential explanation for the apparent non-existence of a linear targeting motif in galectin-1 that directs sorting to the nonclassical export pathway. Moreover, these data suggest a direct role of counter receptors as export adaptors and the β-galactoside binding motif of galectin-1 as the primary targeting element. Recent experiments performed in our laboratory suggest a similar involvement of heparan sulfate proteoglycans in the secretion of FGF2. It was shown *in vitro* that inside-out

vesicles derived from the plasma membrane of CHO cells translocate FGF2 and galectin-1 into the lumen of the vesicles in presence of cytosol. However, if vesicles derived from CHO cells treated with sodium chlorate to inhibit sulfatation of heparan sulfates (Baeuerle and Huttner, 1986; Safaiyan et al., 1999), FGF2 was not shown to translocate into inside-out vesicles (Schäfer et al., 2004). Accordingly, *in vivo* experiments were conducted to examine the secretion efficiency of CHO cells treated with high-salt containing buffer. It was demonstrated that FGF2-GFP was secreted less efficiently from these cells as analyzed by FACS analysis and IP (unpublished data). Moreover, a mutant CHO cell line (CHOpgsA-745), defective in the synthesis of glycosaminoglycans due to lack of activity of xylosyl transferase (Esko et al., 1985) was retrovirally transduced with FGF2-GFP resulting in FGF2-GFP expression in a doxicycline-dependent manner. Because of lacking HSPGs on the cell surface, FGF2-GFP is not able to bind to the cell surface, but would remain in the medium if secretion occurs. It was not possible to detect neither FGF2-GFP bound to the cell surface nor FGF2-GFP present in the medium of the cells, suggesting a FGF2-GFP secretion deficiency (unpublished data). Most strikingly, when CHOpgsA-745 expressing FGF2-GFP were cultivated with $CHO_{MCAT/TAM2}$ cells on the same culture plate but spatially separated by different cover slips, FGF2-GFP could not be detected on the cell surface of $CHO_{MCAT/TAM2}$ cells. However, when both cell lines were in close contact due to cultivation on the same cover slip, FGF2-GFP appeared on the cell surface of $CHO_{MCAT/TAM2}$ cells (unpublished data). These results strongly suggest that heparan sulfate proteoglycans are required for the secretion of FGF2-GFP. A major aim of this thesis was therefore to generate non-heparin binding mutants of FGF2 in order to clarify the role of heparan sulfate proteoglycans in the secretion mechanism of FGF2. In contrast to galectin-1 and as discussed in the previous sections, FGF2 single-site mutations were not able to cause binding deficiency. Additionally, N-terminal truncations, thereby deleting a predicted binding motif did not result in binding or secretion deficiency. However, Heparin binding of FGF2 is proposed to be mainly mediated by two C-terminal residues. It was demonstrated that mutation of two lysines to glutamine (K128Q and K138Q) leads to a significantly reduced affinity of FGF2 to heparin (Li et al., 1994). Therefore, truncations were generated to delete the C-terminal heparin binding motif of FGF2 by performing a PCR using specific primers to delete C-terminal amino acids (for cloning strategy see section 3.3.1.4). The various constructs were stably integrated into the

genome of $CHO_{MCAT/TAM2}$ cells using a retroviral gene transfer system and followed by FACS sortings in absence and presence of doxicycline to generate cell pools expressing the truncated fusion proteins in a doxicycline-dependent manner (refer to section 3.1). These cell pools were finally characterized with regard to unconventional secretion, as well as binding efficiency to heparin and HSPGs employing the four read-out systems described in section 3.3.2. The analysis of these truncations demonstrated that the C-terminus of FGF2 plays a major role in heparin binding efficiency. In contrast to point mutations and N-terminal truncations, removing the C-terminal binding motifs leads to a loss of binding to heparin and heparan sulfate proteoglycans. All truncations demonstrated a significantly reduced signal for intracellular fusion protein as observed by FACS analysis. Interestingly, no truncation was found to be able to bind to heparan sulfate proteoglycans. These results suggest that a correctly folded, intact and complete protein is necessary to ensure protein stability and to be bound to HSPG. However, affinity of FGF2 to heparin and heparan sulfate proteoglycans are shown to be different throughout different truncations, because deletion of 19 amino acids from the C-terminus of FGF2 does not influence affinity of FGF2 to heparin, although this truncation is not able to bind to HSPGs, indicating a different affinity of FGF2 to heparin as to heparan sulfate proteoglycans. By truncating 29 amino acids, the heparin binding efficiency is reduced to about 50% as compared to wild-type protein, probably because of impairing the heparin binding motifs (predicted by Li et al., 1994). Further truncation of FGF2 led to a complete heparin binding deficiency. The standardised read-out systems were used to analyze the secretion efficiency of the truncated FGF2-GFP versions. Since the truncations were shown to be negative for binding to HSPGs *in vivo*, a signal for secreted FGF2-GFP versions was not expected and finally also not shown by performing the standard assays (FACS analysis and cell surface biotinylation). However, the truncated versions of the fusion protein, if secreted from cells, should be present in the medium of the cells. Therefore, an additional experiment was performed to precipitate secreted fusion protein potentially present in the medium (section 3.4.1). Anti-GFP antibodies were used in order to precipitate FGF2-GFP wild-type protein, as well as the different truncated versions of the fusion protein, but it was not possible to immunoprecipitate any fusion protein from the conditioned medium. This experiment shows that wild-type FGF2 is completely bound to the cell surface and thus not detectable in the medium but since the

truncations were also not precipitated from the medium as analyzed by IP, it appears possible that C-terminal truncated versions of FGF2 are not secreted from cells. However, it has been reported, that binding to heparan sulfate proteoglycans stabilizes FGF2 from degradation (Ornitz and Itoh, 2001), therefore it remains to be verified whether these observation are caused by secretion deficiency or by rapid degradation of the C-terminal truncated versions of FGF2. During this thesis, heparin-binding deficient truncations of FGF2 were successfully generated and if they prove to be also secretion deficient, evidence would be provided for a requirement of heparan sulfate proteoglycans in the secretion process of FGF2.

4.4.5 Detailed analysis of mutant 156 with regard to secretion efficiency, protein stability, heparin and heparan sulfate binding efficiency

The mutant rM 156, consisting of three individual amino acid changes (E87K, K128E and R129Q), was analyzed during the screening process of mutants generated by random mutagenesis and showed thereby striking differences to wild-type cells regarding unconventional secretion and binding efficiency to heparan sulfate proteoglycans. The secretion efficiency of rM 156 was significantly reduced compared to wild-type protein as demonstrated by the standard assays described in section 3.3.2. Additionally, this mutant was shown to be deficient for heparan sulfate proteoglycan binding *in vivo*, but strikingly, was able to bind to heparin *in vitro*. To elucidate if one amino acid change or a combination of the three mutations in rM 156 mediate secretion- and HSPG-binding deficiency, individual point mutations, identical to those of mutant rM 156, were generated by site-directed mutagenesis. They were already analyzed during the screening process of point mutations. In this screening, the mutants 36 (E87K), 45 (K128E) and 46 (R129Q) did not demonstrate a difference in secretion efficiency and heparin binding characteristics as compared to wild-type protein, indicating that a combination of all amino acid changes is necessary to loose affinity of FGF2 to heparan sulfate proteoglycans and to reduce secretion efficiency. These mutants were further characterized with regard to degradation and binding affinity to heparan sulfate proteoglycans.

To exclude that the reduced signal of secreted FGF2 bound to the cell surface observed in the secretion assays for rM 156 is caused by less available fusion protein due to a higher degree of protein degradation, the fate of the fusion protein in

the medium was monitored by the following experiment (figure 3.121). The different fusion proteins obtained from mutant rM 156, 36, 45 and 46 were incubated in conditioned medium derived from CHO cells for 24 h at 4°C. The mutated versions of FGF2-GFP were analysed by SDS-PAGE and Western blotting and the signal detected was about 50% as compared to the positive control for both wild-type and mutated proteins, showing that FGF2-GFP, independently of mutations, was degraded to the same extent at 4°C as well as after performing a temperature shift to 37°C. This result provides evidence that introduction of these specific mutations into FGF2 does not influence the degree of protein degradation, suggesting that the signal observed for rM 156 is not reduced due to a decreased amount of available fusion protein in the medium caused by degradation. A second experiment was conducted to test the ability of the different fusion proteins to bind to heparan sulfate proteoglycans. It remains possible that the signal for cell surface associated, secreted FGF2 is reduced because of the missing ability of the FGF2 mutant to bind to heparan sulfate proteoglycans. Therefore, the binding of FGF2 and mutants to HSPGs was verified using cell free supernatant derived from wild-type, rM 156 and point mutation 36 cells (see figure 3.122). The various proteins were incubated with $CHO_{MCAT/TAM2}$ cells for different periods of time and at different temperatures to mediate binding to cell surface-associated HSPGs. Cells were then prepared and analyzed by flow cytometry. This experiment suggests that binding of wild-type fusion protein to the cell surface is temperature-sensitive, since only 15% of the fusion protein still binds to the cell surface at 4°C after 1 h as compared to incubation at 37°C for 1 h. Prolonging the incubation time or shifting the temperature to 37°C did not result in a different signal as observed before for 1 h at 4°C. It is most likely that the reduced signal detected at 4°C is caused by temperature sensitive binding of FGF2 to HSPGs and that the signal observed for protein incubated for 16 h at 37°C is reduced by proteolytical degradation of the fusion protein. This result was confirmed by the analysis of point mutation 36, because the results for this mutant are similar to those made for wild-type FGF2-GFP, although the ability to bind to HSPGs at 4°C is slightly enhanced. Strikingly, in contrast to wild-type protein, cell surface staining could not be detected with flow cytometry for the mutant rM 156, indicating a total defect in binding of the mutated fusion protein to HSPGs, irrespective of temperature and incubation time. Because of the degradation experiment described previously in this section, it has to be excluded that a higher

degree of degradation for mutant rM 156 compared to wild-type protein is responsible for the reduced signal in this assay.

To verify the results obtained by the screening of mutants obtained by random mutagenesis and point mutations, the standardised screening assays were repeated using the mutant cell lines described in this section. Unfortunately the result obtained in previous experiments could no longer be observed. Performing flow cytometry and cell surface biotinylation of the mutant rM 156 revealed that the amount of FGF2-GFP bound to the cell surface is comparable for the mutant and wild-type cells. Strikingly, mutant rM 156 was still negative for HSPG-binding in *in vivo* binding assays. This observation raises an important question: Why is biosynthetic mutated FGF2-GFP secreted from the mutant rM 156 detected in association with cell surface localized heparan sulfate proteoglycans by flow cytometry and cell surface biotinylation, although it was shown to be deficient in HSPG binding? So far, this question remains unanswered. An artefact from the experiments obtained can be excluded, because, as shown in section 4.2, the robust *in vivo* secretion assay using flow cytometry demonstrated a specific detection of FGF2-GFP bound to HSPGs of CHO cells. A hypothesis to explain this discrepancy would be that FGF2-GFP is somehow modified during the transport which causes an enhanced affinity of FGF2 to heparan sulfate proteoglycans. It then appears likely that a modification would occur in the heparin binding motif, because the amino acid changed at position 128 and 129 in mutant rM 156 belong to a predicted heparin-binding motif (Li et al., 1994).

4.4.6 Future perspectives

The FGF2 secretion assay based on flow cytometry described in the first part of this study is a powerful tool for the analysis of the molecular machinery mediating FGF2 export. For example, the systematic testing of candidate proteins (e.g. identified by interaction studies or genetic screening in mammalian cells) can be carried out by transiently inhibiting their biosynthesis based on RNA interference (Elbashir et al., 2001). In this context, a considerable advantage of the FGF2-GFP-based system is that total protein expression (GFP-derived fluorescence) and secreted FGF2-GFP (PE-derived cell surface staining) can be measured independently. Therefore, a phenotype determined by APC-derived cell surface staining can be corrected by normalization based on the degree of total FGF2-GFP expression. Due to the lack of

FGF receptors in CHO cells, another unique feature of the experimental system described is the uncoupling of FGF2 externalization from FGF2 signalling. Therefore, FGF2 export can be studied without the risk of secondary effects provoked by the action of the secreted product.

Another obvious application is a systematic high throughput screening for inhibitors (e.g. derived from natural compound libraries) of FGF2 secretion and the subsequent functional identification of their cellular targets. Given the biological function of FGF2 as a direct stimulator of tumour angiogenesis (Bikfalvi et al., 1997), inhibitors of FGF2 secretion might have strong biomedical implications as potential lead compounds for the development of anti-angiogenic drugs.

In the second part of this study, the secretion assay was used to carry out a genetic screen based on the mutagenesis of FGF2 in order to elucidate a potential motif which targets FGF2 to its transport machinery. Unfortunately, after mutagenesis of FGF2 and characterization of a vast variety of different mutants with regard to unconventional secretion, it was not possible to define a linear amino acid motif that influences FGF2 secretion. However, by performing C-terminal truncations of FGF2, it was possible to impair the heparin binding ability of FGF2. Several observations as already described in detail in section 4.4.4 have been made recently which support the hypothesis that FGF2-GFP secretion might depend on the interaction of heparin binding motifs of FGF2 with heparan sulfate proteoglycans present on the cell surface. Sodium chlorate treatment of cells led to a dramatic decrease of FGF2 secretion efficiency (unpublished data). Strikingly, CHOpgsA-745 cells lacking glycosylaminoglycans were shown to be secretion deficient (unpublished data) and FGF2 export was reconstituted when CHOpgsA-745 cells were in close contact to $CHO_{MCAT/TAM2}$ cells which are suggested to provided the HSPGs required for the unconventional secretion of FGF2-GFP (unpublished data). It remains elusive how the translocation over the plasma membrane of FGF2-GFP is facilitated. A highly speculative model would be that FGF2 is transported through a putative plasma membrane resident pore and heparan sulfate proteoglycans are involved in the translocation as cargo adaptors, exerting a pulling force that is required for the directional transport of FGF2. This model would be consistent to the observation that membrane translocation occurs in a folded state (Backhaus et al., 2004) since only properly folded FGF2 binds to heparin (Seddon et al., 1991). Finally, this model provides a functional basis for quality control in the overall process of FGF2 secretion.

As the heparin binding motif of FGF2 is shown to be the primary target element for secretion, quality control is in place since only properly folded FGF2 will be recognized by the export machinery. The next step would be the analysis of the heparin binding deficient C-terminal truncations with regard to secretion efficiency and degradation in order to verify if heparan sulfate proteoglycans are involved in FGF2 secretion. However, the mutants described in this thesis provide a basis for future studies to analyze the mechanism of FGF2 secretion.

5 Abbreviations

ABC	ATP binding cassette
APC	allophycocyanin
APS	ammonium peroxo disulphate
ATP	adenosin triphosphate
BFA	brefeldin A
bp	basepairs
CDB	cell dissociation buffer
CHO	Chinese hamster ovary (cells)
CRD	carbohydrate recognition domain
C-terminal	carboxy terminal
DMSO	dimethyl sulphoxide
DNA	desoxyribonucleic acid
E.coli	*Escherichia coli*
e.g.	*exempli gratia*
ECL	enhanced chemoluminescence
EDTA	ethylenediaminetetraacetic acid
En2	engrailed 2
ER	endoplasmatic reticulum
et al.	*et altera*
FACS	fluorescence activated cell sorting
FCS	fetal calf serum
FGF2	fibroblast growth factor 2
FGFR	fibroblast growth factor receptor
FV	Foamy virus
g	gravitation
Gal-1	galectin-1
GFP	green fluorescence protein
GTP	guanosine triphosphate
h	hour
HASPB	hydrophilic acylated surface protein B
HCl	hydrochlorid acid
HIV	human immunodeficiency virus

HMGB	high mobility group protein
HRP	horse raddish peroxidase
HS	heparan sulfate
HSPG	heparan sulfate proteoglycans
i.e.	*id est*
IgG	Immunoglobulin G
IL	interleukin
kDa	kilo Dalton
LTR	long terminal repeat
MCAT	Mouse cationic amino acid transporter
MIF	migration inhibtory factor
NLS	nuclear localization signal
nm	Nanometer (wavelength)
ORF	open reading frame
ORF	open reading frame
PAGE	polyacrylamide gel electrophoresis
PBS	phosphate buffered saline
PCR	polymerase chain reaction
PE	phycoerythrin
PTS	peroxisomal targeting sequence
PVDF	polyvinyliden fluoride
RNA	ribonucleic acid
SDS	sodium dodecyl sulfate
SRP	signal recognition particle
Tat	HIV transactivator protein
TEMED	N,N;N´,N´-tetramethylethylenediamine
Tris	Tris[hydroxymethyl]aminoethane
TRX	thioredoxin
Tween 20	polyoxethylene sorbitane monolaureate
U	units (enzyme activity)
v/v	volume/volume relationship
VEGF	vascular endothelian growth factor
w/v	weight/volume relationship
α-MEM	α-modification of Minimal Essential Medium

6 References

Abeijon, C. and Hirschberg, C. B. (1992). Topography of glycosylation reactions in the endoplasmic reticulum. *Trends Biochem Sci* **17**, 32-6.

Abraham, J. A., Whang, J. L., Tumolo, A., Mergia, A., Friedman, J., Gospodarowicz, D. and Fiddes, J. C. (1986). Human basic fibroblast growth factor: nucleotide sequence and genomic organization. *Embo J* **5**, 2523-8.

Ago, H., Kitagawa, Y., Fujishima, A., Matsuura, Y. and Katsube, Y. (1991). Crystal structure of basic fibroblast growth factor at 1.6 A resolution. *J Biochem (Tokyo)* **110**, 360-3.

Aints, A., Guven, H., Gahrton, G., Smith, C. I. and Dilber, M. S. (2001). Mapping of herpes simplex virus-1 VP22 functional domains for inter- and subcellular protein targeting. *Gene Ther* **8**, 1051-6.

Albritton, L. M., Tseng, L., Scadden, D. and Cunningham, J. M. (1989). A putative murine ecotropic retrovirus receptor gene encodes a multiple membrane-spanning protein and confers susceptibility to virus infection. *Cell* **57**, 659-66.

Andrei, C., Dazzi, C., Lotti, L., Torrisi, M. R., Chimini, G. and Rubartelli, A. (1999). The secretory route of the leaderless protein interleukin 1beta involves exocytosis of endolysosome-related vesicles. *Mol Biol Cell* **10**, 1463-75.

Auron, P. E., Warner, S. J., Webb, A. C., Cannon, J. G., Bernheim, H. A., McAdam, K. J., Rosenwasser, L. J., LoPreste, G., Mucci, S. F. and Dinarello, C. A. (1987). Studies on the molecular nature of human interleukin 1. *J Immunol* **138**, 1447-56.

Backhaus, R., Zehe, C., Wegehingel, S., Kehlenbach, A., Schwappach, B. and Nickel, W. (2004). Unconventional protein secretion: membrane translocation of FGF-2 does not require protein unfolding. *J Cell Sci* **117**, 1727-36.

Baeuerle, P. A. and Huttner, W. B. (1986). Chlorate--a potent inhibitor of protein sulfation in intact cells. *Biochem Biophys Res Commun* **141**, 870-7.

Baeuerle, P. A. and Huttner, W. B. (1987). Tyrosine sulfation is a trans-Golgi-specific protein modification. *J Cell Biol* **105**, 2655-64.

Baird, A., Schubert, D., Ling, N. and Guillemin, R. (1988). Receptor- and heparin-binding domains of basic fibroblast growth factor. *Proc Natl Acad Sci U S A* **85**, 2324-8.

Balch, W. E. and Rothman, J. E. (1985). Characterization of protein transport between successive compartments of the Golgi apparatus: asymmetric properties of donor and acceptor activities in a cell-free system. *Arch Biochem Biophys* **240**, 413-25.

Baldin, V., Roman, A. M., Bosc-Bierne, I., Amalric, F. and Bouche, G. (1990). Translocation of bFGF to the nucleus is G1 phase cell cycle specific in bovine aortic endothelial cells. *Embo J* **9**, 1511-7.

Ballensiefen, W., Ossipov, D. and Schmitt, H. D. (1998). Recycling of the yeast v-SNARE Sec22p involves COPI-proteins and the ER transmembrane proteins Ufe1p and Sec20p. *J Cell Sci* **111 (Pt 11)**, 1507-20.

Balmer, Y., Vensel, W. H., Tanaka, C. K., Hurkman, W. J., Gelhaye, E., Rouhier, N., Jacquot, J. P., Manieri, W., Schurmann, P., Droux, M. et al. (2004). Thioredoxin links redox to the regulation of fundamental processes of plant mitochondria. *Proc Natl Acad Sci U S A* **101**, 2642-7.

Barlowe, C., Orci, L., Yeung, T., Hosobuchi, M., Hamamoto, S., Salama, N., Rexach, M. F., Ravazzola, M., Amherdt, M. and Schekman, R. (1994). COPII: a membrane coat formed by Sec proteins that drive vesicle budding from the endoplasmic reticulum. *Cell* **77**, 895-907.

Bechtner, G., Potscher, C. and Gartner, R. (1992). Role of autocrine and paracrine factors in thyroid follicle growth. *Thyroidology* **4**, 1-5.

Becker-Hapak, M., McAllister, S. S. and Dowdy, S. F. (2001). TAT-mediated protein transduction into mammalian cells. *Methods* **24**, 247-56.

Bernhagen, J., Calandra, T. and Bucala, R. (1998). Regulation of the immune response by macrophage migration inhibitory factor: biological and structural features. *J Mol Med* **76**, 151-61.

Bikfalvi, A., Klein, S., Pintucci, G. and Rifkin, D. B. (1997). Biological roles of fibroblast growth factor-2. *Endocr Rev* **18**, 26-45.

Bouche, G., Gas, N., Prats, H., Baldin, V., Tauber, J. P., Teissie, J. and Amalric, F. (1987). Basic fibroblast growth factor enters the nucleolus and stimulates the transcription of ribosomal genes in ABAE cells undergoing G0----G1 transition. *Proc Natl Acad Sci U S A* **84**, 6770-4.

Briles, E. B., Gregory, W., Fletcher, P. and Kornfeld, S. (1979). Vertebrate lectins, Comparison of properties of beta-galactoside-binding lectins from tissues of calf and chicken. *J Cell Biol* **81**, 528-37.

Brodsky, J. L. (1998). Translocation of proteins across the endoplasmic reticulum membrane. *Int Rev Cytol* **178**, 277-328.

Brucato, S., Bocquet, J. and Villers, C. (2002). Cell surface heparan sulfate proteoglycans: target and partners of the basic fibroblast growth factor in rat Sertoli cells. *Eur J Biochem* **269**, 502-11.

Burgess, W. H. and Maciag, T. (1989). The heparin-binding (fibroblast) growth factor family of proteins. *Annu Rev Biochem* **58**, 575-606.

Calandra, T. (2003). Macrophage migration inhibitory factor and host innate immune responses to microbes. *Scand J Infect Dis* **35**, 573-6.

Chang, H. C., Samaniego, F., Nair, B. C., Buonaguro, L. and Ensoli, B. (1997). HIV-1 Tat protein exits from cells via a leaderless secretory pathway and binds to extracellular matrix-associated heparan sulfate proteoglycans through its basic region. *Aids* **11**, 1421-31.

Choi, J., Ko, M. K. and Kay, E. P. (2000). Subcellular localization of the expressed 18 kDa FGF-2 isoform in corneal endothelial cells. *Mol Vis* **6**, 222-231.

Christophe, D., Christophe-Hobertus, C. and Pichon, B. (2000). Nuclear targeting of proteins: how many different signals? *Cell Signal* **12**, 337-41.

Cleves, A. E., Cooper, D. N., Barondes, S. H. and Kelly, R. B. (1996). A new pathway for protein export in Saccharomyces cerevisiae. *J Cell Biol* **133**, 1017-26.

Cleves, A. E. and Kelly, R. B. (1996). Rehearsing the ABCs. Protein translocation. *Curr Biol* **6**, 276-8.

Cooper, D. N. and Barondes, S. H. (1990). Evidence for export of a muscle lectin from cytosol to extracellular matrix and for a novel secretory mechanism. *J Cell Biol* **110**, 1681-91.

Couraud, P. O., Casentini-Borocz, D., Bringman, T. S., Griffith, J., McGrogan, M. and Nedwin, G. E. (1989). Molecular cloning, characterization, and expression of a human 14-kDa lectin. *J Biol Chem* **264**, 1310-6.

Crissman, H. A., Oka, M. S. and Steinkamp, J. A. (1976). Rapid staining methods for analysis of deoxyribonucleic acid and protein in mammalian cells. *J Histochem Cytochem* **24**, 64-71.

Dahl, J. P., Binda, A., Canfield, V. A. and Levenson, R. (2000). Participation of Na,K-ATPase in FGF-2 Secretion: Rescue of Ouabain- Inhibitable FGF-2 Secretion by Ouabain-Resistant Na,K-ATPase alpha Subunits. *Biochemistry* **39**, 14877-14883.

Davey, R. A., Hamson, C. A., Healey, J. J. and Cunningham, J. M. (1997). In vitro binding of purified murine ecotropic retrovirus envelope surface protein to its receptor, MCAT-1. *J. Virol.* **71**, 8096-102.

Denny, P. W., Gokool, S., Russell, D. G., Field, M. C. and Smith, D. F. (2000). Acylation-dependent protein export in Leishmania. *J Biol Chem* **275**, 11017-25.

Derossi, D., Chassaing, G. and Prochiantz, A. (1998). Trojan peptides: the penetratin system for intracellular delivery. *Trends Cell Biol* **8**, 84-7.

Dietrich, L. E., Peplowska, K., LaGrassa, T. J., Hou, H., Rohde, J. and Ungermann, C. (2005). The SNARE Ykt6 is released from yeast vacuoles during an early stage of fusion. *EMBO Rep* **6**, 245-50.

Dinarello, C. A. (1985). An update on human interleukin-1: from molecular biology to clinical relevance. *J Clin Immunol* **5**, 287-97.

Dinarello, C. A. (1997). Interleukin-1. *Cytokine Growth Factor Rev* **8**, 253-65.

Eickhoff, R., Wilhelm, B., Renneberg, H., Wennemuth, G., Bacher, M., Linder, D., Bucala, R., Seitz, J. and Meinhardt, A. (2001). Purification and characterization of macrophage migration inhibitory factor as a secretory protein from rat epididymis: evidences for alternative release and transfer to spermatozoa. *Mol Med* **7**, 27-35.

Elliott, G. and O'Hare, P. (1997). Intercellular trafficking and protein delivery by a herpesvirus structural protein. *Cell* **88**, 223-33.

Elliott, G. and O'Hare, P. (1999). Live-cell analysis of a green fluorescent protein-tagged herpes simplex virus infection. *J Virol* **73**, 4110-9.

Elliott, G. and O'Hare, P. (2000). Cytoplasm-to-nucleus translocation of a herpesvirus tegument protein during cell division [In Process Citation]. *J Virol* **74**, 2131-41.

Endo, T., Yamamoto, H. and Esaki, M. (2003). Functional cooperation and separation of translocators in protein import into mitochondria, the double-membrane bounded organelles. *J Cell Sci* **116**, 3259-67.

Engleka, K. A. and Maciag, T. (1992). Inactivation of human fibroblast growth factor-1 (FGF-1) activity by interaction with copper ions involves FGF-1 dimer formation induced by copper-catalyzed oxidation. *J. Biol. Chem.* **267**, 11307-15.

Engling, A., Backhaus, R., Stegmayer, C., Zehe, C., Seelenmeyer, C., Kehlenbach, A., Schwappach, B., Wegehingel, S. and Nickel, W. (2002). Biosynthetic FGF-2 is targeted to non-lipid raft microdomains following translocation to the extracellular surface of CHO cells. *J Cell Sci* **115**, 3619-31.

Eriksson, A. E., Cousens, L. S., Weaver, L. H. and Matthews, B. W. (1991). Three-dimensional structure of human basic fibroblast growth factor. *Proc Natl Acad Sci U S A* **88**, 3441-5.

Ernst, J. F. and Prill, S. K. (2001). O-glycosylation. *Med Mycol* **39 Suppl 1**, 67-74.

Esko, J. D. and Selleck, S. B. (2002). Order out of chaos: assembly of ligand binding sites in heparan sulfate. *Annu Rev Biochem* **71**, 435-71.

Esko, J. D., Stewart, T. E. and Taylor, W. H. (1985). Animal cell mutants defective in glycosaminoglycan biosynthesis. *Proc Natl Acad Sci U S A* **82**, 3197-201.

Faham, S., Hileman, R. E., Fromm, J. R., Linhardt, R. J. and Rees, D. C. (1996). Heparin structure and interactions with basic fibroblast growth factor. *Science* **271**, 1116-20.

Flaumenhaft, R., Moscatelli, D. and Rifkin, D. B. (1990). Heparin and heparan sulfate increase the radius of diffusion and action of basic fibroblast growth factor. *J Cell Biol* **111**, 1651-9.

Flieger, O., Engling, A., Bucala, R., Lue, H., Nickel, W. and Bernhagen, J. (2003). Regulated secretion of macrophage migration inhibitory factor is mediated by a non-classical pathway involving an ABC transporter. *FEBS Lett* **551**, 78-86.

Flinn, H. M., Rangarajan, D. and Smith, D. F. (1994). Expression of a hydrophilic surface protein in infective stages of Leishmania major. *Mol Biochem Parasitol* **65**, 259-70.

Florkiewicz, R. Z., Anchin, J. and Baird, A. (1998). The inhibition of fibroblast growth factor-2 export by cardenolides implies a novel function for the catalytic subunit of Na+,K+-ATPase. *J Biol Chem* **273**, 544-51.

Florkiewicz, R. Z., Majack, R. A., Buechler, R. D. and Florkiewicz, E. (1995). Quantitative export of FGF-2 occurs through an alternative, energy-dependent, non-ER/Golgi pathway. *J Cell Physiol* **162**, 388-99.

Florkiewicz, R. Z. and Sommer, A. (1989). Human basic fibroblast growth factor gene encodes four polypeptides: three initiate translation from non-AUG codons. *Proc Natl Acad Sci U S A* **86**, 3978-81.

Gardella, S., Andrei, C., Ferrera, D., Lotti, L. V., Torrisi, M. R., Bianchi, M. E. and Rubartelli, A. (2002). The nuclear protein HMGB1 is secreted by monocytes via a non-classical, vesicle-mediated secretory pathway. *EMBO Rep*.

Gilmore, R., Blobel, G. and Walter, P. (1982a). Protein translocation across the endoplasmic reticulum. I. Detection in the microsomal membrane of a receptor for the signal recognition particle. *J Cell Biol* **95**, 463-9.

Gilmore, R., Walter, P. and Blobel, G. (1982b). Protein translocation across the endoplasmic reticulum. II. Isolation and characterization of the signal recognition particle receptor. *J Cell Biol* **95**, 470-7.

Gimenez-Gallego, G., Rodkey, J., Bennett, C., Rios-Candelore, M., DiSalvo, J. and Thomas, K. (1985). Brain-derived acidic fibroblast growth factor: complete amino acid sequence and homologies. *Science* **230**, 1385-8.

Giron, M. L., de The, H. and Saib, A. (1998). An evolutionarily conserved splice generates a secreted env-Bet fusion protein during human foamy virus infection. *J Virol* **72**, 4906-10.

Gkantiragas, I., Brugger, B., Stuven, E., Kaloyanova, D., Li, X. Y., Lohr, K., Lottspeich, F., Wieland, F. T. and Helms, J. B. (2001). Sphingomyelin-enriched microdomains at the Golgi complex. *Mol Biol Cell* **12**, 1819-33.

Gleizes, P. E., Noaillac-Depeyre, J., Amalric, F. and Gas, N. (1995). Basic fibroblast growth factor (FGF-2) internalization through the heparan sulfate proteoglycans-mediated pathway: an ultrastructural approach. *Eur J Cell Biol* **66**, 47-59.

Gloe, T., Sohn, H. Y., Meininger, G. A. and Pohl, U. (2002). Shear stress-induced release of basic fibroblast growth factor from endothelial cells is mediated by matrix interaction via integrin alpha(v)beta3. *J Biol Chem* **277**, 23453-8.

Goldstein, G. (1996). HIV-1 Tat protein as a potential AIDS vaccine. *Nat Med* **2**, 960-4.

Goodson, H. V., Valetti, C. and Kreis, T. E. (1997). Motors and membrane traffic. *Curr Opin Cell Biol* **9**, 18-28.

Gordon, D. M., Dancis, A. and Pain, D. (2000). Mechanisms of mitochondrial protein import. *Essays Biochem* **36**, 61-73.

Gorlich, D. and Kutay, U. (1999). Transport between the cell nucleus and the cytoplasm. *Annu Rev Cell Dev Biol* **15**, 607-60.

Gospodarowicz, D. (1991). Biological activities of fibroblast growth factors. *Ann N Y Acad Sci* **638**, 1-8.

Guimond, S., Maccarana, M., Olwin, B. B., Lindahl, U. and Rapraeger, A. C. (1993). Activating and inhibitory heparin sequences for FGF-2 (basic FGF). Distinct requirements for FGF-1, FGF-2, and FGF-4. *J Biol Chem* **268**, 23906-14.

Guimond, S. E. and Turnbull, J. E. (1999). Fibroblast growth factor receptor signalling is dictated by specific heparan sulphate saccharides. *Curr Biol* **9**, 1343-6.

Guo, W., Grant, A. and Novick, P. (1999). Exo84p is an exocyst protein essential for secretion. *J Biol Chem* **274**, 23558-64.

Hamon, Y., Luciani, M. F., Becq, F., Verrier, B., Rubartelli, A. and Chimini, G. (1997). Interleukin-1beta secretion is impaired by inhibitors of the Atp binding cassette transporter, ABC1. *Blood* **90**, 2911-5.

Hanisch, F. G. (2001). O-glycosylation of the mucin type. *Biol Chem* **382**, 143-9.

Hanson, P. I., Heuser, J. E. and Jahn, R. (1997). Neurotransmitter release - four years of SNARE complexes. *Curr Opin Neurobiol* **7**, 310-5.

Harrison, F. L. (1991). Soluble vertebrate lectins: ubiquitous but inscrutable proteins. *J Cell Sci* **100 (Pt 1)**, 9-14.

Haugsten, E. M., Sorensen, V., Brech, A., Olsnes, S. and Wesche, J. (2005). Different intracellular trafficking of FGF1 endocytosed by the four homologous FGF receptors. *J Cell Sci* **118**, 3869-81.

Heath, W. F., Cantrell, A. S., Mayne, N. G. and Jaskunas, S. R. (1991). Mutations in the heparin-binding domains of human basic fibroblast growth factor alter its biological activity. *Biochemistry* **30**, 5608-15.

Hebert, D. N., Simons, J. F., Peterson, J. R. and Helenius, A. (1995). Calnexin, calreticulin, and Bip/Kar2p in protein folding. *Cold Spring Harb Symp Quant Biol* **60**, 405-15.

Hendil, K. B. and Hartmann-Petersen, R. (2004). Proteasomes: a complex story. *Curr Protein Pept Sci* **5**, 135-51.

Heneine, W., Schweizer, M., Sandstrom, P. and Folks, T. (2003). Human infection with foamy viruses. *Curr Top Microbiol Immunol* **277**, 181-96.

Herr, A. B., Ornitz, D. M., Sasisekharan, R., Venkataraman, G. and Waksman, G. (1997). Heparin-induced self-association of fibroblast growth factor-2. Evidence for two oligomerization processes. *J Biol Chem* **272**, 16382-9.

Hille, A., Rosa, P. and Huttner, W. B. (1984). Tyrosine sulfation: a post-translational modification of proteins destined for secretion? *FEBS Lett* **177**, 129-34.

Hirabayashi, J. and Kasai, K. (1991). Effect of amino acid substitution by sited-directed mutagenesis on the carbohydrate recognition and stability of human 14-kDa beta-galactoside-binding lectin. *J Biol Chem* **266**, 23648-53.

Holmgren, A. (1989). Thioredoxin and glutaredoxin systems. *J Biol Chem* **264**, 13963-6.

Holroyd, C. and Erdmann, R. (2001). Protein translocation machineries of peroxisomes. *FEBS Lett* **501**, 6-10.

Hsia, E., Richardson, T. P. and Nugent, M. A. (2003). Nuclear localization of basic fibroblast growth factor is mediated by heparan sulfate proteoglycans through protein kinase C signaling. *J Cell Biochem* **88**, 1214-25.

Hugel, B., Martinez, M. C., Kunzelmann, C. and Freyssinet, J. M. (2005). Membrane microparticles: two sides of the coin. *Physiology (Bethesda)* **20**, 22-7.

Hughes, C., Stanley, P. and Koronakis, V. (1992). E. coli hemolysin interactions with prokaryotic and eukaryotic cell membranes. *Bioessays* **14**, 519-25.

Hughes, R. C. (1997). The galectin family of mammalian carbohydrate-binding molecules. *Biochem Soc Trans* **25**, 1194-8.

Hughes, R. C. (1999). Secretion of the galectin family of mammalian carbohydrate-binding proteins. *Biochim Biophys Acta* **1473**, 172-85.

Imamura, T., Engleka, K., Zhan, X., Tokita, Y., Forough, R., Roeder, D., Jackson, A., Maier, J. A., Hla, T. and Maciag, T. (1990). Recovery of mitogenic activity of a growth factor mutant with a nuclear translocation sequence. *Science* **249**, 1567-70.

Imamura, T., Tokita, Y. and Mitsui, Y. (1992). Identification of a heparin-binding growth factor-1 nuclear translocation sequence by deletion mutation analysis. *J Biol Chem* **267**, 5676-9.

Ishihara, M., Guo, Y., Wei, Z., Yang, Z., Swiedler, S. J., Orellana, A. and Hirschberg, C. B. (1993). Regulation of biosynthesis of the basic fibroblast growth factor binding domains of heparan sulfate by heparan sulfate-N-deacetylase/N-sulfotransferase expression. *J Biol Chem* **268**, 20091-5.

Ivessa, N. E., De Lemos-Chiarandini, C., Gravotta, D., Sabatini, D. D. and Kreibich, G. (1995). The Brefeldin A-induced retrograde transport from the Golgi apparatus to the endoplasmic reticulum depends on calcium sequestered to intracellular stores. *J Biol Chem* **270**, 25960-7.

Jackson, A., Friedman, S., Zhan, X., Engleka, K. A., Forough, R. and Maciag, T. (1992). Heat shock induces the release of fibroblast growth factor 1 from NIH 3T3 cells. *Proc Natl Acad Sci U S A* **89**, 10691-5.

Jackson, A., Tarantini, F., Gamble, S., Friedman, S. and Maciag, T. (1995). The release of fibroblast growth factor-1 from NIH 3T3 cells in response to temperature involves the function of cysteine residues. *J Biol Chem* **270**, 33-6.

Johnson, T. L. and Olsen, L. J. (2001). Building new models for peroxisome biogenesis. *Plant Physiol* **127**, 731-9.

Joliot, A., Trembleau, A., Raposo, G., Calvet, S., Volovitch, M. and Prochiantz, A. (1997). Association of Engrailed homeoproteins with vesicles presenting caveolae-like properties. *Development* **124**, 1865-75.

Kabsch, W. and Sander, C. (1983). Dictionary of protein secondary structure: pattern recognition of hydrogen-bonded and geometrical features. *Biopolymers* **22**, 2577-637.

Klaassen, C. D. and Boles, J. W. (1997). Sulfation and sulfotransferases 5: the importance of 3'-phosphoadenosine 5'-phosphosulfate (PAPS) in the regulation of sulfation. *Faseb J* **11**, 404-18.

Kobayashi, Y., Yamamoto, K., Saido, T., Kawasaki, H., Oppenheim, J. J. and Matsushima, K. (1990). Identification of calcium-activated neutral protease as a processing enzyme of human interleukin 1 alpha. *Proc Natl Acad Sci U S A* **87**, 5548-52.

Kopitz, J., von Reitzenstein, C., Burchert, M., Cantz, M. and Gabius, H. J. (1998). Galectin-1 is a major receptor for ganglioside GM1, a product of the growth-controlling activity of a cell surface ganglioside sialidase, on human neuroblastoma cells in culture. *J Biol Chem* **273**, 11205-11.

Kuroiwa, T., Sakaguchi, M., Omura, T. and Mihara, K. (1996). Reinitiation of protein translocation across the endoplasmic reticulum membrane for the topogenesis of multispanning membrane proteins. *J Biol Chem* **271**, 6423-8.

Kurt-Jones, E. A., Beller, D. I., Mizel, S. B. and Unanue, E. R. (1985). Identification of a membrane-associated interleukin 1 in macrophages. *Proc Natl Acad Sci U S A* **82**, 1204-8.

Kurzchalia, T. V. and Parton, R. G. (1999). Membrane microdomains and caveolae. *Curr Opin Cell Biol* **11**, 424-31.

Kwan, C. P., Venkataraman, G., Shriver, Z., Raman, R., Liu, D., Qi, Y., Varticovski, L. and Sasisekharan, R. (2001). Probing fibroblast growth factor dimerization and role of heparin-like glycosaminoglycans in modulating dimerization and signaling. *J Biol Chem* **276**, 23421-9.

Laemmli, U. K. (1970). Cleavage of structural proteins during the assembly of the head of bacteriophage T4. *Nature* **227**, 680-5.

Landriscina, M., Bagala, C., Mandinova, A., Soldi, R., Micucci, I., Bellum, S., Prudovsky, I. and Maciag, T. (2001a). Copper induces the assembly of a multiprotein aggregate implicated in the release of fibroblast growth factor 1 in response to stress. *J Biol Chem* **276**, 25549-57.

Landriscina, M., Prudovsky, I., Mouta Carreira, C., Soldi, R., Tarantini, F. and Maciag, T. (2000). Amlexanox reversibly inhibits cell migration and proliferation and induces the Src-dependent disassembly of actin stress fibers in vitro. *J Biol Chem* **275**, 32753-62.

Landriscina, M., Soldi, R., Bagala, C., Micucci, I., Bellum, S., Tarantini, F., Prudovsky, I. and Maciag, T. (2001b). S100a13 participates in the release of fibroblast growth factor 1 in response to heat shock in vitro. *J Biol Chem* **276**, 22544-52.

LaVallee, T. M., Tarantini, F., Gamble, S., Carreira, C. M., Jackson, A. and Maciag, T. (1998). Synaptotagmin-1 is required for fibroblast growth factor-1 release. *J Biol Chem* **273**, 22217-23.

Lecellier, C. H., Vermeulen, W., Bachelerie, F., Giron, M. L. and Saib, A. (2002). Intra- and intercellular trafficking of the foamy virus auxiliary bet protein. *J Virol* **76**, 3388-94.

Lee, M. C., Miller, E. A., Goldberg, J., Orci, L. and Schekman, R. (2004). Bi-directional protein transport between the ER and Golgi. *Annu Rev Cell Dev Biol* **20**, 87-123.

Lee, P. L., Johnson, D. E., Cousens, L. S., Fried, V. A. and Williams, L. T. (1989). Purification and complementary DNA cloning of a receptor for basic fibroblast growth factor. *Science* **245**, 57-60.

Leffler, H. (2001). Galectins structure and function--a synopsis. *Results Probl Cell Differ* **33**, 57-83.

Leifert, J. A., Harkins, S. and Whitton, J. L. (2002). Full-length proteins attached to the HIV tat protein transduction domain are neither transduced between cells, nor exhibit enhanced immunogenicity. *Gene Ther* **9**, 1422-8.

Li, L. Y., Safran, M., Aviezer, D., Bohlen, P., Seddon, A. P. and Yayon, A. (1994). Diminished heparin binding of a basic fibroblast growth factor mutant is associated with reduced receptor binding, mitogenesis, plasminogen activator induction, and in vitro angiogenesis. *Biochemistry* **33**, 10999-1007.

Lippincott-Schwartz, J., Cole, N. B. and Donaldson, J. G. (1998). Building a secretory apparatus: role of ARF1/COPI in Golgi biogenesis and maintenance. *Histochem Cell Biol* **109**, 449-62.

Lippincott-Schwartz, J., Donaldson, J. G., Schweizer, A., Berger, E. G., Hauri, H. P., Yuan, L. C. and Klausner, R. D. (1990). Microtubule-dependent retrograde transport of proteins into the ER in the presence of brefeldin A suggests an ER recycling pathway. *Cell* **60**, 821-36.

Liu, F. T. (2000). Galectins: a new family of regulators of inflammation. *Clin Immunol* **97**, 79-88.

Liu, F. T., Patterson, R. J. and Wang, J. L. (2002). Intracellular functions of galectins. *Biochim Biophys Acta* **1572**, 263-73.

Liu, X., Constantinescu, S. N., Sun, Y., Bogan, J. S., Hirsch, D., Weinberg, R. A. and Lodish, H. F. (2000). Generation of mammalian cells stably expressing multiple genes at predetermined levels. *Anal. Biochem.* **280**, 20-8.

Lu, W. and Ou, J. H. (2002). Phosphorylation of hepatitis C virus core protein by protein kinase A and protein kinase C. *Virology* **300**, 20-30.

Lucocq, J. M., Brada, D. and Roth, J. (1986). Immunolocalization of the oligosaccharide trimming enzyme glucosidase II. *J Cell Biol* **102**, 2137-46.

Lundberg, M. and Johansson, M. (2001). Is VP22 nuclear homing an artifact? *Nat Biotechnol* **19**, 713-4.

Mach, H., Volkin, D. B., Burke, C. J., Middaugh, C. R., Linhardt, R. J., Fromm, J. R., Loganathan, D. and Mattsson, L. (1993). Nature of the interaction of heparin with acidic fibroblast growth factor. *Biochemistry* **32**, 5480-9.

Maciejewski, P. M., Peterson, F. C., Anderson, P. J. and Brooks, C. L. (1995). Mutation of serine 90 to glutamic acid mimics phosphorylation of bovine prolactin. *J Biol Chem* **270**, 27661-5.

MacKenzie, A., Wilson, H. L., Kiss-Toth, E., Dower, S. K., North, R. A. and Surprenant, A. (2001). Rapid secretion of interleukin-1beta by microvesicle shedding. *Immunity* **15**, 825-35.

Maizel, A., Bensaude, O., Prochiantz, A. and Joliot, A. (1999). A short region of its homeodomain is necessary for engrailed nuclear export and secretion. *Development* **126**, 3183-90.

Maizel, A., Tassetto, M., Filhol, O., Cochet, C., Prochiantz, A. and Joliot, A. (2002). Engrailed homeoprotein secretion is a regulated process. *Development* **129**, 3545-53.

Maniatis, T., Fritsch, E. F. and Sambrook, J. (1989). Molecular Cloning: A Laboratory Manual. Cold Spring Harbor: Cold Spring Harbor Laboratory Press.

Martinez, M. C., Tesse, A., Zobairi, F. and Andriantsitohaina, R. (2005). Shed membrane microparticles from circulating and vascular cells in regulating vascular function. *Am J Physiol Heart Circ Physiol* **288**, H1004-9.

Martin-Verdeaux, S., Pombo, I., Iannascoli, B., Roa, M., Varin-Blank, N., Rivera, J. and Blank, U. (2003). Evidence of a role for Munc18-2 and microtubules in mast cell granule exocytosis. *J Cell Sci* **116**, 325-34.

Maxfield, F. R., Willingham, M. C., Davies, P. J. and Pastan, I. (1979). Amines inhibit the clustering of alpha2-macroglobulin and EGF on the fibroblast cell surface. *Nature* **277**, 661-3.

McKeehan, W. L., Wang, F. and Kan, M. (1998). The heparan sulfate-fibroblast growth factor family: diversity of structure and function. *Prog Nucleic Acid Res Mol Biol* **59**, 135-76.

McNeil, P. L., Muthukrishnan, L., Warder, E. and D'Amore, P. A. (1989). Growth factors are released by mechanically wounded endothelial cells. *J Cell Biol* **109**, 811-22.

McNew, J. A. and Goodman, J. M. (1994). An oligomeric protein is imported into peroxisomes in vivo. *J Cell Biol* **127**, 1245-57.

Mehul, B., Bawumia, S. and Hughes, R. C. (1995). Cross-linking of galectin 3, a galactose-binding protein of mammalian cells, by tissue-type transglutaminase. *FEBS Lett* **360**, 160-4.

Mignatti, P., Morimoto, T. and Rifkin, D. B. (1992). Basic fibroblast growth factor, a protein devoid of secretory signal sequence, is released by cells via a pathway independent of the endoplasmic reticulum-Golgi complex. *J Cell Physiol* **151**, 81-93.

Mignatti, P. and Rifkin, D. B. (1991). Release of basic fibroblast growth factor, an angiogenic factor devoid of secretory signal sequence: a trivial phenomenon or a novel secretion mechanism? *J. Cell. Biochem.* **47**, 201-7.

Miki, T., Bottaro, D. P., Fleming, T. P., Smith, C. L., Burgess, W. H., Chan, A. M. and Aaronson, S. A. (1992). Determination of ligand-binding specificity by alternative splicing: two distinct growth factor receptors encoded by a single gene. *Proc Natl Acad Sci U S A* **89**, 246-50.

Miller, A. C., Schattenberg, D. G., Malkinson, A. M. and Ross, D. (1994). Decreased content of the IL1 alpha processing enzyme calpain in murine bone marrow-derived macrophages after treatment with the benzene metabolite hydroquinone. *Toxicol Lett* **74**, 177-84.

Misumi, Y., Miki, K., Takatsuki, A., Tamura, G. and Ikehara, Y. (1986). Novel blockade by brefeldin A of intracellular transport of secretory proteins in cultured rat hepatocytes. *J Biol Chem* **261**, 11398-403.

Miyakawa, K., Hatsuzawa, K., Kurokawa, T., Asada, M., Kuroiwa, T. and Imamura, T. (1999). A hydrophobic region locating at the center of fibroblast growth factor- 9 is crucial for its secretion. *J Biol Chem* **274**, 29352-7.

Miyake, A., Konishi, M., Martin, F. H., Hernday, N. A., Ozaki, K., Yamamoto, S., Mikami, T., Arakawa, T. and Itoh, N. (1998). Structure and expression of a novel member, FGF-16, on the fibroblast growth factor family. *Biochem Biophys Res Commun* **243**, 148-52.

Moscatelli, D. (1987). High and low affinity binding sites for basic fibroblast growth factor on cultured cells: absence of a role for low affinity binding in the stimulation of plasminogen activator production by bovine capillary endothelial cells. *J Cell Physiol* **131**, 123-30.

Moscatelli, D., Presta, M., Joseph-Silverstein, J. and Rifkin, D. B. (1986). Both normal and tumor cells produce basic fibroblast growth factor. *J Cell Physiol* **129**, 273-6.

Mouta Carreira, C., LaVallee, T. M., Tarantini, F., Jackson, A., Lathrop, J. T., Hampton, B., Burgess, W. H. and Maciag, T. (1998). S100A13 is involved in the regulation of fibroblast growth factor-1 and p40 synaptotagmin-1 release in vitro. *J Biol Chem* **273**, 22224-31.

Muesch, A., Hartmann, E., Rohde, K., Rubartelli, A., Sitia, R. and Rapoport, T. A. (1990). A novel pathway for secretory proteins? *Trends Biochem Sci* **15**, 86-8.

Nakamoto, T., Chang, C. S., Li, A. K. and Chodak, G. W. (1992). Basic fibroblast growth factor in human prostate cancer cells. *Cancer Res* **52**, 571-7.

Neupert, W. (1997). Protein import into mitochondria. *Annu Rev Biochem* **66**, 863-917.

Nickel, W. (2003). The mystery of nonclassical protein secretion. *Eur. J. Biochem.* **270**, 2109-2119.

Nickel, W. (2005). Unconventional secretory routes: direct protein export across the plasma membrane of mammalian cells. *Traffic* **6**, 607-14.

Nickel, W., Malsam, J., Gorgas, K., Ravazzola, M., Jenne, N., Helms, J. B. and Wieland, F. T. (1998). Uptake by COPI-coated vesicles of both anterograde and retrograde cargo is inhibited by GTPgammaS in vitro. *J Cell Sci* **111 (Pt 20)**, 3081-90.

Nickel, W., Weber, T., McNew, J. A., Parlati, F., Sollner, T. H. and Rothman, J. E. (1999). Content mixing and membrane integrity during membrane fusion driven by pairing of isolated v-SNAREs and t-SNAREs. *Proc Natl Acad Sci U S A* **96**, 12571-6.

Ogura, K., Nagata, K., Hatanaka, H., Habuchi, H., Kimata, K., Tate, S., Ravera, M. W., Jaye, M., Schlessinger, J. and Inagaki, F. (1999). Solution structure of human acidic fibroblast growth factor and interaction with heparin-derived hexasaccharide. *J Biomol NMR* **13**, 11-24.

Okada-Ban, M., Thiery, J. P. and Jouanneau, J. (2000). Fibroblast growth factor-2. *Int J Biochem Cell Biol* **32**, 263-7.

Okumura, N., Takimoto, K., Okada, M. and Nakagawa, H. (1989). C6 glioma cells produce basic fibroblast growth factor that can stimulate their own proliferation. *J Biochem (Tokyo)* **106**, 904-9.

Ornitz, D. M. and Itoh, N. (2001). Fibroblast growth factors. *Genome Biol* **2**, REVIEWS3005.

Ortega, S., Ittmann, M., Tsang, S. H., Ehrlich, M. and Basilico, C. (1998). Neuronal defects and delayed wound healing in mice lacking fibroblast growth factor 2. *Proc Natl Acad Sci U S A* **95**, 5672-7.

Ozeki, Y., Matsui, T., Yamamoto, Y., Funahashi, M., Hamako, J. and Titani, K. (1995). Tissue fibronectin is an endogenous ligand for galectin-1. *Glycobiology* **5**, 255-61.

Pace, K. E., Lee, C., Stewart, P. L. and Baum, L. G. (1999). Restricted receptor segregation into membrane microdomains occurs on human T cells during apoptosis induced by galectin-1. *J Immunol* **163**, 3801-11.

Passalacqua, M., Zicca, A., Sparatore, B., Patrone, M., Melloni, E. and Pontremoli, S. (1997). Secretion and binding of HMG1 protein to the external surface of the membrane are required for murine erythroleukemia cell differentiation. *FEBS Lett* **400**, 275-9.

Pearse, B. M. (1976). Clathrin: a unique protein associated with intracellular transfer of membrane by coated vesicles. *Proc Natl Acad Sci U S A* **73**, 1255-9.

Pelham, H. R. (1996). The dynamic organisation of the secretory pathway. *Cell Struct Funct* **21**, 413-9.

Pellegrini, L., Burke, D. F., von Delft, F., Mulloy, B. and Blundell, T. L. (2000). Crystal structure of fibroblast growth factor receptor ectodomain bound to ligand and heparin. *Nature* **407**, 1029-34.

Perillo, N. L., Marcus, M. E. and Baum, L. G. (1998). Galectins: versatile modulators of cell adhesion, cell proliferation, and cell death. *J Mol Med* **76**, 402-12.

Perillo, N. L., Pace, K. E., Seilhamer, J. J. and Baum, L. G. (1995). Apoptosis of T cells mediated by galectin-1. *Nature* **378**, 736-9.

Petersen, O. H. and Poulsen, J. H. (1967). Inhibition of salivary secretion and secretory potentials by g-strophantin, dinitrophenol and cyanide. *Acta Physiol Scand* **71**, 194-202.

Plotnikov, A. N., Hubbard, S. R., Schlessinger, J. and Mohammadi, M. (2000). Crystal structures of two FGF-FGFR complexes reveal the determinants of ligand-receptor specificity. *Cell* **101**, 413-24.

Plotnikov, A. N., Schlessinger, J., Hubbard, S. R. and Mohammadi, M. (1999). Structural basis for FGF receptor dimerization and activation. *Cell* **98**, 641-50.

Prats, H., Kaghad, M., Prats, A. C., Klagsbrun, M., Lelias, J. M., Liauzun, P., Chalon, P., Tauber, J. P., Amalric, F., Smith, J. A. et al. (1989). High molecular mass forms of basic fibroblast growth factor are initiated by alternative CUG codons. *Proc Natl Acad Sci U S A* **86**, 1836-40.

Presta, M., Moscatelli, D., Joseph-Silverstein, J. and Rifkin, D. B. (1986). Purification from a human hepatoma cell line of a basic fibroblast growth factor-like molecule that stimulates capillary endothelial cell plasminogen activator production, DNA synthesis, and migration. *Mol Cell Biol* **6**, 4060-6.

Prudovsky, I., Bagala, C., Tarantini, F., Mandinova, A., Soldi, R., Bellum, S. and Maciag, T. (2002). The intracellular translocation of the components of the fibroblast growth factor 1 release complex precedes their assembly prior to export. *J Cell Biol* **158**, 201-8.

Prudovsky, I., Mandinova, A., Soldi, R., Bagala, C., Graziani, I., Landriscina, M., Tarantini, F., Duarte, M., Bellum, S., Doherty, H. et al. (2003). The non-classical export routes: FGF1 and IL-1{alpha} point the way. *J Cell Sci* **116**, 4871-4881.

Pruyne, D. W., Schott, D. H. and Bretscher, A. (1998). Tropomyosin-containing actin cables direct the Myo2p-dependent polarized delivery of secretory vesicles in budding yeast. *J Cell Biol* **143**, 1931-45.

Raggers, R. J., Pomorski, T., Holthuis, J. C., Kalin, N. and van Meer, G. (2000). Lipid traffic: the ABC of transbilayer movement. *Traffic* **1**, 226-34.

Rapoport, T. A., Gorlich, D., Musch, A., Hartmann, E., Prehn, S., Wiedmann, M., Otto, A., Kostka, S. and Kraft, R. (1992). Components and mechanism of protein translocation across the ER membrane. *Antonie Van Leeuwenhoek* **61**, 119-22.

Rapoport, T. A., Jungnickel, B. and Kutay, U. (1996). Protein transport across the eukaryotic endoplasmic reticulum and bacterial inner membranes. *Annu Rev Biochem* **65**, 271-303.

Renko, M., Quarto, N., Morimoto, T. and Rifkin, D. B. (1990). Nuclear and cytoplasmic localization of different basic fibroblast growth factor species. *J Cell Physiol* **144**, 108-14.

Retaux, S., Rogard, M., Bach, I., Failli, V. and Besson, M. J. (1999). Lhx9: a novel LIM-homeodomain gene expressed in the developing forebrain. *J Neurosci* **19**, 783-93.

Ribatti, D., Leali, D., Vacca, A., Giuliani, R., Gualandris, A., Roncali, L., Nolli, M. L. and Presta, M. (1999). In vivo angiogenic activity of urokinase: role of endogenous fibroblast growth factor-2. *J Cell Sci* **112 (Pt 23)**, 4213-21.

Riehle, M., Bereiter-Hahn, J. and Boller, B. (1991). Effects of ouabain and digitoxin on the respiration of chick embryo cardiomyocytes in culture. *Arzneimittelforschung* **41**, 378-84.

Roth, J., Brada, D., Lackie, P. M., Schweden, J. and Bause, E. (1990). Oligosaccharide trimming Man9-mannosidase is a resident ER protein and exhibits a more restricted and local distribution than glucosidase II. *Eur J Cell Biol* **53**, 131-41.

Roth, J., Ziak, M. and Zuber, C. (2003). The role of glucosidase II and endomannosidase in glucose trimming of asparagine-linked oligosaccharides. *Biochimie* **85**, 287-94.

Rothberg, K. G., Heuser, J. E., Donzell, W. C., Ying, Y. S., Glenney, J. R. and Anderson, R. G. (1992). Caveolin, a protein component of caveolae membrane coats. *Cell* **68**, 673-82.

Rothman, J. E. (1990). The reconstitution of intracellular protein transport in cell-free systems. *Harvey Lect* **86**, 65-85.

Rothman, J. E. (1996). The protein machinery of vesicle budding and fusion. *Protein Sci* **5**, 185-94.

Rothman, J. E. and Wieland, F. T. (1996). Protein sorting by transport vesicles. *Science* **272**, 227-34.

Rubartelli, A., Bajetto, A., Allavena, G., Wollman, E. and Sitia, R. (1992). Secretion of thioredoxin by normal and neoplastic cells through a leaderless secretory pathway. *J Biol Chem* **267**, 24161-4.

Rubartelli, A., Bonifaci, N. and Sitia, R. (1995). High rates of thioredoxin secretion correlate with growth arrest in hepatoma cells. *Cancer Res* **55**, 675-80.

Rubartelli, A., Cozzolino, F., Talio, M. and Sitia, R. (1990). A novel secretory pathway for interleukin-1 beta, a protein lacking a signal sequence. *Embo J* **9**, 1503-10.

Rubartelli, A. and Sitia, R. (1991). Interleukin 1 beta and thioredoxin are secreted through a novel pathway of secretion. *Biochem Soc Trans* **19**, 255-9.

Rusnati, M., Urbinati, C., Tanghetti, E., Dell'Era, P., Lortat-Jacob, H. and Presta, M. (2002). Cell membrane GM1 ganglioside is a functional coreceptor for fibroblast growth factor 2. *Proc Natl Acad Sci U S A* **99**, 4367-72.

Sadeghi, H. and Birnbaumer, M. (1999). O-Glycosylation of the V2 vasopressin receptor. *Glycobiology* **9**, 731-7.

Safaiyan, F., Kolset, S. O., Prydz, K., Gottfridsson, E., Lindahl, U. and Salmivirta, M. (1999). Selective effects of sodium chlorate treatment on the sulfation of heparan sulfate. *J Biol Chem* **274**, 36267-73.

Sakaguchi, M., Mihara, K. and Sato, R. (1987). A short amino-terminal segment of microsomal cytochrome P-450 functions both as an insertion signal and as a stop-transfer sequence. *Embo J* **6**, 2425-31.

Salama, N. R. and Schekman, R. W. (1995). The role of coat proteins in the biosynthesis of secretory proteins. *Curr Opin Cell Biol* **7**, 536-43.

Sato, S., Burdett, I. and Hughes, R. C. (1993). Secretion of the baby hamster kidney 30-kDa galactose-binding lectin from polarized and nonpolarized cells: a pathway independent of the endoplasmic reticulum-Golgi complex. *Exp Cell Res* **207**, 8-18.

Schäfer, T., Zentgraf, H., Zehe, C., Brugger, B., Bernhagen, J. and Nickel, W. (2004). Unconventional secretion of fibroblast growth factor 2 is mediated by direct translocation across the plasma membrane of mammalian cells. *J Biol Chem* **279**, 6244-51.

Schatz, G. (1996). The protein import system of mitochondria. *J Biol Chem* **271**, 31763-6.

Schekman, R. and Orci, L. (1996). Coat proteins and vesicle budding. *Science* **271**, 1526-33.

Schulze-Osthoff, K., Risau, W., Vollmer, E. and Sorg, C. (1990). In situ detection of basic fibroblast growth factor by highly specific antibodies. *Am J Pathol* **137**, 85-92.

Seddon, A., Decker, M., Muller, T., Armellino, D., Kovesdi, I., Gluzman, Y. and Bohlen, P. (1991). Structure/activity relationships in basic FGF. *Ann N Y Acad Sci* **638**, 98-108.

Seeger, M. and Payne, G. S. (1992). A role for clathrin in the sorting of vacuolar proteins in the Golgi complex of yeast. *Embo J* **11**, 2811-8.

Seelenmeyer, C., Wegehingel, S., Lechner, J. and Nickel, W. (2003). The cancer antigen CA125 represents a novel counter receptor for galectin-1. *J Cell Sci* **116**, 1305-18.

Seelenmeyer, C., Wegehingel, S., Tews, I., Künzler, M., Aebi, M. and Nickel, W. (2005). *J Biol Chem, in press*.

Shafikhani, S., Siegel, R. A., Ferrari, E. and Schellenberger, V. (1997). Generation of large libraries of random mutants in Bacillus subtilis by PCR-based plasmid multimerization. *Biotechniques* **23**, 304-10.

Sharma, C. B., Lehle, L. and Tanner, W. (1981). N-Glycosylation of yeast proteins. Characterization of the solubilized oligosaccharyl transferase. *Eur J Biochem* **116**, 101-8.

Shi, J., Friedman, S. and Maciag, T. (1997). A carboxyl-terminal domain in fibroblast growth factor (FGF)-2 inhibits FGF-1 release in response to heat shock in vitro. *J Biol Chem* **272**, 1142-7.

Shin, J. T., Opalenik, S. R., Wehby, J. N., Mahesh, V. K., Jackson, A., Tarantini, F., Maciag, T. and Thompson, J. A. (1996). Serum-starvation induces the extracellular appearance of FGF-1. *Biochim Biophys Acta* **1312**, 27-38.

Shishibori, T., Oyama, Y., Matsushita, O., Yamashita, K., Furuichi, H., Okabe, A., Maeta, H., Hata, Y. and Kobayashi, R. (1999). Three distinct anti-allergic drugs, amlexanox, cromolyn and tranilast, bind to S100A12 and S100A13 of the S100 protein family. *Biochem J* **338 (Pt 3)**, 583-9.

Sivaram, M. V., Saporita, J. A., Furgason, M. L., Boettcher, A. J. and Munson, M. (2005). Dimerization of the exocyst protein Sec6p and its interaction with the t-SNARE Sec9p. *Biochemistry* **44**, 6302-11.

Smith, M. D. and Schnell, D. J. (2001). Peroxisomal protein import. the paradigm shifts. *Cell* **105**, 293-6.

Sohn, K., Orci, L., Ravazzola, M., Amherdt, M., Bremser, M., Lottspeich, F., Fiedler, K., Helms, J. B. and Wieland, F. T. (1996). A major transmembrane protein of Golgi-derived COPI-coated vesicles involved in coatomer binding. *J Cell Biol* **135**, 1239-48.

Sollner, T., Whiteheart, S. W., Brunner, M., Erdjument-Bromage, H., Geromanos, S., Tempst, P. and Rothman, J. E. (1993). SNAP receptors implicated in vesicle targeting and fusion. *Nature* **362**, 318-24.

Stegmayer, C., Kehlenbach, A., Tournaviti, S., Wegehingel, S., Zehe, C., Denny, P., Smith, D. F., Schwappach, B. and Nickel, W. (2005). Direct transport across the plasma membrane of mammalian cells of Leishmania HASPB as revealed by a CHO export mutant. *J Cell Sci* **118**, 517-27.

Sterpetti, A. V., Cucina, A., Morena, A. R., Di Donna, S., D'Angelo, L. S., Cavalarro, A. and Stipa, S. (1993). Shear stress increases the release of interleukin-1 and interleukin-6 by aortic endothelial cells. *Surgery* **114**, 911-4.

Stevenson, F. T., Bursten, S. L., Fanton, C., Locksley, R. M. and Lovett, D. H. (1993). The 31-kDa precursor of interleukin 1 alpha is myristoylated on specific lysines within the 16-kDa N-terminal propiece. *Proc Natl Acad Sci U S A* **90**, 7245-9.

Stevenson, F. T., Torrano, F., Locksley, R. M. and Lovett, D. H. (1992). Interleukin 1: the patterns of translation and intracellular distribution support alternative secretory mechanisms. *J Cell Physiol* **152**, 223-31.

Stinchcombe, J., Bossi, G. and Griffiths, G. M. (2004). Linking albinism and immunity: the secrets of secretory lysosomes. *Science* **305**, 55-9.

Stoorvogel, W., Kleijmeer, M. J., Geuze, H. J. and Raposo, G. (2002). The biogenesis and functions of exosomes. *Traffic* **3**, 321-30.

Tanudji, M., Hevi, S. and Chuck, S. L. (2002). Improperly folded green fluorescent protein is secreted via a non-classical pathway. *J Cell Sci* **115**, 3849-57.

Tanudji, M., Hevi, S. and Chuck, S. L. (2003). The non-classical secretion of thioredoxin is not sensitive to redox state. *Am J Physiol Cell Physiol*.

Tarantini, F., Gamble, S., Jackson, A. and Maciag, T. (1995). The cysteine residue responsible for the release of fibroblast growth factor-1 resides in a domain independent of the domain for phosphatidylserine binding. *J Biol Chem* **270**, 29039-42.

Tarantini, F., LaVallee, T., Jackson, A., Gamble, S., Carreira, C. M., Garfinkel, S., Burgess, W. H. and Maciag, T. (1998). The extravesicular domain of synaptotagmin-1 is released with the latent fibroblast growth factor-1 homodimer in response to heat shock. *J Biol Chem* **273**, 22209-16.

Tarantini, F., Micucci, I., Bellum, S., Landriscina, M., Garfinkel, S., Prudovsky, I. and Maciag, T. (2001). The precursor but not the mature form of IL1alpha blocks the release of FGF1 in response to heat shock. *J Biol Chem* **276**, 5147-51.

Tartakoff, A. M. (1983). Perturbation of vesicular traffic with the carboxylic ionophore monensin. *Cell* **32**, 1026-8.

Taverna, S., Ghersi, G., Ginestra, A., Rigogliuso, S., Pecorella, S., Alaimo, G., Saladino, F., Dolo, V., Dell'Era, P., Pavan, A. et al. (2003). Shedding of Membrane Vesicles Mediates Fibroblast Growth Factor-2 Release from Cells. *J Biol Chem* **278**, 51911-51919.

Thompson, L. D., Pantoliano, M. W. and Springer, B. A. (1994). Energetic characterization of the basic fibroblast growth factor-heparin interaction: identification of the heparin binding domain. *Biochemistry* **33**, 3831-40.

Thoren, P. E., Persson, D., Karlsson, M. and Norden, B. (2000). The antennapedia peptide penetratin translocates across lipid bilayers - the first direct observation. *FEBS Lett* **482**, 265-8.

Thornalley, P. J. (1998). Cell activation by glycated proteins. AGE receptors, receptor recognition factors and functional classification of AGEs. *Cell Mol Biol (Noisy-le-grand)* **44**, 1013-23.

Tobaly-Tapiero, J., Bittoun, P. and Saib, A. (2005). Isolation of foamy viruses from peripheral blood lymphocytes. *Methods Mol Biol* **304**, 125-37.

Tooze, J. and Tooze, S. A. (1986). Clathrin-coated vesicular transport of secretory proteins during the formation of ACTH-containing secretory granules in AtT20 cells. *J Cell Biol* **103**, 839-50.

Towbin, H., Staehelin, T. and Gordon, J. (1979). Electrophoretic transfer of proteins from polyacrylamide gels to nitrocellulose sheets: procedure and some applications. In *Proc Natl Acad Sci U S A*, vol. 76, pp. 4350-4.

Tracey, B. M., Feizi, T., Abbott, W. M., Carruthers, R. A., Green, B. N. and Lawson, A. M. (1992). Subunit molecular mass assignment of 14,654 Da to the soluble beta-galactoside-binding lectin from bovine heart muscle and demonstration of intramolecular disulfide bonding associated with oxidative inactivation. *J Biol Chem* **267**, 10342-7.

Trudel, C., Faure-Desire, V., Florkiewicz, R. Z. and Baird, A. (2000). Translocation of FGF2 to the cell surface without release into conditioned media [In Process Citation]. *J Cell Physiol* **185**, 260-8.

Tsuboi, T., Ravier, M. A., Xie, H., Ewart, M. A., Gould, G. W., Baldwin, S. A. and Rutter, G. A. (2005). Mammalian exocyst complex is required for the docking step of insulin vesicle exocytosis. *J Biol Chem* **280**, 25565-70.

Urlinger, S., Baron, U., Thellmann, M., Hasan, M. T., Bujard, H. and Hillen, W. (2000). Exploring the sequence space for tetracycline-dependent transcriptional activators: novel mutations yield expanded range and sensitivity. *Proc. Natl. Acad. Sci. U.S.A.* **97**, 7963-8.

Vega, I. E. and Hsu, S. C. (2001). The exocyst complex associates with microtubules to mediate vesicle targeting and neurite outgrowth. *J Neurosci* **21**, 3839-48.

Wacker, I., Kaether, C., Kromer, A., Migala, A., Almers, W. and Gerdes, H. H. (1997). Microtubule-dependent transport of secretory vesicles visualized in real time with a GFP-tagged secretory protein. *J Cell Sci* **110 (Pt 13)**, 1453-63.

Walter, P., Gilmore, R. and Blobel, G. (1984). Protein translocation across the endoplasmic reticulum. *Cell* **38**, 5-8.

Walton, P. A., Hill, P. E. and Subramani, S. (1995). Import of stably folded proteins into peroxisomes. *Mol Biol Cell* **6**, 675-83.

Wang, J. L., Laing, J. G. and Anderson, R. L. (1991). Lectins in the cell nucleus. *Glycobiology* **1**, 243-52.

Wang, Y. and Becker, D. (1997). Antisense targeting of basic fibroblast growth factor and fibroblast growth factor receptor-1 in human melanomas blocks intratumoral angiogenesis and tumor growth. *Nat Med* **3**, 887-93.

Weber, T., Zemelman, B. V., McNew, J. A., Westermann, B., Gmachl, M., Parlati, F., Sollner, T. H. and Rothman, J. E. (1998). SNAREpins: minimal machinery for membrane fusion. *Cell* **92**, 759-72.

Weis, K. (2003). Regulating access to the genome: nucleocytoplasmic transport throughout the cell cycle. *Cell* **112**, 441-51.

Wessels, H. P. and Spiess, M. (1988). Insertion of a multispanning membrane protein occurs sequentially and requires only one signal sequence. *Cell* **55**, 61-70.

Wiedlocha, A., Falnes, P. O., Madshus, I. H., Sandvig, K. and Olsnes, S. (1994). Dual mode of signal transduction by externally added acidic fibroblast growth factor. *Cell* **76**, 1039-51.

Wiedlocha, A. and Sorensen, V. (2004). Signaling, internalization, and intracellular activity of fibroblast growth factor. *Curr Top Microbiol Immunol* **286**, 45-79.

Wilson, T. J., Firth, M. N., Powell, J. T. and Harrison, F. L. (1989). The sequence of the mouse 14 kDa beta-galactoside-binding lectin and evidence for its synthesis on free cytoplasmic ribosomes. *Biochem J* **261**, 847-52.

Wong, P. and Burgess, W. H. (1998). FGF2-Heparin co-crystal complex-assisted design of mutants FGF1 and FGF7 with predictable heparin affinities. *J Biol Chem* **273**, 18617-22.

Wong-Staal, F. and Haseltine, W. A. (1992). Regulatory genes of human immunodeficiency viruses. *Mol Genet Med* **2**, 189-219.

Wybranietz, W. A., Prinz, F., Spiegel, M., Schenk, A., Bitzer, M., Gregor, M. and Lauer, U. M. (1999). Quantification of VP22-GFP spread by direct fluorescence in 15 commonly used cell lines. *J Gene Med* **1**, 265-74.

Zanetta, J. P. (1998). Structure and functions of lectins in the central and peripheral nervous system. *Acta Anat (Basel)* **161**, 180-95.

Zhan, X., Hu, X., Friedman, S. and Maciag, T. (1992). Analysis of endogenous and exogenous nuclear translocation of fibroblast growth factor-1 in NIH 3T3 cells. *Biochem Biophys Res Commun* **188**, 982-91.

Zhou, Q. and Cummings, R. D. (1990). The S-type lectin from calf heart tissue binds selectively to the carbohydrate chains of laminin. *Arch Biochem Biophys* **281**, 27-35.

Zhou, X., Engel, T., Goepfert, C., Erren, M., Assmann, G. and von Eckardstein, A. (2002). The ATP binding cassette transporter A1 contributes to the secretion of interleukin 1beta from macrophages but not from monocytes. *Biochem Biophys Res Commun* **291**, 598-604.

Zhu, W. Q. and Ochieng, J. (2001). Rapid release of intracellular galectin-3 from breast carcinoma cells by fetuin. *Cancer Res* **61**, 1869-73.

Zuber, C., Spiro, M. J., Guhl, B., Spiro, R. G. and Roth, J. (2000). Golgi apparatus immunolocalization of endomannosidase suggests post-endoplasmic reticulum glucose trimming: implications for quality control. *Mol Biol Cell* **11**, 4227-40.

Acknowledgements

I am deeply indebted to Prof. Dr. rer. nat. Walter Nickel for giving me the opportunity to work in his laboratory on this interesting project as well as for his guidance and help.

I want to thank Prof. Dr. rer. nat. Michael Brunner for being my appraiser.

Special thanks to Dr. rer. nat. Ivo Tews for his support on the structural analysis of FGF2.

I would like to thank Angelika Kehlenbach and Julia Lenz for their generous help with FACS sortings.

I especially thank Carolin Stegmayer, Rafael Backhaus and Christoph Zehe for their support by conducting two experiments regarding FGF2 spreading and FGF2 localization on the plasma membrane.

I am indebted to Christoph Zehe for his critical comments on the manuscript and for very fruitful discussions.

Thanks to all members of the Nickel lab for the nice working atmosphere and their support during this thesis. Without Rafael Backhaus, Lucía Cespón Torrado, Antje Ebert, Tobias Schäfer, Claudia Seelenmeyer, Carolin Stegmayer, Koen Temmerman, Stella Tournaviti, Sabine Wegehingel, Matthias Wuttke, Jaz Woo and Christoph Zehe, the work would have been only half as productive and enjoyable as it finally was.

I would like to express my gratitude to my family. Thank you Mama und Papa for supporting me in good and bad moments. Without you I would not have had the oppurtunity to pursue my PhD degree. I also want to thank my brother for his support.

Last but not least I want to thank Britta Pätzold for her understanding and support.